Mathematical study of multi-resource models in a chemostat

Sarra Nouaoura

University of Tunis El Manar
National Engineering School of Tunis
Doctoral School : Engineering Sciences and Techniques

DOCTORAL THESIS

Specialty: **Applied Mathematics**

Presented by

Sarra NOUAOURA

In partial fulfillment of the requirements of

DOCTORAL DIPLOMA

Mathematical study of multi-resource models in a chemostat

Defended on **June 25th , 2021,** in front of the jury members :

Mr. Maher MOAKHER	Professor, University of Tunis El Manar, Tunisia	President
Mr. Karim YADI	Professor, University of Tlemcen , Algeria	Reviewer
Mr. Alain RAPAPORT	Research Director, INRAE, University of Montpellier, France	Reviewer
Mr. Moncef AOUADI	Professor, University of Carthage, Tunisia	Examiner
Mrs. Nahla ABDELLATIF	Assistant Professor, University of Manouba, Tunisia	Supervisor
Mr. Tewfik SARI	Research Director, INRAE, University of Montpellier, France	Co-Supervisor
Mr. Radhouane FEKIH SALEM	Assistant Professor, University of Monastir, Tunisia	Co-Supervisor

Laboratory of Mathematical and Numerical Modeling in Engineering Sciences
ENIT, B.P.N° 37, 1002 Tunis Belvédère, Tunisia
www.edsti.enit.utm.tn

Acknowledgments

First of all, a big thank you to **ALLAH** the most powerful who gave me the strength and patience to finish my thesis and to overcome the obstacles at difficult times and who is the source of all the successes in my life.

I am so happy to express my thanks and my deep gratitude to my research supervisors:

Mrs. Nahla ABDELLATIF, lecturer at the University of Manouba (ENSI) and researcher at the University of Tunis el Manar (ENIT), for having accepted to supervise me and to have made me discover a field of research which impassioned me from the beginning. I thank her for her precious advice, her encouragement and her listening. Her great erudition and her advice helped me throughout my research and the writing of this thesis. Thank you again for having trusted me throughout these four years.

Mr. Tewfik SARI, research director at INRAE, University of Montpellier, who suggested my research topic and whose great professional and human qualities gave me a great support in the progress of my work. I was very lucky to work with him.

I address my sincere thanks to *Mr. Radhouene FEKIH-SALEM*, assistant professor at the University of Monastir and researcher at the University of Tunis el Manar (ENIT) for the knowledge that he transmitted to me with sincerity, for his precious help and for his devotion to this work. He has greatly contributed to the progress of my thesis. I learned a lot working with him especially in the numerical part of this thesis.

I also extend my most sincere thanks to *Mr. Alain RAPAPORT*, research director at INRAE, University of Montpellier, and *Mr. Karim YADI*, professor at the University of Tlemcen, for the honor they have given me by participating on my jury as reviewers.

I thank *Mr.Maher MOAKHER*, professor at the University of Tunis el Manar (ENIT), for agreeing to swear this thesis as a jury presenter.

I would like to thank *Mr. Moncef AOUADI*, professor at the University of Carthage (ENIB), for accepting to be an examiner and a member of the jury.

My warm thanks go to all the members, teachers-researchers and PhD students, of the LAMSIN laboratory, to its director *Mr. Mourad BELLASSOUED* for having welcomed me in the laboratory during these four years. I was able to work in a particularly pleasant environment. I cannot forget to mention all the administrative staff for their welcome, their help, and their generous attitude.

I feel obliged to take this opportunity to sincerely thank my country, Algeria (represented by the Ministry of Higher Education) for the doctoral scholarship that allowed me to pursue my university studies. This work could not have been accomplished without its financial support.

Without forgetting to thank all my family, in particular, my dear mother **Rahima**, my dear father **Mohammed** and my lovely sisters **Asma** and **Selma**. A big thank you to them for supporting me mentally and physically, for their encouragement and their help not only during the realization of this work but also during all my studies. A big thank you also to my uncles, especially to my uncle **Salah** for his support and help.

In last and not least, a huge thank you from all my heart to my fiance **Marwen**, for his help, his support, his listening at all times with all his strength and energy, and especially his love which has been essential to me these last years. He gave me the courage to reach my goal and he did a lot for me. I thank you very much.

My thoughts also go to my former friends. I thank them warmly for the moments shared even if our reunions are becoming more and more distant.

A big thanks to all those who contributed directly or indirectly to the development of this modest research.

Abstract

This thesis focuses on the mathematical analysis of an anaerobic digestion model involving three species and three resources in a chemostat. The model includes several specific ecological interactions between these species, such that competition, syntrophy, and inhibition. More precisely, we analyze the mechanistic model describing the anaerobic chlorophenol mineralization in a three-tiered microbial food-web. We investigate the effects of including three inflowing concentrations, the mortality of the species, together with the inhibition of the third substrate on the first species. In this general case, we prove that the system can have up to eight types of steady states and we give a complete analysis by determining the necessary and sufficient conditions for their existence, according to the operating parameters. Then, we study the local stability in the case when the maintenance is ignored, where we can reduce the system to a three-dimensional one. We examine the effect of adding the hydrogen input concentration to the chlorophenol mineralization model and analyze the bifurcation diagrams by varying the input concentration of chlorophenol as a bifurcation parameter. We show that the positive steady state, which corresponds to the coexistence of the three microorganisms, can be unstable and that the system exhibits rich behaviors including bistability, coexistence, and emergence of a limit cycle through a supercritical Hopf bifurcation. When the mortality terms are present in the model, we use the Liénard-Chipart stability criterion to determine explicitly the necessary and sufficient local stability properties, when the eigenvalues of the Jacobian matrix can not be calculated. Subsequently, we give a numerical analysis of the bifurcation diagrams which suggested the presence of a supercritical Hopf bifurcation emerging through the positive steady state with the appearance of a stable periodic solution. Finally, we focus on the study of the operating diagrams which illustrate the existence and stability regions of the steady states. Our analytical study results in the discovery of several interesting regions, namely the existence of an instability region of the positive steady state, a fact that has not been detected, previously, by the numerical study.

Résumé

Cette thèse porte sur l'analyse mathématique d'un modèle de la digestion anaérobie qui comprend trois espèces microbiennes et trois ressources dans un chémostat. Le modèle implique plusieurs interactions écologiques spécifiques entre ces espèces, telles que la compétition, la syntrophie et l'inhibition. Plus précisément, nous analysons mathématiquement un modèle décrivant la minéralisation anaérobie du chlorophénol dans une chaîne alimentaire microbienne à trois niveaux. Nous étudions les effets des trois substrats en entrée, de la mortalité des espèces, ainsi que celui de l'inhibition du troisième substrat sur la première espèce. Dans ce cas général, nous prouvons que le système peut avoir huit types d'équilibres et nous donnons une analyse complète en déterminant les conditions nécessaires et suffisantes pour leur existence, en fonction des paramètres opératoires. Ensuite, nous étudions la stabilité locale du modèle sans termes de mortalité qu'on a pu réduire à un modèle en dimension trois. Nous examinons l'effet de l'ajout de l'hydrogène en entrée au modèle de minéralisation du chlorophénol et nous analysons les diagrammes de bifurcation en faisant varier la concentration du chlorophénol en entrée en tant que paramètre de bifurcation. Nous montrons que l'équilibre positif, qui correspond à la coexistence des trois microorganismes, peut être instable, et que le système présente des comportements très riches comprenant la bi-stabilité, la coexistence et l'émergence d'un cycle limite à travers une bifurcation de Hopf super-critique. Lorsque les termes de mortalité sont présents dans le modèle, nous utilisons le critère de stabilité de Liénard-Chipart pour déterminer explicitement les conditions nécessaires et suffisantes de la stabilité locale, quand on ne peut pas calculer les valeurs propres des matrices Jacobiennes. Par la suite, nous donnons une analyse numérique des diagrammes de bifurcation qui a suggéré la présence d'une bifurcation de Hopf super-critique émergeant à travers l'équilibre positif avec l'apparition d'une solution périodique stable. Enfin, nous nous concentrons sur l'étude des diagrammes opératoires qui illustrent les régions d'existence et de stabilité des équilibres. Notre étude analytique aboutit à la découverte de plusieurs régions intéressantes, comme l'existence d'une région d'instabilité de l'équilibre positif, qui n'a pas été détectée, auparavant, par l'étude numérique.

Keywords: Anaerobic digestion, Chlorophenol mineralization, Three-tiered microbial food-web, Chemostat, Coexistence, Bi-stability, Liénard-Chipart criterion, Hopf bifurcation, Limit cycle, Bifurcation diagrams, Operating diagrams.

Mots clés: Digestion anaérobie, Minéralisation du chlorophénol, Chaîne alimentaire microbienne à trois niveaux, Chémostat, Coexistence, Bi-stabilité, Critère de Liénard-Chipart, Bifurcation de Hopf, Cycle limite, Diagrammes de bifurcation, Diagrammes opératoires.

Table of Contents

List of Figures

List of Tables

Glossary and Notations

Symbol	Meaning
AD	Anaerobic Digestion
ADM1	Anaerobic Digestion Model No.1
ODE	Ordinary Differential Equation
OD	Operating Diagram
H_2	Hydrogen
CEP	Competitive Exclusion Principle
GAS	Globally Asymptotically Stable
LES	Locally Exponentially Stable
E_{ijk}	Steady state
SSi	Steady state i
TB	Transcritical Bifurcation
SNB	Saddle-Node Bifurcation
HB	Hopf Bifurcation
S	Stable
U	Unstable
D	Dilution rate
F_{in}	Input flow rate in Figure 1.1
F_{out}	Outflow rate in Figure 1.1
V	Reaction volume in Figure 1.1
s	Substrat in model (1.1)
s^{in}	Inflowing substrate concentration in model (1.1)
x	Bacteria in model (1.1)
γ	Yield of the conversion of substrate into biomass in model (1.1)
μ	Growth rate function in model (1.1)
$\mu_{\max}$	Maximum growth rate of μ in Figure 1.2
X_{ch}	Chlorophenol degrader concentration in model (2.1)
X_{ph}	Phenol degrader concentration in model (2.1)
X_{H_2}	Methanogen concentration in model (2.1)
S_{ch}	Chlorophenol substrate concentration in model (2.1)

S_{ph}	Phenol substrate concentration in model (2.1)
S_{H_2}	Hydrogen substrate concentration in model (2.1)
$S_{\text{ch}}^{\text{in}}$	Chlorophenol substrate concentration in model (2.1)
$S_{\text{ph}}^{\text{in}}$	Phenol substrate concentration in model (2.1)
$S_{\text{H}_2}^{\text{in}}$	Hydrogen substrate concentration in model (2.1)
f_i	Specific growth rate of the species i in model (2.1)
Y_i	Yield coefficients in model (2.1)
m_i	Maximum growth rate of the species i
K_s	Semi-saturation constant
K_I	Inhibition constant
$k_{\text{dec,ch}}$	Maintenance term of the Chlorophenol degrader in model (2.1)
$k_{\text{dec,ph}}$	Maintenance term of the phenol degrader in model (2.1)
$k_{\text{dec,H}_2}$	Maintenance term of the Methanogen in model (2.1)
$K_{S,\text{ch}}$	Semi-saturation constant of the Chlorophenol degrader
$K_{S,\text{ph}}$	Semi-saturation constant of the phenol degrader
K_{S,H_2}	Semi-saturation constant of the Hydrogen
x_0	Chlorophenol degrader concentration in model (2.8)
x_1	Phenol degrader concentration in model (2.8)
x_2	Methanogen concentration in model (2.8)
s_0	Chlorophenol substrate concentration in model (2.8)
s_1	Phenol substrate concentration in model (2.8)
s_2	Hydrogen substrate concentration in model (2.8)
s_0^{in}	Chlorophenol substrate concentration in model (2.8)
s_1^{in}	Phenol substrate concentration in model (2.8)
s_2^{in}	Hydrogen substrate concentration in model (2.8)
a_0	Maintenance (or decay) term of the Chlorophenol degrader in model (2.8)
a_1	Maintenance (or decay) term of the phenol degrader in model (2.8)
a_2	Maintenance (or decay) term of the Methanogen in model (2.8)
μ_i	Specific growth rate of the species i in model (2.8)
M_0	Inverse function of μ_0 with respect to s_0 given in Definition 2.1
M_1	Inverse function of μ_1 with respect to s_1 given in Definition 2.1
M_2	Inverse function of μ_2 given in Definition 2.1
M_3	Inverse function of μ_0 with respect to s_2 given in Definition 2.1
s_2^i	Functions of D defined by (2.21) and given in Table 3.4
I_1, I_2	Intervals defined by (2.22)
Ψ	Function of s_2 and D defined by (2.23)
ϕ_i, φ_i	Functions of D defined by (2.25)
s_2^{*i}	Solutions of (2.26)
ψ_i	Functions of s_i defined by (2.27)
ϕ_4	Function of D, s_0^{in}, s_1^{in} and s_2^{in} defined by (3.2)

N_0	Chlorophenol degrader concentration in model (3.21)
N_1	Phenol degrader concentration in model (3.21)
N_2	Methanogen concentration in model (3.21)
R_0	Chlorophenol substrate concentration in model (3.21)
R_1	Phenol substrate concentration in model (3.21)
R_2	Hydrogen substrate concentration in model (3.21)
ν_i	Growth rate functions in model (3.21)
ω_i	Yield coefficients in model (3.21)
k_i	Decay terms of the species i in model (3.21)

General introduction

The protection of the environment and the preservation of natural resources are major concerns of our world. The fight against pollution is in fact an important issue that requires knowledge of the functioning of microbial ecosystems and an understanding of the mechanisms that allow different microbial species to maintain themselves in ecosystems involved in human or animal health. These microorganisms are sources of contamination of surface water and groundwater, but can also be used to treat wastewater. Water is a renewable resource and the quality of the water is more and more important. Lack of water and/or quality is a big problem in some parts of the world. Consequently, to maintain and improve the quality of water resources we can use biological reactors. As explained in [25], a bioreactor is an enclosure containing a nutrient medium consisting of a cocktail of various substrates which one or more populations of microorganisms grow. Bioreactors are used to perform operations for transforming matter through biological pathways. These bioreactors are classified according to their mode of operation, in other words, the way in which they are supplied with the matter, and depending on whether microorganisms are free in the medium or fixed on support; the latter could itself be fixed or mobile. As a result, it is possible to distinguish continuously-fed systems, systems whose supply is semi-continuous, and those operating in closed mode. For example, the chemostat is a closed biological reactor which makes it possible to reduce the quantity of polluting substances contained in the wastewater so that the water finally released into the natural environment does not degrade the latter. The use of wastewater in agriculture often reduces the environmental impact it would have and can help communities increase their harvests and preserve precious resources of water and nutrient.

Today, treatment techniques and treatment plants are constantly evolving. One of the effective methods for the treatment of wastewater is anaerobic digestion. This process transforms the organic matter in absence of oxygen, into methane and carbon dioxide (biogas) considered as a new form of energy. To understand the biological reactions and to predict the behavior of the processes, we use mathematical theories to model these reactions by nonlinear ordinary differential equations systems. Several models of anaerobic digestion have been proposed in the literature [7, 10, 29, 65, 67, 68]. We list in review some of them in chapter 1.

In this thesis work, we study mathematically some of these models developed around

the decontamination of wastewater and their use, and we propose a model relevant to improvements for applications, that is more in tune with reality. The aim of this thesis is to perform the mathematical analysis of a model of three microbial species and three substrates in a chemostat. The study of these models allows us to understand the different mechanisms that could lead to improve the bioprocesses and control the metabolic pathways of some ecosystems of interest. More precisely, we are interested in a mechanistic model describing the anaerobic mineralization of chlorophenol in a three-tiered food-web in the chemostat. This model has been studied numerically in the literature in [64] and mathematically in the particular cases where the second and the third substrate concentrations are neglected in [51] and where the maintenance is not considered in [57]. We reconsider in this work the three-tiered model and we give the theoretical study in the general case including the three input substrate concentrations as well as maintenance.

The thesis is structured as follows:

In chapter 1, we begin with a working definition of a chemostat and present the minimal model of the chemostat which is a two-dimensional model that describes a single substrate and a single biomass interaction. We expose, as well, extensions of this minimal model which are widely studied in the chemostat literature. We then put in review some two-tiered models and provide some definitions of biological interactions between the species of microorganisms as competition, commensalism, mutualism, and syntrophy. Finally, we briefly describe the process of anaerobic digestion and explain the different phases of this process.

Chapter 2 is dedicated to the analysis of the mathematical model of the three-tiered microbial species in competition on three resources in the chemostat from [64], which takes into account three inflowing concentrations, including the terms of mortality and inhibition of the third substrate on the first species. By considering a general class of growth functions, we provide a complete theoretical description of the steady states of the model and we determine the necessary and sufficient conditions of their existence.

Chapter 3 is devoted to the theoretical analysis of the local stability of the three-tiered model according to the operating (control) parameters in the particular case without maintenance (decay) terms. We give the necessary and sufficient properties of the stability of the steady states. Then, we study the asymptotic behaviors of the chlorophenol model according to the control parameters. Thus, we analyze numerically the bifurcation diagram by varying one-parameter. We prove that the coexistence steady state can be unstable and we give numerical evidence for a supercritical Hopf bifurcation with the appearance of a stable periodic orbit.

In chapter 4, we are interested in analyzing the local stability of the model, by consid-

ering the general case including maintenance terms. We give the necessary and sufficient conditions of the stability of the steady states, with respect to the operating parameters of the process. In previous studies, this stability analysis was performed only numerically. Moreover, we analyze the dynamical behavior of the model with maintenance and we apply our theoretical results on the existence and stability of steady states. We give two bifurcation diagrams, showing that the model can present rich behavior including bistability, coexistence and emergence of the limit cycle due to Hopf bifurcation.

The final chapter 5 deals with the mathematical description of the operating diagrams of the three-tiered model in both cases: with and without decay terms. Using the theoretical results on the existence and local stability of the steady states, provided in previous chapters, we construct the operating diagrams with respect to four operating parameters (the dilution rate and the three input concentrations of the substrates) to analyze the dynamic behavior of the process according to the regions of these diagrams.

Finally, we give a general conclusion on the results obtained and we present perspectives and possible extensions of our work.

CHAPTER 1

Introduction to competition models in a chemostat

Summary

1.1 Introduction

In this chapter, we introduce and discuss the fundamental notions that will be used throughout the thesis. We start to define the experimental device "the chemostat", we present the minimal model of the chemostat, and we expose the extensions of this model which are widely studied in the chemostat literature. Next, we recall some two-step models studied in the literature which describe the different biological interactions between microbial species that are the competition, commensalism, mutualism and syntrophy, and we describe the effects of the maintenance (or decay). Finally, we briefly describe the process of anaerobic digestion by explaining, in the same way, their different phases.

1.2 The Chemostat

The chemostat is an experimental device that is a basic piece of laboratory apparatus. It is used to study microorganisms and especially their growth characteristics on a substrate. We consult [25], which describes in some details the theory of the chemostat, and from which this part was elaborated.

The continuous culture of the species of microorganisms or plant cells produced in a laboratory device called "*Chemostat*", which is defined as an enclosure containing the reaction volume, in which microorganisms (biomass) are put in the presence of a limiting substrate and the other non-limiting resources essential to their development and reproduction. It is used in scientific areas related to the acquisition of knowledge that is both fundamental, such as ecology or evolutionary biology, and applied such as wastewater treatment. There are several works in the literature relating to chemostats both in the biological journals [37, 43] and in mathematical journals [25, 56, 63]. It is also very useful in different fields as explained in [56]. This device presents two main characteristics: its content is assumed to be perfectly homogeneous and its volume V is kept constant. In fact, it is a bioreactor whose mode of feeding is continuous, i.e, the input flow and outflow rates are identical ($F_{in} = F_{out}$), see [25].

In the chemostat, a nutrient element or a substrate s, that is necessary for the growth of a biomass x (bacterium), enters the chemostat with an input flow F_{in} and concentration s^{in}. The dilution rate is equal to

$$D = \frac{F_{in}}{V},$$

which describes the relationship between the flow of the medium F_{in} and the culture volume in the bioreactor V.

We schematize the chemostat as follows:

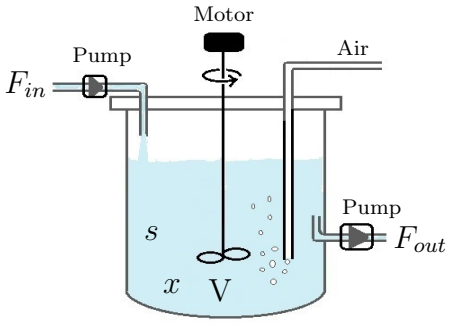

Figure 1.1: The Chemostat.

1.2.1 Simple chemostat model

To establish the chemostat equations, we will start by introducing the simplest possible model of chemostat that is called the "minimal model" of the chemostat, which is based on the transformation of substrate s by the presence of a microorganism x, which is schematized as follows:

$$s \xrightarrow{\mu(s)} x,$$

where μ is a harvesting rate in the first equation of (1.1) and a specific growth rate in the second, which only depends on the substrate concentration s. This schema leads to obtain the minimal model which is written as:

$$\begin{aligned} \frac{ds}{dt} &= D\left(s^{in} - s\right) - \frac{\mu(s)}{\gamma}x \\ \frac{dx}{dt} &= \left(\mu(s) - D\right)x, \end{aligned} \tag{1.1}$$

where s^{in} is the inflowing substrate concentration, γ is the yield of the conversion of substrate into biomass, which is constant. Furthermore, we assume that the function $s \to \mu(s)$ is continuous, has a continuous derivative, is positive and is equal to zero at 0. In the literature there exist several types of growth functions. The most known are the growth functions of Monod-type and Haldane-type.

- **Monod-type function:**

  The most classic growth function of Monod (or function of Michaelis-Menten) is written as follows:

  $$\mu(s) = \mu_{\max}\frac{s}{K_s + s},$$

  where $\mu_{\max}$ is the maximum growth rate of μ and K_s is the semi-saturation constant, noticing that $\mu(K_s) = \mu_{\max}/2$.

  A growth function μ is said to be of Monod-type if it satisfies the following properties:

  - μ is defined for $s \geq 0$ and is bounded.

- $\mu(0) = 0$.
- μ is strictly increasing.

- **Haldane-type function:**

  The growth function of Haldane is written as follows:

$$\mu(s) = \mu_{\max} \frac{s}{s + K_s + s^2/K_I},$$

  where K_I is the inhibition constant.

  A growth function μ is said to be of Haldane-type if it satisfies the following properties:

  - μ is defined for $s \geq 0$, is positive and $\mu(0) = 0$.
  - There exists $s_m > 0$, such that for $s \in [0, s_m[$, $\mu'(s) > 0$ and for $s \in [s_m, +\infty[$, $\mu'(s) < 0$.
  - $\lim_{s \to +\infty} \mu(s) = 0$.

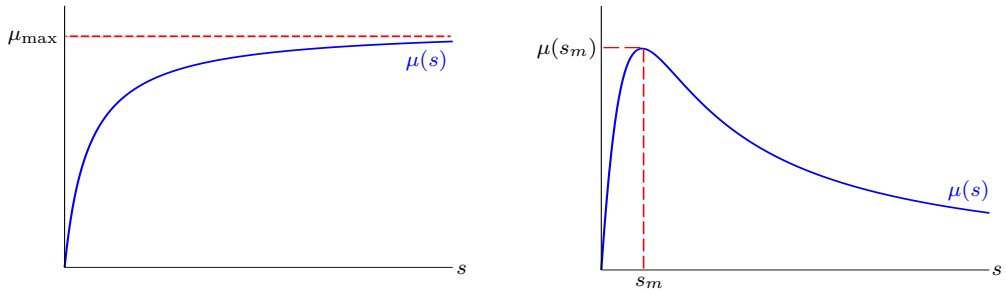

Figure 1.2: Growth functions: On the left, 'Monod-type' and on the right 'Haldane-type'.

The behavior of system (1.1) is well known. Thus, we summarize the behavior of this model in following Tables 1.1 and 1.2 for both types of growth function. The details are given in [25].

Table 1.1: Existence and stability of steady states of (1.1) for the growth rate μ of Monod-type.

Condition	$s^* < s^{\text{in}}$	$s^* \geq s^{\text{in}}$
$\text{SS}_0 = (s^{\text{in}}, 0)$	Unstable	GAS
$\text{SS}_1 = (s^*, x^*)$, $s^* = s^*(D)$ is solution of $\mu(s) = D$ and $x^* = \gamma(s^{\text{in}} - s^*)$	GAS	Does not exist

GAS and LES mean globally asymptotically stable and locally exponentially stable, respectively. In the next section, we will propose two possible extensions of the minimal model.

Table 1.2: Existence and stability of steady states of (1.1) for the growth rate μ of Haldane-type.

Condition	$s^{\text{in}} < s^{1*}$	$s^{1*} < s^{\text{in}} < s^{2*}$	$s^{2*} < s^{\text{in}}$
$\text{SS}_0 = \left(s^{\text{in}}, 0\right)$	LES	Unstable	LES
$\text{SS}_1 = (s^{1*}, x^{1*})$, $s^{1*} = s^{1*}(D) < s^{2*}(D)$ is solution of $\mu(s) = D$ and $x^{1*} = \gamma(s^{\text{in}} - s^{1*})$	Does not exist	LES	LES
$\text{SS}_2 = (s^{2*}, x^{2*})$, $s^{2*} = s^{2*}(D) > s^{1*}(D)$ is solution of $\mu(s) = D$ and $x^{2*} = \gamma(s^{\text{in}} - s^{2*})$	Does not exist	Does not exist	Unstable

1.2.2 Model with several species in the chemostat

In this section, we assume that n species of microorganisms ($n \geq 2$) compete for a single substrate in the chemostat. We assume that the dilution rates of the substrate and species are different, so the minimal model (1.1) becomes:

$$\begin{aligned} \frac{ds}{dt} &= D\left(s^{in} - s\right) - \sum_{i=1}^{n} \frac{\mu_i(s)}{\gamma_i} x_i \\ \frac{dx_i}{dt} &= \left(\mu_i(s) - D_i\right) x_i, \qquad\qquad i = 1, \ldots, n, \end{aligned} \tag{1.2}$$

where x_i is the concentration of the i^{th} species, μ_i is the growth function and D_i represents the disappearance rate of bacteria i, which can be modeled by:

$$D_i = \alpha_i D + a_i,$$

where α_i represents the bacteria proportion that leaves the reactor, and a_i represents the mortality rate of species i.

The mathematical analysis of the competition model of two or more species for a limiting resource can be found in [25, 28, 56]. Using same dilution rates $D = D_i$ and monotonic growth rates, the classical result well-known as the Competitive Exclusion Principle (CEP) is shown, in a generic case, where the microorganism that has the lowest breakeven concentration of substrate outweighs the competition on all other species. Other approaches have been expanded in the literature: a model with the input microorganism concentrations at the chemostat [25, 48]. For example, when bioreactors for the treatment of wastewater with waters to be treated obviously contain all kinds of bacteria. In [25], the authors studied the case of n different species consuming a single substrate in a chemostat with $D = D_i$ and density-dependent growth rates.

1.2.3 Model with several species and multiple substrates in the chemostat

The general model of n species x_i competing for m resources s_j proposed in [36] is:

$$\begin{aligned} \frac{ds_j}{dt} &= D_j\left(s_j^{in} - s_j\right) - \sum_{i=1}^{n} \frac{\mu_{i,j}(S)}{\gamma_{i,j}} x_i, && j = 1\ldots, m, \\ \frac{dx_i}{dt} &= \left(\sum_{j=1}^{m} \mu_{i,j}(S) - D_i\right) x_i, && i = 1, \ldots, n, \end{aligned} \tag{1.3}$$

where $S = (s_1, \ldots, s_m)$, s_j is the concentration of the j^{th} substrates, x_i is the concentration of the i^{th} species, $s_j^{in} > 0$ is the j^{th} input substrate concentration.

In ecosystems, it is common to note that microorganisms occupying the same ecological niche feed on several limiting resources. Resources are defined as entities that stimulate population growth, at least over some range of availability, and which are consumed and include various forms of materials and energy. So it is necessary to introduce important distinctions between resources. Among the different classifications of limiting resources introduced in ecology, we will cite two classifications that are widely used in competition models: substitutable substrates and complementary or essential substrates. Two substrates are called substitutable if one can be replaced by the other. Two substrates are called complementary(essential) if they are both essential for growth (see [33, 59]). There was a lot of research, both experimental and theoretical, concerning the growth of microorganisms on substitutable resources (see [33, 38] and the references therein): the authors have shown that coexistence is possible. There are relatively few studies regarding growth on complementary resources (see [8, 9, 59]).

Several approaches have been proposed in the literature to analyze mathematically models of competition several species on multi-substrates, see for example [34, 36, 60], and more recent works [13, 50] where the authors considered competition models between two species for two resources. In [18, 40, 41, 51, 57, 64], the authors study model (1.3) restricted to three organisms and three substrates. This study has suggested the emergence of interesting dynamical behavior through its specific ecological interactions, which include competition, syntrophy, and product inhibition.

In this thesis, we do not consider this type of competition models.

1.3 Two-tiered models

A two-tiered models are commonly used to describe relationships between two bacterial populations. Several of these models have been proposed in the literature, see for example [4, 6, 11, 15, 45, 53, 58, 70]. They take the form of four-dimensional mathematical models with a cascade of two biological reactions where one substrate s_0 is consumed by one microorganism x_0 in a chemostat to produce a product s_1 that serves as the main limiting

substrate for a second microorganism x_1. This is represented by the following reaction scheme:

$$s_0 \xrightarrow{\mu_0} x_0 + s_1, \qquad\qquad s_1 \xrightarrow{\mu_1} x_1,$$

where μ_0 and μ_1 are the bacterial growth rates, depending eventually on one or both substrates. The substrate concentrations s_0 and s_1 are introduced in the chemostat with the input concentrations s_0^{in} and s_1^{in}, respectively. The model for a two-tiered "food chain", can be written as the following dynamical system of ODEs:

$$\begin{cases} \dot{s}_0 &= D\left(s_0^{\text{in}} - s_0\right) - \mu_0\left(.\right) x_0 \\ \dot{x}_0 &= [\mu_0\left(.\right) - \alpha_0 D - a_0] x_0 \\ \dot{s}_1 &= D\left(s_1^{\text{in}} - s_1\right) + \mu_0\left(.\right) x_0 - \mu_1\left(.\right) x_1 \\ \dot{x}_1 &= [\mu_1\left(.\right) - \alpha_1 D - a_1] x_1 \end{cases} \tag{1.4}$$

where D is a dilution rate. α_0 and α_1 are coefficients that belong to $[0, 1]$, with $a_0 x_0$ and $a_1 x_1$ are the maintenance (decay) terms, a_0 and a_1 are positive parameters.

If the growth rate μ_0 depends only on substrate s_0 and μ_1 depends only on s_1, that is, $\mu_0(.) = \mu_0(s_0)$, $\mu_1(.) = \mu_1(s_1)$, then the system describes a commensalism relationship. The system has a cascade structure and the number of steady states and their stability as functions of model inputs and parameters have be investigated, [4, 5, 47, 53, 55, 58]. An important contribution to the modeling of a two-tiered as a commensalism system is the model of [5]. If μ_0 depends on both substrates s_0 and s_1, and μ_1 depends on substrate s_1, that is, $\mu_0(.) = \mu_0(s_0, s_1)$, $\mu_1(.) = \mu_1(s_1)$, then the system describes a syntrophic relationship. The mathematical analysis of such two-tiered models is more delicate than for commensalism models (see [23] and the references therein).

In [23], the authors have studied a two-tiered microbial food chain, by analyzing the joined effects of syntrophy, mortality, substrate inhibition and input concentrations. Using a general class of growth rates, the operating diagrams illustrate the effects of inhibition and the new input substrate concentration on the reduction of the coexistence region and the emergence of a bi-stability region. They proved that for a large class of models and despite the additional complication of substrate inhibition and distinct removal rates, the maintenance cannot destabilize a two-tiered microbial 'food chain', regardless of the biological parameters.

The two-tiered models may involve several relationships between species, such as competition, commensalism, mutualism, and syntrophy, and may include, maintenance (or decay) terms, which we will detail in the following subsections.

1.3.1 Competition

The competition is a natural biological interaction between two or more organisms or species in which all species are damaged. Competition means a mutually negative interaction between populations. There are two types of competition: the interaction is said to be intraspecific competition when the two microorganisms are of the same

species, while competition between individuals of different species is known as interspecific competition. This interaction can be represented schematically by:

$$x_0 \longleftarrow s_0 \longrightarrow x_1.$$
$$\nwarrow s_1 \nearrow$$

According to the scheme above, this interaction can be mathematically formalized as follows: both species denoted x_0 and x_1 grow on two substrates s_0 and s_1.

The chemostat model predicts that the coexistence of two or more microbial populations competing for a single non-reproducing nutrient is not possible, in the generic case. Only the species with the lowest 'break-even' concentration survives. This result, known as the Competitive Exclusion Principle (CEP), has a long history in the literature of bio-mathematics, [46] and the references therein. Several mathematical models in the literature with competition relationship have been considered, see for instance [1, 19, 20, 22, 30, 56].

In [1], the authors have considered a model with several species in competition for a single resource, they have taken into account the intra-specific interactions. Using a growth rates are increasing and the dilution rates are distinct, the operating diagram illustrates the effect of the intra-specific competition on the coexistence region of the species. In [22], the authors have studied the model of two species competing for a single resource in the chemostat, by taking into account the inter- and intraspecific interactions. The growth functions are monotonic and the dilution rates are distinct. They gave the results of global asymptotic stability for the competition model of two species. The operating diagrams describe the effect of the intra- and interspecific interference on the disappearance of coexistence region and the occurrence of bi-stability region.

1.3.2 Commensalism

The commensalism is a natural biological phenomenon between two living beings. In biology, commensalism means a lasting interaction between individuals of different species where one of the partners derives a benefit from the association while the other finds neither advantage nor real inconvenience. If the host and the commensal populations are indicated by x_0 and x_1, respectively, then the interaction of commensalism can be represented schematically by:

$$s_0 \longrightarrow x_0 \longrightarrow s_1 \longrightarrow x_1.$$

According to the scheme above, the primary substrate s_0 is utilized by the host population x_0, with the simultaneous production of the secondary substrate s_1 which is further consumed by the commensal population x_1 for growth.

There are several examples of mixed cultures of commensal populations [4, 5, 47, 53, 58]. The first of the above cultures have been proposed in [47] for the direct conversion of

cellulosic and hemicellulosic biomass to ethanol. In this paper, the authors have given a mathematical study of a commensalism type model (1.4), where they considered two substrates and two species, with $a_0 = a_1 = 0$ and $\alpha_0 = \alpha_1 = 1$.

1.3.3 Mutualism

The mutualism is a natural biological phenomenon occurring between two or more organisms (or populations) that belong to different species, in which the organisms both benefit from this relationship. During this interaction, there is an interplay benefit (it is not therefore commensalism). Similar actions that occur between individuals of the same species are called cooperation, that is, two organisms mutually cooperate to produce the necessary substrate for the growth of the other type.

If two populations of bacteria are indicated by x_0 and x_1, respectively, then, this interaction can be represented schematically by:

$$x_0 \longrightarrow s_1 \longrightarrow x_1.$$
$$\nwarrow s_0 \swarrow$$

According to the scheme above, this reaction can be mathematically formalized as follows: the first species denoted x_0 grows on a substrate s_0 forming an intermediate product s_1. This intermediate product is necessary for the growth of a second species x_1. Producing substrate s_0 as product which is necessary for the growth of x_0, so the second species x_1 can not develop if the first species x_0 is not present and the first species x_0 can not develop if the second species x_1 is not present.

There are several models in the literature with mutualism relationship, see for instance [2, 16, 61, 66, 72]. In [61], the authors have studied the dynamics of two interacting microbial species in the chemostat. Both species compete for a common resource, while also being mutualists through cross-feeding. They derived an extended Lotka-Volterra model, which has a quadratic term modeling the competition, while the typical linear term describes the mutualistic interaction. They showed that bistability occurs when the mutual dependence on the cross-feeding nutrients is sufficiently high.

1.3.4 Syntrophy

The syntrophy is a biological phenomenon that allows two or more bacteria to multiply in an environment that the necessary growth factors are missing for one of them. A syntrophic relationship is a biological relationship of necessity between bacterial species that can not develop separately.

If two populations of bacteria are indicated by x_0 and x_1, respectively, then, the interaction of syntrophy can be represented schematically by:

$$s_0 \longrightarrow x_0 + s_1, \qquad s_1 \longrightarrow x_1.$$

According to the scheme above, the first species denoted x_0 grows on a substrate s_0 forming an intermediate product s_1. This intermediate product is necessary for the growth of a second species x_1. Then, the second species x_1 can not grow if the first species x_0 is not present, it is a relation of trophic interest.

A syntrophic relationship between two organisms refers to growth functions where μ_0 depends on both substrates s_0 and s_1 and μ_1 depends only on s_1, i.e $\mu_0(.) = \mu_0(s_0, s_1)$ et $\mu_1(.) = \mu_1(s_1)$. There are several models in the literature describing a syntrophic relationship, see for instance [17, 31, 32, 52, 62, 69, 71]. In [69], the authors have studied the interactions of a growing bacterial population on methane. The important results of this study focused on the conditions under which a stable coexistence equilibrium could occur. In [31], the authors have studied model (1.4) for syntrophic associations between H_2-producing acetogenic bacteria and H_2-utilizing bacteria, they have considered the growth functions μ_0 and μ_1 of Monod-type in s_0 and the function μ_0 is decreasing in s_1, $a_0 = a_1 = 0$ and $\alpha_0 = \alpha_1 = 1$, with the absence of an input term of s_1 ($s_1^{in} = 0$). An extension of this work studied in [32], which considers the case where s_0 also appears in μ_1, ($\mu_1(.) = \mu_1(s_0, s_1)$). The authors have showed a bistability behavior that can not be observed when $\mu_1(.)$ depends only on s_0. In [52], the authors considered the general situation of a growth function $\mu_1(.) = \mu_1(s_0, s_1)$, which increases in s_1 and decreases in s_0 with $s_1^{in} = 0$ and have shown, contrary to the case where $\mu_1(.)$ only depends on s_1, that a multiplicity of positive equilibria can occur. Other models for which $\mu_0(.) = \mu_0(s_0, s_1)$ and $\mu_1(.) = \mu_1(s_0, s_1)$, present the multiplicity of positive equilibria, are found in [62]. All these studies do not take into account the terms of maintenance. In [13], using a general class of growth rates, the authors have analyzed the joined effects of syntrophy, mortality, and new input concentrations. The operating diagram shows that, whatever the region of space considered, there exists only one locally exponentially stable steady state.

1.3.5 The effects of decay

As explained in [50], maintenance is the consumption of energy by an organism that is used for all biological processes other than growth. It is modeled either by adding a negative term on the substrate dynamic without associating it to growth or by considering a decay term on the biomass dynamics. For more information about the modeling of maintenance, [39].

Several works have focused on the effect of maintenance (mortality) on the behavior of the system, see for instance [13, 21, 50, 68, 71]. A previous study investigated the effect of maintenance on the stability of a model comprising two species and two substrates [71]. In this work, the authors were the first to consider the effects of maintenance terms in the system (1.4), in particular, in the case where the growth functions are of the form ($\mu_0(.) = \mu_0(s_0, s_1), \mu_1(.) = \mu_1(s_1)$), where μ_0 is increasing in s_0 and decreasing in s_1 and the Monod function for μ_1, and ($a_0 > 0, a_1 > 0$), and $s_1^{in} = 0$ and $\alpha_0 = \alpha_1 = 1$. The authors asserted the possibility of the Hopf bifurcation of the positive steady state in the

case with maintenance.

In [50], the authors have generalized [71] by allowing a larger class of growth functions and they have generalized [17] by taking account the maintenance terms, in particular, in the case where μ_1 is increasing in s_1 with $\alpha_0 = \alpha_1 = 1$ and $s_1^{in} = 0$. They proved that the positive steady state is stable as long as it exists, that is to say, maintenance does not affect the stability of the considered two-tiered microbial 'food chain'. Important and interesting extensions of the two-tiered models are the eight-dimensional mathematical models, which include syntrophy and inhibition [67, 68], and the model with five state variables studied in [7, 17].

1.4 Anaerobic digestion

Introducing an additional microorganism and substrate to the two-tiered model of [71] leads to a three-tiered model describing the chlorophenol mineralization, [64]. This model is considered in the next chapters. This mineralization may occur under aerobic (in presence of oxygen) or anaerobic (in absence of oxygen) conditions. The anaerobic process is called anaerobic digestion or methanisation which is a natural biological process of decomposition of organic matter by microorganisms (bacteria) that are activated under anaerobic conditions. On an industrial scale, this process takes place in a closed bioreactor, to produce biogas rich in methane and some carbon dioxide. This biogas is a source of energy that can be used directly to replace natural gas. This natural process is used mainly for the depollution of wastewater or for converting surplus sludge produced in wastewater treatment plants into more stable products [29], it also makes it possible to treat waste while recovering a renewable energy source.

Under the action of microbial populations, the organic matter converts into biogas through a sequence of stages. Indeed, the process of anaerobic digestion takes place through four stages:

- The first stage is *hydrolysis* which is very important for the anaerobic digestion process since in this phase the organic macromolecules (cellulose, polysaccharides, protein, lipids,...) converts into monomer (sugars, amino acids, fatty acids,...). This step is limiting in the case of anaerobic digestion of insoluble complex substrates.

- In the second stage *acidogenesis*, acidogenic bacteria transforms the products of the previous phase into carbon dioxide, hydrogen, organic acids, alcohols. Acetic acid is a volatile fatty acid.

- The third stage is *acetogenesis* and allows to convert the molecules that result from the second stage into carbon dioxide. But their activity is inhibited by an excess of hydrogen in the medium.

- The final step *methanogenesis* (methane formation) is the anaerobic degradation of organic matter. The microorganisms that perform this step are hydrogenophilic methanogenesis bacteria which convert carbon dioxide to methane with the help of hydrogen and

acetoclate methanogenesis bacteria convert acetate to methane.

The complexity of the anaerobic digestion process has motivated the development of complex models. Several models of anaerobic digestion exist in the literature, see [7, 10, 29, 65, 67, 68], such as the widely used Anaerobic Digestion Model No.1 (ADM1) [29]. In engineered biological systems, mechanistic modeling reached consensus with the development of the Activated Sludge Models [26, 27], for wastewater treatment processes, followed by the Anaerobic Digestion Model No.1, a few years later. The development of ADM1 was enabled largely due to the possibilities for better identification and characterization of functional microbial groups responsible for the chemical transformations within anaerobic digesters. The full (ADM1) model is highly parameterized with a large number of physical, chemical and biological processes described by 32 state variables and numerous algebraic expressions. Whilst suitable for dynamic simulation, a more rigorous mathematical analysis and the control of the model are very difficult which were made on sub-models or reduced models of this model. To the author's knowledge, only numerical investigations of the full model are available in [7]. Due to the analytical intractability of the full (ADM1), simpler mechanistic models of microbial interaction have been proposed in view of a better understanding of the anaerobic digestion process. For a recent review of mathematical modeling of anaerobic digestion, the reader is referred to [65].

1.5 Conclusion

In this first chapter, we gave an overview of some mathematical models of the chemostat. First, we presented the chemostat and its minimal model and exposed some extensions of this minimal model. We then recalled the two-tiered models, treated in the literature. Finally, we described anaerobic digestion and its different phases.

In the next chapters, we will study the extensions of [71], by introducing an additional microorganism and substrate to create a three-tiered feeding chain model, considered in [64]. In chapter 2, we begin by listing all the possible steady states of the system, followed by conditions for their existence and uniqueness. The local stability and the bifurcation diagrams of the model in both cases without and with maintenance terms are presented in chapter 3 and chapter 4. In final in chapter 5, we perform the operating diagrams for showing the asymptotic behaviors of this model.

CHAPTER 2

Three-tiered microbial food-web model

Summary

2.1 Introduction

In this chapter, we study a three-tiered microbial food-web model of the anaerobic digestion in the chemostat, involving three species and three resources, with three input substrates, including the terms of maintenance and inhibition of the third substrate on the first species. The model is a six-dimensional system of ordinary differential equations. This model has recently been proposed and investigated numerically in [64]. Then, by considering the case of a large class of growth rates, we generalize and extend these analytical studies.

This chapter is organized as follows. In section 2.2, we start by presenting the mathematical model of the three-tiered microbial species from [64], which takes into account the phenol and the hydrogen inflowing concentrations as well as the maintenance terms. Next, in section 2.3, we give the general assumptions on the microbial growth functions and we give a preliminary result on positivity and boundedness of solutions, we then describe the steady states of the model and determine the necessary and sufficient conditions of existence of these steady states in the case with maintenance.

2.2 Three-tiered food-web model

The mathematical model developed in [64], by introducing an additional microorganism and substrate into a two-tiered feeding chain model in previous work [71], has six components, three substrate (chlorophenol, phenol and hydrogen) and three organisms (chlorophenol-dechlorinating bacterium, the phenol degrader and the hydrogenotrophic methanogen) variables. As explained in [64], the chlorophenol degrader utilizes both chlorophenol and hydrogen for growth, producing phenol as a product. Phenol is consumed by the phenol degrader forming hydrogen, which also is inhibitory to its growth. The hydrogenotrophic methanogen scavenges this hydrogen and acts as the primary syntroph, as shown in a schematic representation in Figure 2.1. This form of the interaction between microorganisms is called a food-web, that is, an interconnection of food chains, see [44].

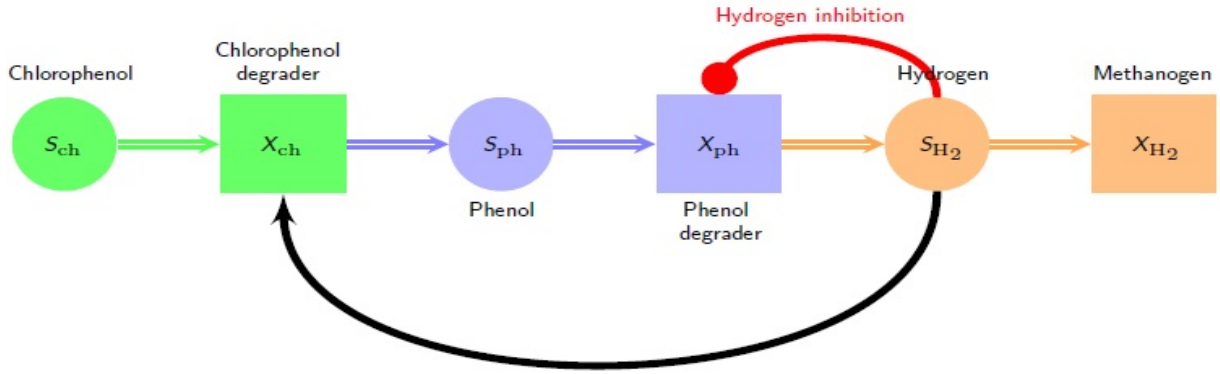

Figure 2.1: The three-tiered chlorophenol mineralizing food-web.

Following [51, 64], the three-step model that we propose to study is:

$$\begin{cases} \dot{X}_{\text{ch}} = (Y_{\text{ch}} f_0\left(S_{\text{ch}}, S_{\text{H}_2}\right) - D - k_{\text{dec,ch}}) X_{\text{ch}} \\ \dot{X}_{\text{ph}} = (Y_{\text{ph}} f_1\left(S_{\text{ph}}, S_{\text{H}_2}\right) - D - k_{\text{dec,ph}}) X_{\text{ph}} \\ \dot{X}_{\text{H}_2} = (Y_{\text{H}_2} f_2\left(S_{\text{H}_2}\right) - D - k_{\text{dec,H}_2}) X_{\text{H}_2} \\ \dot{S}_{\text{ch}} = D\left(S_{\text{ch}}^{\text{in}} - S_{\text{ch}}\right) - f_0\left(S_{\text{ch}}, S_{\text{H}_2}\right) X_{\text{ch}} \\ \dot{S}_{\text{ph}} = D\left(S_{\text{ph}}^{\text{in}} - S_{\text{ph}}\right) + \frac{224}{208}\left(1 - Y_{\text{ch}}\right) f_0\left(S_{\text{ch}}, S_{\text{H}_2}\right) X_{\text{ch}} - f_1\left(S_{\text{ph}}, S_{\text{H}_2}\right) X_{\text{ph}} \\ \dot{S}_{\text{H}_2} = D\left(S_{\text{H}_2}^{\text{in}} - S_{\text{H}_2}\right) - \frac{16}{208} f_0\left(S_{\text{ch}}, S_{\text{H}_2}\right) X_{\text{ch}} + \frac{32}{224}\left(1 - Y_{\text{ph}}\right) f_1\left(S_{\text{ph}}, S_{\text{H}_2}\right) X_{\text{ph}} \\ \qquad - f_2\left(S_{\text{H}_2}\right) X_{\text{H}_2}, \end{cases} \tag{2.1}$$

where X_{ch}, X_{ph} and X_{H_2} denote, respectively, the chlorophenol, phenol and hydrogen degrader concentrations; S_{ch}, S_{ph} and S_{H_2} are the chlorophenol, phenol and hydrogen substrates concentrations; $S_{\text{ch}}^{\text{in}}$, $S_{\text{ph}}^{\text{in}}$ and $S_{\text{H}_2}^{\text{in}}$ are the substrate concentrations in the feed bottle; $k_{\text{dec,ch}}$, $k_{\text{dec,ph}}$ and $k_{\text{dec,H}_2}$ represent the decay rates; D is the dilution rate of the chemostat; Y_{ch}, Y_{ph} and Y_{H_2} are the yield coefficients. $224/208\,(1 - Y_{\text{ch}})$ is the fraction of chlorophenol converted to phenol; $32/224\,(1 - Y_{\text{ph}})$ is the fraction of phenol that is transformed to hydrogen and $16/208$ is the fraction of hydrogen consumed by the chlorophenol degrader X_{ch}. The functions f_0, f_1 and f_2, are the following specific growth rates that take the form:

$$\begin{aligned} f_0\left(S_{\text{ch}}, S_{\text{H}_2}\right) &= \frac{k_{m,\text{ch}} S_{\text{ch}}}{K_{S,\text{ch}} + S_{\text{ch}}} \frac{S_{\text{H}_2}}{K_{S,\text{H}_2,\text{c}} + S_{\text{H}_2}}, \\ f_1\left(S_{\text{ph}}, S_{\text{H}_2}\right) &= \frac{k_{m,\text{ph}} S_{\text{ph}}}{K_{S,\text{ph}} + S_{\text{ph}}} \frac{1}{1 + S_{\text{H}_2}/K_{I,\text{H}_2}}, \quad f_2\left(S_{\text{H}_2}\right) = \frac{k_{m,\text{H}_2} S_{\text{H}_2}}{K_{S,\text{H}_2} + S_{\text{H}_2}}, \end{aligned} \tag{2.2}$$

where $k_{m,\text{i}}$ for $i = \{\text{ch}, \text{ph}, \text{H}_2\}$ are the maximum specific growth rates related to the chlorophenol, phenol, and hydrogen degraders, respectively. $K_{S,\text{i}}$ are the half-saturation coefficients, respectively, for each organism. $K_{S,\text{H}_2,\text{c}}$ is the half-saturation constant for hydrogen in the chlorophenol degrader. K_{I,H_2} is the inhibition term, and $1/(1+S_{\text{H}_2}/K_{I,\text{H}_2})$ represents the inhibition of phenol degrader by the hydrogen.

Several authors have studied this three-tiered model (2.1), see recent works [18, 40, 41, 51, 57, 64]. In [64] most of the results on the existence and stability of steady states of model (2.1) were obtained only numerically, using specific growth rates given in (2.2). They have numerically performed several operating diagrams with respect to the four operating parameters, showing the role, and the importance of each control parameter. Recently, a rigorous mathematical analysis of this model (2.1) was done in [51] with general growth rates but only the chlorophenol inflowing concentration has been taken into account. In this work, the authors show that the system can have at most three types of steady states when $S_{\text{ch}}^{\text{in}} > 0$ and $S_{\text{ph}}^{\text{in}} = S_{\text{H}_2}^{\text{in}} = 0$: the washout steady state, a coexistence steady state of three species and a steady state where only the hydrogen degrader is extinct. The local stability analysis is achieved when the maintenance is excluded from the model, where this six-dimensional model is reduced to a three-dimensional one. A numerical evidence shows that, when maintenance is included, the positive steady state can destabilize through a supercritical Hopf bifurcation with the appearance of a stable periodic orbit [51] which was not depicted in [64]. In [57], the authors have considered the three-tiered model in the case without maintenance and persistence results were analytically proved. Using numerical estimation, it is shown in [57] that the system has a rich dynamics including Hopf, Bogdanov-Takens and Bautin bifurcations. In [18], the three-tiered model of [64] was studied by neglecting the part of hydrogen produced by the phenol degrader as well as maintenance terms, which gives rise to a less realistic model. However, the existence and stability of steady states were analytically studied and a global analysis is performed, proving the asymptotic persistence of the three bacteria. We extende here the results of [51], by considering the three inflowing concentrations ($S_{\text{ch}}^{\text{in}} \geq 0$, $S_{\text{ph}}^{\text{in}} \geq 0$ and $S_{\text{H}_2}^{\text{in}} \geq 0$). We analytically determine the necessary and sufficient conditions of the existence of the steady states in the case with maintenance, for a large class of growth rates, instead of specific kinetics, as in [64].

2.3 Analysis of the model

We use the following simplified notations in (2.1), as given in [51].

$$X_0 = X_{\text{ch}}, \quad X_1 = X_{\text{ph}}, \quad X_2 = X_{\text{H}_2}, \quad S_0 = S_{\text{ch}}, \quad S_1 = S_{\text{ph}}, \quad S_2 = S_{\text{H}_2}. \tag{2.3}$$

The inflowing concentrations are given by:

$$S_0^{\text{in}} = S_{\text{ch}}^{\text{in}}, \quad S_1^{\text{in}} = S_{\text{ph}}^{\text{in}}, \quad S_2^{\text{in}} = S_{\text{H}_2}^{\text{in}}, \tag{2.4}$$

the death rates are $a_0 = k_{\text{dec,ch}}$, $a_1 = k_{\text{dec,ph}}$, $a_2 = k_{\text{dec,H}_2}$ (with units d^{-1}), and the yield coefficients are

$$Y_0 = Y_{\text{ch}}, \quad Y_1 = Y_{\text{ph}}, \quad Y_2 = Y_{\text{H}_2}, \quad Y_3 = \frac{224}{208}(1 - Y_0), \quad Y_4 = \frac{32}{224}(1 - Y_1).$$

With these notations, (2.1) can be written as follows:

$$\begin{cases} \dot{X}_0 = -DX_0 + Y_0 f_0(S_0, S_2) X_0 - a_0 X_0 \\ \dot{X}_1 = -DX_1 + Y_1 f_1(S_1, S_2) X_1 - a_1 X_1 \\ \dot{X}_2 = -DX_2 + Y_2 f_2(S_2) X_2 - a_2 X_2 \\ \dot{S}_0 = D\left(S_0^{\text{in}} - S_0\right) - f_0(S_0, S_2) X_0 \\ \dot{S}_1 = D\left(S_1^{\text{in}} - S_1\right) + Y_3 f_0(S_0, S_2) X_0 - f_1(S_1, S_2) X_1 \\ \dot{S}_2 = D\left(S_2^{\text{in}} - S_2\right) + Y_4 f_1(S_1, S_2) X_1 - Y_5 f_0(S_0, S_2) X_0 - f_2(S_2) X_2. \end{cases} \tag{2.5}$$

To reduce the number of yield parameters and ease the mathematical analysis, we can rescale system (2.5) using the following change of variables proposed in [50, 51]:

$$x_0 = \frac{Y}{Y_0} X_0, \quad x_1 = \frac{Y_4}{Y_1} X_1, \quad x_2 = \frac{1}{Y_2} X_2, \quad s_0 = Y S_0, \quad s_1 = Y_4 S_1, \quad s_2 = S_2, \tag{2.6}$$

where $Y = Y_3 Y_4$, with

$$\omega = \frac{16}{208Y} = \frac{1}{2(1 - Y_0)(1 - Y_1)},$$

which is a positive constant.

$$s_0^{\text{in}} = Y S_0^{\text{in}}, \quad s_1^{\text{in}} = Y_4 S_1^{\text{in}}, \quad s_2^{\text{in}} = S_2^{\text{in}}. \tag{2.7}$$

We obtain the following system:

$$\begin{cases} \dot{x}_0 &= (\mu_0(s_0, s_2) - D - a_0) x_0 \\ \dot{x}_1 &= (\mu_1(s_1, s_2) - D - a_1) x_1 \\ \dot{x}_2 &= (\mu_2(s_2) - D - a_2) x_2 \\ \dot{s}_0 &= D\left(s_0^{\text{in}} - s_0\right) - \mu_0(s_0, s_2) x_0 \\ \dot{s}_1 &= D\left(s_1^{\text{in}} - s_1\right) + \mu_0(s_0, s_2) x_0 - \mu_1(s_1, s_2) x_1 \\ \dot{s}_2 &= D\left(s_2^{\text{in}} - s_2\right) - \omega \mu_0(s_0, s_2) x_0 + \mu_1(s_1, s_2) x_1 - \mu_2(s_2) x_2, \end{cases} \tag{2.8}$$

where s_i, $i = 0, 1, 2$ are the three substrates concentrations (chlorophenol, phenol and hydrogen, in the application); x_i are the three microbial species concentrations; μ_i are the specific growth rates given by (2.9), usually take the form of a double Monod, a Monod with hydrogen inhibition acting on the phenol degrader and represented in μ_1 (see (2.9)), and a Monod kinetics, respectively; s_i^{in} is the input substrate concentration in the chemostat; a_i are the maintenance (or decay) rate for $i = 0, 1, 2$ and corresponding to chlorophenol, phenol and hydrogen, respectively. All the yield coefficients in (2.5) are normalized to one except of ω.

The specific growth functions (2.2) become the following functions satisfying Hypotheses **H1** to **H8**:

$$\mu_0(s_0, s_2) = Y_0 f_0\left(\frac{s_0}{Y}, s_2\right), \quad \mu_1(s_1, s_2) = Y_1 f_1\left(\frac{s_1}{Y_4}, s_2\right), \quad \mu_2(s_2) = Y_2 f_2(s_2).$$

Therefore, the growth functions take the form:

$$\mu_0(s_0, s_2) = \frac{m_0 s_0}{K_0 + s_0}\frac{s_2}{L_0 + s_2},\ \mu_1(s_1, s_2) = \frac{m_1 s_1}{K_1 + s_1}\frac{1}{1 + s_2/K_I},\ \mu_2(s_2) = \frac{m_2 s_2}{K_2 + s_2}, \quad (2.9)$$

where

$$m_0 = Y_0 k_{m,\mathrm{ch}}, \quad K_0 = Y K_{S,\mathrm{ch}}, \quad L_0 = K_{S,\mathrm{H_2,c}}, \quad m_1 = Y_4 k_{m,\mathrm{ph}},$$
$$K_1 = Y_4 K_{S,\mathrm{ph}}, \quad K_I = K_{I,\mathrm{H_2}}, \quad m_2 = Y_2 k_{m,\mathrm{H_2}}, \quad K_2 = K_{S,\mathrm{H_2}}.$$

2.3.1 Assumptions and preliminary result

In this work, we consider a large class of growth rates. Following [50], we assume that the bacterial growth functions are continuously differentiable ($\mathcal{C}^1$) and satisfy the following conditions:

H1 For all $s_0 > 0$ and $s_2 > 0$, it exists $m_0 > 0$, such that $0 < \mu_0(s_0, s_2) \leq m_0 < +\infty$ and $\mu_0(0, s_2) = 0$, $\mu_0(s_0, 0) = 0$.

H2 For all $s_1 > 0$ and $s_2 \geq 0$, it exists $m_1 > 0$, such that $0 < \mu_1(s_1, s_2) \leq m_1 < +\infty$ and $\mu_1(0, s_2) = 0$.

H3 For all $s_2 > 0$, it exists $m_2 > 0$, such that $0 < \mu_2(s_2) \leq m_2 < +\infty$, $\mu_2(0) = 0$.

H4 For all $s_0 > 0$ and $s_2 > 0$, $\dfrac{\partial \mu_0}{\partial s_0}(s_0, s_2) > 0, \quad \dfrac{\partial \mu_0}{\partial s_2}(s_0, s_2) > 0.$

H5 For all $s_1 > 0$ and $s_2 > 0$, $\dfrac{\partial \mu_1}{\partial s_1}(s_1, s_2) > 0, \quad \dfrac{\partial \mu_1}{\partial s_2}(s_1, s_2) < 0.$

H6 For all $s_2 > 0$, $\dfrac{d\mu_2}{ds_2}(s_2) > 0.$

H7 The function $s_2 \mapsto \mu_0(+\infty, s_2)$ is monotonically increasing and the function $s_2 \mapsto \mu_1(+\infty, s_2)$ is monotonically decreasing.

Hypothesis **H1** means that the function μ_0 is uniformly bounded, and that no growth can occur for species x_0 without substrates s_0 and s_2. Hypothesis **H2** means that there is a uniform bound for μ_1, and that no growth can occur for species x_1 without substrate s_1. Hypothesis **H3** means that the function μ_2 is uniformly bounded, and that the production of s_2 is necessary for the growth of the species x_2. Hypothesis **H4** means that the growth rate of species x_0 increases with substrates s_0 and s_2. Hypothesis **H5** means that the growth rate of the species x_1 increases with the substrate s_1 but is auto-inhibited by the production of s_2. Hypothesis **H6** means that the growth rate of species x_2 increases with substrate s_2. Hypothesis **H7** means that the maximum growth rate of the species x_0 and x_1 increase and decreases, respectively, with the concentration of substrate s_2.

Firstly, we give the next result on the solutions of model (2.8), where we prove that they are non-negative and bounded, which is a prerequisite for any reasonable model of the chemostat.

Proposition 2.1. *For any non-negative initial conditions, all solutions of system (2.8) are bounded and remain non-negative for all $t > 0$. Moreover, the set*

$$\Omega = \left\{(x_0, x_1, x_2, s_0, s_1, s_2) \in \mathbb{R}^6_+ : Z = \omega x_0 + x_1 + x_2 + 2s_0 + 2s_1 + s_2 \leq 2s_0^{\text{in}} + 2s_1^{\text{in}} + s_2^{\text{in}}\right\}$$

is positively invariant and is a global attractor for the dynamics (2.8).

Proof. Since the vector field defined by (2.8) is $\mathcal{C}^1$, the uniqueness of solution to initial value problems holds. From (2.8), for $i = 0, 1, 2$,

$$x_i(\tau) = 0, \quad \text{for any} \quad \tau \geqslant 0 \quad \Rightarrow \quad \dot{x}_i(\tau) = 0.$$

If $x_i(0) = 0$, then $x_i(t) = 0$ for all t since the boundary face where $x_i \equiv 0$ is invariant in the vector field $\mathcal{C}^1$ by system (2.8). If $x_i(0) > 0$, then $x_i(t) > 0$ for all t since $x_i \equiv 0$ cannot be reached in finite time by trajectories such that $x_i(0) > 0$ by the uniqueness of solutions. On the other hand, one has

$$\begin{aligned}
&s_0(\tau) = 0, \ \text{for any} \ \tau \geqslant 0 \quad \Rightarrow \quad \dot{s}_0(\tau) = Ds_0^{\text{in}} \\
&s_1(\tau) = 0, \ \text{for any} \ \tau \geqslant 0 \quad \Rightarrow \quad \dot{s}_1(\tau) = Ds_1^{\text{in}} + \mu_0(s_0(\tau), s_2(\tau))x_0(\tau) \\
&s_2(\tau) = 0, \ \text{for any} \ \tau \geqslant 0 \quad \Rightarrow \quad \dot{s}_2(\tau) = Ds_2^{\text{in}} + \mu_1(s_1(\tau), 0)x_1(\tau).
\end{aligned}$$

Similarly to case x_i, if $\dot{s}_i(\tau) = 0$, then $s_i(t) \geqslant 0$ for all t. In addition, if $\dot{s}_i(\tau) > 0$, then $s_i(t) \geqslant 0$ for all t. Indeed, for example, consider the case of s_0 where D and s_0^{in} are positive with $s_0(0) \geqslant 0$. Assume that it exists $\tau > 0$ such that $s_0(\tau) = 0$ and $s_0(t) > 0$ for all $t \in (0, \tau)$. It follows that $\dot{s}_0(\tau) \leqslant 0$, which is the desired contradiction with $\dot{s}_0(\tau) = Ds_0^{\text{in}} > 0$.

Further, by considering $z = \omega x_0 + x_1 + x_2 + 2s_0 + 2s_1 + s_2$, we obtain from (2.8)

$$\dot{z} = D\left(2s_0^{\text{in}} + 2s_1^{\text{in}} + s_2^{\text{in}} - z\right) - \omega a_0 x_0 - a_1 x_1 - a_2 x_2 \leqslant D\left(2s_0^{\text{in}} + 2s_1^{\text{in}} + s_2^{\text{in}} - z\right).$$

Using Gronwall's lemma, we have

$$z(t) \leqslant 2s_0^{\text{in}} + 2s_1^{\text{in}} + s_2^{\text{in}} + \left(z(0) - \left(2s_0^{\text{in}} + 2s_1^{\text{in}} + s_2^{\text{in}}\right)\right)e^{-Dt}, \quad \text{for all} \quad t \geqslant 0. \tag{2.10}$$

Consequently,

$$z(t) \leqslant \max\left(z(0), 2s_0^{\text{in}} + 2s_1^{\text{in}} + s_2^{\text{in}}\right), \quad \text{for all} \quad t \geqslant 0. \tag{2.11}$$

Thus, the solutions of (2.8) are positively bounded and are defined for all $t \geqslant 0$. From (2.11), it can be deduced that the set Ω is positively invariant and from (2.10), it is a global attractor for (2.8).

□

2.3.2 Analysis of the steady states

A steady state of (2.8) is obtained by setting the right-hand sides equal to zero:

$$[\mu_0(s_0, s_2) - D - a_0]\, x_0 = 0 \tag{2.12}$$

$$[\mu_1(s_1, s_2) - D - a_1]\, x_1 = 0 \tag{2.13}$$

$$[\mu_2(s_2) - D - a_2]\, x_2 = 0 \tag{2.14}$$

$$D\left(s_0^{\text{in}} - s_0\right) - \mu_0(s_0, s_2)\, x_0 = 0 \tag{2.15}$$

$$D\left(s_1^{\text{in}} - s_1\right) + \mu_0(s_0, s_2)\, x_0 - \mu_1(s_1, s_2)\, x_1 = 0 \tag{2.16}$$

$$D\left(s_2^{\text{in}} - s_2\right) + \mu_1(s_1, s_2)\, x_1 - \omega\mu_0(s_0, s_2)\, x_0 - \mu_2(s_2)\, x_2 = 0. \tag{2.17}$$

A steady state exists (or is said to be 'meaningful') if and only if all its components are non-negative. This predicts eight possible steady states, that we denote by E_{ijk}, $i, j, k = 0$ or 1, with $i = 0$ if the species $x_0 = 0$, $j = 0$, if the species $x_1 = 0$ and $k = 0$ if the species $x_2 = 0$:

E_{000}, where $x_0 = 0$, $x_1 = 0$ and $x_2 = 0$: the washout steady state where all populations are extinct. This steady state always exists.

E_{001}, where $x_0 = 0$, $x_1 = 0$ and $x_2 > 0$: only the hydrogenotrophic methanogen population is maintained.

E_{100}, where $x_0 > 0$, $x_1 = 0$ and $x_2 = 0$: only the chlorophenol degraders are maintained.

E_{110}, where $x_0 > 0$, $x_1 > 0$ and $x_2 = 0$: the hydrogenotrophic methanogens are washed out.

E_{101}, where $x_0 > 0$, $x_1 = 0$ and $x_2 > 0$: only the phenol degraders are washed out.

E_{111}, where $x_0 > 0$, $x_1 > 0$ and $x_2 > 0$: all three populations are present.

E_{010}, where $x_0 = 0$, $x_1 > 0$ and $x_2 = 0$: only the phenol degraders are present.

E_{011}, where $x_0 = 0$, $x_1 > 0$ and $x_2 > 0$: only the chlorophenol degraders are washed out.

These steady states are denoted in [64], respectively, by SS1, SS2,..., SS8.

Notice that the steady states E_{001}, E_{100}, E_{101}, E_{010} and E_{011} do not exist in the case considered in [51]. In this particular case, only the steady states E_{000}, E_{110} and E_{111} exist, they were labeled in [51] by SS1, SS2 and SS3, respectively.

For the description of steady states, we need to define some auxiliary functions. The existence and definition domains of these functions are all relatively straightforward and can be found in [51].

Definition 2.1. *Let $M_0(y, s_2)$, $M_1(y, s_2)$, $M_2(y)$ and $M_3(s_0, z)$ be defined by:*

- *For $s_2 \geq 0$ and $0 \leq y < \mu_0(+\infty, s_2)$, $s_0 = M_0(y, s_2)$ is the unique solution of equation $\mu_0(s_0, s_2) = y$.*
- *For $s_2 \geq 0$ and $0 \leq y < \mu_1(+\infty, s_2)$, $s_1 = M_1(y, s_2)$ is the unique solution of equation $\mu_1(s_1, s_2) = y$.*
- *For $0 \leq y < \mu_2(+\infty)$, $s_2 = M_2(y)$ is the unique solution of equation $\mu_2(s_2) = y$.*
- *For $s_0 \geq 0$ and $0 \leq z < \mu_0(s_0, +\infty)$, $s_2 = M_3(s_0, z)$ is the unique solution of equation $\mu_0(s_0, s_2) = z$.*

Then, we have the next result.

Lemma 2.1. *Under assumptions* **H4**, **H5** *and* **H6**, *we have:*

- *For all $y \in [0, \mu_i(+\infty, s_2))$, $i = 0, 1$ and $s_2 \geq 0$: $\dfrac{\partial M_0}{\partial s_2}(y, s_2) < 0$, $\dfrac{\partial M_1}{\partial s_2}(y, s_2) > 0$.*
- *For all $y \in [0, \mu_i(+\infty, s_2))$, $i = 0, 1$ and $s_2 \geq 0$: $\dfrac{\partial M_0}{\partial y}(y, s_2) > 0$, $\dfrac{\partial M_1}{\partial y}(y, s_2) > 0$.*
- *For all $y \in [0, \mu_2(+\infty))$, we have: $\dfrac{dM_2}{dy}(y) > 0$.*
- *For all $z \in [0, \mu_0(s_0, +\infty))$ and $s_0 \geq 0$: $\dfrac{\partial M_3}{\partial z}(s_0, z) > 0$.*

Proof. According to the equivalence

$$s_i = M_i(y, s_2) \quad \Longleftrightarrow \quad y = \mu_i(s_i, s_2), \quad i = 0, 1,$$

we have, for all $y \in [0, \mu_i(+\infty, s_2))$ and $s_2 \geq 0$

$$\mu_i\left(M_i(y, s_2), s_2\right) = y. \tag{2.18}$$

The derivative of (2.18), with respect to s_2, implies that

$$\frac{\partial M_i}{\partial s_2}(y, s_2) = -\left[\frac{\partial \mu_i}{\partial s_2}(M_i(y, s_2), s_2)\right]\left[\frac{\partial \mu_i}{\partial s_i}(M_i(y, s_2), s_2)\right]^{-1}.$$

From **H4** and **H5**, it follows that,

$$\frac{\partial M_0}{\partial s_2}(y, s_2) < 0 \quad \text{and} \quad \frac{\partial M_1}{\partial s_2}(y, s_2) > 0.$$

On the other hand, the derivative of equation (2.18), with respect to y, implies that

$$\frac{\partial M_i}{\partial y}\left(y, s_2\right) = \left[\frac{\partial \mu_i}{\partial s_i}\left(M_i\left(y, s_2\right), s_2\right)\right]^{-1}.$$

From **H4** and **H5**, it follows that $\frac{\partial M_i}{\partial y}(y, s_2) > 0$, for $i = 0, 1$.

Next, from the equivalence:

$$s_2 = M_2(y) \quad \Longleftrightarrow \quad y = \mu_2(s_2),$$

we have, for all $y \in [0, \mu_2(+\infty))$

$$\mu_2(M_2(y)) = y. \tag{2.19}$$

Derivating (2.19), with respect to y and using **H6** implies that,

$$\frac{dM_2}{dy}(y) = \left[\frac{d\mu_2}{ds_2}(M_2(y))\right]^{-1} > 0.$$

Finally, according to the equivalence

$$s_2 = M_3(s_0, z) \quad \Longleftrightarrow \quad z = \mu_0(s_0, s_2),$$

we have, for all $z \in [0, \mu_0(s_0, +\infty))$ and $s_0 \geq 0$,

$$\mu_0(s_0, M_3(s_0, z)) = z. \tag{2.20}$$

Derivating (2.20), with respect to z and using **H4**, we obtain

$$\frac{\partial M_3}{\partial z}(s_0, z) = \left[\frac{\partial \mu_0}{\partial s_2}(s_0, M_3(s_0, z))\right]^{-1} > 0.$$

□

For $D \geq 0$ satisfying the conditions $D + a_0 < \mu_0(+\infty, +\infty)$ and $D + a_1 < \mu_1(+\infty, 0)$, there exist unique values $s_2^0 = s_2^0(D)$ and $s_2^1 = s_2^1(D)$ (see Figure 2.2), such that:

$$\mu_0\left(+\infty, s_2^0(D)\right) = D + a_0, \quad \mu_1\left(+\infty, s_2^1(D)\right) = D + a_1. \tag{2.21}$$

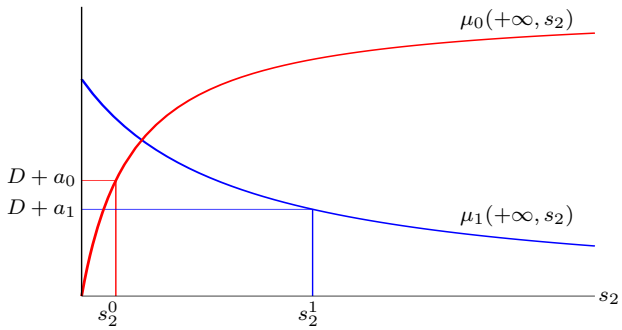

Figure 2.2: Existence conditions of s_2^0 and s_2^1.

Let I_1 and I_2 be the intervals defined by:

$$I_1 = \left\{D \geq 0 : \ s_2^0 < s_2^1\right\}, \quad I_2 = \left\{D \in I_1 : \ s_2^0 < M_2(D + a_2) < s_2^1\right\}. \tag{2.22}$$

Notice that I_1 is not empty, since for D small enough, s_2^0 is close to 0, while s_2^1 goes to $+\infty$ (see Figure 2.2 and Table 3.4 for the expressions of s_2^0 and s_2^1 as functions of D).

Using these notations, we consider the function Ψ defined for $s_2 \in (s_2^0, s_2^1)$ and $D \in I_1$ by:

$$\Psi(s_2, D) = (1-\omega)M_0(D + a_0, s_2) + M_1(D + a_1, s_2) + s_2. \tag{2.23}$$

Lemma 2.2. *The function Ψ satisfies the following properties:*

- *If $\omega < 1$, then, for all $D \in I_1$ the function $s_2 \mapsto \Psi(s_2, D)$ is positive and*

$$\lim_{s_2 \to s_2^0} \Psi(s_2, D) = +\infty, \quad \lim_{s_2 \to s_2^1} \Psi(s_2, D) = +\infty.$$

- *If $\omega = 1$, then, for all $D \in I_1$ the function $s_2 \mapsto \Psi(s_2, D)$ is positive, monotonically increasing and*

$$\Psi\left(s_2^0, D\right) > 0, \quad \lim_{s_2 \to s_2^1} \Psi(s_2, D) = +\infty.$$

- *If $\omega > 1$, then, for all $D \in I_1$ the function $s_2 \mapsto \Psi(s_2, D)$ is monotonically increasing and*

$$\lim_{s_2 \to s_2^0} \Psi(s_2, D) = -\infty, \quad \lim_{s_2 \to s_2^1} \Psi(s_2, D) = +\infty.$$

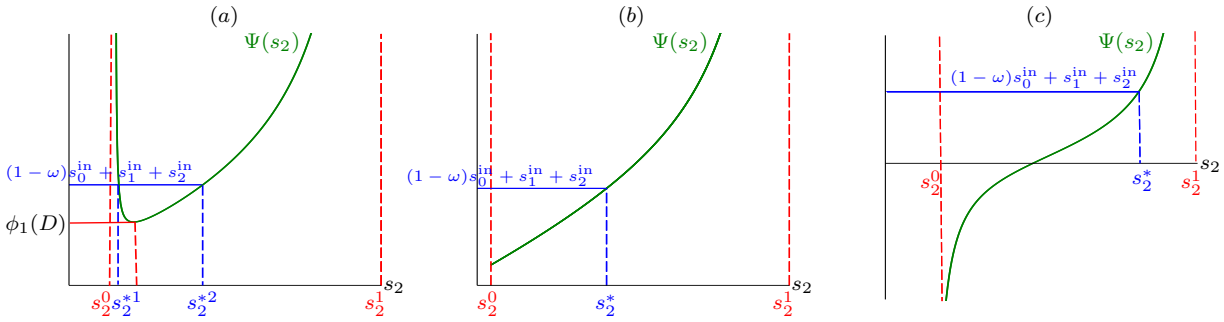

Figure 2.3: Graphical definition of Ψ: (a) case $\omega < 1$, (b) case $\omega = 1$, (c) case $\omega > 1$.

Proof. From (2.21), we have

$$M_0\left(D + a_0, s_2^0\right) = +\infty \quad \text{and} \quad M_1\left(D + a_1, s_2^1\right) = +\infty.$$

It follows that (see Figure 2.3):

$$\text{for all } \omega \geq 0, \text{ we have } \lim_{s_2 \to s_2^1} \Psi(s_2, D) = +\infty.$$

$$\text{for all } \omega > 1, \text{ we have } \lim_{s_2 \to s_2^0} \Psi(s_2, D) = -\infty.$$

$$\text{for all } \omega < 1, \text{ we have } \lim_{s_2 \to s_2^0} \Psi(s_2, D) = +\infty.$$

From Lemma 2.1, we have,

$$\frac{\partial \Psi}{\partial s_2}(s_2, D) = (1-\omega)\frac{\partial M_0}{\partial s_2}(D + a_0, s_2) + \frac{\partial M_1}{\partial s_2}(D + a_1, s_2) + 1 > 0, \quad \text{for } \omega \geq 1, \tag{2.24}$$

Therefore, for $\omega \geq 1$ the function $s_2 \mapsto \Psi(s_2, D)$ is monotonically increasing.

□

Following [51], we add a hypothesis on the function Ψ which then assures that there are at most two steady states of the form E_{110}.

H8 In the case $\omega < 1$, the function Ψ has a unique minimum $\overline{s}_2$ on the interval (s_2^0, s_2^1), such that $\dfrac{\partial \Psi}{\partial s_2}(s_2, D) < 0$ on $(s_2^0, \overline{s}_2)$ and $\dfrac{\partial \Psi}{\partial s_2}(s_2, D) > 0$ on $(\overline{s}_2, s_2^1)$.

Hypothesis **H8** is fulfilled with the specific growth rates (2.9) of chapter 3.

Definition 2.2. *The functions ϕ_1 be defined for I_1, ϕ_2 and ϕ_3 be defined for I_2 and φ_i, $i = 0, 1$ are defined for $D \in \{D \geq 0 : s_2^0 < M_2(D + a_2)\}$ and $D \in \{D \geq 0 : M_2(D + a_2) < s_2^1\}$ by:*

$$\begin{aligned}
&\phi_1(D) = \inf_{s_2^0 < s_2 < s_2^1} \Psi(s_2, D) = \Psi(\overline{s}_2(D), D), \\
&\phi_2(D) = \Psi\left(M_2(D + a_2), D\right), \qquad \phi_3(D) = \frac{\partial \Psi}{\partial s_2}\left(M_2(D + a_2), D\right), \\
&\varphi_0(D) = M_0(D + a_0, M_2(D + a_2)), \qquad \varphi_1(D) = M_1(D + a_1, M_2(D + a_2)).
\end{aligned} \tag{2.25}$$

Remark 2.1. From Lemma 2.2, we have $\phi_1(D) = -\infty$ if $\omega > 1$ and $\phi_1(D) > 0$ if $\omega \leq 1$ (see Figure 2.3). Moreover, if $\omega = 1$ then, $\phi_1(D) = \Psi\left(s_2^0, D\right)$. Since Ψ is convex, the equation

$$\Psi(s_2, D) = (1-\omega)s_0^{\text{in}} + s_1^{\text{in}} + s_2^{\text{in}} \tag{2.26}$$

has a solution $s_2 = s_2\left(D, s_0^{\text{in}}, s_1^{\text{in}}, s_2^{\text{in}}\right)$ if and only if

$$(1-\omega)s_0^{\text{in}} + s_1^{\text{in}} + s_2^{\text{in}} \geq \phi_1(D).$$

If $\omega \geq 1$ then, s_2, if it exists, is unique. If $\omega < 1$ then, there exist at least two solutions $s_2^{*1} < s_2^{*2}$ in the interval (s_2^0, s_2^1), which are equal when $(1-\omega)s_0^{\text{in}} + s_1^{\text{in}} + s_2^{\text{in}} = \phi_1(D)$, such that

$$\frac{\partial \Psi}{\partial s_2}\left(s_2^{*1}, D\right) < 0 \quad \text{and} \quad \frac{\partial \Psi}{\partial s_2}\left(s_2^{*2}, D\right) > 0.$$

The solutions s_2^{*1} and s_2^{*2} lead to two steady states E_{110}^1 and E_{110}^2.

Definition 2.3. *Let ψ_0 and ψ_1 be the functions defined for $s_0 \in \left[\max\left(0, s_0^{\text{in}} - s_2^{\text{in}}/\omega\right), +\infty\right)$ and $s_1 \in \left[0, s_1^{\text{in}} + s_2^{\text{in}}\right]$, respectively, by:*

$$\psi_0\left(s_0\right) = \mu_0\left(s_0, s_2^{\text{in}} - \omega\left(s_0^{\text{in}} - s_0\right)\right), \quad \psi_1\left(s_1\right) = \mu_1\left(s_1, s_1^{\text{in}} + s_2^{\text{in}} - s_1\right). \tag{2.27}$$

Lemma 2.3. *The equation $\psi_0(s_0) = y$ has a solution in the interval*

$$J_0 = \left[\max\left(0, s_0^{\text{in}} - s_2^{\text{in}}/\omega\right), s_0^{\text{in}}\right),$$

if and only if $\mu_0\left(s_0^{\text{in}}, s_2^{\text{in}}\right) > y$. If it exists, this solution is unique. The equation $\psi_1(s_1) = y$ has a solution in the interval

$$J_1 = \left[0, s_1^{\text{in}}\right)$$

if and only if $\mu_1\left(s_1^{\text{in}}, s_2^{\text{in}}\right) > y$. If it exists, this solution is unique.

Proof. We have

$$\frac{d\psi_0}{ds_0}(s_0) = \frac{\partial \mu_0}{\partial s_0}(s_0, s_2^{\text{in}} - \omega(s_0^{\text{in}} - s_0)) + \omega \frac{\partial \mu_0}{\partial s_2}(s_0, s_2^{\text{in}} - \omega(s_0^{\text{in}} - s_0)),$$

which is positive thanks to **H4**. Therefore, ψ_0 is monotonically increasing. Moreover, if $s_2^{\text{in}} - \omega s_0^{\text{in}} > 0$, one has

$$\psi_0(0) = \mu_0\left(0, s_2^{\text{in}} - \omega s_0^{\text{in}}\right) = 0,$$

and if $s_2^{\text{in}} - \omega s_0^{\text{in}} \leq 0$ one has $s_0^{\text{in}} - s_2^{\text{in}}/\omega \geq 0$, so that,

$$\psi_0\left(s_0^{\text{in}} - s_2^{\text{in}}/\omega\right) = \mu_0\left(s_0^{\text{in}} - s_2^{\text{in}}/\omega, 0\right) = 0.$$

Thus, $\psi_0\left(\max\left(0, s_0^{\text{in}} - s_2^{\text{in}}/\omega\right)\right) = 0$. On the other hand, $\psi_0\left(s_0^{\text{in}}\right) = \mu_0\left(s_0^{\text{in}}, s_2^{\text{in}}\right)$. Therefore, there exists a unique $s_0 \in J_0$ satisfying $\psi_0(s_0) = y$, if and only if $\mu_0\left(s_0^{\text{in}}, s_2^{\text{in}}\right) > y$. We have

$$\frac{d\psi_1}{ds_1}(s_1) = \frac{\partial \mu_1}{\partial s_1}\left(s_1, s_1^{\text{in}} + s_2^{\text{in}} - s_1\right) - \frac{\partial \mu_1}{\partial s_2}\left(s_1, s_1^{\text{in}} + s_2^{\text{in}} - s_1\right),$$

which is positive thanks to **H5**. Therefore, ψ_1 is monotonically increasing. On the other hand,

$$\psi_1(0) = \mu_1\left(0, s_1^{\text{in}} + s_2^{\text{in}}\right) = 0 \quad \text{and} \quad \psi_1(s_1^{\text{in}}) = \mu_1\left(s_1^{\text{in}}, s_2^{\text{in}}\right).$$

Thus, there exists a unique $s_1 \in J_1$ satisfying $\psi_1(s_1) = y$ if and only if $\mu_1(s_1^{\text{in}}, s_2^{\text{in}}) > y$. □

2.3.3 Existence of the steady states

We can state now the necessary and sufficient conditions of existence of the steady states in the following Theorem.

Theorem 2.1. *Assume that Hypotheses* **H1** *to* **H6** *hold. The steady states* E_{000}, E_{001},..., E_{011}, *of* (2.8) *are given in* Table 2.1. *Assume also that* **H7** *and* **H8** *hold. The necessary and sufficient conditions of existence of the steady states are given in* Table 2.2.

Table 2.1: The steady states of (2.8). The functions M_0, M_1 and M_2 are given in Definition 2.1, φ_0 and φ_1 are given in Definition 2.2 and Ψ is defined by (2.23).

	$s_0,\ s_1,\ s_2$	$x_0,\ x_1,\ x_2$
E_{000}	$s_0 = s_0^{\text{in}},\ s_1 = s_1^{\text{in}},\ s_2 = s_2^{\text{in}}$	$x_0 = 0,\ x_1 = 0,\ x_2 = 0$
E_{001}	$s_0 = s_0^{\text{in}},\ s_1 = s_1^{\text{in}},\ s_2 = M_2(D+a_2)$	$x_0 = 0,\ x_1 = 0,\ x_2 = \frac{D}{D+a_2}\left(s_2^{\text{in}} - M_2(D+a_2)\right)$
E_{100}	$s_0 = s_0\left(D, s_0^{\text{in}}, s_2^{\text{in}}\right)$ is a solution of $\psi_0(s_0) = D + a_0$ $s_1 = s_1^{\text{in}} + s_0^{\text{in}} - s_0$ $s_2 = s_2^{\text{in}} - \omega\left(s_0^{\text{in}} - s_0\right)$	$x_0 = \frac{D}{D+a_0}\left(s_0^{\text{in}} - s_0\right)$ $x_1 = 0$ $x_2 = 0$
E_{110}	$s_2 = s_2\left(D, s_0^{\text{in}}, s_1^{\text{in}}, s_2^{\text{in}}\right)$ is a solution of $\Psi\left(s_2, D\right) = (1-\omega)s_0^{\text{in}} + s_1^{\text{in}} + s_2^{\text{in}}$ $s_0 = M_0\left(D + a_0, s_2\right)$ $s_1 = M_1\left(D + a_1, s_2\right)$	$x_0 = \frac{D}{D+a_0}\left(s_0^{\text{in}} - s_0\right)$ $x_1 = \frac{D}{D+a_1}\left(s_0^{\text{in}} - s_0 + s_1^{\text{in}} - s_1\right)$ $x_2 = 0$
E_{101}	$s_0 = \varphi_0(D),\ \ s_1 = s_0^{\text{in}} + s_1^{\text{in}} - s_0$ $s_2 = M_2(D+a_2)$	$x_0 = \frac{D}{D+a_0}\left(s_0^{\text{in}} - s_0\right),\ x_1 = 0$ $x_2 = \frac{D}{D+a_2}\left(s_2^{\text{in}} - s_2 - \omega\left(s_0^{\text{in}} - s_0\right)\right)$
E_{111}	$s_0 = \varphi_0(D)$ $s_1 = \varphi_1(D)$ $s_2 = M_2(D+a_2)$	$x_0 = \frac{D}{D+a_0}\left(s_0^{\text{in}} - s_0\right)$ $x_1 = \frac{D}{D+a_1}\left(s_0^{\text{in}} + s_1^{\text{in}} - s_1 - s_0\right)$ $x_2 = \frac{D}{D+a_2}\left((1-\omega)(s_0^{\text{in}} - s_0) + s_1^{\text{in}} - s_1 + s_2^{\text{in}} - s_2\right)$
E_{010}	$s_0 = s_0^{\text{in}},\ s_1 = s_1\left(D, s_1^{\text{in}}, s_2^{\text{in}}\right)$ is a solution of $\psi_1(s_1) = D + a_1$ $s_2 = s_1^{\text{in}} - s_1 + s_2^{\text{in}}$	$x_0 = 0,\ x_1 = \frac{D}{D+a_1}\left(s_1^{\text{in}} - s_1\right)$ $x_2 = 0$
E_{011}	$s_0 = s_0^{\text{in}},\ s_1 = \varphi_1(D)$ $s_2 = M_2(D+a_2)$	$x_0 = 0,\ x_1 = \frac{D}{D+a_1}\left(s_1^{\text{in}} - s_1\right)$ $x_2 = \frac{D}{D+a_2}\left(s_1^{\text{in}} - s_1 + s_2^{\text{in}} - s_2\right)$

Proof. Adding (2.15) to (2.12), substrating (2.12) from (2.13)+(2.16) and adding (2.12) multiplied by ω to (2.14) and (2.17) and substrating (2.13), we obtain the set of equations

$$\begin{cases} D\left(s_0^{\text{in}} - s_0\right) - (D+a_0)\,x_0 = 0 \\ D\left(s_1^{\text{in}} - s_1\right) + (D+a_0)\,x_0 - (D+a_1)\,x_1 = 0 \\ D\left(s_2^{\text{in}} - s_2\right) - \omega\,(D+a_0)\,x_0 + (D+a_1)\,x_1 - (D+a_2)\,x_2 = 0. \end{cases} \tag{2.28}$$

We can solve (2.28) and obtain x_0, x_1 and x_2 with respect of s_0, s_1 and s_2:

$$x_0 = \frac{D}{D+a_0}\left(s_0^{\text{in}} - s_0\right) \tag{2.29}$$

$$x_1 = \frac{D}{D+a_1}\left(s_0^{\text{in}} - s_0 + s_1^{\text{in}} - s_1\right) \tag{2.30}$$

$$x_2 = \frac{D}{D+a_2}\left((1-\omega)\left(s_0^{\text{in}} - s_0\right) + s_1^{\text{in}} - s_1 + s_2^{\text{in}} - s_2\right). \tag{2.31}$$

Table 2.2: The necessary and sufficient existence conditions of steady states of (2.8). The functions M_0, M_1 and M_2 are given in Definition 2.1, ϕ_1, ϕ_2, φ_0 and φ_1 are given in Definition 2.2, while μ_i and Ψ are given by (2.9) and (2.23).

Steady states	Existence conditions
E_{000}	Always exists
E_{001}	$\mu_2\left(s_2^{\text{in}}\right) > D + a_2$
E_{100}	$\mu_0\left(s_0^{\text{in}}, s_2^{\text{in}}\right) > D + a_1$
E_{110}	$(1-\omega)s_0^{\text{in}} + s_1^{\text{in}} + s_2^{\text{in}} \geq \phi_1(D)$, $s_0^{\text{in}} > M_0(D + a_0, s_2)$ and $s_0^{\text{in}} + s_1^{\text{in}} > M_0(D + a_0, s_2) + M_1(D + a_1, s_2)$ with s_2 is solution of $\Psi(s_2) = (1-\omega)s_0^{\text{in}} + s_1^{\text{in}} + s_2^{\text{in}}$
E_{101}	$s_0^{\text{in}} > \varphi_0(D)$ and $s_2^{\text{in}} - \omega s_0^{\text{in}} > M_2(D + a_2) - \omega\varphi_0(D)$
E_{111}	$(1-\omega)s_0^{\text{in}} + s_1^{\text{in}} + s_2^{\text{in}} > \phi_2(D)$, $s_0^{\text{in}} > \varphi_0(D)$ and $s_0^{\text{in}} + s_1^{\text{in}} > \varphi_0(D) + \varphi_1(D)$
E_{010}	$\mu_1\left(s_1^{\text{in}}, s_2^{\text{in}}\right) > D + a_1$
E_{011}	$s_1^{\text{in}} > \varphi_1(D)$ and $s_1^{\text{in}} + s_2^{\text{in}} > \varphi_1(D) + M_2(D + a_2)$

We can also solve (2.28) and obtain s_0, s_1 and s_2 with respect of x_0, x_1 and x_2:

$$s_0 = s_0^{\text{in}} - \frac{D + a_0}{D} x_0 \tag{2.32}$$

$$s_1 = s_1^{\text{in}} + \frac{D + a_0}{D} x_0 - \frac{D + a_1}{D} x_1 \tag{2.33}$$

$$s_2 = s_2^{\text{in}} - \omega\frac{D + a_0}{D} x_0 + \frac{D + a_1}{D} x_1 - \frac{D + a_2}{D} x_2. \tag{2.34}$$

For E_{000}, $x_0 = x_1 = x_2 = 0$. Hence, (2.32), (2.33) and (2.34) result in

$$s_0 = s_0^{\text{in}}, \quad s_1 = s_1^{\text{in}} \quad \text{and} \quad s_2 = s_2^{\text{in}}.$$

This steady state always exists.

For E_{001}, $x_0 = x_1 = 0$ and $x_2 > 0$. Hence, (2.32) and (2.33) result in

$$s_0 = s_0^{\text{in}} \quad \text{and} \quad s_1 = s_1^{\text{in}}.$$

Therefore, (2.31) results in

$$x_2 = \frac{D}{D + a_2}\left(s_2^{\text{in}} - s_2\right). \tag{2.35}$$

Since $x_2 > 0$, (2.14) results in $\mu_2(s_2) = D + a_2$. Therefore,

$$s_2 = M_2(D + a_2). \tag{2.36}$$

E_{001} exists if and only if $x_2 > 0$, that is to say $s_2^{\text{in}} > M_2(D + a_2)$, which is equivalent to

$$\mu_2\left(s_2^{\text{in}}\right) > D + a_2,$$

thanks to **H6**.

For E_{100}, $x_1 = x_2 = 0$ and $x_0 > 0$. (2.29) results in

$$x_0 = \frac{D}{D + a_0}\left(s_0^{\text{in}} - s_0\right). \tag{2.37}$$

Using this expression together with $x_1 = x_2 = 0$ in (2.33) and (2.34) result in

$$s_1 = s_1^{\text{in}} + s_0^{\text{in}} - s_0 \quad \text{and} \quad s_2 = s_2^{\text{in}} - \omega(s_0^{\text{in}} - s_0). \tag{2.38}$$

Since $x_0 > 0$, (2.12) results in

$$\mu_0(s_0, s_2) = D + a_0. \tag{2.39}$$

Replacing s_2 by its expression (2.38) with respect of s_0 in (2.39) results in

$$\psi_0(D) = D + a_0, \tag{2.40}$$

where ψ_0 is the function defined in (2.27). E_{100} exists if and only if equation (2.40) has a positive solution and x_0, s_1 and s_2 defined by (2.37) and (2.38), respectively, are positive. This condition is equivalent to say that

$$0 < s_0 < s_0^{\text{in}} \quad \text{and} \quad s_0 > s_0^{\text{in}} - s_2^{\text{in}}/\omega.$$

Therefore, (2.40) must have a solution in the interval J_0. Using Lemma 2.3, (2.40) has a unique solution in the interval J_0 if and only if

$$\mu_0\left(s_0^{\text{in}}, s_2^{\text{in}}\right) > D + a_0.$$

For E_{110}, $x_0 > 0$, $x_1 > 0$ and $x_2 = 0$. Hence, (2.29) and (2.30) result in

$$x_0 = \frac{D}{D + a_0}\left(s_0^{\text{in}} - s_0\right) \quad \text{and} \quad x_1 = \frac{D}{D + a_1}\left(s_0^{\text{in}} - s_0 + s_1^{\text{in}} - s_1\right). \tag{2.41}$$

Using $x_0 > 0$ and $x_1 > 0$, (2.12) and (2.13) result in

$$\mu_0(s_0, s_2) = D + a_0 \quad \text{and} \quad \mu_1(s_1, s_2) = D + a_1.$$

Therefore, using the definitions of M_0 and M_1, we have

$$s_0 = M_0(D + a_0, s_2) \quad \text{and} \quad s_1 = M_1(D + a_1, s_2). \tag{2.42}$$

Using (2.41) together with $x_2 = 0$ in (2.34), we have

$$s_2 = s_2^{\text{in}} - \omega\left(s_0^{\text{in}} - s_0\right) + s_0^{\text{in}} - s_0 + s_1^{\text{in}} - s_1. \tag{2.43}$$

Replacing s_0 and s_1 by their expressions (2.42) with respect of s_2 in (2.43), it follows that, s_2 is a solution of

$$\Psi(s_2, D) = (1 - \omega)s_0^{\text{in}} + s_1^{\text{in}} + s_2^{\text{in}}, \tag{2.44}$$

where Ψ is the function defined by (2.23). According to Remark 2.1 E_{110} exists if and only if

$$(1-\omega)s_0^{\text{in}} + s_1^{\text{in}} + s_2^{\text{in}} \geq \phi_1(D),$$

and the solution s_2 of (2.44) is such that x_0 and x_1-components are positive, which is equivalent to

$$s_0^{\text{in}} > M_0(D+a_0, s_2) \text{ and } s_0^{\text{in}} + s_1^{\text{in}} > M_0(D+a_0, s_2) + M_1(D+a_1, s_2).$$

The existence of a unique or two steady states of the form E_{110} according to ω follow immediately from Remark 2.1.

For E_{101}, $x_0 > 0$, $x_2 > 0$ and $x_1 = 0$. (2.29) results in

$$x_0 = \frac{D}{D+a_0}\left(s_0^{\text{in}} - s_0\right). \tag{2.45}$$

Using this expression together with $x_1 = 0$ in (2.33) results in

$$s_1 = s_1^{\text{in}} - s_0 + s_0^{\text{in}}. \tag{2.46}$$

Using this expression in (2.34) results in

$$x_2 = \frac{D}{D+a_2}\left(s_2^{\text{in}} - s_2 - \omega\left(s_0^{\text{in}} - s_0\right)\right). \tag{2.47}$$

Using $x_0 > 0$ and $x_2 > 0$, (2.12) and (2.14) result in

$$\mu_0(s_0, s_2) = D + a_0 \quad \text{and} \quad \mu_2(s_2) = D + a_2.$$

Therefore, using the definitions of M_0, M_2 and φ_0, we find that

$$s_2 = M_2(D+a_2) \quad \text{and} \quad s_0 = \varphi_0(D). \tag{2.48}$$

E_{101} exists if and only if x_0, s_1 and x_2-components are positive. This condition is equivalent to

$$s_0^{\text{in}} > \varphi_0(D) \quad \text{and} \quad s_2^{\text{in}} - \omega s_0^{\text{in}} > M_2(D+a_2) - \omega\varphi_0(D).$$

For E_{111}, $x_0 > 0$, $x_1 > 0$ and $x_2 > 0$. Then, as a consequence of (2.12)-(2.14), we obtain

$$\mu_0(s_0, s_2) = D + a_0, \quad \mu_1(s_1, s_2) = D + a_1, \quad \mu_2(s_2) = D + a_2.$$

Using the definitions of M_0, M_1, M_2, φ_0 and φ_1 yields

$$s_2 = M_2(D+a_2), \quad s_0 = \varphi_0(D), \quad s_1 = \varphi_1(D).$$

The x-components of E_{111} are given by (2.29), (2.30) and (2.31). Thus, E_{111} exists if and only if its x-components are positive, that is,

$$s_0^{\text{in}} > \varphi_0(D),\ s_1^{\text{in}} + s_0^{\text{in}} > \varphi_0(D) + \varphi_1(D) \quad \text{and} \quad (1-\omega)s_0^{\text{in}} + s_1^{\text{in}} + s_2^{\text{in}} > \phi_2(D).$$

For E_{010}, $x_0 = x_2 = 0$ and $x_1 > 0$. Hence, (2.32) results in

$$s_0 = s_0^{\text{in}}.$$

From (2.30), we have

$$x_1 = \frac{D}{D + a_1}\left(s_1^{\text{in}} - s_1\right). \tag{2.49}$$

Using this expression together with $x_0 = x_2 = 0$ in (2.34) results in

$$s_2 = s_1^{\text{in}} - s_1 + s_2^{\text{in}}. \tag{2.50}$$

Since $x_1 > 0$, then, as a consequence of (2.13), we obtain

$$\mu_1(s_1, s_2) = D + a_1. \tag{2.51}$$

Replacing s_2 by its expression (2.50) with respect of s_1 results in

$$\psi_1(D) = D + a_1. \tag{2.52}$$

E_{010} exists if and only if (2.52) has a positive solution and x_1 and s_2 defined by (2.49) and (2.50), respectively, are positive. This last condition is equivalent to $0 < s_1 < s_1^{\text{in}}$. Consequently, (2.52) must have a solution in the interval J_1. Using Lemma 2.3, there exists a unique $s_1 \in J_1$, satisfying (2.52), if and only if

$$\mu_1(s_1^{\text{in}}, s_2^{\text{in}}) > D + a_1.$$

For E_{011}, $x_0 = 0$, $x_1 > 0$ and $x_2 > 0$. Hence, (2.32) results in

$$s_0 = s_0^{\text{in}}.$$

Using this expression in (2.30) and (2.31) results in

$$x_1 = \frac{D}{D + a_1}\left(s_1^{\text{in}} - s_1\right), \quad x_2 = \frac{D}{D + a_2}\left(s_1^{\text{in}} - s_1 + s_2^{\text{in}} - s_2\right).$$

Since $x_1 > 0$ and $x_2 > 0$, as a consequence of (2.13) and (2.14), we have

$$\mu_1(s_1, s_2) = D + a_1 \quad \text{and} \quad \mu_2(s_2) = D + a_2.$$

Therefore, using the definitions of the functions M_2 and φ_1, it follows that

$$s_2 = M_2(D + a_2), \quad s_1 = \varphi_1(D).$$

For the components x_1 and x_2 to be positive, the necessary and sufficient condition is that

$$s_1^{\text{in}} > \varphi_1(D) \quad \text{and} \quad s_1^{\text{in}} + s_2^{\text{in}} > \varphi_1(D) + M_2(D + a_2).$$

□

Remark 2.2. Recall from Remark 2.1 that $\phi_1(D) = -\infty$ when $\omega > 1$. Therefore, in this case, the condition $(1-\omega)s_0^{\text{in}} + s_1^{\text{in}} + s_2^{\text{in}} \geq \phi_1(D)$ of existence of E_{110} is always satisfied.

In the particular cases, where $s_1^{\text{in}} = 0$ or $s_2^{\text{in}} = 0$, some of the steady states described in Theorem 2.1 do not exist and the existence conditions of the existing steady states can be simplified. More precisely, we have the following result.

Proposition 2.2. *If* $s_1^{\text{in}} = 0$ *then,* E_{010} *and* E_{011} *do not exist. If* $s_2^{\text{in}} = 0$, E_{001}, E_{100} *and* E_{101} *do not exist. If* $s_1^{\text{in}} = s_2^{\text{in}} = 0$, *we have:*

- *The steady states* E_{001}, E_{100}, E_{101}, E_{010} *and* E_{011} *do not exist.*
- *If* $\omega \geqslant 1$, E_{110} *and* E_{111} *do not exist. If* $\omega < 1$, E_{110} *and* E_{111} *exist, respectively, if and only if*

$$(1-\omega)s_0^{\text{in}} \geqslant \phi_1(D) \quad \textit{and} \quad (1-\omega)s_0^{\text{in}} > \phi_2(D). \tag{2.53}$$

Proof. If $s_1^{\text{in}} = 0$, then $\mu_1\left(s_1^{\text{in}}, s_2^{\text{in}}\right) = 0$, so that the conditions

$$\mu_1\left(s_1^{\text{in}}, s_2^{\text{in}}\right) > D + a_1 \quad \text{and} \quad s_1^{\text{in}} > \varphi_1(D)$$

of existence of E_{010} and E_{011}, respectively, cannot be satisfied. Therefore, E_{010} and E_{011} do not exist. If $s_2^{\text{in}} = 0$, then $\mu_2\left(s_2^{\text{in}}\right) = 0$ and $\mu_0\left(s_0^{\text{in}}, s_2^{\text{in}}\right) = 0$, so that the existence conditions

$$\mu_2\left(s_2^{\text{in}}\right) > D + a_2 \quad \text{and} \quad \mu_0\left(s_0^{\text{in}}, s_2^{\text{in}}\right) > D + a_0$$

of E_{001} and E_{100} cannot be satisfied, respectively. Moreover, the second existence condition of E_{101} implies that

$$s_0^{\text{in}} < \varphi_0(D) - \frac{M_2(D+a_2)}{\omega} < \varphi_0(D),$$

which is in contradiction with the first existence condition of E_{101}. Therefore, E_{001}, E_{100} and E_{101} do not exist. This confirms the results obtained in [51] in the case where $s_1^{\text{in}} = s_2^{\text{in}} = 0$, where the steady states E_{001}, E_{100}, E_{101}, E_{010} and E_{011} do not exist.

Assume that $s_1^{\text{in}} = s_2^{\text{in}} = 0$. If $\omega = 1$, the first existence condition of E_{110} in Table 2.2 is written $0 \geqslant \phi_1(D)$. This condition cannot be satisfied, since $\phi_1(D) = \Psi\left(s_2^0, D\right) > 0$ from Remark 2.1. Thus, E_{110} does not exist if $\omega = 1$. When $\omega > 1$, we have s_2 is solution of equation

$$(1-\omega)\left(s_0^{\text{in}} - s_0\right) = s_1 + s_2.$$

Since $s_1 > 0$ and $s_2 > 0$, then we have necessarily

$$(1-\omega)\left(s_0^{\text{in}} - s_0\right) > 0,$$

so that $s_0^{\text{in}} - s_0 < 0$, which contradicts the positivity of the x_0-component of E_{110} in Table 2.1. Thus, E_{110} does not exist if $\omega > 1$. When $s_1^{\text{in}} = s_2^{\text{in}} = 0$, the s_2-component of E_{110} becomes the solution of equation

$$s_0^{\text{in}} = M_0\left(D + a_0, s_2\right) + \frac{M_1\left(D + a_1, s_2\right) + s_2}{(1-\omega)}.$$

If $0 < \omega < 1$, then

$$s_0^{\text{in}} > M_0\left(D + a_0, s_2\right) + M_1\left(D + a_1, s_2\right) > M_0\left(D + a_0, s_2\right),$$

thus, the second and the third existence conditions of E_{110} in Table 2.2 are satisfied when $\omega < 1$. Therefore, E_{110} exists if and only if $(1-\omega)s_0^{\text{in}} \geqslant \phi_1(D)$.

Regarding the steady state E_{111} in the particular case $s_1^{\text{in}} = s_2^{\text{in}} = 0$, the first existence condition in Table 2.2 becomes

$$(1-\omega)s_0^{\text{in}} > \phi_2(D), \tag{2.54}$$

which is equivalent to

$$(1-\omega)\left(s_0^{\text{in}} - \varphi_0(D)\right) > \varphi_1(D) + M_2(D + a_2).$$

When $\omega \geqslant 1$, this last inequality cannot hold, since $s_0^{\text{in}} > \varphi_0(D)$, so that E_{111} does not exist. If $\omega < 1$, condition (2.54) implies that

$$(1-\omega)s_0^{\text{in}} > (1-\omega)\varphi_0(D) + (1-\omega)\varphi_1(D),$$

that is,

$$s_0^{\text{in}} > \varphi_0(D) + \varphi_1(D) > \varphi_0(D),$$

which are the second and the third existence conditions of E_{111} in Table 2.2. Thus, (2.54) is the only existence condition of E_{111}.

□

Remark 2.3. From Tables 2.1 and 2.2, we can see that:

- E_{000} and E_{001} coalesce, when $D + a_2 = \mu_2\left(s_2^{\text{in}}\right)$.
- E_{000} and E_{100} coalesce, when $D + a_0 = \mu_0\left(s_0^{\text{in}}, s_2^{\text{in}}\right)$.
- E_{000} and E_{010} coalesce, when $D + a_1 = \mu_1\left(s_1^{\text{in}}, s_2^{\text{in}}\right)$.
- E_{001} and E_{101} coalesce, when $s_0^{\text{in}} = \varphi_0(D)$.
- E_{100} and E_{101} coalesce, when $s_2^{\text{in}} - \omega s_0^{\text{in}} = M_2(D + a_2) - \omega\varphi_0(D)$.
- E_{011} and E_{001} coalesce, when $s_1^{\text{in}} = \varphi_1(D)$.
- E_{110}^1 and E_{110}^2 coalesce, when $s_0^{\text{in}}(1-\omega) = \phi_1(D) - s_1^{\text{in}} - s_2^{\text{in}}$.
- E_{011} and E_{111} coalesce, when $s_0^{\text{in}} = \varphi_0(D)$.
- E_{101} and E_{111} coalesce, when $s_0^{\text{in}} + s_1^{\text{in}} = \varphi_0(D) + \varphi_1(D)$.
- E_{110} and E_{111} coalesce, when $s_0^{\text{in}}(1-\omega) = \phi_2(D) - s_1^{\text{in}} - s_2^{\text{in}}$.

- E_{010} and E_{011} coalesce, when $s_1^{in} + s_2^{in} = M_2(D + a_2) + \varphi_1(D)$.

Remark 2.4. Assume that $s_1^{in} = s_2^{in} = 0$. Then, only the steady states E_{000}, E_{110} and E_{111} can exist. The existence conditions (2.53) of E_{110} and E_{111}, respectively, are equivalent to the following conditions given in Lemmas 3 and 4 of [51]:

$$s_0^{in} \geqslant F_1(D) := \frac{\phi_1(D)}{1-\omega} \quad \text{and} \quad s_0^{in} > F_2(D) := \frac{\phi_2(D)}{1-\omega}.$$

Hence, we recover the results of [51] where the study is restricted to the case $s_1^{in} = s_2^{in} = 0$.

2.4 Conclusion

In this chapter, we have investigated mathematically the steady states of the three-tiered chlorophenol mineralizing "food-web" model proposed by [64] involving three organisms and three substrates with general growth functions and by considering the effects of the phenol and the hydrogen inflowing concentrations as well as the maintenance terms. We have described all steady states of system (2.8) and we have provided the existence conditions according to the control parameters. The analysis of the steady states of system (2.8) proves the existence of eight types of steady states: the washout steady state which always exists, a coexistence steady state where all degrader populations are maintained and six other steady states corresponding to the extinction of one or two degrader populations. Each type of steady state is unique, if it exists, except that of the exclusion only of the hydrogen degraders (E_{110}). Using Hypothesis **H8** which satisfies the specific growth rates (2.9), there are at most two steady states of type E_{110}.

In the following chapter, we determine the local stability analysis of the three-tiered model in the particular case, when the maintenance (decay) is excluded from the model. We illustrate the change in the asymptotic behavior of the chlorophenol model by bifurcation diagrams according to one-parameter, by using the results of this chapter.

The results of this chapter have been published in [40].

CHAPTER 3

Stability of the three-tiered food-web model without decay

Summary

3.1 Introduction

In this chapter, we are interested in analyzing the local stability of the three-tiered microbial model, by considering a large class of growth rates, instead of specific kinetics, when the maintenance is excluded.

This chapter is organized as follows. In section 3.2, we present the three-step food-web model with three input substrate concentrations, when the terms of maintenance are zero and describe the steady states of the model and their existing conditions. Next, in section 3.3, we determine explicitly the necessary and sufficient local stability conditions of the steady states according to the operating parameters, followed by the bifurcation diagram with respect to the chlorophenol input concentration as a bifurcating parameter in section 3.4. In section 3.5, we give some numerical simulations to illustrate the theoretical results.

3.2 Three-tiered model without decay terms

Putting the mortality terms equal to zero $a_i = 0$, for $i = 0, 1, 2$ in model (2.8), which corresponds to ($k_{\text{dec,ch}} = k_{\text{dec,ph}} = k_{\text{dec,H}_2} = 0$) of model (2.1), leads to the following model:

$$\begin{cases} \dot{x}_0 &= \mu_0(s_0, s_2)x_0 - Dx_0 \\ \dot{x}_1 &= \mu_1(s_1, s_2)x_1 - Dx_1 \\ \dot{x}_2 &= \mu_2(s_2)x_2 - Dx_2 \\ \dot{s}_0 &= D\left(s_0^{\text{in}} - s_0\right) - \mu_0(s_0, s_2)x_0 \\ \dot{s}_1 &= D\left(s_1^{\text{in}} - s_1\right) + \mu_0(s_0, s_2)x_0 - \mu_1(s_1, s_2)x_1 \\ \dot{s}_2 &= D\left(s_2^{\text{in}} - s_2\right) - \omega\mu_0(s_0, s_2)x_0 + \mu_1(s_1, s_2)x_1 - \mu_2(s_2)x_2. \end{cases} \tag{3.1}$$

We suppose that the growth functions μ_i, $i = 0, 1, 2$ in system (3.1) satisfy the assumptions **H1** to **H8** of chapter 2. The solutions of system (3.1) verify Proposition 2.1, with the set Ω in this case is given by

$$\Omega = \left\{(x_0, x_1, x_2, s_0, s_1, s_2) \in \mathbb{R}_+^6 : Z = \omega x_0 + x_1 + x_2 + 2s_0 + 2s_1 + s_2 = 2s_0^{\text{in}} + 2s_1^{\text{in}} + s_2^{\text{in}}\right\}.$$

In Table 3.1, the steady states of (3.1) and their necessary and sufficient existence conditions are easily deduced from Table 2.1 and Table 2.2, respectively, in chapter 2 by putting $a_i = 0$, $i = 0, 1, 2$.

3.3 Local stability of the steady states

In this section, we determine the local stability conditions of steady states of model (3.1). Any reference to steady state stability should be considered as local exponential

Table 3.1: The steady states of (3.1) and their necessary and sufficient existence conditions.

Steady state	Existence condition
$\mathrm{E}_{000} = \left(0, 0, 0, s_0^{\mathrm{in}}, s_1^{\mathrm{in}}, s_2^{\mathrm{in}}\right)$	Always exists
$\mathrm{E}_{001} = \left(0, 0, \mathrm{s}_2^{\mathrm{in}} - \mathrm{M}_2(\mathrm{D}), \mathrm{s}_0^{\mathrm{in}}, \mathrm{s}_1^{\mathrm{in}}, \mathrm{M}_2(\mathrm{D})\right)$	$\mu_2\left(s_2^{\mathrm{in}}\right) > D$
$\mathrm{E}_{100} = \left(\mathrm{s}_0^{\mathrm{in}} - \mathrm{s}_0, 0, 0, \mathrm{s}_0, \mathrm{s}_1, \mathrm{s}_2\right)$, where $s_0 = s_0\left(D, s_0^{\mathrm{in}}, s_2^{\mathrm{in}}\right)$ is a solution of $\psi_0(s_0) = D$, $s_1 = s_1^{\mathrm{in}} + s_0^{\mathrm{in}} - s_0$, $s_2 = s_2^{\mathrm{in}} - \omega\left(s_0^{\mathrm{in}} - s_0\right)$	$\mu_0\left(s_0^{\mathrm{in}}, s_2^{\mathrm{in}}\right) > D$
$\mathrm{E}_{110} = \left(\mathrm{s}_0^{\mathrm{in}} - \mathrm{s}_0, \mathrm{s}_0^{\mathrm{in}} - \mathrm{s}_0 + \mathrm{s}_1^{\mathrm{in}} - \mathrm{s}_1, 0, \mathrm{s}_0, \mathrm{s}_1, \mathrm{s}_2\right)$, where $s_0 = M_0\left(D, s_2\right)$, $s_1 = M_1\left(D, s_2\right)$ and $s_2 = s_2\left(D, s_0^{\mathrm{in}}, s_1^{\mathrm{in}}, s_2^{\mathrm{in}}\right)$ is a solution of $\Psi\left(s_2, D\right) = (1-\omega)s_0^{\mathrm{in}} + s_1^{\mathrm{in}} + s_2^{\mathrm{in}}$	$(1-\omega)s_0^{\mathrm{in}} + s_1^{\mathrm{in}} + s_2^{\mathrm{in}} \geq \phi_1\left(D\right)$ and the solution s_2 satisfies $s_0^{\mathrm{in}} > M_0\left(D, s_2\right)$ and $s_0^{\mathrm{in}} + s_1^{\mathrm{in}} > M_0\left(D, s_2\right) + M_1\left(D, s_2\right)$
$\mathrm{E}_{101} = \left(\mathrm{s}_0^{\mathrm{in}} - \mathrm{s}_0, 0, \mathrm{s}_2^{\mathrm{in}} - \mathrm{s}_2 - \omega\left(\mathrm{s}_0^{\mathrm{in}} - \mathrm{s}_0\right), \mathrm{s}_0, \mathrm{s}_1, \mathrm{s}_2\right)$, where $s_0 = M_0(D, s_2)$, $s_1 = s_0^{\mathrm{in}} + s_1^{\mathrm{in}} - s_0$, $s_2 = M_2(D)$	$s_0^{\mathrm{in}} > \varphi_0(D)$ and $s_2^{\mathrm{in}} - \omega s_0^{\mathrm{in}} > M_2(D) - \omega\varphi_0(D)$
$\mathrm{E}_{111} = (\mathrm{x}_0, \mathrm{x}_1, \mathrm{x}_2, \mathrm{s}_0, \mathrm{s}_1, \mathrm{s}_2)$, where $s_0 = M_0(D, s_2)$, $s_1 = M_1(D, s_2)$, $s_2 = M_2(D)$ $x_0 = s_0^{\mathrm{in}} - s_0$, $x_1 = s_1^{\mathrm{in}} + s_0^{\mathrm{in}} - s_1 - s_0$, $x_2 = (1-\omega)(s_0^{\mathrm{in}} - s_0) + s_1^{\mathrm{in}} - s_1 + s_2^{\mathrm{in}} - s_2$	$(1-\omega)s_0^{\mathrm{in}} + s_1^{\mathrm{in}} + s_2^{\mathrm{in}} > \phi_2\left(D\right)$, $s_0^{\mathrm{in}} > \varphi_0(D)$ and $s_0^{\mathrm{in}} + s_1^{\mathrm{in}} > \varphi_0(D) + \varphi_1(D)$
$\mathrm{E}_{010} = \left(0, \mathrm{s}_1^{\mathrm{in}} - \mathrm{s}_1, 0, \mathrm{s}_0^{\mathrm{in}}, \mathrm{s}_1, \mathrm{s}_1^{\mathrm{in}} - \mathrm{s}_1 + \mathrm{s}_2^{\mathrm{in}}\right)$, where $s_1 = s_1\left(D, s_1^{\mathrm{in}}, s_2^{\mathrm{in}}\right)$ is a solution of $\psi_1(s_1) = D$	$\mu_1\left(s_1^{\mathrm{in}}, s_2^{\mathrm{in}}\right) > D$
$\mathrm{E}_{011} = \left(0, \mathrm{s}_1^{\mathrm{in}} - \mathrm{s}_1, \mathrm{s}_1^{\mathrm{in}} - \mathrm{s}_1 + \mathrm{s}_2^{\mathrm{in}} - \mathrm{s}_2, \mathrm{s}_0^{\mathrm{in}}, \mathrm{s}_1, \mathrm{s}_2\right)$, where $s_1 = M_1\left(D, s_2\right)$, $s_2 = M_2\left(D\right)$	$s_1^{\mathrm{in}} > \varphi_1(D)$ and $s_1^{\mathrm{in}} + s_2^{\mathrm{in}} > \varphi_1(D) + M_2(D)$

stability (LES). Indeed, the local exponential stability is given by the sign of the real parts of the eigenvalues of the Jacobian matrix of system (3.1) evaluated at the steady states, or by the stability criterions in the more complicated cases, as the Routh-Hurwitz criterion and the Liénard-Chipart stability criterion. These stability criterions allow us to conclude to the local stability of a steady state without explicitly calculating the eigenvalues of the Jacobian matrix.

The study of the stability of E_{111} requires the following definition.

Definition 3.1. *Let* $\left(D, s_0^{\mathrm{in}}, s_1^{\mathrm{in}}, s_2^{\mathrm{in}}\right) \mapsto \phi_4\left(D, s_0^{\mathrm{in}}, s_1^{\mathrm{in}}, s_2^{\mathrm{in}}\right)$ *be defined by:*

$$\begin{aligned}\phi_4(D, s_0^{\mathrm{in}}, s_1^{\mathrm{in}}, s_2^{\mathrm{in}}) =& (EIx_0x_2 + EG\phi_3(D)x_0x_1)(Ix_2 + (G+H)x_1 + (E+\omega F)x_0) \\ &+ (Ix_2 + (G+H)x_1 + \omega F x_0)GIx_1x_2,\end{aligned} \tag{3.2}$$

where

$$\begin{aligned}E &= \frac{\partial \mu_0}{\partial s_0}(s_0, s_2), \quad F = \frac{\partial \mu_0}{\partial s_2}(s_0, s_2), \quad G = \frac{\partial \mu_1}{\partial s_1}(s_1, s_2), \\ H &= -\frac{\partial \mu_1}{\partial s_2}(s_1, s_2), \quad I = \frac{d\mu_2}{ds_2}(s_2).\end{aligned} \tag{3.3}$$

and are evaluated at the steady state E_{111}. *We have used the opposite sign of the partial derivative* $H = -\partial\mu_1/\partial s_2$, *such that all constants involved in the computation become positive.*

Now, we state our main result.

Theorem 3.1. *Assume that* **H1** *to* **H8** *hold. The necessary and sufficient stability conditions of the steady states of* (3.1) *are given in Table 3.2.*

Table 3.2: The necessary and sufficient conditions of local stability of steady states of (3.1).

	Stability conditions
E_{000}	$\mu_0\left(s_0^{\mathrm{in}}, s_2^{\mathrm{in}}\right) < D, \quad \mu_1\left(s_1^{\mathrm{in}}, s_2^{\mathrm{in}}\right) < D$ and $\mu_2\left(s_2^{\mathrm{in}}\right) < D$
E_{001}	$s_0^{\mathrm{in}} < \varphi_0(D)$ and $s_1^{\mathrm{in}} < \varphi_1(D)$
E_{100}	$\mu_1\left(s_0^{\mathrm{in}} + s_1^{\mathrm{in}} - s_0, s_2^{\mathrm{in}} - \omega\left(s_0^{\mathrm{in}} - s_0\right)\right) < D$ and $s_2^{\mathrm{in}} - \omega s_0^{\mathrm{in}} < M_2(D) - \omega\varphi_0(D)$, with s_0 solution of equation $\psi_0(s_0) = D$
E_{110}	$(1-\omega)s_0^{\mathrm{in}} + s_1^{\mathrm{in}} + s_2^{\mathrm{in}} < \phi_2(D)$, $\phi_3(D) > 0$ and $\dfrac{\partial\Psi}{\partial s_2}(s_2, D) > 0$, with s_2 solution of equation $\Psi(s_2, D) = (1-\omega)s_0^{\mathrm{in}} + s_1^{\mathrm{in}} + s_2^{\mathrm{in}}$
E_{101}	$s_0^{\mathrm{in}} + s_1^{\mathrm{in}} < \varphi_0(D) + \varphi_1(D)$
E_{111}	$\phi_3(D) \geq 0 \quad$ or $\quad \phi_3(D) < 0$ and $\phi_4(D, s_0^{\mathrm{in}}, s_1^{\mathrm{in}}, s_2^{\mathrm{in}}) > 0$
E_{010}	$s_1^{\mathrm{in}} + s_2^{\mathrm{in}} < M_3\left(s_0^{\mathrm{in}}, D\right) + M_1\left(D, M_3\left(s_0^{\mathrm{in}}, D\right)\right)$ and $s_1^{\mathrm{in}} + s_2^{\mathrm{in}} < M_2(D) + \varphi_1(D)$
E_{011}	$s_0^{\mathrm{in}} < \varphi_0(D)$

Proof. To facilitates the local stability analysis, we use the following change of variables:

$$z_0 = x_0 + s_0, \quad z_1 = x_1 + s_1 - x_0, \quad z_2 = \omega x_0 - x_1 + x_2 + s_2. \tag{3.4}$$

Therefore, model (3.1) can be reduced to a cascade system which takes the form:

$$\begin{cases} \dot{x}_0 &= -Dx_0 + \mu_0\left(z_0 - x_0, z_2 - \omega x_0 + x_1 - x_2\right) x_0 \\ \dot{x}_1 &= -Dx_1 + \mu_1\left(z_1 + x_0 - x_1, z_2 - \omega x_0 + x_1 - x_2\right) x_1 \\ \dot{x}_2 &= -Dx_2 + \mu_2\left(z_2 - \omega x_0 + x_1 - x_2\right) x_2 \\ \dot{z}_0 &= D\left(s_0^{\mathrm{in}} - z_0\right) \\ \dot{z}_1 &= D\left(s_1^{\mathrm{in}} - z_1\right) \\ \dot{z}_2 &= D\left(s_2^{\mathrm{in}} - z_2\right) \end{cases} \tag{3.5}$$

The steady states E_{000}, E_{001},..., E_{011} of (3.5) now take the form $\left(x_0, x_1, x_2, s_0^{\mathrm{in}}, s_1^{\mathrm{in}}, s_2^{\mathrm{in}}\right)$, where the x_i-components of each steady state are given by those in Table 3.1. The Jacobian

matrix of (3.5) has the block triangular form:

$$\mathcal{J} = \begin{bmatrix} \mathbf{J_1} & \mathbf{J_2} \\ 0 & \mathbf{J_3} \end{bmatrix},$$

where

$$\mathbf{J_1} = \begin{bmatrix} \mu_0(s_0, s_2) - D - (E + \omega F)x_0 & Fx_0 & -Fx_0 \\ (G + \omega H)x_1 & \mu_1(s_1, s_2) - D - (G + H)x_1 & Hx_1 \\ -\omega I x_2 & Ix_2 & \mu_2(s_2) - D - Ix_2 \end{bmatrix}, \tag{3.6}$$

$$\mathbf{J_2} = \begin{bmatrix} Ex_0 & 0 & Fx_0 \\ 0 & Gx_1 & -Hx_1 \\ 0 & 0 & Ix_2 \end{bmatrix}, \qquad \mathbf{J_3} = \begin{bmatrix} -D & 0 & 0 \\ 0 & -D & 0 \\ 0 & 0 & -D \end{bmatrix},$$

where the functions E, F, G, H and I, defined by (3.3), are evaluated at the steady state. Since $\mathcal{J}$ is a block triangular matrix, its eigenvalues are $-D$ with multiplicity 3, together with the eigenvalues of the 3×3 upper-left matrix $\mathbf{J_1}$. Thus, the local exponential stability (LES) of the steady states is determined by the sign of the real parts of the eigenvalues of $\mathbf{J_1}$.

For E_{000}, the matrix $\mathbf{J_1}$ is:

$$\mathbf{J_1} = \begin{bmatrix} \mu_0\left(s_0^{\text{in}}, s_2^{\text{in}}\right) - D & 0 & 0 \\ 0 & \mu_1\left(s_1^{\text{in}}, s_2^{\text{in}}\right) - D & 0 \\ 0 & 0 & \mu_2\left(s_2^{\text{in}}\right) - D \end{bmatrix}.$$

The eigenvalues of $\mathbf{J_1}$ are

$$\lambda_1 = \mu_0\left(s_0^{\text{in}}, s_2^{\text{in}}\right) - D, \quad \lambda_2 = \mu_1\left(s_1^{\text{in}}, s_2^{\text{in}}\right) - D \quad \text{and} \quad \lambda_3 = \mu_2\left(s_2^{\text{in}}\right) - D.$$

Therefore, for E_{000} to be stable, it is necessary and sufficient that $\lambda_1 < 0$, $\lambda_2 < 0$ and $\lambda_3 < 0$. Thus, E_{000} is stable if and only if

$$\mu_0\left(s_0^{\text{in}}, s_2^{\text{in}}\right) < D, \quad \mu_1\left(s_1^{\text{in}}, s_2^{\text{in}}\right) < D \quad \text{and} \quad \mu_2\left(s_2^{\text{in}}\right) < D,$$

which are the same as the stability conditions of E_{000} in Table 3.2.

For E_{001}, the matrix $\mathbf{J_1}$ is:

$$\mathbf{J_1} = \begin{bmatrix} \mu_0\left(s_0^{\text{in}}, M_2(D)\right) - D & 0 & 0 \\ 0 & \mu_1\left(s_1^{\text{in}}, M_2(D)\right) - D & 0 \\ -\omega I x_2 & Ix_2 & -Ix_2 \end{bmatrix}.$$

The eigenvalues of $\mathbf{J_1}$ are

$$\lambda_1 = \mu_0\left(s_0^{\text{in}}, M_2(D)\right) - D, \quad \lambda_2 = \mu_1\left(s_1^{\text{in}}, M_2(D)\right) - D \quad \text{and} \quad \lambda_3 = -Ix_2.$$

Therefore, for E_{001} to be stable, it is necessary and sufficient that $\lambda_1 < 0$ and $\lambda_2 < 0$. Thus, E_{001} is stable if and only if

$$\mu_0\left(s_0^{\text{in}}, M_2(D)\right) < D \quad \text{and} \quad \mu_1\left(s_1^{\text{in}}, M_2(D)\right) < D.$$

Since M_0 and M_1 are increasing (see Lemma 2.1), these conditions are equivalent to

$$s_0^{\text{in}} < M_0(D, M_2(D)) \quad \text{and} \quad s_1^{\text{in}} < M_1(D, M_2(D)),$$

which are the same as the stability conditions of E_{001} in Table 3.2.

For E_{100}, the matrix $\mathbf{J_1}$ is:

$$\mathbf{J_1} = \begin{bmatrix} -(E+\omega F)x_0 & Fx_0 & -Fx_0 \\ 0 & \mu_1\left(s_0^{\text{in}} + s_1^{\text{in}} - s_0, s_2^{\text{in}} - \omega\left(s_0^{\text{in}} - s_0\right)\right) - D & 0 \\ 0 & 0 & \mu_2\left(s_2^{\text{in}} - \omega\left(s_0^{\text{in}} - s_0\right)\right) - D \end{bmatrix}.$$

The eigenvalues of $\mathbf{J_1}$ are

$$\lambda_1 = -(E+\omega F)x_0, \quad \lambda_2 = \mu_1\left(s_0^{\text{in}} + s_1^{\text{in}} - s_0, s_2^{\text{in}} - \omega\left(s_0^{\text{in}} - s_0\right)\right) - D$$
$$\text{and} \quad \lambda_3 = \mu_2\left(s_2^{\text{in}} - \omega\left(s_0^{\text{in}} - s_0\right)\right) - D.$$

Therefore, for E_{100} to be stable, it is necessary and sufficient that $\lambda_2 < 0$ and $\lambda_3 < 0$. Thus, E_{100} is stable if and only if

$$\mu_1\left(s_0^{\text{in}} + s_1^{\text{in}} - s_0, s_2^{\text{in}} - \omega\left(s_0^{\text{in}} - s_0\right)\right) < D \quad \text{and} \quad \mu_2\left(s_2^{\text{in}} - \omega\left(s_0^{\text{in}} - s_0\right)\right) < D, \tag{3.7}$$

where s_0 is the solution in the interval J_0 of equation $\psi_0(s_0) = D$. Since M_2 is increasing (see Lemma 2.1), the second condition of (3.7) is equivalent to

$$s_2^{\text{in}} - \omega\left(s_0^{\text{in}} - s_0\right) < M_2(D) \iff s_0 < \left(M_2(D) - s_2^{\text{in}}\right)/\omega + s_0^{\text{in}}. \tag{3.8}$$

As the function ψ_0 is increasing, (3.8) is equivalent to

$$\psi_0(s_0) < \psi_0\left(\left(M_2(D) - s_2^{\text{in}}\right)/\omega + s_0^{\text{in}}\right). \tag{3.9}$$

From the definition of the function ψ_0 together with the condition $\psi_0(s_0) = D$ defining s_0, we deduce that (3.9) is equivalent to

$$D < \mu_0\left(\left(M_2(D) - s_2^{\text{in}}\right)/\omega + s_0^{\text{in}}, M_2(D)\right).$$

Since M_0 is increasing (see Lemma 2.1), then E_{100} is stable if and only if

$$\mu_1\left(s_0^{\text{in}} + s_1^{\text{in}} - s_0, s_2^{\text{in}} - \omega\left(s_0^{\text{in}} - s_0\right)\right) < D \text{ and } M_0(D, M_2(D)) < \left(M_2(D) - s_2^{\text{in}}\right)/\omega + s_0^{\text{in}},$$

which are the same as the stability conditions of E_{100} in Table 3.2.

For E_{110}, the matrix $\mathbf{J_1}$ is:

$$\mathbf{J_1} = \begin{bmatrix} -(E+\omega F)x_0 & Fx_0 & -Fx_0 \\ (G+\omega H)x_1 & -(G+H)x_1 & Hx_1 \\ 0 & 0 & \mu_2(s_2) - D \end{bmatrix}.$$

The eigenvalue is simply

$$\lambda_1 = \mu_2(s_2) - D.$$

The others are those of the matrix

$$\begin{bmatrix} -(E+\omega F)x_0 & Fx_0 \\ (G+\omega H)x_1 & -(G+H)x_1 \end{bmatrix}.$$

The eigenvalues of this matrix are λ_2 and λ_3, such that

$$\lambda_2\lambda_3 = (E(G+H) - (1-\omega)FG)\, x_0x_1 \text{ and } \lambda_2 + \lambda_3 = -\left((E+\omega F)x_0 + (G+H)x_1\right) < 0.$$

Hence, the eigenvalues λ_2 and λ_3 are of a negative real part if and only if

$$E(G+H) - (1-\omega)FG > 0. \tag{3.10}$$

Let us prove that this condition (3.10) is equivalent to $\frac{\partial \Psi}{\partial s_2}(s_2, D) > 0$. Using (3.3) and Lemma 2.1, we obtain

$$\frac{\partial M_0}{\partial s_2}(D, s_2) = -\frac{F}{E} \quad \text{and} \quad \frac{\partial M_1}{\partial s_2}(D, s_2) = \frac{H}{G}.$$

Using (2.24), it follows that

$$\frac{\partial \Psi}{\partial s_2}(s_2, D) = \frac{F}{E}(\omega - 1) + \frac{H}{G} + 1 = \frac{E(G+H) + (\omega-1)FG}{EG}. \tag{3.11}$$

Since E and G are positive, condition (3.10) is equivalent to $\frac{\partial \Psi}{\partial s_2}(s_2, D) > 0$. Consequently, as μ_2 is increasing, E_{110} is stable if and only if

$$s_2 < M_2(D) \quad \text{and} \quad \frac{\partial \Psi}{\partial s_2}(s_2, D) > 0. \tag{3.12}$$

When $s_2^1 \leq M_2(D)$, the s_2-component of E_{110} satisfies $s_2 < s_2^1 \leq M_2(D)$. Thus, E_{110} is stable if and only if the first and the second conditions of (3.12) hold. When $M_2(D) < s_2^1$, we will prove that (3.12) is equivalent to the stability conditions of E_{110} given in Table 3.2. To this end, assume first that $\omega \geqslant 1$. If $s_2 < M_2(D)$, then $s_2^0 \leq s_2 < M_2(D) < s_2^1$. From Lemma 2.3, the mapping $s_2 \mapsto \Psi(s_2, D)$ is increasing for all $s_2 \in (s_2^0, s_2^1)$ (see Figure 2.3(b-c)). Hence, the condition $s_2 < M_2(D)$ is equivalent to

$$(1-\omega)s_0^{\text{in}} + s_1^{\text{in}} + s_2^{\text{in}} = \Psi(s_2, D) < \Psi\left(M_2(D), D\right) = \phi_2(D). \tag{3.13}$$

In addition, $s_2 < M_2(D)$ implies that $\phi_3(D) > 0$ for all $D \in I_2$. Now, when $\omega < 1$, from Lemma 2.3 and using **H8**, equation (2.44) has at most two solutions $s_2^{*1} < s_2^{*2}$, such that $\dfrac{\partial \Psi}{\partial s_2}(s_2^{*1}, D) < 0$ and $\dfrac{\partial \Psi}{\partial s_2}(s_2^{*2}, D) > 0$ (see Figure 2.3(a)). Thus, the steady state E^1_{110} corresponding to s_2^{*1} is unstable. For the steady state E^2_{110} corresponding to s_2^{*2}, the condition $s_2^{*2} < M_2(D)$ implies the first and the second stability conditions of E_{110} since the mapping $s_2 \mapsto \Psi(s_2, D)$ is increasing on $(\overline{s}_2, s_2^1)$. On the other hand, if the first stability condition of E_{110} or equivalently (3.13) holds, then

$$s_2^{*2} < M_2(D) \quad \text{or} \quad s_2^0 < M_2(D) < s_2^{*1}.$$

This last condition is in contradiction with the second condition of stability of E_{110}. Therefore, E_{110} is stable if and only if

$$(1-\omega)s_0^{\mathrm{in}} + s_1^{\mathrm{in}} + s_2^{\mathrm{in}} < \phi_2(D), \quad \phi_3(D) > 0 \quad \text{and} \quad \frac{\partial \Psi}{\partial s_2}(s_2, D) > 0.$$

For E_{101}, the matrix $\mathbf{J_1}$ is:

$$\mathbf{J_1} = \begin{bmatrix} -(E+\omega F)x_0 & Fx_0 & -Fx_0 \\ 0 & \mu_1\left(s_0^{\mathrm{in}} + s_1^{\mathrm{in}} - M_0(D, M_2(D)), M_2(D)\right) - D & 0 \\ -\omega I x_2 & I x_2 & -I x_2 \end{bmatrix}.$$

Its known eigenvalue is

$$\lambda_1 = \mu_1\left(s_0^{\mathrm{in}} + s_1^{\mathrm{in}} - M_0(D, M_2(D)), M_2(D)\right) - D.$$

The two other are those of the matrix:

$$\begin{bmatrix} -(E+\omega F)x_0 & -Fx_0 \\ -\omega I x_2 & -I x_2 \end{bmatrix}.$$

The eigenvalues of this matrix are λ_2 and λ_3 such that,

$$\lambda_2\lambda_3 = EIx_0x_2 > 0 \quad \text{and} \quad \lambda_2 + \lambda_3 = -\left((E+\omega F)x_0 + Ix_2\right) < 0.$$

Hence, the real parts of the eigenvalues λ_2 and λ_3 are negative. Therefore, E_{101} is stable if and only if

$$\mu_1\left(s_0^{\mathrm{in}} + s_1^{\mathrm{in}} - M_0(D, M_2(D)), M_2(D)\right) < D,$$

which is equivalent to

$$s_0^{\mathrm{in}} + s_1^{\mathrm{in}} < M_1(D, M_2(D)) + M_0(D, M_2(D)),$$

which is the same as the stability condition of E_{101} in Table 3.2.

For E_{111}, the matrix $\mathbf{J_1}$ is:

$$\mathbf{J_1} = \begin{bmatrix} -(E+\omega F)x_0 & Fx_0 & -Fx_0 \\ (G+\omega H)x_1 & -(G+H)x_1 & Hx_1 \\ -\omega I x_2 & Ix_2 & -Ix_2 \end{bmatrix}.$$

The eigenvalues are given by the characteristic polynomial P_3, which is given by:

$$P_3 = \lambda^3 + c_1\lambda^2 + c_2\lambda + c_3 = 0, \tag{3.14}$$

where

$$\begin{aligned} &c_1 = Ix_2 + (G+H)x_1 + (E+\omega F)x_0, \\ &c_2 = (E(G+H) - (1-\omega)FG)x_0x_1 + EIx_0x_2 + GIx_1x_2, \quad c_3 = EGIx_0x_1x_2. \end{aligned} \tag{3.15}$$

To satisfy the Routh-Hurwitz criterion, we require $c_i > 0$, for $i = 1, 3$ and $c_1c_2 - c_3 > 0$. Notice that:

$$\begin{aligned} c_1c_2 - c_3 =& (EIx_0x_2 + EG\phi_3(D)x_0x_1)(Ix_2 + (G+H)x_1 + (E+\omega F)x_0) \\ &+ (Ix_2 + (G+H)x_1 + \omega Fx_0)GIx_1x_2. \end{aligned} \tag{3.16}$$

Then, we always have $c_1 > 0$ and $c_3 > 0$. From (3.11), we deduce that

$$(E(G+H) - (1-\omega)FG) = EG\phi_3(D).$$

Therefore, if $\phi_3(D) \geq 0$, then, $(E(G+H) - (1-\omega)FG) \geq 0$. Hence, $c_1c_2 - c_3 > 0$, so that E_{111} is LES.
On the other hand, since we always have $c_1 > 0$ and $c_3 > 0$, according to the Routh-Hurwitz criterion, E_{111} is LES if and only if

$$\phi_4\left(D, s_0^{\text{in}}, s_1^{\text{in}}, s_2^{\text{in}}\right) := c_1c_2 - c_3 > 0,$$

where the function ϕ_4 can be written as its expression (3.2).

For E_{010}, the matrix $\mathbf{J_1}$ is:

$$\mathbf{J_1} = \begin{bmatrix} \mu_0\left(s_0^{\text{in}}, s_1^{\text{in}} - s_1 + s_2^{\text{in}}\right) - D & 0 & 0 \\ (G+\omega H)x_1 & -(G+H)x_1 & Hx_1 \\ 0 & 0 & \mu_2\left(s_1^{\text{in}} - s_1 + s_2^{\text{in}}\right) - D \end{bmatrix}.$$

The eigenvalues of $\mathbf{J_1}$ are

$$\lambda_1 = \mu_0\left(s_0^{\text{in}}, s_1^{\text{in}} - s_1 + s_2^{\text{in}}\right) - D, \quad \lambda_2 = -(G+H)x_1 \quad \text{and} \quad \lambda_3 = \mu_2\left(s_1^{\text{in}} - s_1 + s_2^{\text{in}}\right) - D.$$

Therefore, for E_{010} to be stable, it is necessary and sufficient that $\lambda_1 < 0$ and $\lambda_3 < 0$. Thus, E_{010} is stable if and only if

$$\mu_0\left(s_0^{\text{in}}, s_1^{\text{in}} - s_1 + s_2^{\text{in}}\right) < D \quad \text{and} \quad \mu_2\left(s_1^{\text{in}} - s_1 + s_2^{\text{in}}\right) < D, \tag{3.17}$$

where s_1 is the solution in the interval J_1 of equation $\psi_1(D) = D$. Recall that the functions M_2 and M_3 are increasing (see Lemma 2.1). Thus,

$$\mu_0\left(s_0^{\text{in}}, s_1^{\text{in}} - s_1 + s_2^{\text{in}}\right) < D \quad \Longleftrightarrow \quad s_1 > s_1^{\text{in}} + s_2^{\text{in}} - M_3(s_0^{\text{in}}, D)$$

and

$$\mu_2\left(s_1^{\text{in}} - s_1 + s_2^{\text{in}}\right) < D \quad \Longleftrightarrow \quad s_1 > s_1^{\text{in}} + s_2^{\text{in}} - M_2(D).$$

As the function ψ_1 is increasing, then, we deduced that

$$\psi_1(s_1) > \psi_1\left(s_1^{\text{in}} + s_2^{\text{in}} - M_3(s_0^{\text{in}}, D)\right) \quad \text{and} \quad \psi_1(s_1) > \psi_1\left(s_1^{\text{in}} + s_2^{\text{in}} - M_2(D)\right).$$

From $\psi_1(s_1) = \mu_1\left(s_1, s_1^{\text{in}} - s_1 + s_2^{\text{in}}\right) = D$, then, the conditions of the stability of E_{010} are equivalent to

$$\mu_1\left(s_1^{\text{in}} + s_2^{\text{in}} - M_3(s_0^{\text{in}}, D), M_3(s_0^{\text{in}}, D)\right) < D \quad \text{and} \quad \mu_1\left(s_1^{\text{in}} + s_2^{\text{in}} - M_2(D), M_2(D)\right) < D.$$

Since M_1 is increasing. Thus, E_{010} is stable if and only if

$$s_1^{\text{in}} + s_2^{\text{in}} < M_1\left(D, M_3(s_0^{\text{in}}, D)\right) + M_3(s_0^{\text{in}}, D) \text{ and } s_1^{\text{in}} + s_2^{\text{in}} < M_1\left(D, M_2(D)\right) + M_2(D),$$

which are the same as the stability conditions of E_{010} in Table 3.2.

For E_{011}, the matrix $\mathbf{J_1}$ is:

$$\mathbf{J_1} = \begin{bmatrix} \mu_0\left(s_0^{\text{in}}, M_2(D)\right) - D & 0 & 0 \\ (G + \omega H)x_1 & -(G+H)x_1 & Hx_1 \\ -\omega I x_2 & I x_2 & -I x_2 \end{bmatrix}.$$

Its known eigenvalue is

$$\lambda_1 = \mu_0\left(s_0^{\text{in}}, M_2(D)\right) - D.$$

The two other are those of the matrix:

$$\begin{bmatrix} -(G+H)x_1 & Hx_1 \\ \\ I x_2 & -I x_2 \end{bmatrix}.$$

The eigenvalues of this matrix are λ_2 and λ_3 such that,

$$\lambda_2\lambda_3 = GIx_1x_2 > 0 \quad \text{and} \quad \lambda_2 + \lambda_3 = -\left((G+H)x_1 + Ix_2\right) < 0.$$

Hence, the real parts of the eigenvalues λ_2 and λ_3 are negative. Therefore, E_{011} is stable if and only if

$$\mu_0\left(s_0^{\text{in}}, M_2(D)\right) < D,$$

which is equivalent to

$$s_0^{\text{in}} < M_0(D, M_2(D)),$$

which is the same as the stability condition of E_{011} in Table 3.2.

□

Remark 3.1. From Remark 2.1, when it exists, E^1_{110} is unstable. When E^2_{110} exists, the third stability condition $\dfrac{\partial \Psi}{\partial s_2}(s_2^{*2}, D) > 0$ in Table 3.2 is always satisfied. However, the other stability conditions can be not satisfied, so that, this steady state can be unstable.

3.4 Bifurcation diagram

In this section, we study numerically the qualitative behavior of system (3.1) when considering $S_{\text{ch}}^{\text{in}}$ as the bifurcation parameter. Throughout this section, we assume that the biological parameters are fixed at the values provided in Table 3.3.

Table 3.3: Nominal parameter values, where $i = \{\text{ch}, \text{ph}, \text{H}_2\}$. Units are expressed in Chemical Oxygen Demand (COD).

Parameter	Wade et al. [64]	Unit
$k_{m,\text{ch}}$	29	
$k_{m,\text{ph}}$	26	$\text{kgCOD}_\text{S}/\text{kgCOD}_\text{X}/\text{d}$
k_{m,H_2}	35	
$K_{S,\text{ch}}$	0.053	
$K_{S,\text{H}_2,\text{c}}$	10^{-6}	
$K_{S,\text{ph}}$	0.302	kgCOD/m^3
K_{I,H_2}	3.5×10^{-6}	
K_{S,H_2}	2.5×10^{-5}	
Y_{ch}	0.019	
Y_{ph}	0.04	$\text{kgCOD}_\text{X}/\text{kgCOD}_\text{S}$
Y_{H_2}	0.06	
$k_{\text{dec,i}}$	0	d^{-1}

For the specific kinetics (2.9), straightforward computations show that the various functions M_i, s_2^0, s_2^1, Ψ, ϕ_i, φ_i and ψ_i are given by the expressions in Table 3.4. Notice that, from the expression of Ψ in Table 3.4, a straightforward calculation shows that, for all $s_2 \in (s_2^0, s_2^1)$,

$$\frac{\partial^2 \psi}{\partial s_2^2}(s_2, D) = \frac{(1-\omega)2K_0(D+a_0)}{m_0 - D - a_0}\frac{L_0 + s_2^0}{(s_2 - s_2^0)^3} + \frac{2K_1(K_I + s_2^1)}{(s_2^1 - s_2)^3},$$

which is positive since $\omega < 1$ and $m_0 > D + a_0$. Thus, the function $s_2 \mapsto \Psi(s_2, D)$ is convex and fulfills **H8** (see Figure 2.3(a)). Furthermore, model (2.1) is of the form (2.8) where the growth functions (2.9) satisfy Hypotheses **H1** to **H8**, where $k_{\text{dec,i}} = 0$. Consequently, the results of this section apply to model (2.1). For this section, we put $a_i = 0$, for $i = 0, 1, 2$ in Table 3.4.

Now, we fix the following input concentrations with the dilution rate

$$S_{\text{ph}}^{\text{in}} = 0, \quad S_{\text{H}_2}^{\text{in}} = 2.67\times10^{-5} \quad \text{and} \quad D = 0.01,$$

corresponding to Figure 3(a) in [64] when $k_{\text{dec,i}} = 0$, $i = \{\text{ch}, \text{ph}, \text{H}_2\}$ and plot the one-parameter bifurcation diagram in $S_{\text{ch}}^{\text{in}}$. As a consequence of Table 3.1 and Theorem 3.1, we obtain the following result which determines the existence and the stability of the steady states of (2.1) with respect to the input concentration $S_{\text{ch}}^{\text{in}}$.

Table 3.4: Notations, intervals and auxiliary functions in the case of growth functions given by (2.9).

Auxiliary functions	Definition domain
$M_0(y,s_2)=\dfrac{yK_0(L_0+s_2)}{m_0s_2-y(L_0+s_2)}$	Defined for $0\leq y<\dfrac{m_0s_2}{L_0+s_2}$.
$M_1(y,s_2)=\dfrac{yK_1(K_I+s_2)}{m_1K_I-y(K_I+s_2)}$	Defined for $0\leq y<\dfrac{m_1K_I}{K_I+s_2}$.
$M_2(y)=\dfrac{yK_2}{m_2-y}$	Defined for $0\leq y<m_2$.
$M_3(s_0,z)=\dfrac{zL_0(K_0+s_0)}{m_0s_0-z(K_0+s_0)}$	Defined for $0\leq z<\dfrac{m_0s_0}{K_0+s_0}$.
$s_2^0(D)=\dfrac{L_0(D+a_0)}{m_0-D-a_0}$	Defined for $D+a_0<m_0$.
$s_2^1(D)=\dfrac{K_I(m_1-D-a_1)}{D+a_1}$	Defined for $D+a_1<m_1$.
$\Psi(s_2,D)=(1-\omega)\dfrac{(D+a_0)K_0(L_0+s_2)}{m_0s_2-(D+a_0)(L_0+s_2)}+\dfrac{(D+a_1)K_1(K_I+s_2)}{m_1K_I-(D+a_1)(K_I+s_2)}+s_2$	Defined for $D\in I_1$ and $s_2^0(D)<s_2<s_2^1(D)$.
$\phi_1(D)=\inf\limits_{s_2^0(D)<s_2<s_2^1(D)}\Psi(s_2,D)$	Defined for $D\in I_1$.
$\phi_2(D)=\Psi(M_2(D+a_2),D)$	Defined for $D\in I_2$.
$\phi_3(D)=\frac{\partial\Psi}{\partial s_2}(M_2(D+a_2),D)$	Defined for $D\in I_2$.
$\varphi_0(D)=M_0(D+a_0,(M_2(D+a_2)))$	Defined for $D\in\{D\geq 0: s_2^0<M_2(D+a_2)\}$.
$\varphi_1(D)=M_1(D+a_1,(M_2(D+a_2)))$	Defined for $D\in\{D\geq 0: M_2(D+a_2)<s_2^1\}$.
$\psi_0(s_0)=\dfrac{m_0s_0\left(s_2^{\text{in}}-\omega\left(s_0^{\text{in}}-s_0\right)\right)}{(K_0+s_0)\left(L_0+s_2^{\text{in}}-\omega\left(s_0^{\text{in}}-s_0\right)\right)}$	Defined for $s_0\in\left[\max\left(0,s_0^{\text{in}}-s_2^{\text{in}}/\omega\right),+\infty\right)$.
$\psi_1(s_1)=\dfrac{m_1s_1K_I}{(K_1+s_1)\left(K_I+s_1^{\text{in}}+s_2^{\text{in}}-s_1\right)}$	Defined for $s_1\in\left[0,s_1^{\text{in}}+s_2^{\text{in}}\right)$.

Proposition 3.1. *Assume that the biological parameters in (2.1) are given as in Table 3.3. Assume that* $S_{\text{ph}}^{\text{in}}=0$, $S_{\text{H}_2}^{\text{in}}=2.67\times10^{-5}$, $D=0.01$ *and* $k_{\text{dec,ch}}=k_{\text{dec,ph}}=k_{\text{dec,H}_2}=0$. *Let* σ_i, $i=1,\dots,6$ *be the bifurcation values defined in Table 3.5. The existence and stability of steady states of (2.1), with respect to the input concentration* $S_{\text{ch}}^{\text{in}}$ *is given in Table 3.6. The nature of the bifurcations when* $S_{\text{ch}}^{\text{in}}$ *crosses the values* σ_i, $i=1,\dots,6$ *is given in*

Table 3.7.

Table 3.5: Definitions of the critical values of σ_i, $i = 1, \ldots, 6$. All functions are given in Table 3.4, while ϕ_4 is given by (3.2).

Definition	Value
$\sigma_1 = M_0\left(D, S_{H_2}^{in}\right)/Y$	0.001017
$\sigma_2 = (\phi_1(D) - S_{H_2}^{in})/((1-\omega)Y)$	0.009159
$\sigma_3 = \varphi_0(D)/Y$	0.010846
$\sigma_4 = (S_{H_2}^{in} - M_2(D) + \omega\varphi_0(D))/(\omega Y)$	0.011191
$\sigma_5 = (\phi_2(D) - S_{H_2}^{in})/((1-\omega)Y)$	0.016575
σ_6 is the solution of equation $\phi_4(S_{ch}^{in}) = 0$	0.029877

Table 3.6: Existence and stability of steady states, with respect to S_{ch}^{in}. In the following, the letter S (resp. U) means that the corresponding steady state is stable (resp. unstable). No letter means that the steady state does not exist.

Interval of S_{ch}^{in}	E_{000}	E_{001}	E_{100}	E_{110}^1	E_{110}^2	E_{101}	E_{111}
$(0, \sigma_1)$	U	S					
(σ_1, σ_2)	U	S	U				
(σ_2, σ_3)	U	S	U	U	U		
(σ_3, σ_4)	U	U	U	U	U	S	
(σ_4, σ_5)	U	U	S	U	U		
(σ_5, σ_6)	U	U	S	U	U		U
$(\sigma_6, +\infty)$	U	U	S	U	U		S

Table 3.7: Nature of the bifurcations corresponding to the critical values of σ_i, $i = 1, \ldots, 6$, defined in Table 3.5. There exists also a critical value $\sigma^* \simeq 0.029638$ corresponding to the value of S_{ch}^{in} where the stable limit cycle disappears when S_{ch}^{in} is decreasing.

	Type of the bifurcation
σ_1	Transcritical bifurcation of E_{000} and E_{100}
σ_2	Saddle-node bifurcation of E_{110}^1 and E_{110}^2
σ_3	Transcritical bifurcation of E_{001} and E_{101}
σ_4	Transcritical bifurcation of E_{100} and E_{101}
σ_5	Transcritical bifurcation of E_{110}^1 and E_{111}
σ^*	Disappearance of the stable limit cycle
σ_6	Supercritical Hopf bifurcation

Proof. Using the change of variables (2.7) and from Tables 3.1 and 3.2, the necessary and sufficient conditions of existence and stability of steady states of (2.1) are summarized in Table 3.8 when $S_{\text{ph}}^{\text{in}} = 0$ and $k_{\text{dec,i}} = 0$. Since $s_1^{\text{in}} = Y_4 S_{\text{ph}}^{\text{in}} = 0$, E_{010} and E_{011} do not exist, as shown in Proposition 2.2. Using Table 3.8, we see that:

Table 3.8: Existence and local stability conditions of steady states of (2.1), when $S_{\text{ph}}^{\text{in}} = 0$ and $k_{\text{dec,i}} = 0$. All functions are given in Table 3.4, while μ_i and ϕ_4 are given by (2.9) and (3.2).

	Existence conditions	Stability conditions
E_{000}	Always exists	$\mu_0\left(YS_{\text{ch}}^{\text{in}}, S_{\text{H}_2}^{\text{in}}\right) < D$, $\mu_2\left(S_{\text{H}_2}^{\text{in}}\right) < D$
E_{001}	$\mu_2\left(S_{\text{H}_2}^{\text{in}}\right) > D$	$YS_{\text{ch}}^{\text{in}} < \varphi_0(D)$
E_{100}	$\mu_0\left(YS_{\text{ch}}^{\text{in}}, S_{\text{H}_2}^{\text{in}}\right) > D$	$\mu_1\left(YS_{\text{ch}}^{\text{in}} - s_0, S_{\text{H}_2}^{\text{in}} - \omega\left(YS_{\text{ch}}^{\text{in}} - s_0\right)\right) < D$ $S_{\text{H}_2}^{\text{in}} - \omega YS_{\text{ch}}^{\text{in}} < M_2(D) - \omega\varphi_0(D)$ with s_0 solution of $\psi_0(s_0) = D$
E_{110}	$(1-\omega)YS_{\text{ch}}^{\text{in}} + S_{\text{H}_2}^{\text{in}} \geqslant \phi_1(D)$, $YS_{\text{ch}}^{\text{in}} > M_0(D, s_2) + M_1(D, s_2)$ with s_2 solution of $\Psi(s_2, D) = (1-\omega)YS_{\text{ch}}^{\text{in}} + S_{\text{H}_2}^{\text{in}}$	$(1-\omega)YS_{\text{ch}}^{\text{in}} + S_{\text{H}_2}^{\text{in}} < \phi_2(D)$, $\frac{\partial\Psi}{\partial s_2}(s_2, D) > 0, \quad \phi_3(D) > 0$
E_{101}	$YS_{\text{ch}}^{\text{in}} > \varphi_0(D)$, $S_{\text{H}_2}^{\text{in}} - \omega YS_{\text{ch}}^{\text{in}} > M_2(D) - \omega\varphi_0(D)$	$YS_{\text{ch}}^{\text{in}} < \varphi_0(D) + \varphi_1(D)$
E_{111}	$(1-\omega)YS_{\text{ch}}^{\text{in}} + S_{\text{H}_2}^{\text{in}} > \phi_2(D)$, $YS_{\text{ch}}^{\text{in}} > \varphi_0(D) + \varphi_1(D)$	$\phi_3(D) \geqslant 0$ or $\phi_3(D) < 0$ and $\phi_4(D, S_{\text{ch}}^{\text{in}}, S_{\text{H}_2}^{\text{in}}) > 0$

- E_{000} always exists and is unstable since the second stability condition in Table 3.8 does not hold, as
$$\mu_2\left(S_{\text{H}_2}^{\text{in}}\right) \simeq 1.0845 > D = 0.01. \tag{3.18}$$
- E_{001} exists, since the existence condition in Table 3.8 holds from (3.18). It is stable if and only if
$$S_{\text{ch}}^{\text{in}} < \varphi_0(D)/Y =: \sigma_3.$$
- E_{100} exists if and only if $\mu_0\left(YS_{\text{ch}}^{\text{in}}, S_{\text{H}_2}^{\text{in}}\right) > D$, which is equivalent to
$$S_{\text{ch}}^{\text{in}} > (M_0(D, S_{\text{H}_2}^{\text{in}}))/Y =: \sigma_1.$$
For $S_{\text{ch}}^{\text{in}} = \sigma_1$, there is a transcritical bifurcation of E_{100} and E_{000}, which have the same components at σ_1 (see Table 3.1). Consider the function $y = F(S_{\text{ch}}^{\text{in}})$ defined by:
$$F(S_{\text{ch}}^{\text{in}}) = \mu_1(YS_{\text{ch}}^{\text{in}} - s_0, S_{\text{H}_2}^{\text{in}} - \omega(YS_{\text{ch}}^{\text{in}} - s_0)), \tag{3.19}$$
where s_0 depends also on $S_{\text{ch}}^{\text{in}}$. The first stability condition of E_{100} in Table 3.8 is written $F\left(S_{\text{ch}}^{\text{in}}\right) < D$. Figure 3.1 shows that this condition holds for all $S_{\text{ch}}^{\text{in}} > \sigma_1$,

since the maximum of the function F is smaller than 0.0013 and $D = 0.01$. From the second stability condition, E_{100} is stable if and only if

$$S_{ch}^{in} > \frac{S_{H_2}^{in} - M_2(D) + \omega\varphi_0(D)}{\omega Y} =: \sigma_4.$$

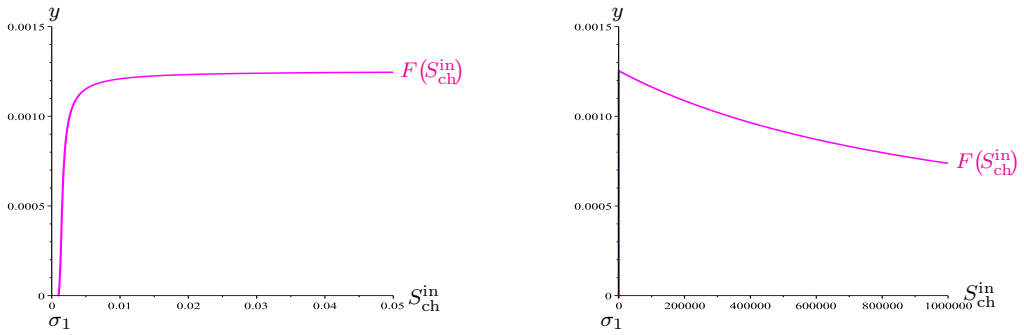

Figure 3.1: Curve of the function $y = F\left(S_{ch}^{in}\right)$ showing that $F\left(S_{ch}^{in}\right) < 0.0013$, for all $S_{ch}^{in} > \sigma_1$.

- Recall that $\omega \simeq 0.53 < 1$ for the set of parameters given in Table 3.3. Therefore, equation $\Psi(s_2, D) = (1-\omega)YS_{ch}^{in} + S_{H_2}^{in}$ admits two solutions s_2^{*1} and s_2^{*2} which correspond to two steady states E_{110}^1 and E_{110}^2, respectively. When it exists, E_{110}^1 is unstable, as stated in Remark 3.1. From Table 3.8, the first existence condition of these steady states holds if and only if

$$S_{ch}^{in} \geq \frac{\phi_1(D) - S_{H_2}^{in}}{(1-\omega)Y} =: \sigma_2.$$

  Figure 3.2 shows that the second existence condition of E_{110}^1 and E_{110}^2 in Table 3.8 holds, for all $S_{ch}^{in} \in [\sigma_2, 0.05]$, since the straight line of equation $y = YS_{ch}^{in}$ is above the curves of the functions $y = M_0\left(D, s_2^{*i}\right) + M_1\left(D, s_2^{*i}\right)$, for $i = 1, 2$, respectively. E_{110}^2 is unstable since the third stability condition does not hold as $\phi_3(D) \simeq -6513 < 0$. Therefore, E_{110}^1 and E_{110}^2 exist and are unstable for all $S_{ch}^{in} \geq \sigma_2$. They disappear for $S_{ch}^{in} < \sigma_2$. For $S_{ch}^{in} = \sigma_2$ there is a saddle-node bifurcation. For $S_{ch}^{in} = \sigma_5$ there is a transcritical bifurcation of E_{110}^1 and E_{111}.

- From Table 3.8, E_{101} exists if and only if

$$\sigma_3 := \frac{\varphi_0(D)}{Y} < S_{ch}^{in} < \frac{S_{H_2}^{in} - M_2(D) + \omega\varphi_0(D)}{\omega Y} =: \sigma_4.$$

  For $S_{ch}^{in} = \sigma_3$, there is a transcritical bifurcation of E_{101} and E_{001}. For $S_{ch}^{in} = \sigma_4$, there is a transcritical bifurcation of E_{101} and E_{100}. When it exists, E_{101} is stable since

$$S_{ch}^{in} < \sigma_4 \simeq 0.011191 < \frac{\varphi_0(D) + \varphi_1(D)}{Y} \simeq 0.013717.$$

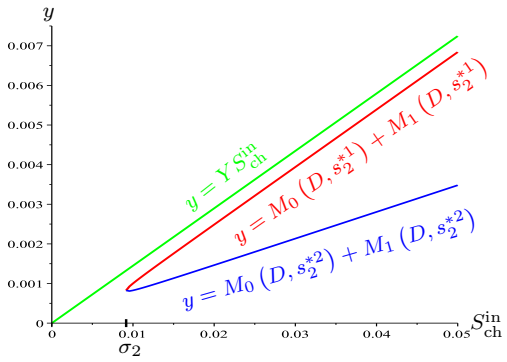

Figure 3.2: The green line of equation $y = Y S^{\text{in}}_{\text{ch}}$ is above the red and blue curves of the functions $M_0(D, s_2^{*i}) + M_1(D, s_2^{*i})$, $i = 1, 2$.

- From Table 3.8, E_{111} exists if and only if

$$S^{\text{in}}_{\text{ch}} > \frac{\phi_2(D) - S^{\text{in}}_{\text{H}_2}}{(1-\omega)Y} =: \sigma_5 \simeq 0.016575, \quad S^{\text{in}}_{\text{ch}} > \frac{\varphi_0(D) + \varphi_1(D)}{Y} \simeq 0.013717.$$

  Then, E_{111} exists if and only if $S^{\text{in}}_{\text{ch}} > \sigma_5$. For the stability of E_{111}, we have $\phi_3(D) < 0$ and we plot the functions ϕ_4 with respect to $S^{\text{in}}_{\text{ch}}$. Figure 3.3 shows that the equation $\phi_4(S^{\text{in}}_{\text{ch}}) = 0$ has a unique solution $\sigma_6 \simeq 0.029877$ such that $\phi_4(S^{\text{in}}_{\text{ch}}) < 0$, for all $\sigma_5 < S^{\text{in}}_{\text{ch}} < \sigma_6$ and $\phi_4(S^{\text{in}}_{\text{ch}}) > 0$, for all $S^{\text{in}}_{\text{ch}} > \sigma_6$.

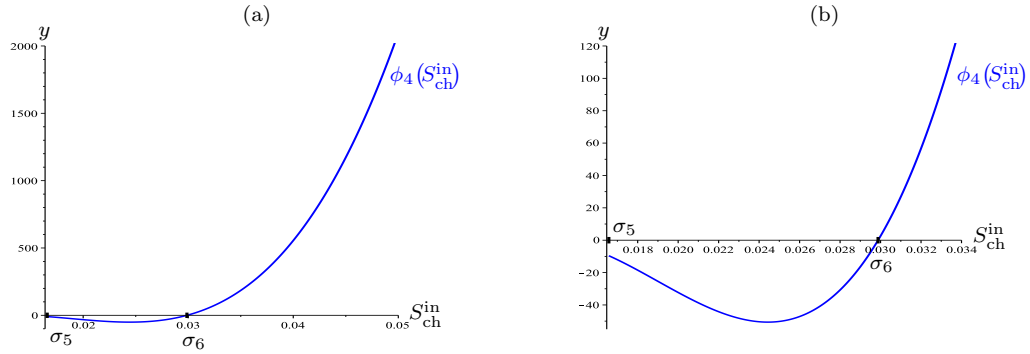

Figure 3.3: (a) Curve of the function ϕ_4, for $S^{\text{in}}_{\text{ch}} > \sigma_5$ and the solution σ_6 of equation $\phi_4\left(S^{\text{in}}_{\text{ch}}\right) = 0$. (b) Magnification for $S^{\text{in}}_{\text{ch}} \in (\sigma_5, 0.034)$.

To give numerical evidence of the Hopf bifurcation occurring through the positive steady state E_{111} as $S^{\text{in}}_{\text{ch}}$ varies, we determine the eigenvalues of the matrix $\mathbf{J_1}$ defined by (3.6) and evaluated at this steady state. Figure 3.4(a) shows that one eigenvalue $\lambda_1\left(S^{\text{in}}_{\text{ch}}\right)$ remains negative for all $S^{\text{in}}_{\text{ch}} \in (\sigma_5, 0.05]$. Figure 3.4(b) shows that the two other eigenvalues are real and distinct for all $S^{\text{in}}_{\text{ch}} \in (\sigma_5, \sigma^\star)$ and we denote them by $\lambda_2\left(S^{\text{in}}_{\text{ch}}\right)$ and $\lambda_3\left(S^{\text{in}}_{\text{ch}}\right)$, then, they become a complex-conjugate pair for all $S^{\text{in}}_{\text{ch}} \in (\sigma^\star, 0.05)$, and we denote them by

$$\lambda_{2,3}\left(S^{\text{in}}_{\text{ch}}\right) = \alpha\left(S^{\text{in}}_{\text{ch}}\right) \pm i\beta\left(S^{\text{in}}_{\text{ch}}\right),$$

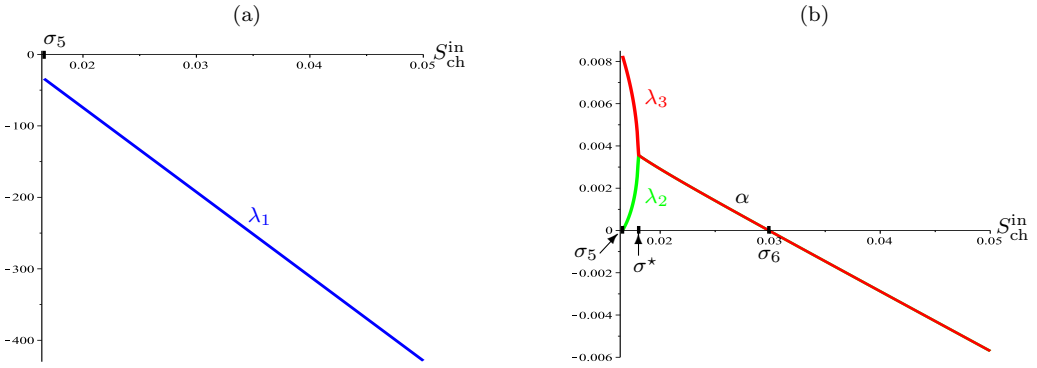

Figure 3.4: Three eigenvalues of the matrix $\mathbf{J_1}$ evaluated at E_{111} as functions of S_{ch}^{in}. (b) Real part of the pair of eigenvalues $\lambda_{2,3}$, for $S_{ch}^{in} \in (\sigma^\star, 0.05]$ where $\sigma^\star = 0.018$.

which becomes purely imaginary for the particular value $S_{ch}^{in} = \sigma_6$ such that $\alpha(\sigma_6) = 0$, with $\beta(\sigma_6) \neq 0$. Moreover, one has

$$\frac{d\alpha}{dS_{ch}^{in}}(\sigma_6) < 0.$$

Therefore, E_{111} changes its stability through a supercritical Hopf bifurcation with the emergence of a stable limit cycle.

□

To detect the limit cycle, we take an initial condition closes enough to the positive steady state E_{111} of size order $\varepsilon = 10^{-2}$. Figures 3.5 and 3.6 depict the bifurcation

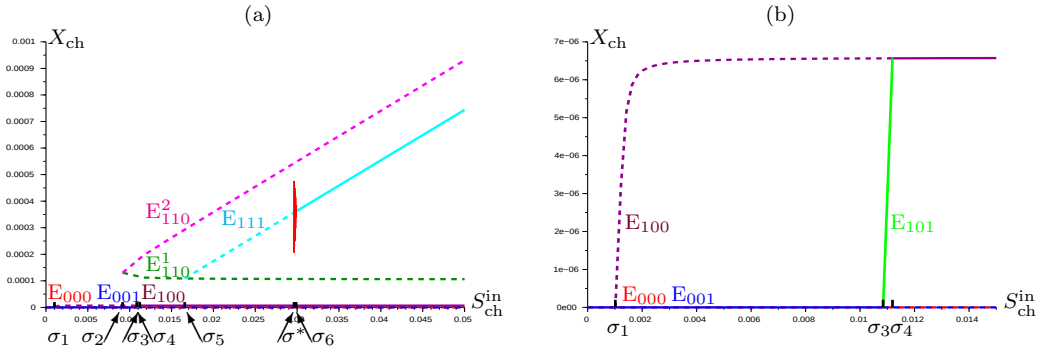

Figure 3.5: (a) Projections of the ω-limit set in variable X_{ch} as a function of $S_{ch}^{in} \in [0, 0.05]$. (b) Magnification of the transcritical bifurcations occurring at σ_1, σ_3 and σ_4 when $S_{ch}^{in} \in [0, 0.015]$.

diagrams of system (2.1) where X_{ch} and X_{H_2} are represented as functions of the bifurcation parameter S_{ch}^{in} and show the existence of a stable limit cycle for a certain range of the values of S_{ch}^{in}. Figures 3.5(b), 3.6(b) and 3.7 show magnifications of the bifurcation diagrams illustrating the transcritical bifurcations occurring at σ_1, σ_3, σ_4 and σ_5, the saddle-node bifurcation occurring at σ_2, the Hopf bifurcation occurring at σ_6, and the disappearance

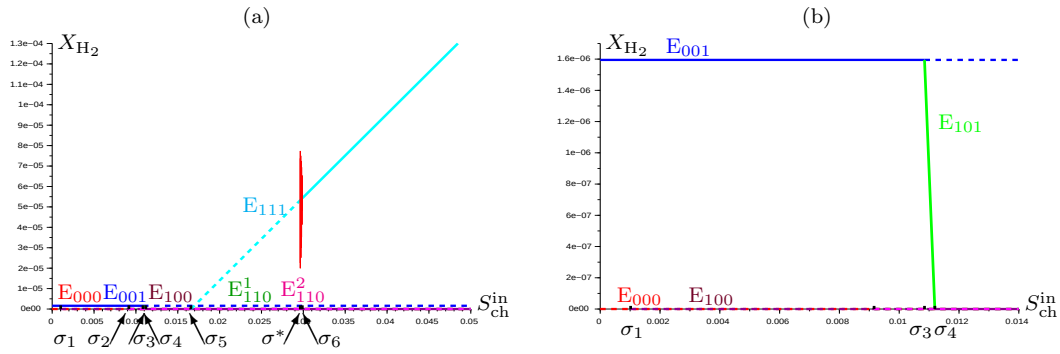

Figure 3.6: (a) Projections of the ω-limit set in variable X_{H_2} as functions of $S^{in}_{ch} \in [0, 0.11]$, reveal the occurrence and disappearance of stable limit cycles. (b) Magnification of the transcritical bifurcations when $S^{in}_{ch} \in [0, 0.018]$.

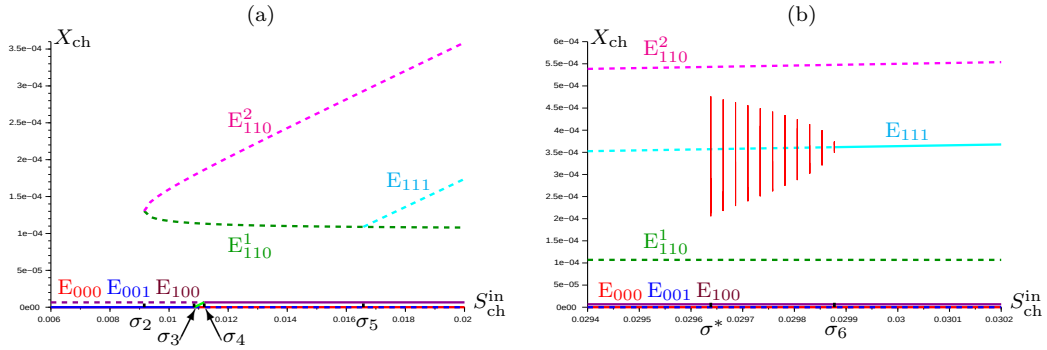

Figure 3.7: (a) Magnification of saddle-node bifurcation at $S^{in}_{ch} = \sigma_2$ and the transcritical bifurcation at $S^{in}_{ch} = \sigma_5$ when $S^{in}_{ch} \in [0.006, 0.02]$. (b) Magnification of the appearance and disappearance of stable limit cycles when $S^{in}_{ch} \in [0.0294, 0.0302]$.

of the cycle occurring at σ^*. In Figure 4.13(b), the steady states E_{000} and E_{001} cannot be distinguished since they have both a zero X_{ch}-component. Since for $S^{in}_{ch} < \sigma_3$, E_{001} is stable and E_{000} is unstable, the $X_{ch} = 0$ axis is plotted in blue, which is the color for E_{001} in Table 3.9. In Figure 3.6(b) E_{000} and E_{001} are distinguished but it is not the case for E_{000} and E_{100}, since they have both a zero X_{H_2}-component. As E_{100} is stable and E_{000} is unstable for $S^{in}_{ch} > \sigma_4$, the $X_{H_2} = 0$ axis is plotted in purple as the color of E_{100} in Table 3.9.

Table 3.9: Colors used in Figures 3.5 and 3.7. The solid (resp. dashed) lines are used for stable (resp. unstable) steady states.

E_{000}	E_{001}	E_{100}	E^1_{110}	E^2_{110}	E_{101}	E_{111}
Red	Blue	Purple	Dark Green	Magenta	Green	Cyan

In [57], a numerical study of the bifurcation diagram with respect to the parameter D is given in the case without maintenance and $s^{in}_1 = s^{in}_2 = 0$. Figure 6 in [57] shows that the disappearance of the stable limit cycle occurs through a saddle-node bifurcation with

another unstable limit cycle. We conjecture that in our case also the stable limit cycle disappears by a confluence with an unstable limit cycle at $S_{\mathrm{ch}}^{\mathrm{in}} = \sigma^*$.

3.5 Numerical simulations

We present in this section, several numerical simulations which illustrate the main results of the last section namely the bistability with convergence either to E_{100} or to a stable limit cycle according to the initial conditions, when $S_{\mathrm{ch}}^{\mathrm{in}} \in (\sigma^*, \sigma_6)$, and bistability with convergence toward E_{100} or E_{111}, when $S_{\mathrm{ch}}^{\mathrm{in}} > \sigma_6$.

For the numerical simulations presented in the following figures, we used the dimensionless form of (2.1) used in [64]. Indeed, in the original form (2.1), numerical instabilities arise in numerical schemes. To reduce the number of parameters describing the dynamics and facilitate numerical simulations, the following rescaling of the variables was used in [64]:

$$\begin{aligned} N_0 &= \frac{X_{\mathrm{ch}}}{K_{\mathrm{S,ch}} Y_{\mathrm{ch}}}, \quad N_1 = \frac{X_{\mathrm{ph}}}{K_{\mathrm{S,ph}} Y_{\mathrm{ph}}}, \quad N_2 = \frac{X_{\mathrm{H_2}}}{K_{\mathrm{S,H_2}} Y_{\mathrm{H_2}}}, \\ R_0 &= \frac{S_{\mathrm{ch}}}{K_{\mathrm{S,ch}}}, \quad R_1 = \frac{S_{\mathrm{ph}}}{K_{\mathrm{S,ph}}}, \quad R_2 = \frac{S_{\mathrm{H_2}}}{K_{\mathrm{S,H_2}}}, \quad \tau = k_{\mathrm{m,ch}} Y_{\mathrm{ch}} t. \end{aligned} \tag{3.20}$$

Then, with these changes of variables, the system given in (2.1) reduced to system

$$\begin{cases} \frac{dN_0}{d\tau} = (\nu_0(R_0, R_2) - \alpha - k_0) N_0 \\ \frac{dN_1}{d\tau} = (\nu_1(R_1, R_2) - \alpha - k_1) N_1 \\ \frac{dN_2}{d\tau} = (\nu_2(R_2) - \alpha - k_2) N_2 \\ \frac{dR_0}{d\tau} = \alpha(u_0 - R_0) - \nu_0(R_0, R_2) N_0 \\ \frac{dR_1}{d\tau} = \alpha(u_1 - R_1) + \omega_0 \nu_0(R_0, R_2) N_0 - \nu_1(R_1, R_2) N_1 \\ \frac{dR_2}{d\tau} = \alpha(u_2 - R_2) - \omega_2 \nu_0(R_0, R_2) N_0 + \omega_1 \nu_1(R_1, R_2) N_1 - \nu_2(R_2) N_2. \end{cases} \tag{3.21}$$

The operating parameters are

$$\alpha = \frac{D}{k_{\mathrm{m,ch}} Y_{\mathrm{ch}}}, \quad u_0 = \frac{S_{\mathrm{ch}}^{\mathrm{in}}}{K_{\mathrm{S,ch}}}, \quad u_1 = \frac{S_{\mathrm{ph}}^{\mathrm{in}}}{K_{\mathrm{S,ph}}}, \quad u_2 = \frac{S_{\mathrm{H_2}}^{\mathrm{in}}}{K_{\mathrm{S,H_2}}}.$$

The yield coefficients are

$$\omega_0 = \frac{K_{\mathrm{S,ch}}}{K_{\mathrm{S,ph}}} \frac{224}{208} (1 - Y_{\mathrm{ch}}), \quad \omega_1 = \frac{K_{\mathrm{S,ph}}}{K_{\mathrm{S,H_2}}} \frac{32}{224} (1 - Y_{\mathrm{ph}}), \quad \omega_2 = \frac{16}{208} \frac{K_{\mathrm{S,ch}}}{K_{\mathrm{S,H_2}}}.$$

The death rates are

$$k_0 = \frac{k_{\mathrm{dec,ch}}}{k_{\mathrm{m,ch}} Y_{\mathrm{ch}}}, \quad k_1 = \frac{k_{\mathrm{dec,ph}}}{k_{\mathrm{m,ch}} Y_{\mathrm{ch}}}, \quad k_2 = \frac{k_{\mathrm{dec,H_2}}}{k_{\mathrm{m,ch}} Y_{\mathrm{ch}}}.$$

The growth functions are

$$\nu_0(R_0, R_2) = \frac{R_0}{1 + R_0} \frac{R_2}{K_P + R_2}, \ \nu_1(R_1, R_2) = \frac{\phi_1 R_1}{1 + R_1} \frac{R_2}{1 + K_I R_2}, \ \nu_2(R_2) = \frac{\phi_2 R_2}{1 + R_2}, \tag{3.22}$$

where the biological parameters are given by

$$\phi_1 = \frac{k_{\mathrm{m,ph}} Y_{\mathrm{ph}}}{k_{\mathrm{m,ch}} Y_{\mathrm{ch}}}, \quad \phi_2 = \frac{k_{\mathrm{m,H_2}} Y_{\mathrm{H_2}}}{k_{\mathrm{m,ch}} Y_{\mathrm{ch}}}, \quad K_P = \frac{K_{\mathrm{S,H_2,C}}}{K_{\mathrm{S,H_2}}}, \quad K_I = \frac{K_{\mathrm{S,H_2}}}{K_{\mathrm{I,H_2}}}.$$

For this section, we put $k_i = 0$, for $i = 0, 1, 2$ in (3.21). In the following, the projections of the orbits of the six-dimensional phase space into the three-dimensional space $(X_{\mathrm{ch}}, X_{\mathrm{ph}}, X_{\mathrm{H_2}})$ illustrate the appearance and disappearance of limit cycles for different values of $S_{\mathrm{ch}}^{\mathrm{in}}$ where E_{000}, E_{001}, E_{110}^1 and E_{110}^2 are unstable. Then, we have the following possible pictures.

- For $S_{\mathrm{ch}}^{\mathrm{in}} \in (\sigma_5, \sigma^*)$, E_{111} is a saddle-focus and the numerical simulations show the convergence for any initial condition to the stable node E_{100}, where there is the competitive exclusion of the second and third species. Figure 3.8 shows the convergence to

  $$\mathrm{E}_{100} \simeq (6.582 \times 10^{-6}, 0, 0, 0.029204, 3.660 \times 10^{-4}, 5.38 \times 10^{-8}),$$

  for an initial condition in a neighborhood of

  $$\mathrm{E}_{111} \simeq (3.55 \times 10^{-4}, 6.69 \times 10^{-4}, 5.29 \times 10^{-5}, 0.0108, 0.00303, 1.2 \times 10^{-7}),$$

  of size order 2×10^{-3}.

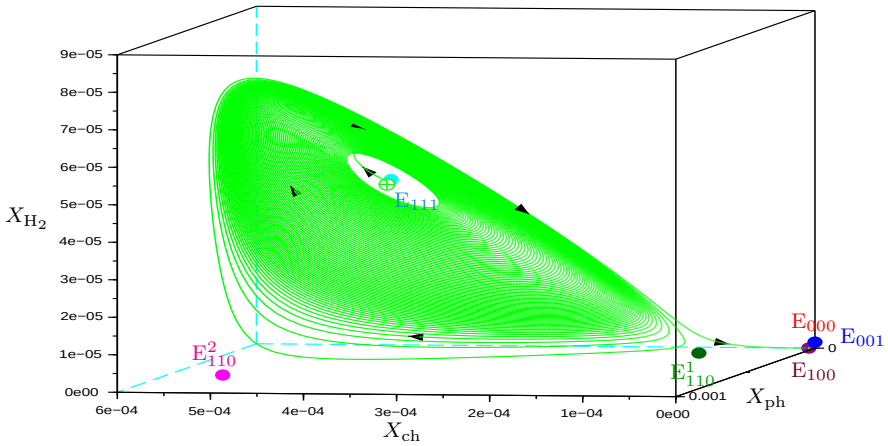

Figure 3.8: Case $S_{\mathrm{ch}}^{\mathrm{in}} = 0.02955 < \sigma^*$: the solution of (2.1) converges to E_{100}.

- For $S_{\mathrm{ch}}^{\mathrm{in}} \in (\sigma^*, \sigma_6)$, the system exhibits sustained oscillations, which implies that limit cycle is stable. Figure 3.9 shows bistability with two basins of attraction: one toward the limit cycle and the second toward E_{100}. Indeed, for initial conditions in a neighborhood of

  $$\mathrm{E}_{111} \simeq (0.539, 0.089, 59.995, 0.257, 0.032, 0.014),$$

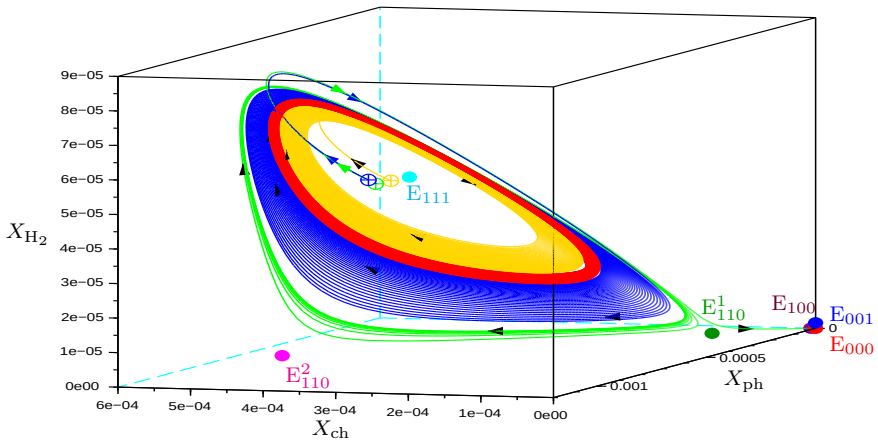

Figure 3.9: Case $S^{in}_{ch} = 0.029639 \in (\sigma^*, \sigma_6)$: bistability of the limit cycle (in red) and E_{100}.

of size order 5.5×10^{-3} and 9.8×10^{-3}, the trajectories in yellow and blue converge toward the stable limit cycle in red, while the green trajectory converges toward the steady state

$$E_{100} \simeq (0.002, 0, 0, 1.870, 0.001, 0.003),$$

for the initial condition in a neighborhood of E_{111} of size order 1.001×10^{-2}.

- For $S^{in}_{ch} > \sigma_6$, E_{111} changes its stability and becomes a stable focus point via a supercritical Hopf bifurcation. Figure 3.10 shows the bistability of

$$E_{100} \simeq (4.8 \times 10^{-8}, 0, 0, 0.0347, 3.66 \times 10^{-4}, 0.00351) \quad \text{and}$$
$$E_{111} \simeq (4.59 \times 10^{-4}, 8.99 \times 10^{-4}, 7.51 \times 10^{-5}, 0.0108, 0.00303, 1.2 \times 10^{-7}),$$

where the blue trajectory converges to the stable focus E_{111} for the initial condition in a neighborhood of E_{111} of size order 2.1×10^{-2}, and the green trajectory converges to E_{100} for the initial condition in a neighborhood of E_{111} of size order 4×10^{-2}.

Figure 3.11 illustrates the time course of system (2.1) in the case of exclusion of the second and the third species and the convergence to the steady state E_{100}. Figure 3.12 illustrates a positive, periodic, solution representing the coexistence of the three species. The sustained oscillations prove the stability of the limit cycle. However, Figure 3.13 shows the time course of the green trajectory in Figure 3.9. Finally, Figure 3.14 illustrates the convergence of the positive steady state which becomes a stable focus. Figure 3.15 shows the time course of the green trajectory in Figure 3.10.

Remark 3.2. The plots of Figures 3.1 to 3.4 were performed with Maple [35], which is used, in particular, for the computations the eigenvalues of the Jacobian matrix evaluated at E_{111}. The plots of Figures 3.5 to 3.7 were performed with Scilab [54] by using the formulas of the steady state components given in Table 3.4. The plots of Figures 3.8 to 3.15 were performed with Scilab [54], which the trajectories in these figures presented according to

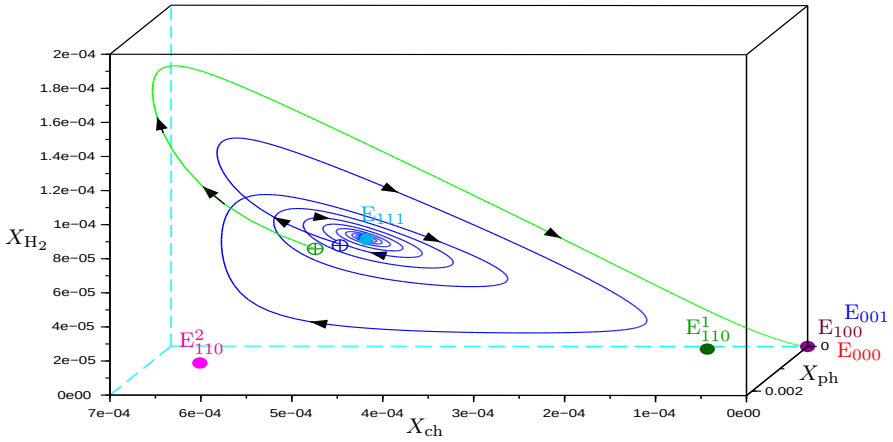

Figure 3.10: The case $\sigma_6 < S^{in}_{ch} = 0.035$: bistability with convergence either to E_{111} or to E_{100}.

the variables of model (2.1), using the change of variables (3.20). The plot of the limit cycle was obtained by solving the ordinary differential equations using the default solver "*lsoda*" from the ODEPACK package in Scilab.

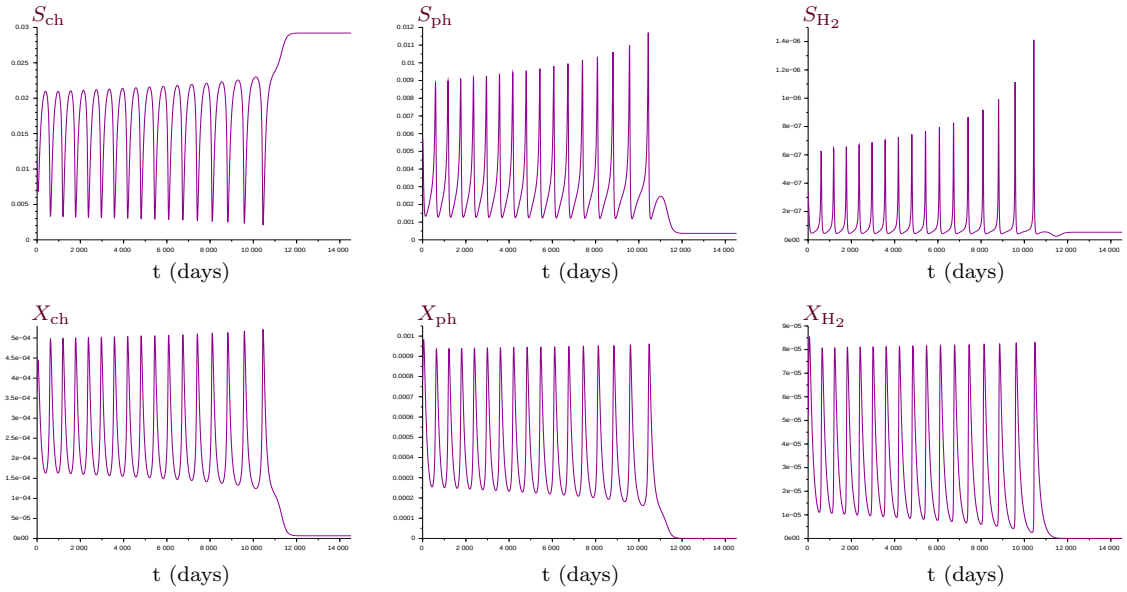

Figure 3.11: Trajectories of $S_{ch}, S_{ph}, S_{H_2}, X_{ch}, X_{ph}$ and X_{H_2} for $S^{in}_{ch} = 0.02955$ (in kgCOD/m^3): Convergence to the stable steady state E_{100}.

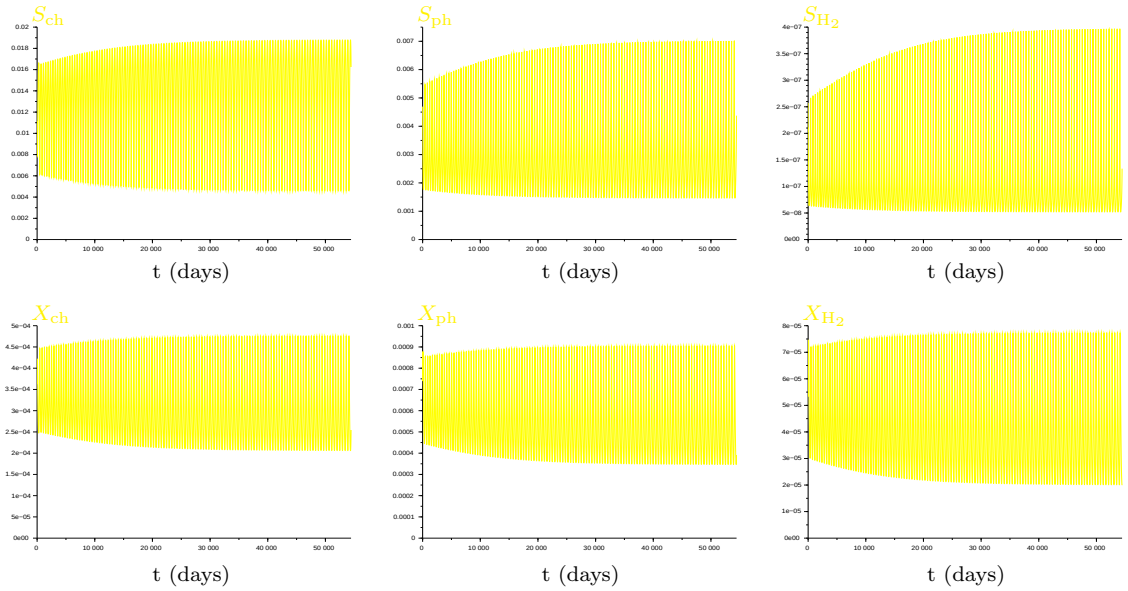

Figure 3.12: Trajectories of $S_{ch}, S_{ph}, S_{H_2}, X_{ch}, X_{ph}$ and X_{H_2} for $S_{ch}^{in} = 0.029639$ (in kgCOD/m^3): Convergence to the stable limit cycle.

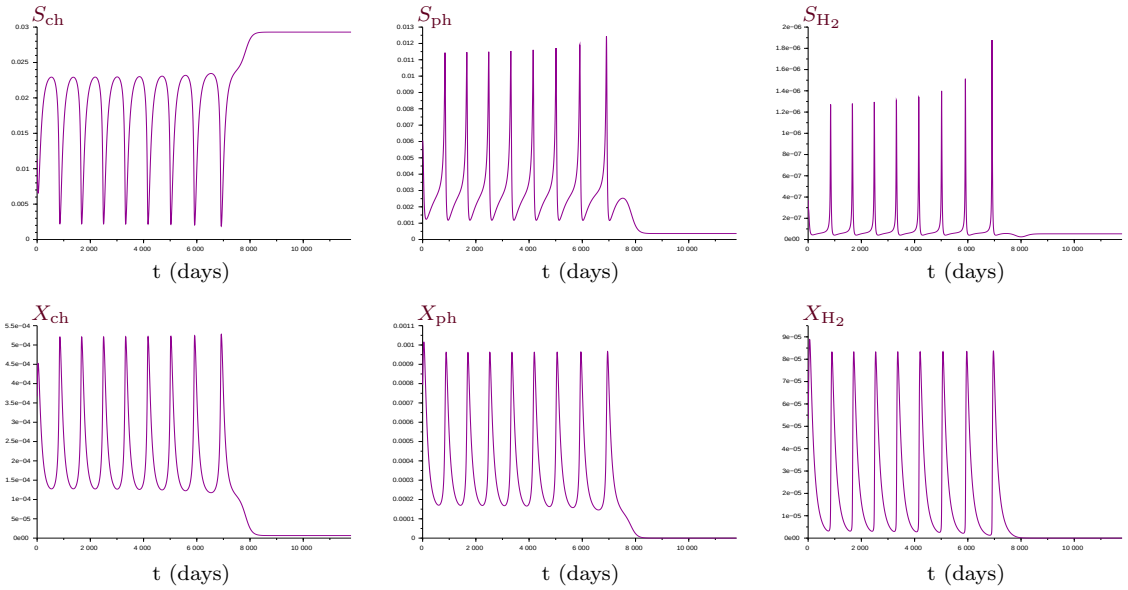

Figure 3.13: Trajectories of $S_{ch}, S_{ph}, S_{H_2}, X_{ch}, X_{ph}$ and X_{H_2} for $S_{ch}^{in} = 0.029639$ (in kgCOD/m^3): Convergence to the stable steady state E_{100}.

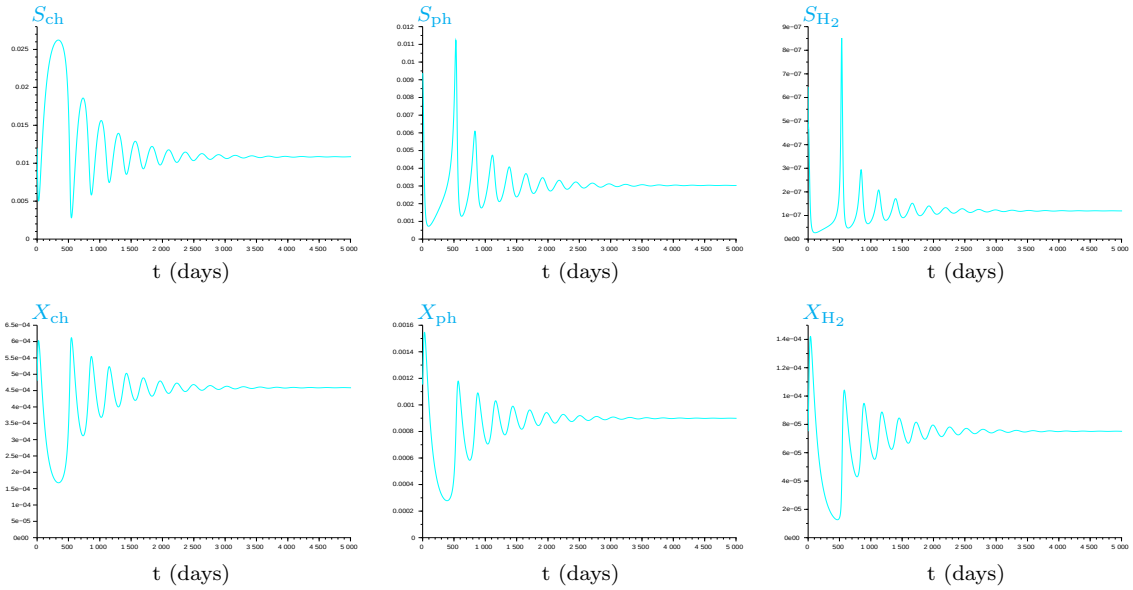

Figure 3.14: Trajectories of $S_{ch}, S_{ph}, S_{H_2}, X_{ch}, X_{ph}$ and X_{H_2} for $S_{ch}^{in} = 0.035$ (in kgCOD/m^3): Convergence to the positive steady state E_{111}.

3.6 Conclusion

In this chapter, we were interested in determining the local stability of the steady states of the three-tiered model (2.1), in the particular case where maintenance is ignored. We consider general growth rates. The phenol and the hydrogen input concentrations are taken into account. We analytically determined the necessary and sufficient conditions of stability of all steady states according to the operating parameters. We have analyzed the bifurcation diagrams of system (2.1) by varying the chlorophenol input concentration when $s_1^{in} = 0$. It shows that the system exhibits a bi-stability where the coexistence steady state can destabilize undergoing a supercritical Hopf bifurcation with the occurrence of a stable limit cycle. These interesting phenomena have been already depicted in [51], in the particular case $s_0^{in} > 0$ and $s_1^{in} = s_2^{in} = 0$. The possibility of the Hopf bifurcation of the positive steady state is analytically proved in [57], in the case without maintenance. The destabilization of the positive steady state was not detected by the numerical analysis of the operating diagrams in [64].

We focus in chapter 4 on the analysis of the stability of system (2.1), by considering the maintenance terms, where the system cannot be reduced to a three-dimensional one, and we illustrate the effects of the maintenance terms on the behavior of the process.

The results of this chapter have been published in [40].

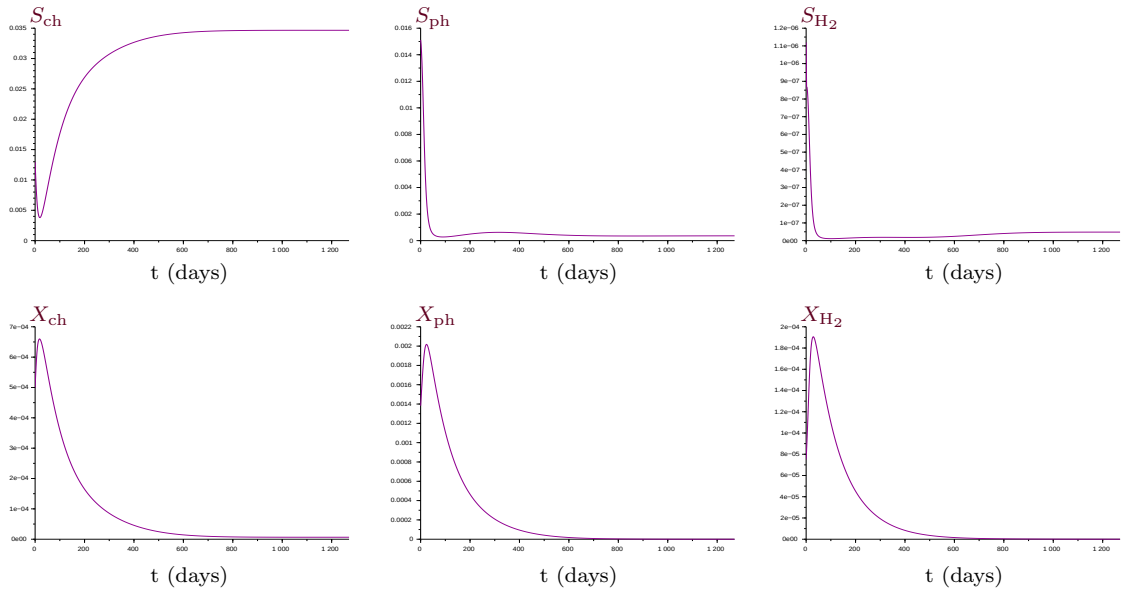

Figure 3.15: Trajectories of $S_{\text{ch}}, S_{\text{ph}}, S_{\text{H}_2}, X_{\text{ch}}, X_{\text{ph}}$ and X_{H_2} for $S_{\text{ch}}^{\text{in}} = 0.035$ (in kgCOD/m^3): Convergence to the steady state E_{100}.

CHAPTER

4 Stability of the three-tiered food-web model with decay

Summary

4.1 Introduction

In this chapter, we describe the local stability analysis of the three-tiered microbial model in the case including decay terms. In this case, we cannot reduce it to a three-dimensional one.

This chapter is structured as follows. In section 4.2, we give the necessary and sufficient local stability properties of all steady states. We give the bifurcation diagrams with respect to the dilution rate, first, and then to the chlorophenol input concentration as the bifurcating parameters in section 4.4. We illustrate our results by numerical simulations in section 4.5.

4.2 Local stability of the steady states

In this section, we are interested to study analytically the local stability of each steady state of system (2.8). In view of using the Liénard-Chipart stability criterion. The asymptotic stability of E_{111} requires a new definition and notations.

$$J = \mu_0(s_0, s_2), \quad K = \mu_1(s_1, s_2), \quad L = \mu_2(s_2). \tag{4.1}$$

Definition 4.1. *The characteristic polynomial of the matrix Jacobian for system (2.8) evaluted at* E_{111} *is given by:*

$$P_6(\lambda) = \lambda^6 + c_1\lambda^5 + c_2\lambda^4 + c_3\lambda^3 + c_4\lambda^2 + c_5\lambda + c_6,$$

where the c_i *are defined in Table 4.1.*

Our main result is stated in Theorem 4.1. To prove our statement, we need the Liénard-Chipart stability criterion (see Gantmacher [24], Theorem 11) which represents almost half that of the Routh-Hurwitz theorem which facilitates the study of the asymptotic behavior of dynamic systems especially for dimensions beyond five. It is known that for a polynomial of degree four the Routh-Hurwitz conditions can be written as in the following Lemmas, see, for instance, Theorem 11 [12].

Lemma 4.1. *Consider the fourth-order polynomial* $P(\lambda)$ *with real coefficients given by:*

$$P(\lambda) = c_0\lambda^4 + c_1\lambda^3 + c_2\lambda^2 + c_3\lambda + c_4.$$

All of the roots of the polynomial $P(\lambda)$ *have a negative real part if and only if*

$$c_i > 0, \quad \textit{for} \quad i = 1, 3, 4 \quad \textit{and} \quad r_1 = c_3r_0 - c_1^2c_4 > 0, \tag{4.2}$$

where $r_0 = c_1c_2 - c_0c_3$.

Table 4.1: The Liénard-Chipart coefficients for E_{111}. The functions E, F, G, H, I, J, K and L, defined by (3.3) and (4.1), are evaluated at the components of E_{111} given in Table 2.1. Notice that they are depending on the operating parameter D.

$$
\begin{aligned}
c_1 &= 3D + (E + Fw)x_0 + (G + H)x_1 + Ix_2 \\
c_2 &= 3D^2 + (2D + J)(E + \omega F)x_0 + (2D + K)(G + H)x_1 + EIx_0x_2 + GIx_1x_2 \\
&\quad +(2D + L)Ix_2 + (E(G + H) - (1 - \omega)FG)x_0x_1 \\
c_3 &= D^3 + D(D + 2J)(E + \omega F)x_0 + D(D + 2K)(G + H)x_1 + D(D + 2L)Ix_2 \\
&\quad +EI(D + J + L)x_0x_2 + GI(D + K + L)x_1x_2 + EGIx_0x_1x_2 + (E(G + H) \\
&\quad -(1 - \omega)FG)(D + J + K)x_0x_1 \\
c_4 &= D^2(E + \omega F)Jx_0 + D^2(G + H)Kx_1 + D^2ILx_2 + EI(DJ + DL + JL)x_0x_2 \\
&\quad +GI\left(DK + DL + KL\right)x_1x_2 + EGI(J + K + L)x_0x_1x_2 + (E(G + H) \\
&\quad -(1 - \omega)FG)(DJ + DK + JK)x_0x_1 \\
c_5 &= DEIJLx_0x_2 + DGIKLx_1x_2 + D(E(G + H) - (1 - \omega)FG)JKx_0x_1 \\
&\quad +EGI\left(JK + JL + KL\right)x_0x_1x_2 \\
c_6 &= EGIJKLx_0x_1x_2 \\
\hline
r_0 &= c_1c_2 - c_3, \quad r_1 = c_1c_4 - c_5, \quad r_2 = c_3r_0 - c_1r_1, \quad r_3 = c_5r_0 - c_1^2c_6 \\
r_4 &= r_1r_2 - r_0r_3, \quad r_5 = r_3r_4 - c_1c_6r_2^2
\end{aligned}
$$

Proof. From the Liénard-Chipart stability criterion (see Gantmacher [24], Theorem 11), all of the roots of the polynomial P have a negative real part if and only if

$$c_i > 0, \quad i = 1, 3, 4, \quad \det(\Delta_2) > 0 \quad \text{and} \quad \det(\Delta_4) > 0, \tag{4.3}$$

where Δ_2 and Δ_4 are the Hurwitz matrices defined by:

$$\Delta_2 = \begin{bmatrix} c_1 & c_3 \\ c_0 & c_2 \end{bmatrix} \quad \text{and} \quad \Delta_4 = \begin{bmatrix} c_1 & c_3 & 0 & 0 \\ c_0 & c_2 & c_4 & 0 \\ 0 & c_1 & c_3 & 0 \\ 0 & c_0 & c_2 & c_4 \end{bmatrix}.$$

Conditions (4.3) are equivalent to

$$c_i > 0, \quad i = 1, 3, 4, \quad r_0 = c_1c_2 - c_0c_3 > 0 \quad \text{and} \quad r_1 = c_3r_0 - c_1^2c_4 > 0. \tag{4.4}$$

When all conditions (4.4) hold, the condition $r_1 > 0$ implies that $r_0 > 0$. Thus, conditions (4.4) are equivalent to (4.2).

□

Lemma 4.2. *Consider the six-order polynomial $P(\lambda)$ with real coefficients given by:*

$$P(\lambda) = c_0\lambda^6 + c_1\lambda^5 + c_2\lambda^4 + c_3\lambda^3 + c_4\lambda^2 + c_5\lambda + c_6.$$

All of the roots of the polynomial $P(\lambda)$ have a negative real part if and only if

$$c_i > 0, \quad i = 1, 3, 5, 6, \quad r_4 > 0 \quad \textit{and} \quad r_5 > 0, \tag{4.5}$$

where $r_4 = r_1 r_2 - r_0 r_3$ *and* $r_5 = r_3 r_4 - c_1 c_6 r_2^2$, *with*

$$r_0 = c_1 c_2 - c_0 c_3, \; r_1 = c_1 c_4 - c_0 c_5, \; r_2 = c_3 r_0 - c_1 r_1 \; \textit{and} \; r_3 = c_5 r_0 - c_1^2 c_6.$$

Proof. From the Liénard-Chipart stability criterion (see Gantmacher [24], Theorem 11), all of the roots of the polynomial P have a negative real part if and only if

$$c_i > 0, \quad i = 1, 3, 5, 6, \quad \det(\Delta_2) > 0, \quad \det(\Delta_4) > 0 \quad \text{and} \quad \det(\Delta_6) > 0, \tag{4.6}$$

where Δ_2, Δ_4 and Δ_6 are the Hurwitz matrices defined by:

$$\Delta_2 = \begin{bmatrix} c_1 & c_3 \\ c_0 & c_2 \end{bmatrix}, \; \Delta_4 = \begin{bmatrix} c_1 & c_3 & c_5 & 0 \\ c_0 & c_2 & c_4 & c_6 \\ 0 & c_1 & c_3 & c_5 \\ 0 & c_0 & c_2 & c_4 \end{bmatrix}, \; \Delta_6 = \begin{bmatrix} c_1 & c_3 & c_5 & 0 & 0 & 0 \\ c_0 & c_2 & c_4 & c_6 & 0 & 0 \\ 0 & c_1 & c_3 & c_5 & 0 & 0 \\ 0 & c_0 & c_2 & c_4 & c_6 & 0 \\ 0 & 0 & c_1 & c_3 & c_5 & 0 \\ 0 & 0 & c_0 & c_2 & c_4 & c_6 \end{bmatrix}.$$

Conditions (4.6) are equivalent to

$$c_i > 0, \; i = 1, 3, 5, 6, \; r_0 > 0, \; r_4 = r_1 r_2 - r_0 r_3 > 0, \; r_5 = r_3 r_4 - c_1 c_6 r_2^2 > 0. \tag{4.7}$$

When all conditions (4.7) hold, the condition $r_5 > 0$ implies that $r_3 > 0$, that is, $c_5 r_0 > c_6 c_1^2$ which implies that $r_0 > 0$. Hence, conditions (4.7) are equivalent to (4.5).

□

We can now state and prove our main result.

Theorem 4.1. *Assume that* **H1** *to* **H8** *hold. The necessary and sufficient conditions of local stability of the steady states of* (2.8) *when the maintenance is included are given in Table 4.2.*

Proof. The local stability of the steady states is determined by the eigenvalues of the Jacobian matrix of system (2.8) evaluated at the steady state. The Jacobian matrix of (2.8) corresponds to the 6×6 matrix:

$$\mathcal{J} = \begin{bmatrix} J - D - a_0 & 0 & 0 & Ex_0 & 0 & Fx_0 \\ 0 & K - D - a_1 & 0 & 0 & Gx_1 & -Hx_1 \\ 0 & 0 & L - D - a_2 & 0 & 0 & Ix_2 \\ -J & 0 & 0 & -D - Ex_0 & 0 & -Fx_0 \\ J & -K & 0 & Ex_0 & -D - Gx_1 & Fx_0 + Hx_1 \\ -\omega J & K & -L & -\omega Ex_0 & Gx_1 & -D - \omega Fx_0 - Hx_1 - Ix_2 \end{bmatrix},$$

where the functions E, F, G, H, I, J, K and L are defined by (3.3) and (4.1), and are evaluated at the steady state.

Table 4.2: The necessary and sufficient conditions of local stability of steady states of (2.8).

	Stability conditions
E_{000}	$\mu_0\left(s_0^{in}, s_2^{in}\right) < D + a_0$, $\mu_1\left(s_1^{in}, s_2^{in}\right) < D + a_1$, $\mu_2\left(s_2^{in}\right) < D + a_2$
E_{001}	$s_0^{in} < \varphi_0(D)$ and $s_1^{in} < \varphi_1(D)$
E_{100}	$\mu_1\left(s_0^{in} + s_1^{in} - s_0, s_2^{in} - \omega\left(s_0^{in} - s_0\right)\right) < D + a_1$ and $s_2^{in} - \omega s_0^{in} < M_2(D + a_2) - \omega\varphi_0(D)$, with s_0 solution of equation $\psi_0(s_0) = D + a_0$.
E_{110}	$(1-\omega)s_0^{in} + s_1^{in} + s_2^{in} < \phi_2(D)$, $\phi_3(D) > 0$ and $\frac{\partial \Psi}{\partial s_2}(s_2, D) > 0$, with s_2 solution of equation $\Psi(s_2, D) = (1-\omega)s_0^{in} + s_1^{in} + s_2^{in}$.
E_{101}	$s_0^{in} + s_1^{in} < \varphi_0(D) + \varphi_1(D)$
E_{111}	$c_3 > 0$, $c_5 > 0$, $r_4 > 0$ and $r_5 > 0$
E_{010}	$s_1^{in} + s_2^{in} < M_3\left(s_0^{in}, D + a_0\right) + M_1\left(D + a_1, M_3\left(s_0^{in}, D + a_0\right)\right)$ $s_1^{in} + s_2^{in} < M_2(D + a_2) + \varphi_1(D)$
E_{011}	$s_0^{in} < \varphi_0(D)$

For E_{000}, the Jacobian matrix $\mathcal{J}$ evaluated at E_{000} is:

$$\mathcal{J} = \begin{bmatrix} J - D - a_0 & 0 & 0 & 0 & 0 & 0 \\ 0 & K - D - a_1 & 0 & 0 & 0 & 0 \\ 0 & 0 & L - D - a_2 & 0 & 0 & 0 \\ -J & 0 & 0 & -D & 0 & 0 \\ J & -K & 0 & 0 & -D & 0 \\ -\omega J & K & -L & 0 & 0 & -D \end{bmatrix}.$$

Thus, E_{000} is stable if and only if

$$\mu_0\left(s_0^{in}, s_2^{in}\right) < D + a_0, \quad \mu_1\left(s_1^{in}, s_2^{in}\right) < D + a_1 \quad \text{and} \quad \mu_2\left(s_2^{in}\right) < D + a_2,$$

which are the same as the stability conditions of E_{000} in Table 4.2.

For E_{001}, the Jacobian matrix $\mathcal{J}$ evaluated at E_{001} is:

$$\mathcal{J} = \begin{bmatrix} J - D - a_0 & 0 & 0 & 0 & 0 & 0 \\ 0 & K - D - a_1 & 0 & 0 & 0 & 0 \\ 0 & 0 & 0 & 0 & 0 & Ix_2 \\ -J & 0 & 0 & -D & 0 & 0 \\ J & -K & 0 & 0 & -D & 0 \\ -\omega J & K & -L & 0 & 0 & -D - Ix_2 \end{bmatrix}.$$

By developing the determinant of the matrix $\mathcal{J} - \lambda I_d$, where I_d is the 6×6 identity matrix, with respect to the first, second, fourth and fifth lines, respectively, we obtain, the

eigenvalues

$$\lambda_1 = \mu_0\left(s_0^{\text{in}}, M_2(D+a_2)\right) - D - a_0,\ \lambda_2 = \mu_1\left(s_1^{\text{in}}, M_2(D+a_2)\right) - D - a_1,\ \lambda_3 = \lambda_4 = -D.$$

The other eigenvalues λ_5 and λ_6 are given by the characteristic polynomial of the following matrix:

$$\mathcal{J}_2 = \begin{bmatrix} 0 & Ix_2 \\ -L & -D - Ix_2 \end{bmatrix}.$$

Thus,

$$\lambda_5\lambda_6 = LIx_2 > 0 \quad \text{and} \quad \lambda_5 + \lambda_6 = -(D + Ix_2) < 0.$$

Hence, the eigenvalues λ_5 and λ_6 are of negative real parts. Therefore, E_{001} is stable if and only if

$$\mu_0\left(s_0^{\text{in}}, M_2(D+a_2)\right) < D + a_0 \quad \text{and} \quad \mu_1\left(s_1^{\text{in}}, M_2(D+a_2)\right) < D + a_1.$$

Since M_0 and M_1 are increasing (see Lemma 2.1), these conditions are equivalent to

$$s_0^{\text{in}} < M_0(D+a_0, M_2(D+a_2)) \quad \text{and} \quad s_1^{\text{in}} < M_1(D+a_1, M_2(D+a_2)),$$

which are the same as the stability conditions of E_{001} in Table 4.2.

For E_{100}, the Jacobian matrix $\mathcal{J}$ evaluated at E_{100} is:

$$\mathcal{J} = \begin{bmatrix} 0 & 0 & 0 & Ex_0 & 0 & Fx_0 \\ 0 & K - D - a_1 & 0 & 0 & 0 & 0 \\ 0 & 0 & L - D - a_2 & 0 & 0 & 0 \\ -J & 0 & 0 & -D - Ex_0 & 0 & -Fx_0 \\ J & -K & 0 & Ex_0 & -D & Fx_0 \\ -\omega J & K & -L & -\omega Ex_0 & 0 & -D - \omega Fx_0 \end{bmatrix}.$$

By developing the determinant of the matrix $\mathcal{J} - \lambda I_d$, with respect to the second and third lines, and the fifth column, respectively, we obtain, the eigenvalues

$$\lambda_1 = \mu_1\left(s_0^{\text{in}} - s_0 + s_1^{\text{in}}, s_2^{\text{in}} - \omega\left(s_0^{\text{in}} - s_0\right)\right) - D - a_1,$$
$$\lambda_2 = \mu_2\left(s_2^{\text{in}} - \omega\left(s_0^{\text{in}} - s_0\right)\right) - D - a_2, \quad \lambda_3 = -D.$$

The other eigenvalues are given by the characteristic polynomial P_3 of the following matrix:

$$\mathcal{J}_3 = \begin{bmatrix} 0 & Ex_0 & Fx_0 \\ -J & -D - Ex_0 & -Fx_0 \\ -\omega J & -\omega Ex_0 & -D - \omega Fx_0 \end{bmatrix}.$$

Denote C_i and L_i, $i = 1, 2, 3$, the columns and lines of the matrix $\mathcal{J}_3 - \lambda I_d$. The replacements of L_3 by $L_3 - \omega L_2$ and C_2 by $C_2 + \omega C_3$ preserve the determinant and lead to

$$P_3(\lambda) = -(\lambda + D)\begin{vmatrix} -\lambda & (E + \omega F)x_0 \\ -J & -(\lambda + D + (E + \omega F)x_0) \end{vmatrix}.$$

The eigenvalues of $\mathcal{J}_3$ are $\lambda_4 = -D$, λ_5 and λ_6 such that

$$\lambda_5\lambda_6 = J(E+\omega F)x_0 > 0 \quad \text{and} \quad \lambda_5+\lambda_6 = -D-(E+\omega F)x_0 < 0.$$

Hence, the real parts of λ_5 and λ_6 are negative. Therefore, E_{100} is stable if and only if

$$\mu_1\left(s_0^{\text{in}} - s_0 + s_1^{\text{in}}, s_2^{\text{in}} - \omega\left(s_0^{\text{in}} - s_0\right)\right) < D+a_1 \text{ and } \mu_2\left(s_2^{\text{in}} - \omega\left(s_0^{\text{in}} - s_0\right)\right) < D+a_2, \quad (4.8)$$

with s_0 is the solution in the interval J_0 of equation $\mu_0\left(s_0, s_2^{\text{in}} - \omega\left(s_0^{\text{in}} - s_0\right)\right) = D + a_0$. Since M_2 is increasing, we have the following equivalence:

$$\mu_2\left(s_2^{\text{in}} - \omega\left(s_0^{\text{in}} - s_0\right)\right) < D + a_2 \quad \Longleftrightarrow \quad s_0 < \frac{M_2(D+a_2) - s_2^{\text{in}}}{\omega} + s_0^{\text{in}}.$$

As the function ψ_0 is increasing, we deduce that, $\psi_0(s_0) < \psi_0\left(\dfrac{M_2(D+a_2) - s_2^{\text{in}}}{\omega} + s_0^{\text{in}}\right)$. From $\psi_0(s_0) = \mu_0\left(s_0, s_2^{\text{in}} - \omega\left(s_0^{\text{in}} - s_0\right)\right) = D + a_0$, we deduce that, the second condition of the stability of E_{100} is equivalent to

$$D + a_0 < \mu_0\left(\frac{M_2(D+a_2) - s_2^{\text{in}}}{\omega} + s_0^{\text{in}}, M_2(D+a_2)\right).$$

Hence, we have

$$s_2^{\text{in}} - \omega s_0^{\text{in}} < M_2(D+a_2) - \omega M_0\left(D+a_0, M_2(D+a_2)\right).$$

Consequently, E_{100} is stable if and only if

$$\mu_1\left(s_0^{\text{in}} - s_0 + s_1^{\text{in}}, s_2^{\text{in}} - \omega\left(s_0^{\text{in}} - s_0\right)\right) < D+a_1,\ s_2^{\text{in}} - \omega s_0^{\text{in}} < M_2(D+a_2) - \omega M_0(D+a_0, M_2(D+a_2)).$$

Then, these conditions are the same as stability conditions of E_{100} in Table 4.2.

For E_{110}, the Jacobian matrix $\mathcal{J}$ evaluated at E_{110} is:

$$\mathcal{J} = \begin{bmatrix} 0 & 0 & 0 & Ex_0 & 0 & Fx_0 \\ 0 & 0 & 0 & 0 & Gx_1 & -Hx_1 \\ 0 & 0 & L-D-a_2 & 0 & 0 & 0 \\ -J & 0 & 0 & -D-Ex_0 & 0 & -Fx_0 \\ J & -K & 0 & Ex_0 & -D-Gx_1 & Fx_0+Hx_1 \\ -\omega J & K & -L & -\omega Ex_0 & Gx_1 & -D-\omega Fx_0-Hx_1 \end{bmatrix}.$$

By developing the determinant of the matrix $\mathcal{J} - \lambda I_d$, with respect to the third line, we obtain the eigenvalue $\lambda_1 = \mu_2(s_2) - D - a_2$. The other eigenvalues are given by the characteristic polynomial P_5 of the following matrix:

$$\mathcal{J}_5 = \begin{bmatrix} 0 & 0 & Ex_0 & 0 & Fx_0 \\ 0 & 0 & 0 & Gx_1 & -Hx_1 \\ -J & 0 & -D-Ex_0 & 0 & -Fx_0 \\ J & -K & Ex_0 & -D-Gx_1 & Fx_0+Hx_1 \\ -\omega J & K & -\omega Ex_0 & Gx_1 & -D-\omega Fx_0-Hx_1 \end{bmatrix}.$$

Denote C_i and L_i, $i = 1, ..., 5$, the columns and lines of the matrix $\mathcal{J}_5 - \lambda I_d$. The replacements of L_5 by $L_5 + L_4 + (1-\omega)L_3$, C_3 by $C_3 - C_4 + \omega C_5$, C_4 by $C_4 - C_5$ and then L_4 by $L_3 + L_4$ preserve the determinant and lead to

$$P_5(\lambda) = -(\lambda + D) \begin{vmatrix} -\lambda & 0 & (E+\omega F)x_0 & -Fx_0 \\ 0 & -\lambda & -(G+\omega H)x_1 & (G+H)x_1 \\ -J & 0 & -\lambda - D - (E+\omega F)x_0 & Fx_0 \\ 0 & -K & (G+\omega H)x_1 & -\lambda - D - (G+H)x_1 \end{vmatrix}.$$

Hence, we obtain, the eigenvalue $\lambda_2 = -D$. The other eigenvalues are given by the following characteristic polynomial:

$$P_4(\lambda) = \lambda^4 + c_1\lambda^3 + c_2\lambda^2 + c_3\lambda + c_4 = 0,$$

where the coefficients c_i for $i = 1, \ldots, 4$ are given by

$$\begin{aligned} c_1 =& 2D + (E+\omega F)x_0 + (G+H)x_1, \\ c_2 =& D^2 + (E+\omega F)(D+J)x_0 + (G+H)(D+K)x_1 + (E(G+H) - (1-\omega)FG)x_0x_1, \\ c_3 =& D(E+\omega F)Jx_0 + D(G+H)Kx_1 + (E(G+H) - (1-\omega)FG)(J+K)x_0x_1, \\ c_4 =& (E(G+H) - (1-\omega)FG)JKx_0x_1. \end{aligned}$$

From Lemma 4.1, all of the roots of the fourth-order polynomial have negative real parts if and only if

$$c_i > 0, \quad \text{for} \quad i = 1, 3, 4 \quad \text{and} \quad r_1 = c_1c_2c_3 - c_1^2c_4 - c_3^2 > 0. \tag{4.9}$$

We always have $c_1 > 0$. Moreover, $c_3 > 0$ and $c_4 > 0$ if and only if

$$E(G+H) - (1-\omega)FG > 0. \tag{4.10}$$

Let us denote

$$A = G + H, \quad B = \frac{E(G+H) - (1-\omega)FG}{G+H} \quad \text{and} \quad C = \frac{G+\omega H}{G+H}F.$$

Note that $B > 0$ if and only if condition (4.10) is satisfied. Then, we can write c_i, for $i = 1, \ldots, 4$ and r_1 as follows:

$$\begin{aligned} c_1 &= 2D + (B+C)x_0 + Ax_1, \\ c_2 &= D^2 + (B+C)(D+J)x_0 + A(D+K)x_1 + ABx_0x_1, \\ c_3 &= D(B+C)Jx_0 + DAKx_1 + AB(J+K)x_0x_1, \quad c_4 = ABJKx_0x_1, \end{aligned}$$

We can write r_1 as follows:

$$\begin{aligned} r_1 =& DJ\left[(D+J)(B+C)^3 - B^3J\right]x_0^3 + D^2A^3Kx_1^3 + B^2A^2(B+C)(J+K)x_0^3x_1^2 \\ &+ B^2A^3(J+K)x_0^2x_1^3 + BA\left[D(2J+K)(B+C)^2 + CJ^2(2B+C)\right]x_0^3x_1 \\ &+ DBA^3(J+2K)x_0x_1^3 + 3D^3A^2Kx_1^2 + D^2J\left[3D(B+C)^2 + CJ(2B+C)\right]x_0^2 \\ &+ BA^2\left[D(J+K)(5B+3C) + C\left(J^2+K^2\right)\right]x_0^2x_1^2 + DA\left[C\left(DC(2J+K)\right.\right. \\ &\left.\left.+CJ(J+2K) + DB(9J+5K) + 2BJ^2\right) + DB^2(7J+4K)\right]x_0^2x_1 + DA^2[DB(4J \\ &+ 7K) + CK(2J+K) + DC(J+2K)]x_0x_1^2 + 2D^4J(B+C)x_0 + 2D^4AKx_1 \\ &+ D^2A[D(J+K)(5B+3C) + 2CJK]x_0x_1 + \left(D^2 + DBx_0 + DAx_1 + BAx_0x_1\right) \\ &(BJx_0 - AKx_1)^2. \end{aligned}$$

Hence, conditions (4.9) are verified if and only if (4.10) is satisfied. Let us prove that condition (4.10) is equivalent to $\dfrac{\partial \Psi}{\partial s_2}(s_2, D) > 0$. Using (3.3), we obtain

$$\frac{\partial M_0}{\partial s_2}(D+a_0, s_2) = -\frac{F}{E} \quad \text{and} \quad \frac{\partial M_1}{\partial s_2}(D+a_1, s_2) = \frac{H}{G}.$$

Using (2.24), it follows that

$$\frac{\partial \Psi}{\partial s_2}(s_2, D) = -\frac{F}{E}(1-\omega) + \frac{H}{G} + 1 = \frac{E(G+H) - (1-\omega)FG}{EG}.$$

Since E and G are positive, condition (4.10) is equivalent to $\dfrac{\partial \Psi}{\partial s_2}(s_2, D) > 0$. Consequently, since μ_2 is increasing, it follows that E_{110} is stable if and only if

$$s_2 < M_2(D+a_2) \quad \text{and} \quad \frac{\partial \Psi}{\partial s_2}(s_2, D) > 0, \tag{4.11}$$

which are equivalent to the stability conditions in Table 4.2 because this first condition of (4.11) is equivalent the first and the second one of E_{110} in Table 4.2 (similarly to the proof of Theorem 3.1 in previous chaptre).

For E_{101}, the Jacobian matrix $\mathcal{J}$ evaluated at E_{101} is:

$$\mathcal{J} = \begin{bmatrix} 0 & 0 & 0 & Ex_0 & 0 & Fx_0 \\ 0 & K-D-a_1 & 0 & 0 & 0 & 0 \\ 0 & 0 & 0 & 0 & 0 & Ix_2 \\ -J & 0 & 0 & -D-Ex_0 & 0 & -Fx_0 \\ J & -K & 0 & Ex_0 & -D & Fx_0 \\ -\omega J & K & -L & -\omega Ex_0 & 0 & -D-\omega Fx_0 - Ix_2 \end{bmatrix}.$$

By developing the determinant of the matrix $\mathcal{J} - \lambda I_d$, with respect to the second and fifth lines, respectively, we obtain, the eigenvalues

$$\lambda_1 = \mu_1\left(s_0^{\text{in}} + s_1^{\text{in}} - M_0(D+a_0, M_2(D+a_2)), M_2(D+a_2)\right) - D - a_1 \quad \text{and} \quad \lambda_2 = -D.$$

The other eigenvalues are given by the characteristic polynomial:

$$P_4(\lambda) = \lambda^4 + c_1\lambda^3 + c_2\lambda^2 + c_3\lambda + c_4 = 0,$$

where

$$\begin{aligned}
c_1 &= 2D + (E + \omega F)x_0 + Ix_2,\\
c_2 &= D^2 + (E + \omega F)(D + J)x_0 + I(D + L)x_2 + EIx_0x_2,\\
c_3 &= D(E + \omega F)Jx_0 + DILx_2 + EI(J + L)x_0x_2,\\
c_4 &= EIJLx_0x_2.
\end{aligned}$$

From Lemma 4.2 the roots of the fourth-order polynomial are of negative real parts if and only if

$$c_i > 0, \quad \text{for} \quad i = 1, 3, 4 \quad \text{and} \quad r_1 = c_1c_2c_3 - c_1^2c_4 - c_3^2 > 0. \tag{4.12}$$

We always have:

$$c_i > 0, \quad \text{for} \quad i = 1, 3, 4.$$

We show that: $r_1 > 0$. Indeed, we can write that:

$$\begin{aligned}
r_1 =& DJ\left[(D + J)(E + \omega F)^3 - E^3J\right]x_0^3 + D^2I^3Lx_2^3 + E^2I^2(E + \omega F)(J + L)x_0^3x_2^2\\
&+ E^2I^3(J + L)x_0^2x_2^3 + \left[DEI(2J + L)(E + \omega F)^2 + EF\omega IJ^2(2E + \omega F)\right]x_0^3x_2\\
&+ DEI^3(J + 2L)x_0x_2^3 + 3D^3I^2Lx_2^2\left[3D^3J(E + \omega F)^2 + D^2F\omega J^2(2E + \omega F)\right]x_0^2\\
&+ EI^2\left[D(J + L)(5E + 3\omega F) + F\omega\left(J^2 + L^2\right)\right]x_0^2x_2^2 + DI\left[F\omega\left(DF\omega(2J + L)\right.\right.\\
&\left.\left.+F\omega J(J + 2L) + DE(9J + 5L) + 2EJ^2\right) + DE^2(7J + 4L)\right]x_0^2x_2 + DI^2\left[DE\left(4J\right.\right.\\
&\left.\left.+7L) + F\omega L(2J + L) + DF\omega(J + 2L)\right]x_0x_2^2 + 2D^4J(E + \omega F)x_0 + 2D^4ILx_2\\
&+ D^2I\left[D(J + L)(5E + 3\omega F) + 2F\omega JL\right]x_0x_2 + \left(D^2 + DEx_0 + DIx_2 + EIx_0x_2\right)\\
&(EJx_0 - ILx_2)^2.
\end{aligned}$$

Thus, $r_1 > 0$. Consequently, the conditions (4.12) are satisfied. Therefore, E_{101} is stable if and only if $\lambda_1 < 0$, that is to say

$$\mu_1\left(s_0^{\mathrm{in}} + s_1^{\mathrm{in}} - M_0(D + a_0, M_2(D + a_2)), M_2(D + a_2)\right) < D + a_1.$$

Since M_1 is increasing (see Lemma 2.1), this condition is equivalent to

$$s_0^{\mathrm{in}} + s_1^{\mathrm{in}} < M_0(D + a_0, M_2(D + a_2)) + M_1(D + a_1, M_2(D + a_2)),$$

which is the same as the stability condition of E_{101} in Table 4.2.

For E_{111}, the Jacobian matrix $\mathcal{J}$ evaluated at $\mathrm{E}_{111} = (\mathrm{x}_0, \mathrm{x}_1, \mathrm{x}_2, \mathrm{s}_0, \mathrm{s}_1, \mathrm{s}_2)$ is given by:

$$\mathcal{J} = \begin{bmatrix}
0 & 0 & 0 & Ex_0 & 0 & Fx_0\\
0 & 0 & 0 & 0 & Gx_1 & -Hx_1\\
0 & 0 & 0 & 0 & 0 & Ix_2\\
-J & 0 & 0 & -D - Ex_0 & 0 & -Fx_0\\
J & -K & 0 & Ex_0 & -D - Gx_1 & Fx_0 + Hx_1\\
-\omega J & K & -L & -\omega Ex_0 & Gx_1 & -D - \omega Fx_0 - Hx_1 - Ix_2
\end{bmatrix}.$$

The characteristic polynomial is given by:

$$P_6(\lambda) = \lambda^6 + c_1\lambda^5 + c_2\lambda^4 + c_3\lambda^3 + c_4\lambda^2 + c_5\lambda + c_6,$$

where c_i are defined in Table 4.1. Note that, c_1 and c_6 are positive. From Lemma 4.2 all of the roots of the sixth-order polynomial have the negative real part if and only if

$$c_i > 0, \quad i = 3, 5 \qquad \text{and} \qquad r_j > 0, \quad j = 4, 5, \tag{4.13}$$

where r_j are defined in Table 4.1.

For E_{010}, the Jacobian matrix $\mathcal{J}$ evaluated at E_{010} is:

$$\mathcal{J} = \begin{bmatrix} J - D - a_0 & 0 & 0 & 0 & 0 & 0 \\ 0 & 0 & 0 & 0 & Gx_1 & -Hx_1 \\ 0 & 0 & L - D - a_2 & 0 & 0 & 0 \\ -J & 0 & 0 & -D & 0 & 0 \\ J & -K & 0 & 0 & -D - Gx_1 & Hx_1 \\ -\omega J & K & -L & 0 & Gx_1 & -D - Hx_1 \end{bmatrix}.$$

By developing the determinant of the matrix $\mathcal{J} - \lambda I_d$, with respect to the first, third and fourth lines, respectively, we obtain, the eigenvalues

$$\lambda_1 = \mu_0\left(s_0^{\text{in}}, s_1^{\text{in}} - s_1 + s_2^{\text{in}}\right) - D - a_0, \quad \lambda_2 = \mu_2\left(s_1^{\text{in}} - s_1 + s_2^{\text{in}}\right) - D - a_2 \quad \text{and} \quad \lambda_3 = -D.$$

The other eigenvalues are given by the characteristic polynomial P_3 of the following matrix:

$$\mathcal{J}_3 = \begin{bmatrix} 0 & Gx_1 & -Hx_1 \\ -K & -D - Gx_1 & Hx_1 \\ K & Gx_1 & -D - Hx_1 \end{bmatrix}.$$

Denote C_i and L_i, $i = 1, 2, 3$, the columns and lines of the matrix $\mathcal{J}_3 - \lambda I_d$. The replacements of L_3 by $L_2 + L_3$ and C_2 by $C_2 - C_3$ preserve the determinant and lead to

$$P_3(\lambda) = -(\lambda + D)\begin{vmatrix} -\lambda & (G+H)x_1 \\ -K & -(\lambda + D + (G+H)x_1) \end{vmatrix}.$$

The eigenvalues of $\mathcal{J}_3$ are $\lambda_4 = -D$, λ_5 and λ_6 such that

$$\lambda_5\lambda_6 = K(G+H)x_1 > 0 \quad \text{and} \quad \lambda_5 + \lambda_6 = -D - (G+H)x_1 < 0.$$

Hence, the real parts of λ_5 and λ_6 are negative. Therefore, E_{010} is stable if and only if

$$\mu_0\left(s_0^{\text{in}}, s_1^{\text{in}} - s_1 + s_2^{\text{in}}\right) < D + a_0 \quad \text{and} \quad \mu_2\left(s_1^{\text{in}} - s_1 + s_2^{\text{in}}\right) < D + a_2,$$

with s_1 is the solution in the interval J_1 of equation $\mu_1\left(s_1, s_1^{\text{in}} - s_1 + s_2^{\text{in}}\right) = D + a_1$. Recall that, the functions M_2 and M_3 are increasing thanks to Lemma 2.1. Thus,

$$\mu_0\left(s_0^{\text{in}}, s_1^{\text{in}} - s_1 + s_2^{\text{in}}\right) < D + a_0 \quad \Longleftrightarrow \quad s_1 > s_1^{\text{in}} + s_2^{\text{in}} - M_3(s_0^{\text{in}}, D + a_0),$$

$$\mu_2\left(s_1^{\text{in}} - s_1 + s_2^{\text{in}}\right) < D + a_2 \quad \Longleftrightarrow \quad s_1 > s_1^{\text{in}} + s_2^{\text{in}} - M_2(D + a_2).$$

As the function ψ_1 is increasing, then, we deduced that

$$\psi_1(s_1) > \psi_1\left(s_1^{\text{in}} + s_2^{\text{in}} - M_3(s_0^{\text{in}}, D + a_0)\right) \quad \text{and} \quad \psi_1(s_1) > \psi_1\left(s_1^{\text{in}} + s_2^{\text{in}} - M_2(D + a_2)\right).$$

From $\psi_1(s_1) = \mu_1\left(s_1, s_1^{\text{in}} - s_1 + s_2^{\text{in}}\right) = D + a_1$, then, the conditions of the stability of E_{010} are equivalent to

$$\mu_1\left(s_1^{\text{in}} + s_2^{\text{in}} - M_3(s_0^{\text{in}}, D + a_0), M_3(s_0^{\text{in}}, D + a_0)\right) < D + a_1,$$

$$\mu_1\left(s_1^{\text{in}} + s_2^{\text{in}} - M_2(D + a_2), M_2(D + a_2)\right) < D + a_1.$$

Since M_1 is increasing (see Lemma 2.1), then, E_{010} is stable if and only if

$$s_1^{\text{in}} + s_2^{\text{in}} < M_1\left(D + a_1, M_3(s_0^{\text{in}}, D + a_0)\right) + M_3(s_0^{\text{in}}, D + a_0),$$

$$s_1^{\text{in}} + s_2^{\text{in}} < M_1\left(D + a_1, M_2(D + a_2)\right) + M_2(D + a_2),$$

which are the same as the stability conditions of E_{010} in Table 4.2.

For E_{011}, the Jacobian matrix $\mathcal{J}$ evaluated at E_{011} is:

$$\mathcal{J} = \begin{bmatrix} J - D - a_0 & 0 & 0 & 0 & 0 & 0 \\ 0 & 0 & 0 & 0 & Gx_1 & -Hx_1 \\ 0 & 0 & 0 & 0 & 0 & Ix_2 \\ -J & 0 & 0 & -D & 0 & 0 \\ J & -K & 0 & 0 & -D - Gx_1 & Hx_1 \\ -\omega J & K & -L & 0 & Gx_1 & -D - Hx_1 - Ix_2 \end{bmatrix}.$$

By developing the determinant of the matrix $\mathcal{J} - \lambda I_d$, with respect to the first and fourth lines, respectively, we obtain, the eigenvalues

$$\lambda_1 = \mu_0\left(s_0^{\text{in}}, M_2(D + a_2)\right) - D - a_0 \quad \text{and} \quad \lambda_2 = -D.$$

The other eigenvalues are given by the characteristic polynomial:

$$P_4(\lambda) = \lambda^4 + c_1\lambda^3 + c_2\lambda^2 + c_3\lambda + c_4 = 0,$$

where

$$\begin{aligned} c_1 &= 2D + (G + H)x_1 + Ix_2, \\ c_2 &= D^2 + (G + H)(D + K)x_1 + I(D + L)x_2 + GIx_1x_2, \\ c_3 &= D(G + H)Kx_1 + DILx_2 + GI(K + L)x_1x_2, \\ c_4 &= GIKLx_1x_2. \end{aligned}$$

From Lemma 4.2 the roots of the fourth-order polynomial are of negative real parts if and only if

$$c_i > 0, \quad \text{for} \quad i = 1, 3, 4 \quad \text{and} \quad r_1 = c_1c_2c_3 - c_1^2c_4 - c_3^2 > 0. \tag{4.14}$$

We always have:

$$c_i > 0, \quad \text{for} \quad i = 1, 3, 4.$$

We show that: $r_1 > 0$. Indeed, we can write that:

$$\begin{aligned} r_1 =& DK\left[(D+K)(G+H)^3 - G^3K\right]x_1^3 + D^2I^3Lx_2^3 + G^2I^2(G+H)(K+L)x_1^3x_2^2 \\ &+ G^2I^3(K+L)x_1^2x_2^3 + \left[DGI(2K+L)(G+H)^2 + GHIK^2(2G+H)\right]x_1^3x_2 \\ &+ DGI^3(K+2L)x_1x_2^3 + 3D^3I^2Lx_2^2 + \left[3D^3K(G+H)^2 + D^2HK^2(2G+H)\right]x_1^2 \\ &+ GI^2\left[D(K+L)(5G+3H) + H\left(K^2+L^2\right)\right]x_1^2x_2^2 + DI\left[H\left(DH(2K+L)\right.\right. \\ &\left.\left.+HK(K+2L) + DG(9K+5L) + 2GK^2\right) + DG^2(7K+4L)\right]x_1^2x_2 + DI^2\left[DG(4K\right. \\ &\left.+7L) + HL(2K+L) + DH(K+2L)\right]x_1x_2^2 + 2D^4K(G+H)x_1 + 2D^4ILx_2 \\ &+ D^2I\left[D(K+L)(5G+3H) + 2HKL\right]x_1x_2 + \left(D^2 + DGx_1 + DIx_2 + GIx_1x_2\right) \\ &(GKx_1 - ILx_2)^2. \end{aligned}$$

Thus, $r_1 > 0$. Consequently, the conditions (4.14) are satisfied. Finally, E_{011} is stable if and only if

$$\mu_0\left(s_0^{\mathrm{in}}, M_2(D+a_2)\right) < D + a_0.$$

Since M_0 is increasing (see Lemma 2.1), this condition is equivalent to

$$s_0^{\mathrm{in}} < M_0(D+a_0, M_2(D+a_2)),$$

which is the same as the stability condition of E_{011} in Table 4.2.

□

Remark 4.1. For all steady states, except for the positive one E_{111}, we see that $-D$ is an eigenvalue whose multiplicity corresponds to the number of extinct species.

From Tables 2.2 and 4.2, we have the following results, which are also valid in the case without maintenance (see Tables 3.1 and 3.2).

Corollary 4.1.

- *If* E_{001} *or* E_{100} *or* E_{010} *exists then,* E_{000} *is unstable.*
- *If* E_{111} *exists then,* E_{001}*,* E_{110}*,* E_{101} *and* E_{011} *are unstable.*
- *If* E_{101} *exists then,* E_{001} *and* E_{100} *are unstable.*
- *If* E_{010} *exists then,* E_{010} *is unstable.*

Proof. If E_{001} exists then, its condition of existence $\mu_2\left(s_2^{\mathrm{in}}\right) > D + a_2$ holds. Therefore, the condition $\mu_2\left(s_2^{\mathrm{in}}\right) < D + a_2$ of stability of E_{000} is not satisfied.

If E_{100} exists then, its condition of existence $\mu_0\left(s_0^{\mathrm{in}}, s_2^{\mathrm{in}}\right) > D + a_0$ holds. Therefore, the condition $\mu_0\left(s_0^{\mathrm{in}}, s_2^{\mathrm{in}}\right) < D + a_0$ of stability of E_{000} is not satisfied.

If E_{010} exists then, its condition of existence $\mu_1\left(s_1^{\mathrm{in}}, s_2^{\mathrm{in}}\right) > D + a_1$ holds. Therefore, the condition $\mu_1\left(s_1^{\mathrm{in}}, s_2^{\mathrm{in}}\right) < D + a_1$ of stability of E_{000} is not satisfied.

If E_{111} exists then, the conditions

$$(1-\omega)s_0^{in} + s_1^{in} + s_2^{in} > \phi_2(D),\ s_0^{in} > \varphi_0(D),\ s_0^{in} + s_1^{in} > \varphi_0(D) + \varphi_1(D)$$

hold. Therefore, the condition $s_0^{in} < \varphi_0(D)$ of stability of E_{001} or E_{011} is not satisfied, the condition $(1-\omega)s_0^{in} + s_1^{in} + s_2^{in} < \phi_2(D)$ of stability of E_{110} is not satisfied, and the condition $s_0^{in} + s_1^{in} < \varphi_0(D) + \varphi_1(D)$ of stability of E_{101} is not satisfied.

If E_{101} exists, then, its conditions of existence

$$s_0^{in} > \varphi_0(D) \quad \text{and} \quad s_2^{in} - \omega s_0^{in} > M_2(D+a_2) - \omega\varphi_0(D)$$

hold. Therefore, the condition $s_0^{in} < \varphi_0(D)$ of stability of E_{001} or E_{011} is not satisfied and the condition $s_2^{in} - \omega s_0^{in} < M_2(D+a_2) - \omega\varphi_0(D)$ of stability of E_{100} is not satisfied.

If E_{011} exists, then, its conditions of existence $s_1^{in} + s_2^{in} > \varphi_1(D) + M_2(D+a_2)$ holds. Therefore, the condition $s_1^{in} + s_2^{in} < \varphi_1(D) + M_2(D+a_2)$ of stability of E_{010} is not satisfied. □

4.3 Proofs for the results of [64] on existence and stability of the steady states of the model

The aim of this section is to give rigorous proofs for the results of [64] on existence and stability of the steady states of model (2.1). Notice that the results in [64] were given with respect to the dimensionless form (3.21) of (2.1) by using the variables (3.20) and the growth functions (3.22). The variables (3.20) are related to our variables (2.6) by the formulas

$$x_0 = N_0K_0,\ x_1 = N_1K_1,\ x_2 = N_2K_2,\ s_0 = R_0K_0,\ s_1 = R_1K_1,\ s_2 = R_2K_2,\ t = \tau/m_0.$$

Hence, results given in variables (3.20) can be easily translated into results given in variables (2.6) and vice versa.

From Tables 2.2 and 4.2, the existence and stability of steady states of model (2.1) can be determine for the specific growth functions (2.9). Using the functions and notations given in Table 3.4, we have the following results:

$E_{000} = \left(0, 0, 0, s_0^{in}, s_1^{in}, s_2^{in}\right)$ always exists. It is stable if and only if

$$\mu_0\left(s_0^{in}, s_2^{in}\right) < D + a_0, \quad \mu_1\left(s_1^{in}, s_2^{in}\right) < D + a_1 \quad \text{and} \quad \mu_2\left(s_2^{in}\right) < D + a_2.$$

These conditions are equivalent to the conditions of E_{000} (SS1) were established in [64], section C1, given in terms of variables (3.20) and growth functions (3.22).

$E_{001} = (0, 0, x_2, s_0, s_1, s_2)$ is given by:

$$s_0 = s_0^{in}, \quad s_1 = s_1^{in}, \quad s_2 = \frac{K_2(D+a_2)}{m_2 - D - a_2}, \quad x_2 = \frac{D}{D+a_2}\left(s_2^{in} - s_2\right). \tag{4.15}$$

It exists if and only if $s_2^{\text{in}} > s_2$, where s_2 is given by (4.15). It is stable if and only if

$$\mu_0\left(s_0^{\text{in}}, s_2\right) < D + a_0 \quad \text{and} \quad \mu_1\left(s_1^{\text{in}}, s_2\right) < D + a_1.$$

Formulas (4.15) together with the conditions of existence and stability of E_{001} (SS2) were established in [64], section C2, using variables (3.20) and growth functions (3.22).

$E_{100} = (x_0, 0, 0, s_0, s_1, s_2)$ is given by:

$$x_0 = \frac{D}{D + a_0}\left(s_0^{\text{in}} - s_0\right), \quad s_1 = s_1^{\text{in}} + s_0^{\text{in}} - s_0, \quad s_2 = s_2^{\text{in}} - \omega\left(s_0^{\text{in}} - s_0\right), \tag{4.16}$$

where s_0 is a solution of equation

$$\frac{m_0 s_0\left(s_2^{\text{in}} - \omega\left(s_0^{\text{in}} - s_0\right)\right)}{(K_0 + s_0)\left(L_0 + s_2^{\text{in}} - \omega\left(s_0^{\text{in}} - s_0\right)\right)} = D + a_0. \tag{4.17}$$

Notice that (4.17) is a quadratic equation. Only its solution in the interval

$$J_0 = \left[\max\left(0, s_0^{\text{in}} - s_2^{\text{in}}/\omega\right), s_0^{\text{in}}\right)$$

is to be considered. E_{100} exists if and only if the following condition holds

$$\mu_0\left(s_0^{\text{in}}, s_2^{\text{in}}\right) > D + a_0. \tag{4.18}$$

It is stable if and only if

$$\begin{aligned} &\mu_1\left(s_0^{\text{in}} - s_0 + s_1^{\text{in}}, s_2^{\text{in}} - \omega\left(s_0^{\text{in}} - s_0\right)\right) < D + a_1, \\ &s_2^{\text{in}} - \omega s_0^{\text{in}} < M_2(D + a_2) - \omega M_0\left(D + a_0, M_2(D + a_2)\right), \end{aligned} \tag{4.19}$$

where s_0 is the solution in the interval J_0 of equation (4.17). Formulas (4.16) together with equation (4.17) giving s_0 and the stability condition (4.19) were established in [64], section C3, using variables (3.20) and growth functions (3.22). However, neither condition (4.18) of existence of E_{100} (SS3) nor the signs of other eigenvalues of the Jacobian matrix were explicitly established in [64], section C3, where the existence and stability of E_{100} (SS3) were checked only numerically by considering the roots of polynomials of degrees 2 and 3, respectively, see formulas (C.3) and (C.7) in [64].

$E_{110} = (x_0, x_1, 0, s_0, s_1, s_2)$ is given by:

$$\begin{aligned} s_0 &= \frac{(D + a_0)K_0(L_0 + s_2)}{m_0 s_2 - (D + a_0)(L_0 + s_2)}, \quad s_1 = \frac{(D + a_1)K_1(K_I + s_2)}{m_1 K_I - (D + a_1)(K_I + s_2)}, \\ x_0 &= \frac{D}{D + a_0}\left(s_0^{\text{in}} - s_0\right), \quad x_1 = \frac{D}{D + a_1}\left(s_0^{\text{in}} - s_0 + s_1^{\text{in}} - s_1\right), \end{aligned} \tag{4.20}$$

where s_2 is a solution of equation

$$\begin{aligned} &(1 - \omega)\frac{(D + a_0)K_0(L_0 + s_2)}{m_0 s_2 - (D + a_0)(L_0 + s_2)} + \frac{(D + a_1)K_1(K_I + s_2)}{m_1 K_I - (D + a_1)(K_I + s_2)} + s_2 \\ &= (1 - \omega)s_0^{\text{in}} + s_1^{\text{in}} + s_2^{\text{in}}. \end{aligned} \tag{4.21}$$

Notice that (4.21) reduces to a cubic equation in s_2. Only its solutions in the interval (s_2^0, s_2^1) are to be considered. The steady states E_{110}^1 and E_{110}^2 exist if and only if the following conditions hold

$$s_0^{\text{in}} > s_0, \quad s_0^{\text{in}} + s_1^{\text{in}} > s_0 + s_1 \quad \text{and} \quad (1-\omega)s_0^{\text{in}} + s_1^{\text{in}} + s_2^{\text{in}} \geq \phi_1(D), \tag{4.22}$$

where s_0 and s_1 are defined by (4.20). E_{110}^1 is unstable whenever it exists and E_{110}^2 is stable if and only if

$$(1-\omega)s_0^{\text{in}} + s_1^{\text{in}} + s_2^{\text{in}} < \phi_2(D), \quad \text{and} \quad \phi_3(D) > 0. \tag{4.23}$$

Here ϕ_2 and ϕ_3 are defined in Table 3.4. Formulas (4.20) together with equation (4.21) giving s_2 were established in [64], section C4, using variables (3.20) and growth functions (3.22). However, neither condition (4.22) of existence of E_{110} (SS4) nor its condition of stability (4.23) have been established explicitly in [64], section C4, where the existence and stability of E_{110} (SS4) were checked only numerically by considering the roots of a polynomial of degree 5, see formula (C.20) in [64].

$\mathrm{E}_{101} = (\mathrm{x}_0, 0, \mathrm{x}_2, \mathrm{s}_0, \mathrm{s}_1, \mathrm{s}_2)$ is given by:

$$\begin{aligned} s_2 &= \frac{(D+a_2)K_2}{m_2 - D - a_2}, \quad s_0 = \frac{(D+a_0)K_0(L_0+s_2)}{m_0 s_2 - (D+a_0)(L_0+s_2)}, \quad s_1 = s_0^{\text{in}} - s_0 + s_1^{\text{in}}, \\ x_0 &= \frac{D}{D+a_0}\left(s_0^{\text{in}} - s_0\right), \quad x_2 = \frac{D}{D+a_2}\left(s_2^{\text{in}} - s_2 - \omega\left(s_0^{\text{in}} - s_0\right)\right). \end{aligned} \tag{4.24}$$

It exists if and only if the following conditions hold

$$s_0^{\text{in}} > s_0, \quad s_2^{\text{in}} - \omega s_0^{\text{in}} > s_2 - \omega s_0, \tag{4.25}$$

where s_0 and s_2 are given by (4.24). E_{101} is stable if and only if

$$s_0^{\text{in}} + s_1^{\text{in}} < M_0\left(D + a_0, M_2(D+a_2)\right) + M_1\left(D + a_1, M_2(D+a_2)\right). \tag{4.26}$$

Formulas (4.24) together with conditions (4.25) of existence and (4.26) of stability of E_{101} (SS5) were established in [64], section C5, using variables (3.20) and growth functions (3.22). However, the signs of other eigenvalues of the Jacobian matrix have been checked only numerically by considering the roots of a polynomial of degree 4, see formula (C.31) in [64].

$\mathrm{E}_{111} = (\mathrm{x}_0, \mathrm{x}_1, \mathrm{x}_2, \mathrm{s}_0, \mathrm{s}_1, \mathrm{s}_2)$ is given by:

$$\begin{aligned} s_2 &= \frac{(D+a_2)K_2}{m_2 - D - a_2}, \quad s_0 = \frac{(D+a_0)K_0(L_0+s_2)}{m_0 s_2 - (D+a_0)(L_0+s_2)}, \quad s_1 = \frac{(D+a_1)K_1(K_I+s_2)}{m_1 K_I - (D+a_1)(K_I+s_2)}, \\ x_0 &= \frac{D}{D+a_0}\left(s_0^{\text{in}} - s_0\right), \quad x_1 = \frac{D}{D+a_1}\left(s_0^{\text{in}} - s_0 + s_1^{\text{in}} - s_1\right), \\ x_2 &= \frac{D}{D+a_2}\left((1-\omega)\left(s_0^{\text{in}} - s_0\right) + s_1^{\text{in}} - s_1 + s_2^{\text{in}} - s_2\right). \end{aligned} \tag{4.27}$$

It exists if and only if the following conditions hold

$$s_0^{\text{in}} > s_0, \quad s_0^{\text{in}} + s_1^{\text{in}} > s_0 + s_1, \quad (1-\omega)s_0^{\text{in}} + s_1^{\text{in}} + s_2^{\text{in}} > \phi_2(D), \tag{4.28}$$

where s_0 and s_1 are given by (4.27). E_{111} is stable if and only if

$$c_i > 0, \quad i = 3, 5, \quad \text{and} \quad r_j > 0, \quad j = 4, 5, \tag{4.29}$$

where c_i and r_j are defined in Table 4.1. Formulas (4.27) together with conditions (4.28) of existence of E_{111} (SS6) were established in [64], section C6, using variables (3.20) and growth functions (3.22). However, the Liénard-Chipart stability conditions (4.29) were not considered in [64], where the stability of E_{111} (SS6) was checked only numerically by considering the roots of a polynomial of degree 6, see formula (C.42) in [64].

$\mathrm{E}_{010} = (0, \mathrm{x}_1, 0, \mathrm{s}_0, \mathrm{s}_1, \mathrm{s}_2)$ is given by:

$$s_0 = s_0^{\text{in}}, \quad x_1 = \frac{D}{D + a_1}\left(s_1^{\text{in}} - s_1\right), \quad s_2 = s_1^{\text{in}} - s_1 + s_2^{\text{in}}, \tag{4.30}$$

where s_1 is a unique solution of equation

$$\frac{m_1 s_1 K_I}{(K_1 + s_1)\left(K_I + s_1^{\text{in}} + s_2^{\text{in}} - s_1\right)} = D + a_1. \tag{4.31}$$

Notice that (4.31) is a quadratic equation. Only its solution in the interval

$$J_1 = \left[0, s_1^{\text{in}}\right)$$

is to be considered. E_{010} exists if and only if the following condition holds

$$\mu_1\left(s_1^{\text{in}}, s_2^{\text{in}}\right) > D + a_1. \tag{4.32}$$

E_{010} is stable if and only if

$$\begin{aligned} &s_1^{\text{in}} + s_2^{\text{in}} < M_1\left(D + a_1, M_3\left(s_0^{\text{in}}, D + a_0\right)\right) + M_3\left(s_0^{\text{in}}, D + a_0\right), \\ &s_1^{\text{in}} + s_2^{\text{in}} < M_1(D + a_1, M_2(D + a_2)) + M_2(D + a_2). \end{aligned} \tag{4.33}$$

Formulas (4.30) together with equation (4.31) giving s_1 and stability condition (4.33) were established in [64], section C7, using variables (3.20) and growth functions (3.22). However, condition (4.32) of existence of E_{010} (SS7) has not been established explicitly in [64], section C7, where the existence of E_{010} (SS7) and the signs of other eigenvalues of the Jacobian matrix were checked only numerically by considering the roots of a polynomial of degree 3, see formula (C.53) in [64].

$\mathrm{E}_{011} = (0, \mathrm{x}_1, \mathrm{x}_2, \mathrm{s}_0, \mathrm{s}_1, \mathrm{s}_2)$ is given by:

$$\begin{aligned} &s_0 = s_0^{\text{in}}, \quad s_2 = \frac{(D + a_2)K_2}{m_2 - D - a_2}, \quad s_1 = \frac{(D + a_1)K_1(K_I + s_2)}{m_1 K_I - (D + a_1)(K_I + s_2)}, \\ &x_1 = \frac{D}{D + a_1}\left(s_1^{\text{in}} - s_1\right), \quad x_2 = \frac{D}{D + a_2}\left(s_1^{\text{in}} - s_1 + s_2^{\text{in}} - s_2\right). \end{aligned} \tag{4.34}$$

It exists if and only if the following conditions hold

$$s_1^{\text{in}} > s_1, \quad s_1^{\text{in}} + s_2^{\text{in}} > s_1 + s_2, \tag{4.35}$$

where s_1 and s_2 are given by (4.34). E_{011} is stable if and only if

$$s_0^{\text{in}} < M_0\left(D + a_0, M_2(D + a_2)\right). \tag{4.36}$$

Formulas (4.34) together with conditions (4.35) of existence and (4.36) of stability of E_{011} (SS8) were established in [64], section C8, using variables (3.20) and growth functions (3.22). However, the signs of other eigenvalues of the Jacobian matrix have been checked only numerically by considering the roots of a polynomial of degree 4, see formula (C.62) in [64].

4.4 Bifurcation diagrams

In this section, we determine numerically the asymptotic behaviors of the three-tiered model by including decay terms. We assume that the biological parameter values are the same in Table 3.3, except for $k_{\text{dec,i}} = a_i = 0.02$. To compare with the findings of the numerical study of [64] in the case including decay, we perform the bifurcation diagrams with respect to the parameter D, and then to $S_{\text{ch}}^{\text{in}}$, to examine the effects of decay terms on the behavior of model (2.1). We compare our results to those in the case without maintenance terms. We consider the same values of the two input concentrations $S_{\text{ph}}^{\text{in}} = 0$ and $S_{\text{H}_2}^{\text{in}} = 2.67 \times 10^{-5}$ of Figure 3(a) in [64]. In this case, the steady states E_{010} and E_{011} do not exist, see Proposition 2.2.

4.4.1 Bifurcation diagram with respect to D

Giving a fixed value for $S_{\text{ch}}^{\text{in}} = 0.1$. Using the results of the existence conditions in Table 2.2 in previous chapter 2 and from Table 4.2, we have the following result, which determines the existence and the stability of the steady states of (2.1) with respect to the dilution rate D.

Proposition 4.1. *Let $S_{\text{ph}}^{\text{in}} = 0$, $S_{\text{H}_2}^{\text{in}} = 2.67 \times 10^{-5}$ and $S_{\text{ch}}^{\text{in}} = 0.1$. Using the biological parameter values in Table 3.3, while $k_{\text{dec,i}} = 0.02$, the bifurcation values δ_i, $i = 1, \ldots, 7$ are provided in Table 4.3. The bifurcation analysis of (2.1) according to D is given in Table 4.4. The bifurcation types at the critical values δ_i are defined in Table 4.5.*

Proof. Using the change of variables (2.7) and Tables 2.2 and 4.2. The necessary and sufficient existence and stability conditions of steady states of (2.1) are summarized in Table 4.6 when $S_{\text{ph}}^{\text{in}} = 0$, $S_{\text{H}_2}^{\text{in}} = 2.67 \times 10^{-5}$ and $S_{\text{ch}}^{\text{in}} = 0.1$. Using Table 4.6, we see that:

E_{000} always exists and it is stable if and only if

$$D > \mu_0\left(Y S_{\text{ch}}^{\text{in}}, S_{\text{H}_2}^{\text{in}}\right) - a_0 := \delta_6 \quad \text{and} \quad D > \mu_2\left(S_{\text{H}_2}^{\text{in}}\right) - a_2 := \delta_7.$$

Table 4.3: Critical parameter values δ_i, for $i = 1, \ldots, 7$. All functions are given in Table 3.4, while μ_i and r_5 are given in (2.9) and Table 4.1.

Definition	Value
δ_1 is the largest root of equation $r_5 = 0$	0.010412
δ_2 is the root of $\phi_2(D) - S_{\mathrm{H}_2}^{\mathrm{in}} - (1-\omega)YS_{\mathrm{ch}}^{\mathrm{in}} = 0$	0.068641
δ_3 is the root of $\phi_1(D) - S_{\mathrm{H}_2}^{\mathrm{in}} - (1-\omega)YS_{\mathrm{ch}}^{\mathrm{in}} = 0$	0.068814
δ_4 is the root of $S_{\mathrm{H}_2}^{\mathrm{in}} + \omega\left(\varphi_0(D) - YS_{\mathrm{ch}}^{\mathrm{in}}\right) - M_2(D + a_2) = 0$	0.267251
δ_5 is the root of $\varphi_0(D) - YS_{\mathrm{ch}}^{\mathrm{in}} = 0$	0.267636
$\delta_6 = \mu_0\left(YS_{\mathrm{ch}}^{\mathrm{in}}, S_{\mathrm{H}_2}^{\mathrm{in}}\right) - a_0$	0.327130
$\delta_7 = \mu_2\left(S_{\mathrm{H}_2}^{\mathrm{in}}\right) - a_2$	1.064526

Table 4.4: Existence and stability of steady states, with respect to D. The bifurcation values δ_i, $i = 1, \ldots, 7$ are given in Table 4.3.

Interval	E_{000}	E_{001}	E_{100}	E_{110}^1	E_{110}^2	E_{101}	E_{111}
$0 < D < \delta_1$	U	U	S	U	U		U
$\delta_1 < D < \delta_2$	U	U	S	U	U		S
$\delta_2 < D < \delta_3$	U	U	S	U	S		
$\delta_3 < D < \delta_4$	U	U	S				
$\delta_4 < D < \delta_5$	U	U	U			S	
$\delta_5 < D < \delta_6$	U	S	U				
$\delta_6 < D < \delta_7$	U	S					
$\delta_7 < D$	S						

Table 4.5: Bifurcation types corresponding to the critical values of δ_i, $i = 1, \ldots, 7$, defined in Table 4.3. There exists also a critical value $\delta^* \simeq 0.009879 < \delta_1$ corresponding to the value of D where the stable limit cycle disappears when D is increasing.

	Bifurcation types
δ^*	Disappearance of the stable limit cycle
δ_1	Supercritical Hopf bifurcation
δ_2	Transcritical bifurcation of E_{110}^2 and E_{111}
δ_3	Saddle-node bifurcation of E_{110}^1 and E_{110}^2
δ_4	Transcritical bifurcation of E_{100} and E_{101}
δ_5	Transcritical bifurcation of E_{001} and E_{101}
δ_6	Transcritical bifurcation of E_{000} and E_{100}
δ_7	Transcritical bifurcation of E_{000} and E_{001}

Table 4.6: Existence and local stability conditions of steady states of (2.1), when $S_{\text{ph}}^{\text{in}} = 0$.

	Existence conditions	Stability conditions
E_{000}	Always exists	$\mu_0\left(YS_{\text{ch}}^{\text{in}}, S_{\text{H}_2}^{\text{in}}\right) < D + a_0$, $\mu_2\left(S_{\text{H}_2}^{\text{in}}\right) < D + a_2$
E_{001}	$\mu_2\left(S_{\text{H}_2}^{\text{in}}\right) > D + a_2$	$YS_{\text{ch}}^{\text{in}} < \varphi_0(D)$
E_{100}	$\mu_0\left(YS_{\text{ch}}^{\text{in}}, S_{\text{H}_2}^{\text{in}}\right) > D + a_0$	$\mu_1\left(YS_{\text{ch}}^{\text{in}} - s_0, S_{\text{H}_2}^{\text{in}} - \omega\left(YS_{\text{ch}}^{\text{in}} - s_0\right)\right) < D + a_1$ $S_{\text{H}_2}^{\text{in}} - \omega YS_{\text{ch}}^{\text{in}} < M_2(D + a_2) - \omega\varphi_0(D)$ with s_0 solution of $\psi_0(s_0) = D + a_0$
E_{110}	$(1-\omega)YS_{\text{ch}}^{\text{in}} + S_{\text{H}_2}^{\text{in}} \geq \phi_1(D)$, $YS_{\text{ch}}^{\text{in}} > M_0(D+a_0, s_2) + M_1(D+a_1, s_2)$ with s_2 solution of $\Psi(s_2, D) = (1-\omega)YS_{\text{ch}}^{\text{in}} + S_{\text{H}_2}^{\text{in}}$	$(1-\omega)YS_{\text{ch}}^{\text{in}} + S_{\text{H}_2}^{\text{in}} < \phi_2(D)$, $\phi_3(D) > 0$ $\frac{\partial\Psi}{\partial s_2}(s_2, D) > 0$
E_{101}	$YS_{\text{ch}}^{\text{in}} > \varphi_0(D)$, $S_{\text{H}_2}^{\text{in}} - \omega YS_{\text{ch}}^{\text{in}} > M_2(D + a_2) - \omega\varphi_0(D)$	$YS_{\text{ch}}^{\text{in}} < \varphi_0(D) + \varphi_1(D)$
E_{111}	$(1-\omega)YS_{\text{ch}}^{\text{in}} + S_{\text{H}_2}^{\text{in}} > \phi_2(D)$, $YS_{\text{ch}}^{\text{in}} > \varphi_0(D) + \varphi_1(D)$	$c_3 > 0$, $c_5 > 0$, $r_4 > 0$, $r_5 > 0$

Thus, E_{000} is stable if and only if $D > \max(\delta_6, \delta_7) = \delta_7$ (see Table 4.3 for all critical parameter values δ_i, $i = 1, \ldots, 7$).

From Table 4.6, E_{001} exists if and only if $D < \delta_7$. From the eigenvalues λ_1 and λ_2 of $\mathcal{J}$ evaluated at E_{001}, we deduce that E_{001} is stable if and only if

$$F_1(D) := \mu_0\left(YS_{\text{ch}}^{\text{in}}, M_2(D + a_2)\right) - D - a_0 < 0 \quad \Longleftrightarrow \quad \delta_5 < D < \delta_7,$$

where δ_5 is the solution of equation $F_1(D) = 0$ (see Figure 4.1).

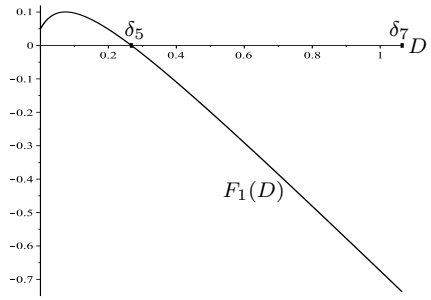

Figure 4.1: Stability of E_{001}, for all $D \in (\delta_5, \delta_7)$: change of sign of the function F_1.

E_{100} exists if and only if $D < \delta_6$ and it is stable if and only if

$$F_2(D) := \mu_1\left(S_{\text{ch}}^{\text{in}}Y - s_0, S_{\text{H}_2}^{\text{in}} - \omega\left(S_{\text{ch}}^{\text{in}}Y - s_0\right)\right) - D - a_1 < 0,$$
$$F_3(D) := S_{\text{H}_2}^{\text{in}} + \omega\left(\varphi_0(D) - YS_{\text{ch}}^{\text{in}}\right) - M_2(D + a_2) < 0,$$

that is, $D < \delta_4$, where δ_4 is the solution of equation $F_3(D) = 0$ (see Figure 4.2).

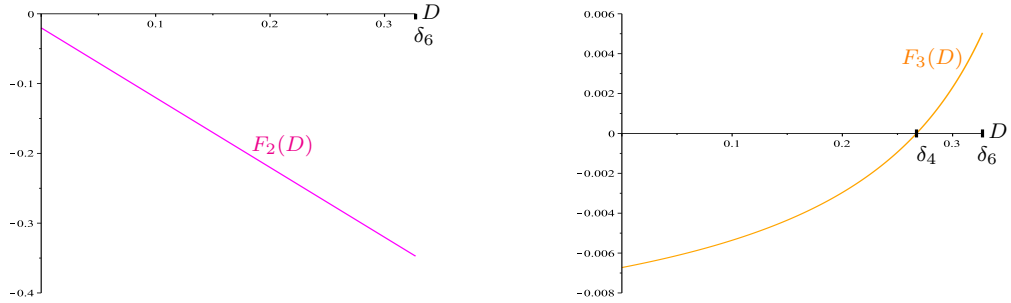

Figure 4.2: Stability of E_{100}, for all $D < \delta_4$: signs of the functions F_2 and F_3.

From Remark 2.1, the system can have at most two steady states of the form E_{110} denoted by E^1_{110} and E^2_{110} as $\omega \simeq 0.53 < 1$. Their first existence condition in Table 4.6 holds if and only if

$$F_4(D) := \phi_1(D) - S^{in}_{H_2} - (1-\omega)YS^{in}_{ch} \leq 0 \quad \Longleftrightarrow \quad D \leq \delta_3,$$

where δ_3 is the solution of equation $F_4(D) = 0$ (see Figure 4.3(a)). Their second existence condition holds for all $D \leq \delta_3$, since the straight line of equation $y = YS^{in}_{ch}$ is above the curve of the function $y = M_0\left(D + a_0, s_2^{*i}\right) + M_1\left(D + a_1, s_2^{*i}\right)$, for $i = 1, 2$, which correspond to E^1_{110} and E^2_{110}, respectively, see Figure 4.3(b). From Remark 2.1 and Table 4.6, E^1_{110} is

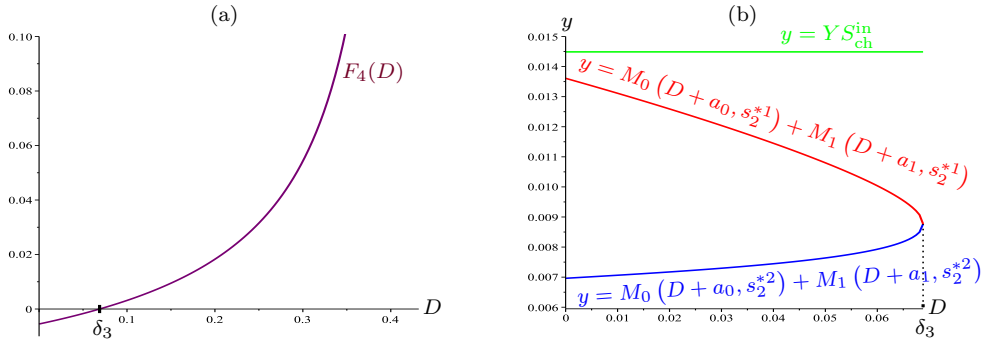

Figure 4.3: Existence of E_{110}, for all $D \leq \delta_3$: (a) change of sign of the function F_4. (b) the green line of equation $y = YS^{in}_{ch}$ is above the red and blue curves of the functions $M_0\left(D + a_0, s_2^{*i}\right) + M_1\left(D + a_1, s_2^{*i}\right)$, $i = 1, 2$, respectively.

unstable for all $0 < D < \delta_3$ while E^2_{110} is stable if and only if

$$F_5(D) := \phi_2(D) - S^{in}_{H_2} - (1-\omega)YS^{in}_{ch} > 0 \quad \text{and} \quad \phi_3(D) > 0,$$

that is, $D \in (\delta_2, \delta_3)$ where δ_2 is the solution of equation $F_5(D) = 0$ (see Figure 4.4). Indeed, $F_5(D) > 0$ for all $D \in (\delta_2, \delta_3)$ and $\phi_3(D) > 0$ for all $D \in (\delta'_2, \delta_3)$ where $\delta'_2 \simeq 0.057865$ is the solution of equation $\phi_3(D) = 0$ such that $\delta'_2 < \delta_2$.

E_{101} exists if and only if $F_1(D) > 0$ and $F_3(D) > 0$, that is, $\delta_4 < D < \delta_5$. E_{101} is stable if and only if

$$F_6(D) := \varphi_0(D) + \varphi_1(D) - YS^{in}_{ch} > 0,$$

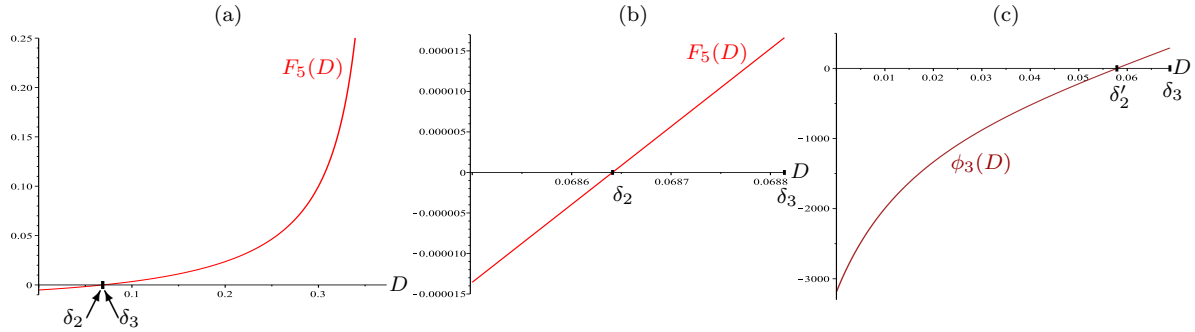

Figure 4.4: Stability of E_{110}, for all $D \in (\delta_2, \delta_3)$: (a) Curve of the function F_5. (b) Magnification of F_5, for $D \in [0.0685, 0.0688]$. (c) Curve of the function ϕ_3.

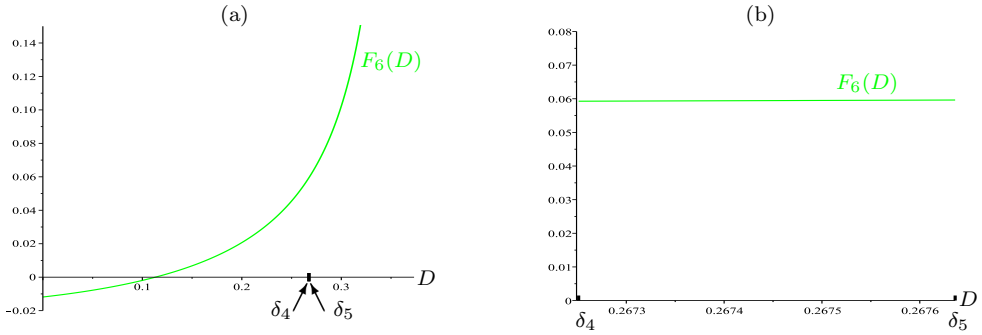

Figure 4.5: Stability of E_{101}, for all $D \in (\delta_4, \delta_5)$ and existence of E_{111} for all $D < \delta_2$: (a) curve of the function F_6. (b) Magnification of $F_6(D)$, for $D \in [\delta_4, \delta_5]$.

that is, for all $D \in (\delta_4, \delta_5)$ (see Figure 4.5).

E_{111} exists if and only if $F_5(D) < 0$ and $F_6(D) < 0$, that is, for all $D < \delta_2$ where δ_2 is the solution of the equation $F_5(D) = 0$ (see Figure 4.4(a-b) and Figure 4.5). Indeed, $F_5(D) < 0$ for all $D < \delta_2$ and $F_6(D) < 0$ for all $D < \delta_2''$ where $\delta_2'' \simeq 0.113033$ is the solution of equation $F_6(D) = 0$ such that $\delta_2 < \delta_2''$. To determine the stability of E_{111}, the functions c_3, c_5, r_4 and r_5 are plotted with respect to $D < \delta_2$. Figure 4.6 shows that $c_3(D)$, $c_5(D)$, $r_4(D)$ and $r_5(D)$ are all positive if and only if $\delta_1 < D < \delta_2$ where $\delta_1 \simeq 0.010412$ is the solution of equation $r_5(D) = 0$.

To give numerical evidence of the Hopf bifurcation occurring for $D = \delta_1$, we determine numerically the eigenvalues of the Jacobian matrix of system (2.1) at E_{111} and we plot them with respect to D. Figure 4.7(a-b) shows that two eigenvalues denoted by $\lambda_1(D)$ and $\lambda_2(D)$ are real and remain negative for all $D \in [0, \delta_2)$. Figure 4.7(c) shows that the two other eigenvalues $\lambda_3(D)$ and $\lambda_4(D)$ form a complex-conjugate pair denoted by

$$\lambda_{3,4}(D) = \alpha_{3,4}(D) \pm i\beta_{3,4}(D), \quad \text{for all} \quad D \in [0, \delta^\star),$$

where the real part $\alpha_{3,4}$ remains negative and $\delta^\star \simeq 0.068504$. Then, they become real, negative and distinct for all $D \in (\delta^\star, \delta_2)$. Similarly, Figure 4.7(d) shows that the two last eigenvalues $\lambda_5(D)$ and $\lambda_6(D)$ form a complex-conjugate pair denoted by

$$\lambda_{5,6}(D) = \alpha_{5,6}(D) \pm i\beta_{5,6}(D), \quad \text{for all} \quad D \in [0, \delta^\star),$$

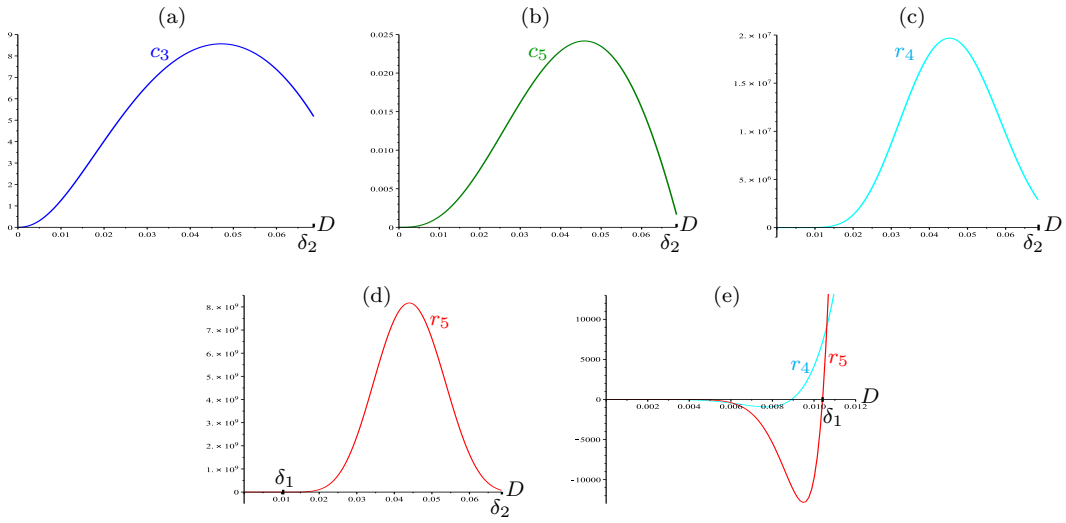

Figure 4.6: (a-b-c-d) Curves of c_3, c_5, r_4 and r_5 as functions of D, for $0 < D < \delta_2$. (e) Magnification of the curves of r_4 and r_5, for $D \in [0, 0.012]$.

where the real part $\alpha_{5,6}$ is positive for all $D \in [0, \delta_1)$ and negative for all $D \in (\delta_1, \delta^\star)$. Then, for all $D \in (\delta^\star, \delta_2)$, they become real, negative and distinct. At the particular value $D = \delta_1$, the pair $\lambda_{5,6}(D)$ is purely imaginary such that $\alpha_{5,6}(\delta_1) = 0$, with $\beta_{5,6}(\delta_1) \neq 0$. Moreover, one has

$$\frac{d\alpha_{5,6}}{dD}(\delta_1) < 0.$$

This is consistent with Figure 4.8(b) showing that, as D decreases and crosses δ_1, the steady state E_{111} becomes unstable and we have a supercritical Hopf bifurcation, leading to the appearance, from the steady state E_{111}, of small-amplitude periodic oscillations.

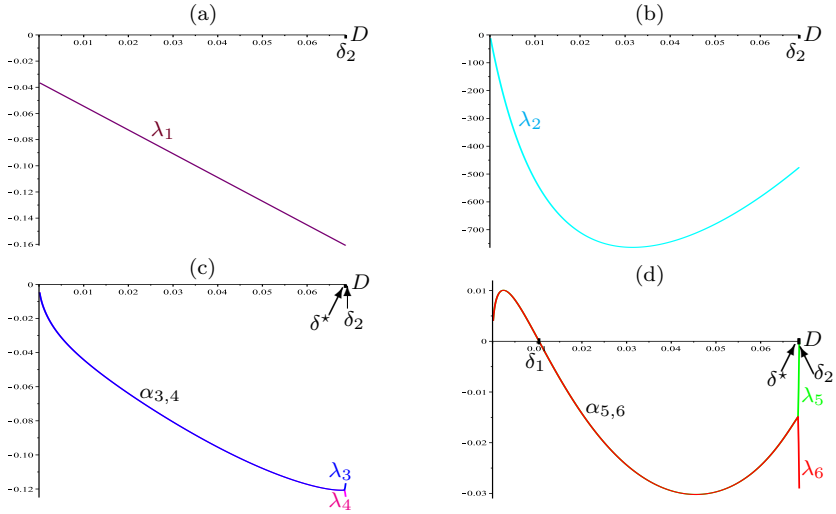

Figure 4.7: The eigenvalues of the Jacobian matrix at E_{111} as functions of D, when $S_{ch}^{in} = 0.1$, $S_{ph}^{in} = 0$ and $S_{H_2}^{in} = 2.67 \times 10^{-5}$. (c-d) The real parts $\alpha_{3,4}$ and $\alpha_{5,6}$ for $D \in [0, \delta^\star)$.

□

To illustrate the emergence of limit cycle and to understand what happens with the limit cycle born via the supercritical Hopf bifurcation when D is varied, we present in Figure 4.8 the one-parameter bifurcation diagram for system (2.1) of X_{ch} depending on the dilution rate D when all other parameters are fixed. When magnified, we observe more clearly the disappearance of the limit cycle at δ^*, the Hopf bifurcation at δ_1, the transcritical bifurcations at δ_2, δ_4 and δ_5 and the saddle-node bifurcation at δ_3, see Figure 4.8(b-c-d). In Figure 4.8, E_{000} and E_{001} cannot be distinguished since they have both a zero X_{ch}-component. As E_{001} is stable and E_{000} is unstable for $D < \delta_7$, the $X_{\text{ch}} = 0$ axis is plotted in blue as the color of E_{001} in Table 3.9.

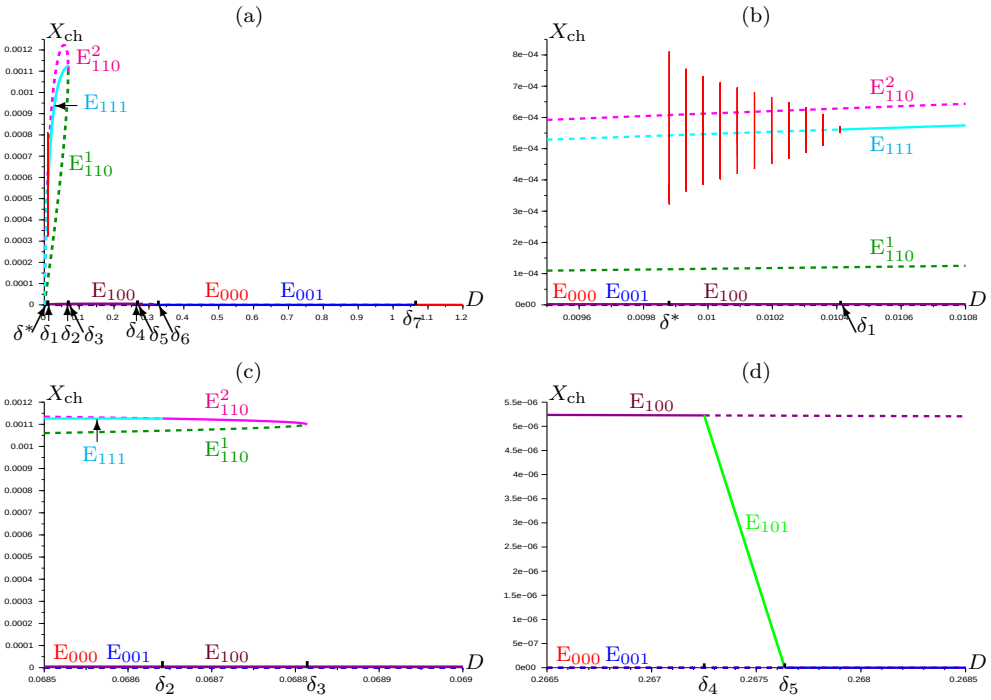

Figure 4.8: (a) Bifurcation diagram of X_{ch} versus $D \in [0, 1.2]$ in model (2.1). (b) Magnification on the appearance and disappearance of stable limit cycles for $D \in [0.0095, 0.0108]$. (c) Magnification on the transcritical bifurcation at $D = \delta_2$ and the saddle-node bifurcation at $D = \delta_3$ for $D \in [0.0685, 0.069]$. (d) Magnification on the transcritical bifurcations for $D \in [0.2665, 0.2685]$.

Remark 4.2. Following [41], not all of the behaviors described in Table 4.4 were reported in [64]. For $S^{\text{in}}_{\text{ch}} = 0.1$. Note that the destabilization of E_{111} (SS6) via a Hopf bifurcation with the emergence of a stable limit cycle has not been observed in [64]. Moreover, the region of existence and stability of E_{101} (SS5), which was depicted in Figure 3(b) of [64] in the case where $S^{\text{in}}_{\text{H}_2} = 2.67 \times 10^{-2}$, was not reported in Figure 3(a) of [64]. Our results show that this region also exists when $S^{\text{in}}_{\text{H}_2} = 2.67 \times 10^{-5}$, and explain why it was not detected by the numerical analysis given in Figure 3(a) of [64]: E_{101} (SS5) occurs in a very small region since, for $S^{\text{in}}_{\text{ch}} = 0.1$ it corresponds to $\delta_4 < D < \delta_5$, where $\delta_4 \simeq 0.267251$ and $\delta_5 \simeq 0.267636$, with $\delta_5 - \delta_4$ of order 10^{-4}. However, while from a mathematical point

of view the diagram shown in [64] is incorrectly labeled, in biological terms, such a small region of E_{101} (SS5) would likely not be attained.

4.4.2 Bifurcation diagram with respect to S_{ch}^{in}

Now, we constructe the bifurcation diagram according to the chlorophenol input concentration as the bifurcating parameter S_{ch}^{in}. We consider $S_{ph}^{in} = 0$ and $S_{H_2}^{in} = 2.67 \times 10^{-5}$, corresponding to Figure 3(a) in [64] and we fix $D = 0.01$. Using Table 4.6, we have the following result.

Proposition 4.2. *Let $S_{ph}^{in} = 0$, $S_{H_2}^{in} = 2.67 \times 10^{-5}$ and $D = 0.01$. Using the biological parameter values in Table 3.3, while $k_{dec,i} = 0.02$, the bifurcation values σ_i, $i = 1, \ldots, 6$ are provided in Table 4.7. The bifurcation analysis of (2.1) according to S_{ch}^{in} is given in Table 4.8. The bifurcation types at the critical values σ_i are defined in Table 4.9.*

Table 4.7: Critical parameter values σ_i, for $i = 1, \ldots, 6$. All functions are given in Table 3.4, while r_5 is given in Table 4.1. Note that $\sigma_1 < \sigma_3 < \sigma_4 < \sigma_2 < \sigma_5 < \sigma_6$, compare with the case without maintenance.

Definition	Value
$\sigma_1 = M_0\left(D + a_0, S_{H_2}^{in}\right)/Y$	0.003173
$\sigma_2 = (\phi_1(D) - S_{H_2}^{in})/((1-\omega)Y)$	0.029402
$\sigma_3 = \varphi_0(D)/Y$	0.013643
$\sigma_4 = (S_{H_2}^{in} - M_2(D + a_2) + \omega\varphi_0(D))/(\omega Y)$	0.013985
$\sigma_5 = (\phi_2(D) - S_{H_2}^{in})/((1-\omega)Y)$	0.033292
σ_6 is the largest root of equation $r_5 = 0$	0.1025

Table 4.8: Existence and stability of steady states, with respect to S_{ch}^{in}. The bifurcation values σ_i, $i = 1, \ldots, 6$ are given in Table 4.7.

Interval	E_{000}	E_{001}	E_{100}	E_{110}^1	E_{110}^2	E_{101}	E_{111}
$0 < S_{ch}^{in} < \sigma_1$	U	S					
$\sigma_1 < S_{ch}^{in} < \sigma_3$	U	S	U				
$\sigma_3 < S_{ch}^{in} < \sigma_4$	U	U	U			S	
$\sigma_4 < S_{ch}^{in} < \sigma_2$	U	U	S				
$\sigma_2 < S_{ch}^{in} < \sigma_5$	U	U	S	U	U		
$\sigma_5 < S_{ch}^{in} < \sigma_6$	U	U	S	U	U		U
$\sigma_6 < S_{ch}^{in}$	U	U	S	U	U		S

Table 4.9: Bifurcation types corresponding to the critical values of σ_i, $i = 1, \ldots, 6$, defined in Table 4.7. There exists also a critical value $\sigma^* \simeq 0.099295 \in (\sigma_5, \sigma_6)$ corresponding to the value of $S_{\text{ch}}^{\text{in}}$ where the stable limit cycle disappears when $S_{\text{ch}}^{\text{in}}$ is decreasing.

	Bifurcation types
σ_1	Transcritical bifurcation of E_{000} and E_{100}
σ_2	Saddle-node bifurcation of E_{110}^1 and E_{110}^2
σ_3	Transcritical bifurcation of E_{001} and E_{101}
σ_4	Transcritical bifurcation of E_{100} and E_{101}
σ_5	Transcritical bifurcation of E_{110}^1 and E_{111}
σ_6	Supercritical Hopf bifurcation
σ^*	Disappearance of the stable limit cycle

Proof. From Table 4.6, we have:

Since the second stability condition of E_{000} in Table 4.6 does not hold

$$\mu_2\left(S_{\text{H}_2}^{\text{in}}\right) \simeq 1.0845 > D + a_2 = 0.03, \tag{4.37}$$

E_{000} always exists and is unstable.

Since the existence condition of E_{001} in Table 4.6 holds (see inequality (4.37)), E_{001} exists and is stable if and only if

$$S_{\text{ch}}^{\text{in}} < \varphi_0(D)/Y =: \sigma_3.$$

E_{100} exists if and only if

$$S_{\text{ch}}^{\text{in}} > M_0\left(D + a_0, S_{\text{H}_2}^{\text{in}}\right)/Y =: \sigma_1.$$

Let $F\left(S_{\text{ch}}^{\text{in}}\right)$ be the function defined by

$$F\left(S_{\text{ch}}^{\text{in}}\right) = \mu_1\left(S_{\text{ch}}^{\text{in}}Y - s_0, S_{\text{H}_2}^{\text{in}} - \omega\left(S_{\text{ch}}^{\text{in}}Y - s_0\right)\right). \tag{4.38}$$

The first stability condition of E_{100} in Table 4.6 holds for all $S_{\text{ch}}^{\text{in}} > \sigma_1$, that is, $F\left(S_{\text{ch}}^{\text{in}}\right) < D + a_1$ since the maximum of F is smaller than 0.0013 while $D + a_1 = 0.03$ (see Figure 4.9). From the second stability condition in Table 4.6, E_{100} is stable if and only if

$$S_{\text{ch}}^{\text{in}} > \left(S_{\text{H}_2}^{\text{in}} - M_2(D + a_2) + \omega\varphi_0(D)\right)/(\omega Y) =: \sigma_4.$$

The first existence condition of E_{110} in Table 4.6 holds, if and only if

$$S_{\text{ch}}^{\text{in}} \geq \left(\phi_1(D) - S_{\text{H}_2}^{\text{in}}\right)/((1-\omega)Y) =: \sigma_2.$$

Their second existence condition holds, for all $S_{\text{ch}}^{\text{in}} \in [\sigma_2, 0.11]$, since the straight line of equation $y = S_{\text{ch}}^{\text{in}}Y$ is above the curves of the functions $y = M_0\left(D + a_0, s_2^{*i}\right) + M_1\left(D + a_1, s_2^{*i}\right)$,

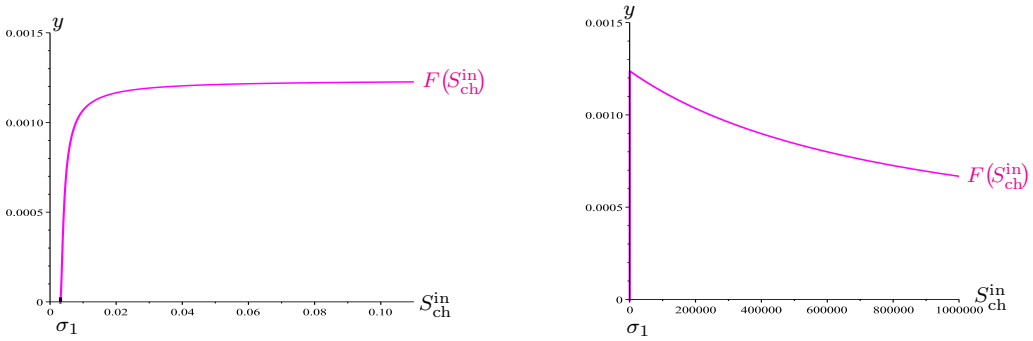

Figure 4.9: Curve of the function $y = F\left(S_{\text{ch}}^{\text{in}}\right)$ defined by (4.38).

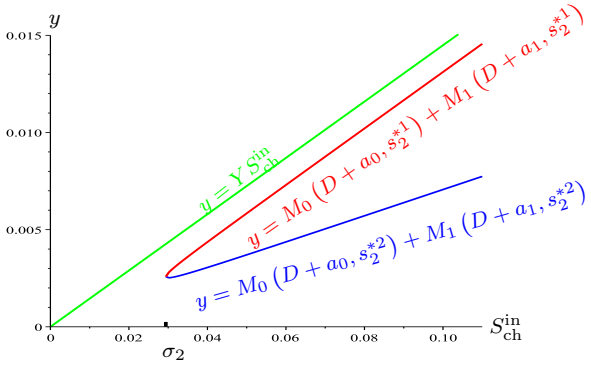

Figure 4.10: The green line of equation $y = Y S_{\text{ch}}^{\text{in}}$ is above the red and blue curves of the functions $M_0\left(D + a_0, s_2^{*i}\right) + M_1\left(D + a_1, s_2^{*i}\right)$, for $i = 1, 2$, which correspond to E_{110}^1 and E_{110}^2, respectively.

for $i = 1, 2$, respectively (see Figure 4.10). Thus, E_{110}^1 and E_{110}^2 exist and are unstable for all $S_{\text{ch}}^{\text{in}} > \sigma_2$ since the second stability condition does not hold where $\phi_3(D) \simeq -1996.917 < 0$.

E_{101} exists if and only if $\sigma_3 := \varphi_0(D)/Y < S_{\text{ch}}^{\text{in}} < \sigma_4$. When it exists, E_{101} is stable since

$$S_{\text{ch}}^{\text{in}} < \sigma_4 \simeq 0.013985 < (\varphi_0(D) + \varphi_1(D))/Y \simeq 0.02304.$$

E_{111} exists if and only if

$$S_{\text{ch}}^{\text{in}} > \frac{\phi_2(D) - S_{\text{H}_2}^{\text{in}}}{(1-\omega)Y} =: \sigma_5 \simeq 0.033292, \quad S_{\text{ch}}^{\text{in}} > \frac{\varphi_0(D) + \varphi_1(D)}{Y} \simeq 0.02304.$$

Hence, E_{111} exists if and only if $S_{\text{ch}}^{\text{in}} > \sigma_5$. To determine the stability of E_{111}, the functions c_3, c_5, r_4 and r_5 are plotted with respect to $S_{\text{ch}}^{\text{in}} > \sigma_5$. Figure 4.11 shows that $c_3(S_{\text{ch}}^{\text{in}})$, $c_5(S_{\text{ch}}^{\text{in}})$, $r_4(S_{\text{ch}}^{\text{in}})$ and $r_5(S_{\text{ch}}^{\text{in}})$ are all positive if and only if $S_{\text{ch}}^{\text{in}} > \sigma_6$ where $\sigma_6 \simeq 0.1025$ is the largest root of equation $r_5\left(S_{\text{ch}}^{\text{in}}\right) = 0$.

To give numerical evidence of the Hopf bifurcation occurring for $S_{\text{ch}}^{\text{in}} = \sigma_6$, we determine numerically the eigenvalues of the Jacobian matrix of system (2.1) at E_{111} and we plot them with respect to $S_{\text{ch}}^{\text{in}}$. Figure 4.12(a-b) shows that two eigenvalues denoted by $\lambda_1\left(S_{\text{ch}}^{\text{in}}\right)$ and $\lambda_2\left(S_{\text{ch}}^{\text{in}}\right)$ are real and remain negative for all $S_{\text{ch}}^{\text{in}} \in (\sigma_5, 0.11]$. Figure 4.12(c) shows

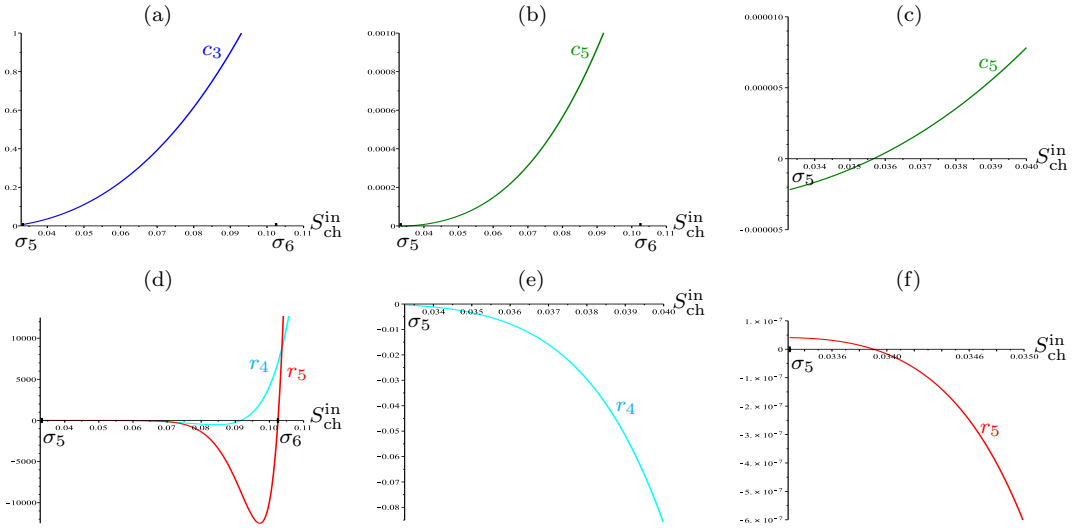

Figure 4.11: (a-b-d) Curves of c_3, c_5, r_4 and r_5 as functions of S_{ch}^{in}, for $S_{ch}^{in} > \sigma_5$. (c-e-f) Magnifications of the curves c_5 and r_4, for $S_{ch}^{in} \in [\sigma_5, 0.04]$ and of r_5, for $S_{ch}^{in} \in [\sigma_5, 0.035]$.

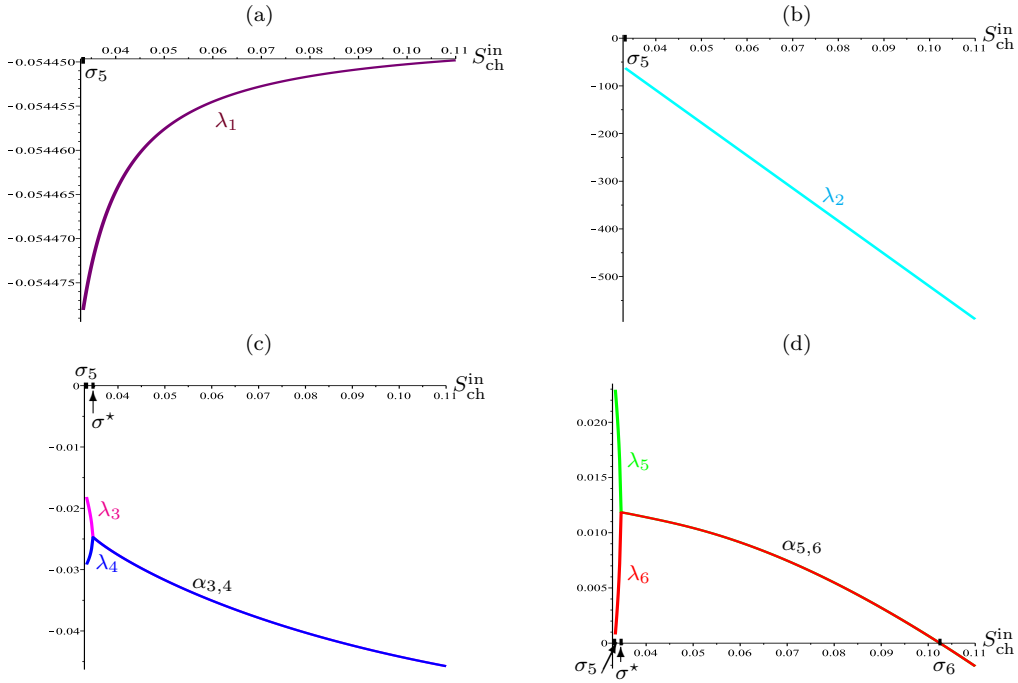

Figure 4.12: The eigenvalues of the Jacobian matrix at E_{111} as functions of S_{ch}^{in}, when $D = 0.01$, $S_{ph}^{in} = 0$ and $S_{H_2}^{in} = 2.67\times10^{-5}$. (c-d) The real parts $\alpha_{3,4}$ and $\alpha_{5,6}$, for $S_{ch}^{in} \in (\sigma^\star, 0.11]$.

that the two other eigenvalues $\lambda_3\left(S_{ch}^{in}\right)$ and $\lambda_4\left(S_{ch}^{in}\right)$ are real, negative and distinct for all $S_{ch}^{in} \in (\sigma_5, \sigma^\star)$ where $\sigma^\star \simeq 0.03467$. Then, they become a complex-conjugate pair denoted by

$$\lambda_{3,4}\left(S_{ch}^{in}\right) = \alpha_{3,4}\left(S_{ch}^{in}\right) \pm i\beta_{3,4}\left(S_{ch}^{in}\right), \quad \text{for all} \quad S_{ch}^{in} \in (\sigma^\star, 0.11],$$

where the real part $\alpha_{3,4}$ remains negative.

Figure 4.12(d) shows that the two last eigenvalues $\lambda_5\left(S_{\text{ch}}^{\text{in}}\right)$ and $\lambda_6\left(S_{\text{ch}}^{\text{in}}\right)$ are real, positive and distinct for all $S_{\text{ch}}^{\text{in}} \in (\sigma_5, \sigma^\star]$. Then, they become a complex-conjugate pair denoted by

$$\lambda_{5,6}\left(S_{\text{ch}}^{\text{in}}\right) = \alpha_{5,6}\left(S_{\text{ch}}^{\text{in}}\right) \pm i\beta_{5,6}\left(S_{\text{ch}}^{\text{in}}\right), \quad \text{for all} \quad S_{\text{ch}}^{\text{in}} \in (\sigma^\star, 0.11],$$

so that the real part $\alpha_{5,6}$ is positive for all $S_{\text{ch}}^{\text{in}} \in (\sigma^\star, \sigma_6)$ and negative for all $S_{\text{ch}}^{\text{in}} \in (\sigma_6, 0.11]$. At the particular value $S_{\text{ch}}^{\text{in}} = \sigma_6$, the pair $\lambda_{5,6}\left(S_{\text{ch}}^{\text{in}}\right)$ is purely imaginary such that $\alpha_{5,6}(\sigma_6) = 0$, with $\beta_{5,6}(\sigma_6) \neq 0$. Moreover, one has

$$\frac{d\alpha_{5,6}}{dS_{\text{ch}}^{\text{in}}}(\sigma_6) < 0.$$

This is consistent with Figures 4.13, 4.14 and 4.15, showing that, as $S_{\text{ch}}^{\text{in}}$ decreases and crosses σ_6, the steady state E_{111} changes its stability through a supercritical Hopf bifurcation with the emergence of a stable limit cycle that we illustrate in Figures 4.19 and 4.17.

□

Figures 4.13 and 4.14 show the one-parameter bifurcation diagrams of X_{ch} and X_{H_2} versus $S_{\text{ch}}^{\text{in}}$ in system (2.1), respectively. The magnifications of the bifurcation diagrams are illustrated in Figure 4.13(b), Figure 4.14(b) and Figure 4.15 showing the transcritical bifurcations at σ_1, σ_3, σ_4 and σ_5, the saddle-node bifurcation at σ_2, the Hopf bifurcation at σ_6 and the disappearance of the cycle at σ^*. In Figure 4.13(b), E_{000} and E_{001} cannot be distinguished since they have both a zero X_{ch}-component. As E_{001} is stable and E_{000} is unstable for $S_{\text{ch}}^{\text{in}} < \sigma_3$, the $X_{\text{ch}} = 0$ axis is plotted in blue as the color of E_{001} in Table 3.9. In Figure 4.14(b), E_{000} and E_{001} are distinguished but it is not the case for E_{000} and E_{100}, since they have both a zero X_{H_2}-component. As E_{100} is stable and E_{000} is unstable for $S_{\text{ch}}^{\text{in}} > \sigma_4$, the $X_{\text{H}_2} = 0$ axis is plotted in purple as the color of E_{100} in Table 3.9.

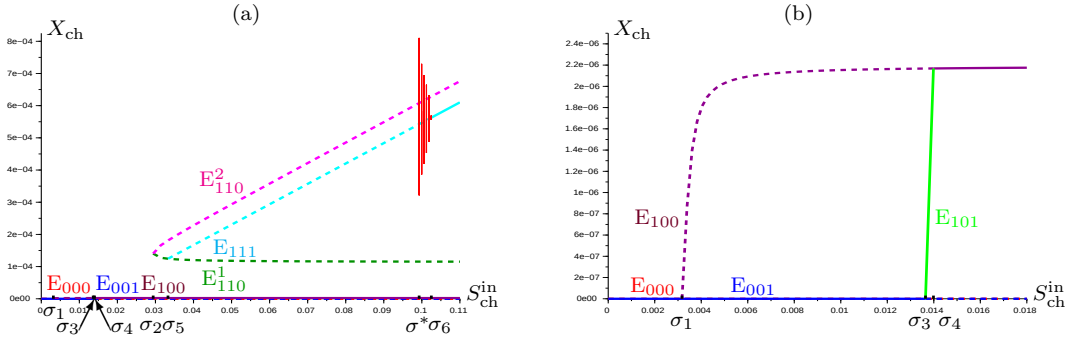

Figure 4.13: (a) Bifurcation diagram of X_{ch} versus $S_{\text{ch}}^{\text{in}} \in [0, 0.11]$ in model (2.1) showing the appearance and disappearance of stable limit cycles. (b) Magnification on the transcritical bifurcations for $S_{\text{ch}}^{\text{in}} \in [0, 0.018]$.

Remark 4.3. As explained in Remark 4.2, the operating diagram of Figure 3(a) in [64] for $D = 0.01$ does not accurately describe the transition from the region labeled E_{001}

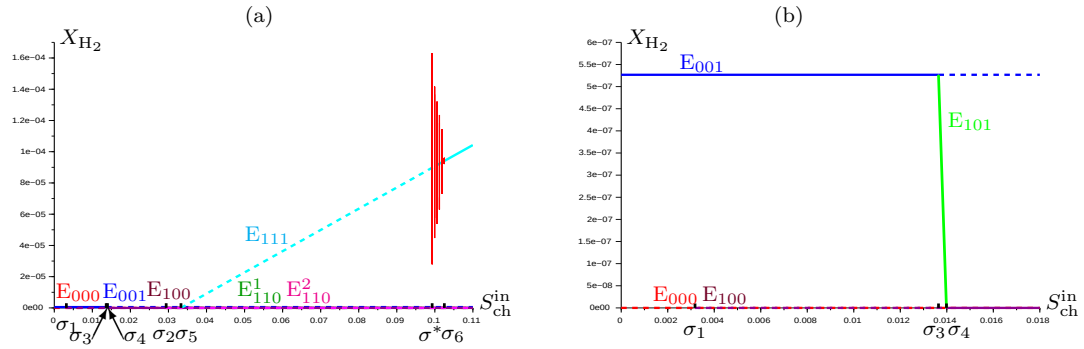

Figure 4.14: (a) Bifurcation diagram of X_{H_2} versus $S^{in}_{ch} \in [0, 0.11]$ in model (2.1). (b) Magnification on the transcritical bifurcations for $S^{in}_{ch} \in [0, 0.018]$.

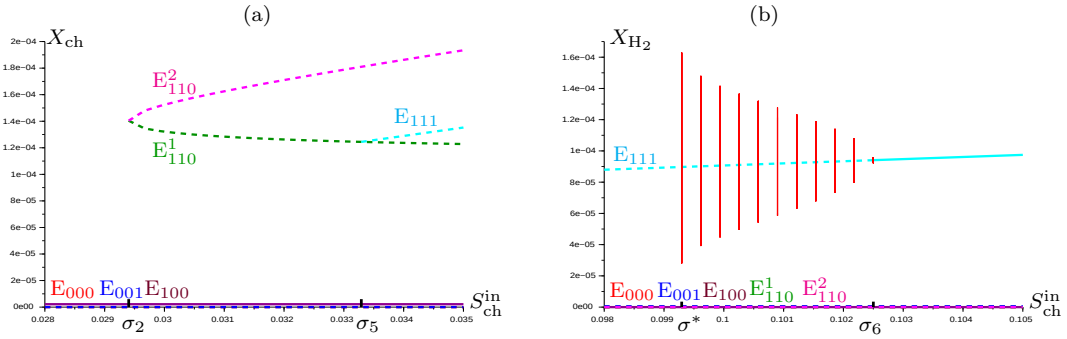

Figure 4.15: (a) Magnification on the saddle-node bifurcation at $S^{in}_{ch} = \sigma_2$ and the transcritical bifurcation at $S^{in}_{ch} = \sigma_5$ for $S^{in}_{ch} \in [0.028, 0.035]$. (b) Magnification on the limit cycles for $S^{in}_{ch} \in [0.098, 0.105]$.

(corresponding to the stability of (SS2)) to the E_{100} region (corresponding to the stability of (SS3)). Our results show that this transition is via a E_{101} (SS5) region, which is very thin, since it corresponds to $\sigma_3 < S^{in}_{ch} < \sigma_4$, where $\sigma_3 \simeq 0.013643$ and $\sigma_4 \simeq 0.013985$. This region was missing in Figure 3(a) in [64], since $\sigma_4 - \sigma_3$ is of order 10^{-4}. Indeed, the limitations of the operating diagram in Figure 3(a) in [64] is due to the numerical resolution: the stability of E_{101} (SS5) occurs in a very small region and may not be detected if the step size was for example an order of magnitude greater than $\sigma_4 - \sigma_3$.

Remark 4.4. As explained in Remark 4.3, except for E_{111}, the maintenance does not destabilize the steady states. Only their regions of existence and stability, with respect to the operating parameters, can be modified. For E_{111}, it is more difficult to answer the question of whether or not it can be destabilized by including maintenance terms. The bifurcations diagrams depicted in Figures 4.13, 4.14 and 4.15, and the results given in Proposition 4.2, permit to answer this question at least for the following values of the operating parameters $S^{in}_{ph} = 0$, $S^{in}_{H_2} = 2.67 \times 10^{-5}$, $D = 0.01$ and $S^{in}_{ch} \geq 0$. The comparison of the results obtained in Table 4.8 with those given in Table 3.6 shows only minor changes in the bifurcation values σ_i, $i = 1, \ldots, 6$. Therefore, even for E_{111}, the maintenance does not destabilize the system: only the regions of stability, with respect to the operating parameters, are slightly modified. Note that the change of the bifurcation values σ_i is

predictable since their formulas in Table 4.7 involve the added decay terms. However, the saddle-node bifurcation at σ_2 arises after and not before the transcritical bifurcations at σ_3 and σ_4 as in the case without maintenance.

4.5 Numerical simulations

In this section, we confirm the main findings in the previous section. Using the rescaling of the variables (3.20) given in [64], and the dimensionless form (3.21) of (2.1), we perform numerical simulations which show the behavior of system according to initial conditions given in Table 4.10. We illustrate, in particular, the three-dimensional phase plot in three interesting cases where the steady states E_{000}, E_{001}, E^1_{110} and E^2_{110} are unstable:

Table 4.10: The initial conditions of solutions of model (2.1) in Figures 4.16 - 4.22. The initial conditions of (3.21) are given by $X_i(0) = X_i^* + \varepsilon$ and $S_i(0) = S_i^* + \varepsilon$, $i = 0, 1, 2$ where X_i^* and S_i^* are the components of E_{111} and ε is given in the second column. When there is more than one trajectory in the figure, its color is indicated in the first column.

Figure Color	ε	$(X_{\mathrm{ch}}(0), X_{\mathrm{ph}}(0), X_{\mathrm{H_2}}(0), S_{\mathrm{ch}}(0), S_{\mathrm{ph}}(0), S_{\mathrm{H_2}}(0))$
Figure 4.16	$9.7\,10^{-3}$	$(5.44\,10^{-4}, 1.17\,10^{-3}, 8.80\,10^{-5}, 1.42\,10^{-2}, 1.29\,10^{-2}, 6.05\,10^{-7})$
Figure 4.17		
Pink	10^{-2}	$(5.54\,10^{-4}, 1.20\,10^{-3}, 9.00\,10^{-5}, 1.42\,10^{-2}, 1.29\,10^{-2}, 6.12\,10^{-7})$
Blue	$3.2\,10^{-2}$	$(5.76\,10^{-4}, 1.46\,10^{-3}, 9.00\,10^{-5}, 1.53\,10^{-2}, 1.96\,10^{-2}, 1.16\,10^{-6})$
Green	$3.5\,10^{-2}$	$(5.79\,10^{-4}, 1.50\,10^{-3}, 9.00\,10^{-5}, 1.55\,10^{-2}, 2.05\,10^{-2}, 1.24\,10^{-6})$
Figure 4.18		
Blue	$6\,10^{-2}$	$(6.71\,10^{-4}, 1.95\,10^{-3}, 1.04\,10^{-4}, 1.68\,10^{-2}, 2.80\,10^{-2}, 1.86\,10^{-6})$
Green	$7\,10^{-2}$	$(6.81\,10^{-4}, 2.07\,10^{-3}, 1.04\,10^{-4}, 1.74\,10^{-2}, 3.11\,10^{-2}, 2.11\,10^{-6})$
Figure 4.19	$2\,10^{-3}$	$(5.46\,10^{-4}, 1.10\,10^{-3}, 9.00\,10^{-5}, 1.37\,10^{-2}, 1.05\,10^{-2}, 4.12\,10^{-7})$
Figure 4.20	$3.5\,10^{-2}$	$(5.79\,10^{-4}, 1.50\,10^{-3}, 9.00\,10^{-5}, 1.55\,10^{-2}, 2.05\,10^{-2}, 1.24\,10^{-6})$
Figure 4.21	$6\,10^{-2}$	$(6.71\,10^{-4}, 1.95\,10^{-3}, 1.04\,10^{-4}, 1.68\,10^{-2}, 2.80\,10^{-2}, 1.86\,10^{-6})$
Figure 4.22	$7\,10^{-2}$	$(6.81\,10^{-4}, 2.07\,10^{-3}, 1.04\,10^{-4}, 1.74\,10^{-2}, 3.11\,10^{-2}, 2.11\,10^{-6})$

- For $S_{\mathrm{ch}}^{\mathrm{in}} \in (\sigma_5, \sigma^*)$, the numerical simulations done for various positive initial conditions permit to conjecture the global asymptotic stability of E_{100}. Figure 4.16 shows that the trajectorie in green converges toward the stable steady state

$$\mathrm{E}_{100} \simeq \left(2.19\,10^{-6}, 0, 0, 9.77\,10^{-2}, 3.65\,10^{-4}, 9.17\,10^{-8}\right).$$

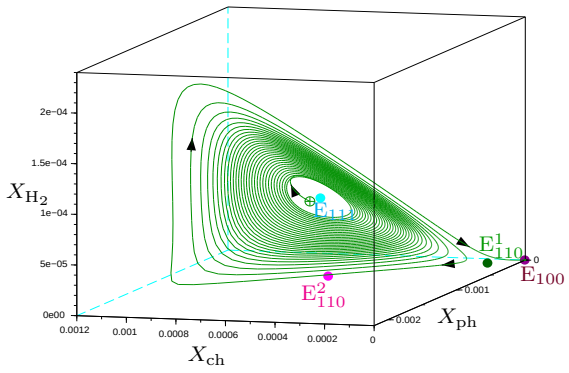

Figure 4.16: Case $S^{in}_{ch} = 0.098 < \sigma^*$: the solution of (2.1) converges to E_{100}.

- For $S^{in}_{ch} \in (\sigma^*, \sigma_6)$, the system exhibits bistability with two basins of attraction: one toward the stable limit cycle and the second toward E_{100}. Figure 4.17 illustrates that the trajectories in pink and blue converge toward the stable limit cycle in red, while the green trajectory converges toward

$$E_{100} \simeq \left(2.19\,10^{-6}, 0, 0, 9.92\,10^{-2}, 3.65\,10^{-4}, 9.12\,10^{-8}\right).$$

  For the initial condition in Table 4.10, the time course in Figure 4.19 illustrates the positive, periodic solution representing the coexistence of the three species. The sustained oscillations prove the stability of the limit cycle. However, Figure 4.20 shows the time course of the green trajectory in Figure 4.17.

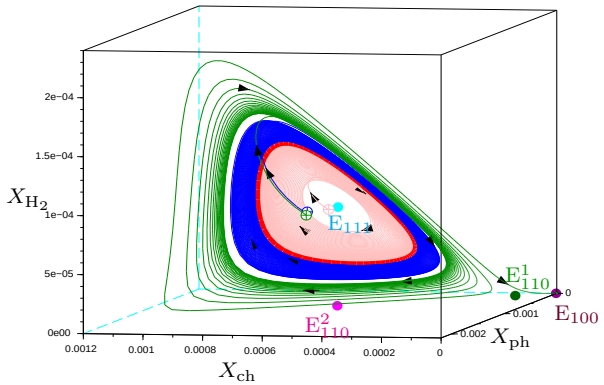

Figure 4.17: Case $\sigma^* < S^{in}_{ch} = 0.0995 < \sigma_6$: bistability with convergence either to the stable limit cycle (in red) or to E_{100}.

- For $S^{in}_{ch} > \sigma_6$, the system exhibits bistability between E_{111} and E_{100}. Figure 4.18 shows that the blue trajectory converges to the stable focus

$$E_{111} \simeq \left(6.10\,10^{-4}, 1.22\,10^{-3}, 1.04\,10^{-4}, 1.36\,10^{-2}, 9.93\,10^{-3}, 3.62\,10^{-7}\right),$$

  while the green trajectory converges to

$$E_{100} \simeq \left(2.19\,10^{-6}, 0, 0, 1.10\,10^{-1}, 3.65\,10^{-4}, 8.79\,10^{-8}\right).$$

Figures 4.21 and 4.22 illustrate the time courses corresponding to the blue and the green trajectories in Figure 4.18, respectively.

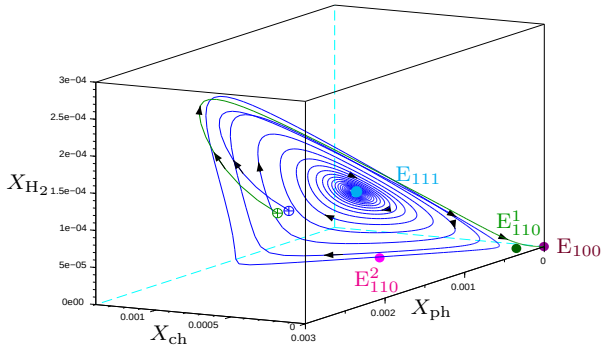

Figure 4.18: Case $\sigma_6 < S_{ch}^{in} = 0.11$: bistability with convergence either to E_{111} or to E_{100}.

Numerical simulations have shown that the stable limit cycle disappears at the critical value $\sigma^* \in (\sigma_5, \sigma_6)$ as S_{ch}^{in} decreases. Similarly to the numerical study of the bifurcation diagram with respect to the parameter D in [57] in the case without maintenance and $s_1^{in} = s_2^{in} = 0$, we conjecture that in our case also the stable limit cycle disappears through a saddle-node bifurcation with another unstable limit cycle when S_{ch}^{in} decreases.

Remark 4.5. The plots of Figures 4.1 to 4.7 and 4.9 to 4.12 were performed with Maple [35]. The plots of Figure 4.8 and Figures 4.13 to 4.18 were performed with Scilab [54]. Using the same method as in the previous chapter.

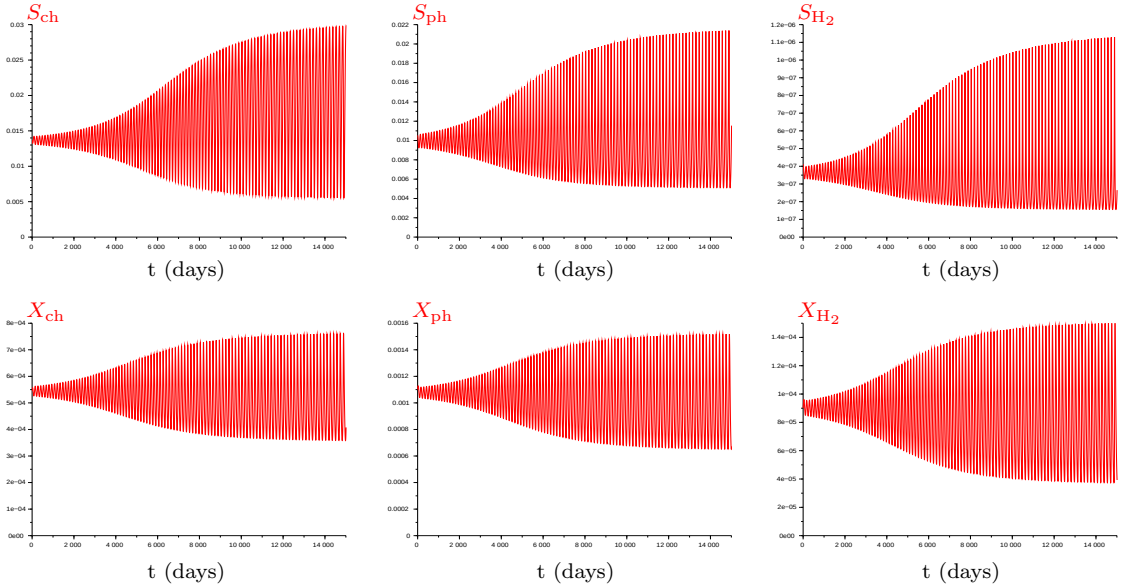

Figure 4.19: Trajectories of $S_{ch}, S_{ph}, S_{H_2}, X_{ch}, X_{ph}$ and X_{H_2} for $S_{ch}^{in} = 0.0995$ (in kgCOD/m^3): Convergence to the stable limit cycle.

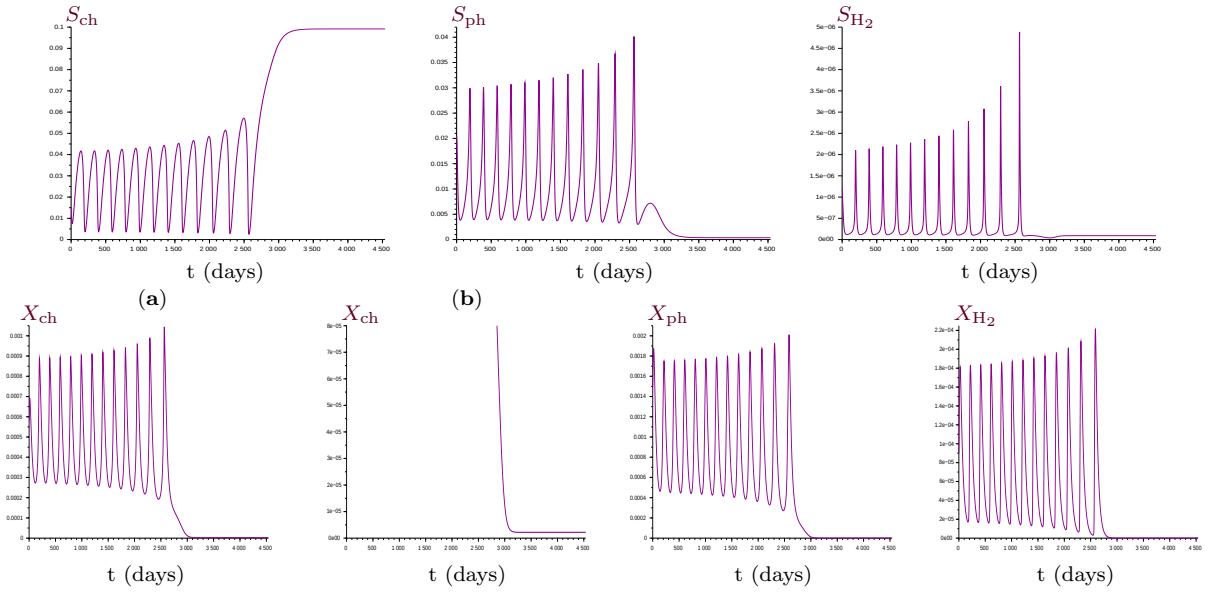

Figure 4.20: Trajectories of $S_{ch}, S_{ph}, S_{H_2}, X_{ch}, X_{ph}$ and X_{H_2} for $S_{ch}^{in} = 0.0995$ (in kgCOD/m^3): Convergence to the stable steady state E_{100}. (b) Magnification of (a) showing that the solution of (2.1) converges to the nonzero X_{ch}-component of E_{100}.

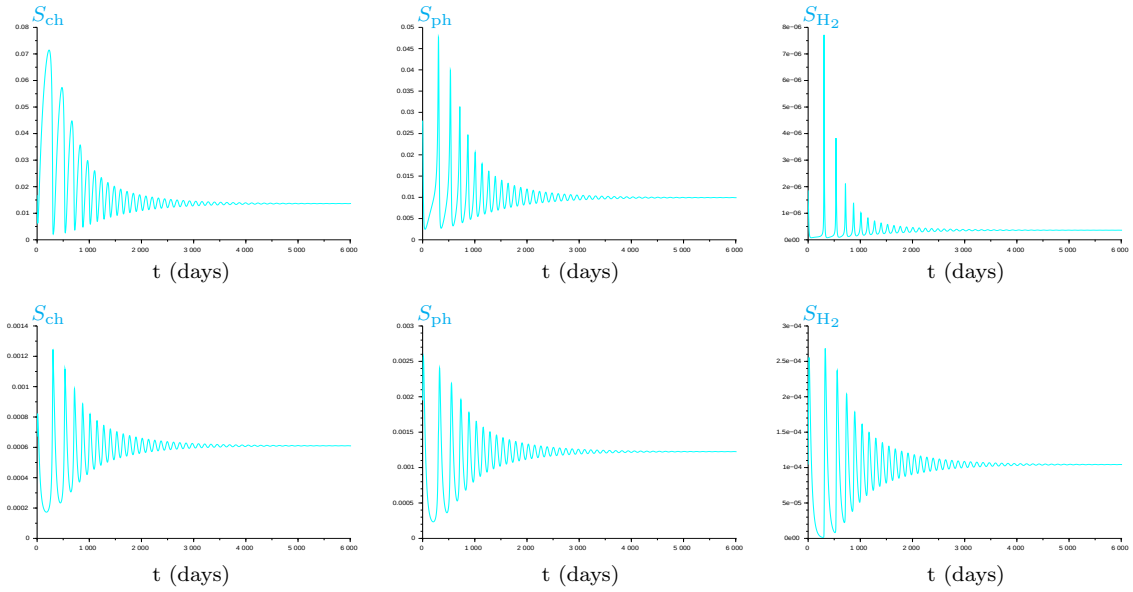

Figure 4.21: Trajectories of $S_{ch}, S_{ph}, S_{H_2}, X_{ch}, X_{ph}$ and X_{H_2} for $S_{ch}^{in} = 0.11$ (in kgCOD/m^3): Convergence to the positive steady state E_{111}.

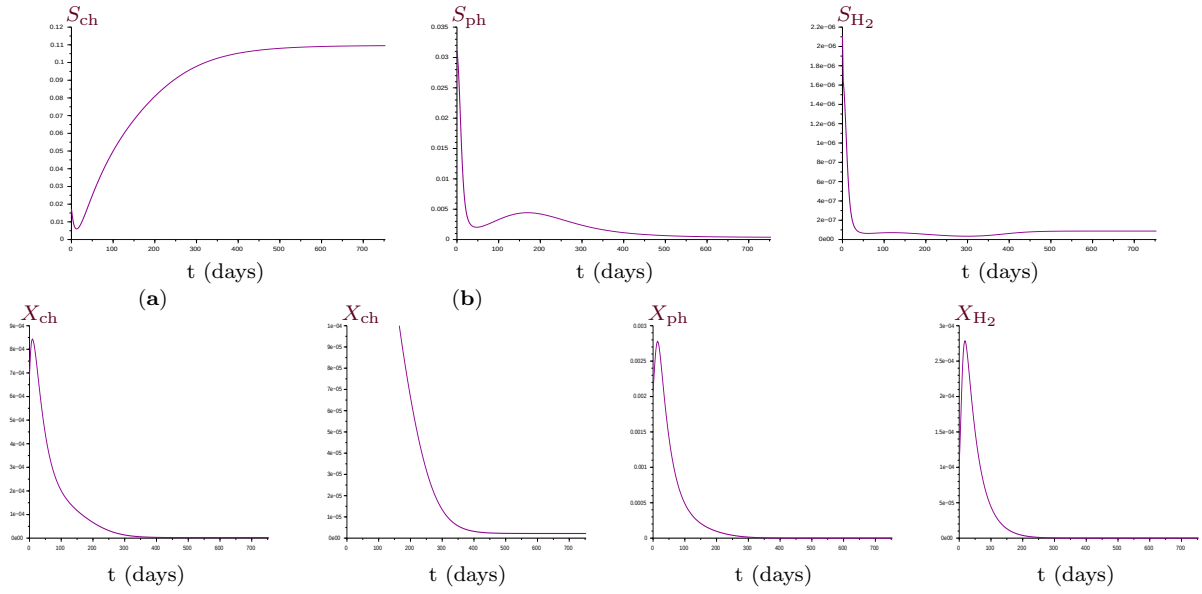

Figure 4.22: Trajectories of $S_{ch}, S_{ph}, S_{H_2}, X_{ch}, X_{ph}$ and X_{H_2} for $S_{ch}^{in} = 0.11$ (in kgCOD/m^3): Convergence to the stable steady state E_{100}. (b) Magnification of (a) showing that the solution of (2.1) converges to the nonzero X_{ch}-component of E_{100}.

4.6 Conclusion

In this chapter, we gave a complete stability analysis of the dynamics of the model (2.1) when the maintenance is included. We have managed to characterize the stability in this six-dimensional system which cannot be reduced to a three-dimensional one as in the case neglecting maintenance, although it is generally accepted that the Routh-Hurwitz theorem is intractable beyond five dimensions. For this, we have used the Liénard-Chipart stability criterion to simplify the mathematical analysis by reducing considerably the number of the Routh-Hurwitz conditions to check. We have performed the bifurcation diagrams, first, with the dilution rate, and second with chlorophenol inflowing concentration as the bifurcating parameters, showing that one of the operating diagrams obtained numerically in [64] has omitted important transition phenomena between steady states. We highlighted several possible asymptotic behaviors in this six-dimensional system, including the bistability between the coexistence steady state and a boundary steady state, or the bistability between a positive limit cycle and a boundary steady state, so that the long term behavior depends on the initial condition. We proved that the positive steady state of coexistence of all species can be unstable and we give numerical evidence for the supercritical Hopf bifurcation, in the case including chlorophenol and hydrogen input concentrations.

We can also show that maintenance does not destabilize the steady states. Then, in chapter 5, we will use the theoretical results of the existence and stability of all steady

states to construct analytically the operating diagrams in both cases with and without decay that give the regions of existence and stability of the steady states, in the space of the four operating parameters which were determined numerically in previous work in [64].

The results of this chapter have been published in [41].

CHAPTER 5

Operating diagrams for a three-tiered food-web model

Summary

5.1 Introduction

In this final chapter, we are interested to illustrate the mathematical study of the three-tiered model by studying analytically the operating diagrams which show the dynamic behavior of the system according to the conventional chemostat operating parameters (the dilution rate and the input concentrations of the substrates) in both cases with and without maintenance, using the analytical findings of the existence and stability of all the steady states, provided in previous chapters.

The operating diagram is the bifurcation diagram for which the values of the biological parameters are fixed. It is very useful for biologists because it allows predicting qualitatively the different asymptotic behaviors of the process according to its control parameters. As it was claimed in [56], the operating diagram probably remains the most useful answer for the analysis of the behavior of the model according to the parameters. This diagram shows how robust or how extensive is the parameter region where some asymptotic behavior emerges. The operating diagram is often performed numerically or theoretically both in the biological literature [53, 64, 71] and the mathematical literature [1, 3, 14, 22, 23, 49–51]. In [64], several operating diagrams have been presented, they have been numerically constructed by varying the four control parameters. The authors did not use the analytical expressions of the curves which separate the regions of existence and stability conditions. They determined numerically the steady states for a realistic range of operational and kinetic parameters and used the numerical method which consists of determining the existence and the stability region point by point at all the steady state. By considering sets of operating parameters and repeating this method with numerous ones, the diagrams are drawn, showing the region of stability of each steady state. The operating diagrams presented in [51] were obtained analytically in the case without maintenance and numerically in the case with maintenance where the authors were able to provide analytical expressions of the boundaries between the different stability regions allowing to give operating diagrams describing the exhaustive behavior of the system.

5.2 Operating diagrams

The operating diagrams show how behaves the system when the operating parameters D, $S_{\text{ch}}^{\text{in}}$, $S_{\text{ph}}^{\text{in}}$ and $S_{\text{H}_2}^{\text{in}}$ are varying in (2.1). These diagrams are used to visualize in particular, for a different set of operating parameters, the existence and local stability of steady states. To plot the operating diagrams, we must fix the values of the biological parameters as in Table 3.3, and two of the four operating parameters D, $S_{\text{ch}}^{\text{in}}$, $S_{\text{ph}}^{\text{in}}$ and $S_{\text{H}_2}^{\text{in}}$ in order to have a better vision and understanding because it is very difficult to visualize all the regions of the operating diagram in four-dimensional space. In what follows, we study the operating diagrams of system (2.1) in the cases with and without maintenance terms. In subsection 5.2.1, we fix $S_{\text{ph}}^{\text{in}}$ and $S_{\text{H}_2}^{\text{in}}$ and we determine the operating diagrams in the plane

$\left(S_{ch}^{in}, D\right)$ and in subsection 5.2.2, we give the operating diagrams in the $\left(S_{H_2}^{in}, S_{ph}^{in}\right)$ plane where S_{ch}^{in} and D being constant.

Using the change of variables (2.7), we summarized the necessary and sufficient existence and stability conditions of steady states of (2.1) in the case with maintenance as stated in Table 5.1, which deduced easily from Tables 2.2 and 4.2 in the previous chapters.

Table 5.1: The necessary and sufficient existence and local stability conditions of steady states of (2.1) in the case of maintenance. All functions are given in Table 3.4, while μ_i and r_5 are given by (2.9) and Table 4.1.

	Existence conditions	Stability conditions
E_{000}	Always exists	$\mu_0\left(S_{ch}^{in}Y, S_{H_2}^{in}\right) < D + a_0$, $\mu_1\left(S_{ph}^{in}Y_4, S_{H_2}^{in}\right) < D + a_1$, $\mu_2\left(S_{H_2}^{in}\right) < D + a_2$
E_{001}	$\mu_2\left(S_{H_2}^{in}\right) > D + a_2$	$S_{ch}^{in}Y < \varphi_0(D)$ and $S_{ph}^{in}Y_4 < \varphi_1(D)$
E_{100}	$\mu_0\left(S_{ch}^{in}Y, S_{H_2}^{in}\right) > D + a_0$	$\mu_1\left(S_{ch}^{in}Y + S_{ph}^{in}Y_4 - s_0, S_{H_2}^{in} - \omega\left(S_{ch}^{in}Y - s_0\right)\right) < D + a_1$ and $S_{H_2}^{in} - \omega S_{ch}^{in}Y < M_2(D + a_2) - \omega\varphi_0(D)$ with s_0 solution of equation $\psi_0(s_0) = D + a_0$
E_{110}	$(1-\omega)S_{ch}^{in}Y + S_{ph}^{in}Y_4 + S_{H_2}^{in} \geq \phi_1(D)$, $S_{ch}^{in}Y > M_0\left(D + a_0, s_2\right)$, $S_{ch}^{in}Y + S_{ph}^{in}Y_4 > M_0\left(D + a_0, s_2\right) + M_1\left(D + a_1, s_2\right)$, with s_2 solution of equation $\Psi(s_2) = (1-\omega)S_{ch}^{in}Y + S_{ph}^{in}Y_4 + S_{H_2}^{in}$	$(1-\omega)S_{ch}^{in}Y + S_{ph}^{in}Y_4 + S_{H_2}^{in} < \phi_2(D)$, $\frac{\partial\Psi}{\partial s_2}(s_2, D) > 0$ and $\phi_3(D) > 0$
E_{101}	$S_{ch}^{in}Y > \varphi_0(D)$, $S_{H_2}^{in} - \omega S_{ch}^{in}Y > M_2(D + a_2) - \omega\varphi_0$	$S_{ch}^{in}Y + S_{ph}^{in}Y_4 < \varphi_0(D) + \varphi_1(D)$
E_{111}	$(1-\omega)S_{ch}^{in}Y + S_{ph}^{in}Y_4 + S_{H_2}^{in} > \phi_2(D)$, $S_{ch}^{in}Y > \varphi_0(D)$, $S_{ch}^{in}Y + S_{ph}^{in}Y_4 > \varphi_0(D) + \varphi_1(D)$	$c_3 > 0$, $c_5 > 0$, $r_4 > 0$, $r_5 > 0$
E_{010}	$\mu_1\left(S_{ph}^{in}Y_4, S_{H_2}^{in}\right) > D + a_1$	$S_{ph}^{in}Y_4 + S_{H_2}^{in} < M_1\left(D + a_1, M_3\left(S_{ch}^{in}Y, D + a_0\right)\right) + M_3\left(S_{ch}^{in}Y, D + a_0\right)$, $S_{ph}^{in}Y_4 + S_{H_2}^{in} < \varphi_1(D) + M_2(D + a_2)$
E_{011}	$S_{ph}^{in}Y_4 > \varphi_1(D)$, $S_{ph}^{in}Y_4 + S_{H_2}^{in} > \varphi_1(D) + M_2(D + a_2)$	$S_{ch}^{in}Y < \varphi_0(D)$

For the case without maintenance, the necessary and sufficient conditions of existence and local stability can be deduced from Table 5.1 by taking $a_i = 0$, $i = 0, 1, 2$, except the stability of E_{111} which is given by

$$\phi_3(D) \geq 0, \quad \text{or} \quad \phi_3(D) < 0 \text{ and } \phi_4(D, S_{ch}^{in}, S_{ph}^{in}, S_{H_2}^{in}) > 0, \tag{5.1}$$

where ϕ_3 and ϕ_4 are given in Definition 2.2 and (3.2).

First, from Table 5.1, we define in Table 5.2 the surfaces Γ_i, $i = 1, \ldots, 18$ which delimited the different regions of the $\left(S_{\text{ch}}^{\text{in}}, S_{\text{ph}}^{\text{in}}, S_{\text{H}_2}^{\text{in}}, D\right)$-space.

Table 5.2: Definitions of the equations of the surfaces Γ_i, $i = 1, \ldots, 18$. All functions are given in Table 3.4, while μ_i and ϕ_4 are given by (2.9) and (3.2), r_5 is given in Table 4.1. s_2^{*i}, $i = 1, 2$ are the solutions of $\Psi(s_2, D) = (1-\omega)YS_{\text{ch}}^{\text{in}} + Y_4 S_{\text{ph}}^{\text{in}} + S_{\text{H}_2}^{\text{in}}$.

Γ_1	$\left\{\left(S_{\text{ch}}^{\text{in}}, S_{\text{ph}}^{\text{in}}, S_{\text{H}_2}^{\text{in}}, D\right),\ S_{\text{ch}}^{\text{in}} Y(1-\omega) = \phi_1(D) - S_{\text{ph}}^{\text{in}} Y_4 - S_{\text{H}_2}^{\text{in}}\right\}$
Γ_2	$\left\{\left(S_{\text{ch}}^{\text{in}}, S_{\text{ph}}^{\text{in}}, S_{\text{H}_2}^{\text{in}}, D\right),\ S_{\text{ch}}^{\text{in}} Y(1-\omega) = \phi_2(D) - S_{\text{ph}}^{\text{in}} Y_4 - S_{\text{H}_2}^{\text{in}}\right\}$
Γ_3	$\left\{\left(S_{\text{ch}}^{\text{in}}, S_{\text{ph}}^{\text{in}}, S_{\text{H}_2}^{\text{in}}, D\right),\ \phi_4\left(D, S_{\text{ch}}^{\text{in}}, S_{\text{ph}}^{\text{in}}, S_{\text{H}_2}^{\text{in}}\right) = 0\right\}$
Γ_4	$\left\{\left(S_{\text{ch}}^{\text{in}}, S_{\text{ph}}^{\text{in}}, S_{\text{H}_2}^{\text{in}}, D\right),\ r_5\left(D, S_{\text{ch}}^{\text{in}}, S_{\text{ph}}^{\text{in}}, S_{\text{H}_2}^{\text{in}}\right) = 0\right\}$
Γ_5	$\left\{\left(S_{\text{ch}}^{\text{in}}, S_{\text{ph}}^{\text{in}}, S_{\text{H}_2}^{\text{in}}, D\right),\ S_{\text{ch}}^{\text{in}} Y = M_0\left(D + a_0, S_{\text{H}_2}^{\text{in}}\right)\right\}$
Γ_6	$\left\{\left(S_{\text{ch}}^{\text{in}}, S_{\text{ph}}^{\text{in}}, S_{\text{H}_2}^{\text{in}}, D\right),\ S_{\text{ch}}^{\text{in}} Y = \varphi_0(D)\right\}$
Γ_7	$\left\{\left(S_{\text{ch}}^{\text{in}}, S_{\text{ph}}^{\text{in}}, S_{\text{H}_2}^{\text{in}}, D\right),\ S_{\text{ch}}^{\text{in}} Y\omega = \mathrm{S}_{\mathrm{H}_2}^{\mathrm{in}} + \omega\varphi_0(\mathrm{D}) - \mathrm{M}_2(\mathrm{D} + \mathrm{a}_2)\right\}$
Γ_8	$\left\{\left(S_{\text{ch}}^{\text{in}}, S_{\text{ph}}^{\text{in}}, S_{\text{H}_2}^{\text{in}}, D\right),\ S_{\text{ch}}^{\text{in}} Y = M_0\left(D + a_0, s_2^{*1}\right)\right\}$
Γ_9	$\left\{\left(S_{\text{ch}}^{\text{in}}, S_{\text{ph}}^{\text{in}}, S_{\text{H}_2}^{\text{in}}, D\right),\ S_{\text{ch}}^{\text{in}} Y = M_0\left(D + a_0, s_2^{*2}\right)\right\}$
Γ_{10}	$\left\{\left(S_{\text{ch}}^{\text{in}}, S_{\text{ph}}^{\text{in}}, S_{\text{H}_2}^{\text{in}}, D\right),\ S_{\text{ch}}^{\text{in}} Y = \varphi_0(D) + \varphi_1(D) - S_{\text{ph}}^{\text{in}} Y_4\right\}$
Γ_{11}	$\left\{\left(S_{\text{ch}}^{\text{in}}, S_{\text{ph}}^{\text{in}}, S_{\text{H}_2}^{\text{in}}, D\right),\ \mu_1\left(S_{\text{ph}}^{\text{in}} Y_4 + S_{\text{ch}}^{\text{in}} Y - s_0, S_{\text{H}_2}^{\text{in}} - \omega\left(S_{\text{ch}}^{\text{in}} Y - s_0\right)\right) = D + a_1\right\}$
Γ_{12}	$\left\{\left(S_{\text{ch}}^{\text{in}}, S_{\text{ph}}^{\text{in}}, S_{\text{H}_2}^{\text{in}}, D\right),\ S_{\text{ch}}^{\text{in}} Y = M_0\left(D + a_0, s_2^{*1}\right) + M_1\left(D + a_1, s_2^{*1}\right) - S_{\text{ph}}^{\text{in}} Y_4\right\}$
Γ_{13}	$\left\{\left(S_{\text{ch}}^{\text{in}}, S_{\text{ph}}^{\text{in}}, S_{\text{H}_2}^{\text{in}}, D\right),\ S_{\text{ch}}^{\text{in}} Y = M_0\left(D + a_0, s_2^{*2}\right) + M_1\left(D + a_1, s_2^{*2}\right) - S_{\text{ph}}^{\text{in}} Y_4\right\}$
Γ_{14}	$\left\{\left(S_{\text{ch}}^{\text{in}}, S_{\text{ph}}^{\text{in}}, S_{\text{H}_2}^{\text{in}}, D\right),\ M_1\left(D + a_1, M_3\left(S_{\text{ch}}^{\text{in}} Y, D + a_0\right)\right) + M_3\left(S_{\text{ch}}^{\text{in}} Y, D + a_0\right) = S_{\text{ph}}^{\text{in}} Y_4 + S_{\text{H}_2}^{\text{in}}\right\}$
Γ_{15}	$\left\{\left(S_{\text{ch}}^{\text{in}}, S_{\text{ph}}^{\text{in}}, S_{\text{H}_2}^{\text{in}}, D\right),\ D + a_1 = \mu_1\left(S_{\text{ph}}^{\text{in}} Y_4, S_{\text{H}_2}^{\text{in}}\right)\right\}$
Γ_{16}	$\left\{\left(S_{\text{ch}}^{\text{in}}, S_{\text{ph}}^{\text{in}}, S_{\text{H}_2}^{\text{in}}, D\right),\ S_{\text{ph}}^{\text{in}} Y_4 + S_{\text{H}_2}^{\text{in}} = M_2(D + a_2) + \varphi_1(D)\right\}$
Γ_{17}	$\left\{\left(S_{\text{ch}}^{\text{in}}, S_{\text{ph}}^{\text{in}}, S_{\text{H}_2}^{\text{in}}, D\right),\ S_{\text{ph}}^{\text{in}} Y_4 = \varphi_1(D)\right\}$
Γ_{18}	$\left\{\left(S_{\text{ch}}^{\text{in}}, S_{\text{ph}}^{\text{in}}, S_{\text{H}_2}^{\text{in}}, D\right),\ D + a_2 = \mu_2\left(S_{\text{H}_2}^{\text{in}}\right)\right\}$

5.2.1 Operating diagrams with respect to $\left(S_{\text{ch}}^{\text{in}}, D\right)$, $S_{\text{ph}}^{\text{in}}$ and $S_{\text{H}_2}^{\text{in}}$ fixed

Giving a fixed value for $S_{\text{ph}}^{\text{in}}$ and $S_{\text{H}_2}^{\text{in}}$, then, the intersections of the surfaces Γ_i, $i = 1, \ldots, 14$ with the $\left(S_{\text{ch}}^{\text{in}}, D\right)$-plane are curves as functions of $S_{\text{ph}}^{\text{in}}$ and $S_{\text{H}_2}^{\text{in}}$. However, the intersections of surfaces Γ_i $i = 15, \ldots, 18$ with this plane are straight lines. Following [64], we consider several cases to examine the effect of the operating parameters $S_{\text{ph}}^{\text{in}}$ and

$S^{in}_{H_2}$ in the cases with and without maintenance on the behavior of the model. First, only chlorophenol input is added to the system ($S^{in}_{ph} = S^{in}_{H_2} = 0$). Then, the hydrogen input is added to the system and the phenol input is excluded, ($S^{in}_{ph} = 0$ and $S^{in}_{H_2} > 0$). Next, the phenol input is added and the hydrogen input is excluded, ($S^{in}_{ph} > 0$ and $S^{in}_{H_2} = 0$). Finally, the hydrogen and phenol inputs are added to the system, ($S^{in}_{ph} > 0$ and $S^{in}_{H_2} > 0$).

Only chlorophenol is in the input

Assume that $S^{in}_{ch} > 0$, $S^{in}_{ph} = S^{in}_{H_2} = 0$. In this case, system (2.1) has only the steady states E_{000}, E^1_{110}, E^2_{110} and E_{111}, see Table 5.1. The operating diagram in the plane $\left(S^{in}_{ch}, D\right)$ is shown in Figure 5.1. Figure 5.1(a) looks very similar to Figure 5.1(b) except near of the origin, as it is shown in the magnifications at the right of Figure 5.1(a-b). In the case with maintenance, the value of S^{in}_{ch}, in which the positive steady state E_{111} is destabilized is greater than in the case without maintenance. Note that, each region that has a different asymptotic behavior is colored by a distinct color as in [64].

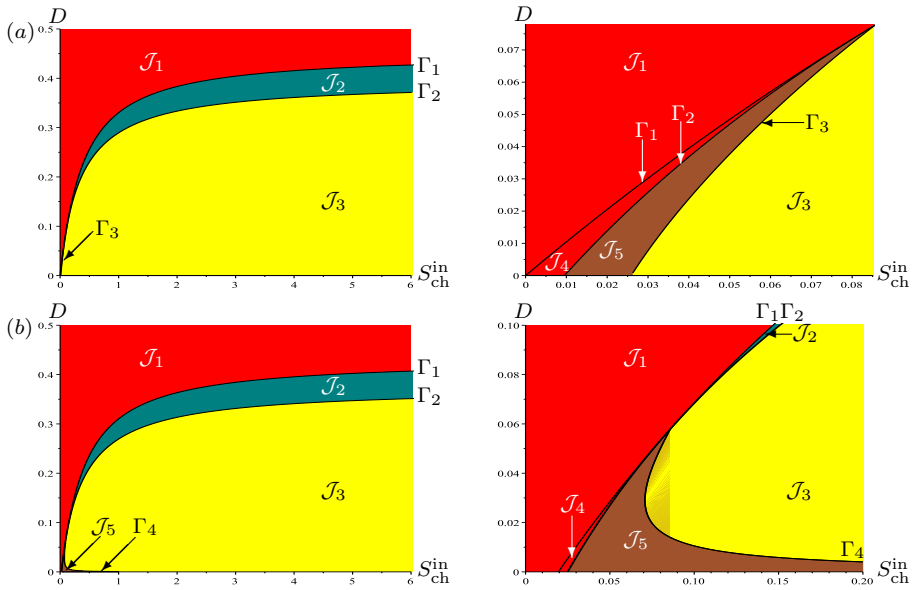

Figure 5.1: Operating diagram in the plane $\left(S^{in}_{ch}, D\right)$, when $S^{in}_{ph} = S^{in}_{H_2} = 0$. (a) case without maintenance and on the right a magnification for $D \in [0, 0.078]$ showing the regions $\mathcal{J}_4$ and $\mathcal{J}_5$. (b) case with maintenance and on the right a magnification for $D \in [0, 0.1]$ showing the regions $\mathcal{J}_4$ and $\mathcal{J}_5$.

The existence and the stability of the steady states of (2.1) in the five regions $\mathcal{J}_i$, $i = 1, \ldots, 5$, of the operating diagrams of Figure 5.1 are determined in Table 5.3.

Remark 5.1. Each region is denoted by its steady states, indicating which are stable and which are unstable. That is, region $\mathcal{J}_k = (ab, cd)$ means that when the operating parameters are taken in $\mathcal{J}_k$, then the steady states SSa and SSb are stable, the steady states SSc and SSd are unstable, and there is no other steady state.

Table 5.3: Existence and stability of steady states in the regions of the operating diagram of Figure 5.1 when $S_{ch}^{in} > 0$ and $S_{ph}^{in} = S_{H_2}^{in} = 0$.

Region	E_{000} SS1	E_{110}^1 SS4^1	E_{110}^2 SS4^2	E_{111} SS6	Color
$\mathcal{J}_1 = (1)$	S				Red
$\mathcal{J}_2 = (14^2, 4^1)$	S	U	S		Teal
$\mathcal{J}_3 = (16, 4^1 4^2)$	S	U	U	S	Yellow
$\mathcal{J}_4 = (1, 4^1 4^2)$	S	U	U		Red
$\mathcal{J}_5 = (1, 4^1 4^2 6)$	S	U	U	U	Sienna

We can deduce from Table 5.3 and Figure 5.1 when $S_{ch}^{in} > 0$ and $S_{ph}^{in} = S_{H_2}^{in} = 0$ that there are no new regions that emerge under the influence of the maintenance terms. Moreover, Figure 5.1(b) corresponds to Figure 2 in [64] and highlights the existence of the region $\mathcal{J}_5$ of instability of E_{111} (SS6), a fact that was not reported in [64]. Actually, the behavior of the system when $S_{ph}^{in} = S_{H_2}^{in} = 0$ was already clarified in [51], where the instability of E_{111} has studied analytically in the case without maintenance, but only numerically in the case including maintenance. In fact, Figure 5.1(a) is the same as Figure 4 in [51]. Both figures are obtained analytically by plotting the curves separating the regions $\mathcal{J}_k$. However, although Figure 5.1(b) shows the same behavior as Figure 9 in [51], our figure is obtained analytically by plotting the curves separating the regions, while Figure 9 in [51] was obtained only numerically. Thus, our theoretical study confirms the numerical findings presented in [51], in the case including maintenance.

These results are supported by numerical experimentation and are proven as in the following.

Construction of Figure 5.1. We illustrate the method used to plot the operating diagram presented in Figure 5.1. We assume that the biological parameter values of model (2.1) are provided in Table 3.3 and $S_{ph}^{in} = S_{H_2}^{in} = 0$. In this case, only the three steady states E_{000}, E_{110} and E_{111} exist (see Proposition 2.2). Using Table 5.1 and from Proposition 2.2, the steady states E_{110} and E_{111} exist, respectively, if and only if

$$(1-\omega)S_{ch}^{in}Y \geq \phi_1(D) \quad \text{and} \quad (1-\omega)S_{ch}^{in}Y > \phi_2(D). \tag{5.2}$$

First, we consider the case with maintenance: E_{000} always exists and it is stable, since all stability conditions in Table 5.1 hold, as

$$\mu_0\left(S_{ch}^{in}Y, S_{H_2}^{in}\right) = \mu_1\left(S_{ph}^{in}Y_4, S_{H_2}^{in}\right) = \mu_2\left(S_{H_2}^{in}\right) = 0 < D + a_i, \qquad i = 0, 1, 2.$$

From the first condition of (5.2), E_{110} exists in the region bounded by the curve Γ_1 defined in Table 5.2 and located at the right of this curve, see Figure 5.2. From Remark 3.1, when it exists, E_{110}^1 is unstable and the second stability condition of E_{110}^2 in Table 5.1 is

always satisfied. The third stability condition of E_{110}^2 holds for all $D > \overline{D}$, where $\overline{D}$ is the unique solution of $\phi_3(D) = 0$ (see Figure 5.3). The first stability condition of E_{110}^2 holds for all $\left(S_{ch}^{in}, D\right)$ in the region bounded by the curve Γ_2 defined in Table 5.2 and located at the left of this curve. Numerical computations show that the curves Γ_1 and Γ_2 are

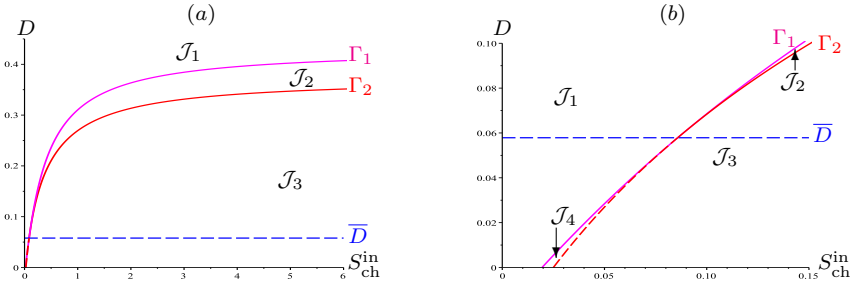

Figure 5.2: The curves Γ_1 and Γ_2 and the line $D = \overline{D}$, in the case with maintenance.

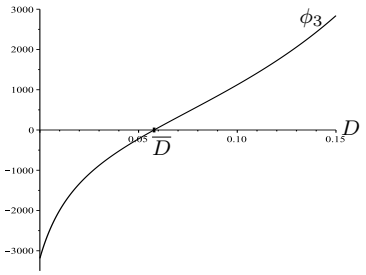

Figure 5.3: The curve of the function ϕ_3 in the case with maintenance.

tangent for $D = \overline{D}$ and $\phi_2(D) < \phi_1(D)$ for all D in their definition domains. Then, E_{110}^2 is stable in the region located between the two curves Γ_1 and Γ_2 and above the line $D = \overline{D}$ (see Figure 5.2).

From the second condition of (5.2), E_{111} exists in the region bounded by the curve Γ_2 and located at the right of this curve, see Figure 5.2. For the stability of E_{111}, we must determine the signs of the various conditions of stability in Table 5.1 in the plane $\left(S_{ch}^{in}, D\right)$, for all $D > 0$ and $S_{ch}^{in} > \sigma(D)$, where $\sigma(D)$ is the existence condition of E_{111} given by $\sigma(D) := \phi_2(D)/(1-\omega)Y$. To this end, we show in Figure 5.4 the signs of the functions $S_{ch}^{in} \mapsto c_3(D, S_{ch}^{in})$, $S_{ch}^{in} \mapsto c_5(D, S_{ch}^{in})$, $S_{ch}^{in} \mapsto r_4(D, S_{ch}^{in})$ and $S_{ch}^{in} \mapsto r_5(D, S_{ch}^{in})$ for several values of $D \in \overline{D}$ and $S_{ch}^{in} > \sigma(D)$. Figure 5.4(a) illustrates the function $c_3(D, S_{ch}^{in})$ is positive. Figure 5.4(b-c-d) illustrate the uniqueness of the solution $S_{ch}^{in,c_i}(D)$, $i = 1, 2, 3$ of equation $c_5(D, S_{ch}^{in}) = 0$, $r_4(D, S_{ch}^{in}) = 0$ and $r_5(D, S_{ch}^{in}) = 0$, respectively.

Using Maple [35], we plot the curves of equations $c_5(D, S_{ch}^{in}) = 0$, $r_4(D, S_{ch}^{in}) = 0$ and $r_5(D, S_{ch}^{in}) = 0$. Then, Figure 5.5 shows that the stability conditions of E_{111} given by

$$c_5(S_{ch}^{in}, D) > 0, \quad r_4(S_{ch}^{in}, D) > 0 \quad \text{and} \quad r_5(S_{ch}^{in}, D) > 0$$

are satisfied for all (S_{ch}^{in}, D) in the region bounded by the curve Γ_4 defined in Table 5.2 and located at the right of this curve, which corresponds to equation $r_5\left(S_{ch}^{in}, D\right) = 0$.

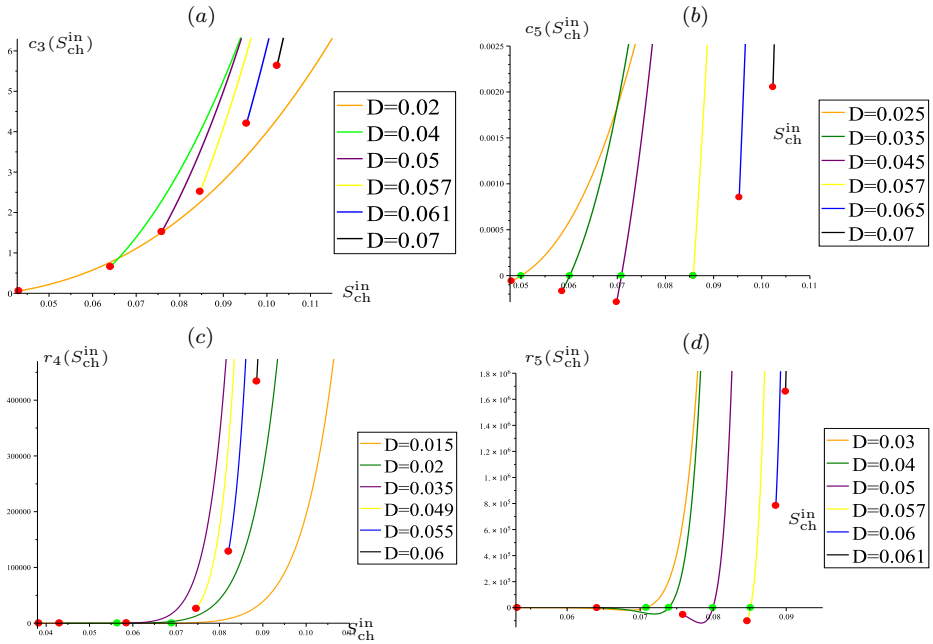

Figure 5.4: The curves of the functions c_3, c_5, r_4 and r_5, for $S_{ch}^{in} > \sigma(D)$ (in red) and for several fixed values of D, showing the solutions in green of $c_5(D, S_{ch}^{in}) = 0$, $r_4(D, S_{ch}^{in}) = 0$ and $r_5(D, S_{ch}^{in}) = 0$.

Therefore, E_{111} is stable (resp. unstable) in the region $\mathcal{J}_3$ (resp. $\mathcal{J}_5$) bounded by the curve Γ_4 and located at the right (resp. left) of this curve (see Figure 5.6).

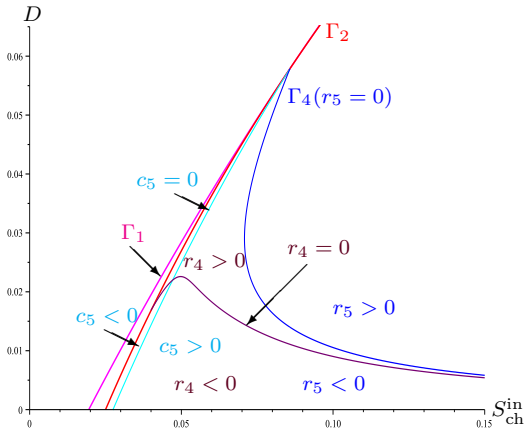

Figure 5.5: Various signs of conditions $c_5 > 0$, $r_4 > 0$ and $r_5 > 0$.

Table 5.4 summarizes the various regions in the operating diagrams in the case with maintenance for the different conditions according to S_{ch}^{in} and D.

Now, in the case without maintenance, we use the same method as in the case with maintenance, we obtain that E_{000} is always exists and it is stable.

E_{110} exists in the region bounded by the curve Γ_1 and located at the right of this curve, see Figure 5.7. E_{110}^1 is unstable, while E_{110}^2 is stable in the region bounded by the curve

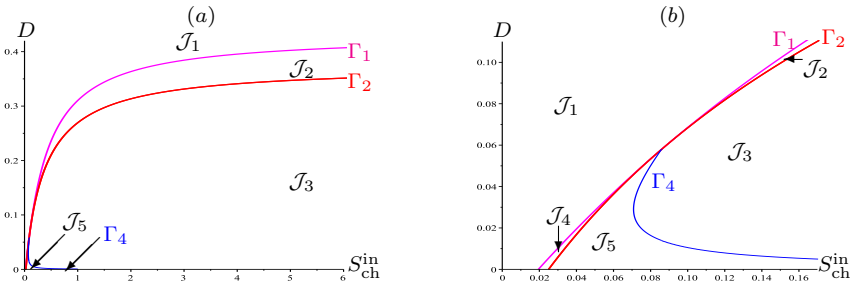

Figure 5.6: The curves Γ_1, Γ_2 and Γ_4 in the case with maintenance.

Table 5.4: Existence and stability of steady states of (2.1) according to the five regions $\mathcal{J}_i$ of the operating diagrams of Figure 5.1(b) in the case with maintenance.

Condition 1	Condition 2	Region	E_{000}	E_{110}^1	E_{110}^2	E_{111}
$D > 0$	$(1-\omega)S_{ch}^{in}Y < \phi_1(D)$	$\mathcal{J}_1$	S			
$D \geq \overline{D}$	$\phi_1(D) < (1-\omega)S_{ch}^{in}Y < \phi_2(D)$	$\mathcal{J}_2$	S	U	S	
	$\phi_2(D) < (1-\omega)S_{ch}^{in}Y$	$\mathcal{J}_3$	S	U	U	S
$D < \overline{D}$	$\phi_2(D) < (1-\omega)S_{ch}^{in}Y$ and $r_5 > 0$	$\mathcal{J}_3$	S	U	U	S
	$\phi_1(D) < (1-\omega)S_{ch}^{in}Y < \phi_2(D)$	$\mathcal{J}_4$	S	U	U	
	$\phi_2(D) < (1-\omega)S_{ch}^{in}Y$ and $r_5 < 0$	$\mathcal{J}_5$	S	U	U	U

Γ_2 and located at the left of this curve.

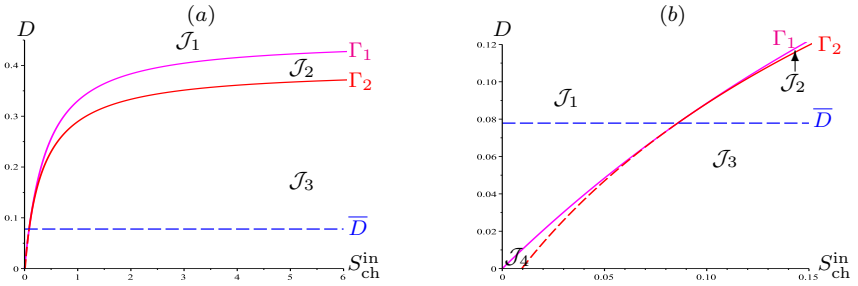

Figure 5.7: The curves Γ_1 and Γ_2 and the line $D = \overline{D}$, in the case without maintenance.

E_{111} exists in the region bounded by the curve Γ_2 and located at the right of this curve, see Figure 5.7. The stability conditions of E_{111} are given by (5.1). Figure 5.8 shows that E_{111} is stable for all $D \geq \overline{D}$. Inversely, when $D < \overline{D}$, we must determine the sign of the function $\phi_4(D, S_{ch}^{in})$. To this end, using similar arguments in the case with maintenance, we show in Figure 5.9 the signs of the function $S_{ch}^{in} \mapsto \phi_4(D, S_{ch}^{in})$ for several values of $D \in [0, \overline{D}[$, illustrate the uniqueness of the solution $S_{ch}^{in,c}(D)$ of equation $\phi_4(D, S_{ch}^{in}) = 0$. Indeed, $\phi_4(D, S_{ch}^{in}) < 0$ for all $S_{ch}^{in} \in [\sigma(D), S_{ch}^{in,c}(D)[$ and $\phi_4(D, S_{ch}^{in}) > 0$ for all $S_{ch}^{in} > S_{ch}^{in,c}(D)$. Using Maple [35], we plot the curve Γ_3 of equation $\phi_4(D, S_{ch}^{in}) = 0$ defined in Table 5.2. We have $\phi_4(D, S_{ch}^{in}) < 0$ in the region bounded by the curve Γ_3 and located at the left of this curve (see Figure 5.10). Inversely, $\phi_4(D, S_{ch}^{in}) > 0$ in the region bounded by the curve Γ_3 and located at the right of this curve (see Figure 5.10).

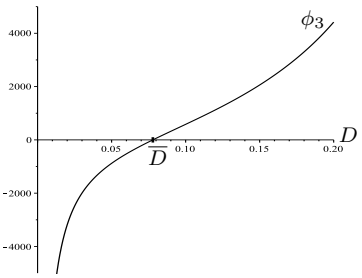

Figure 5.8: The curve of the function ϕ_3 in the case without maintenance.

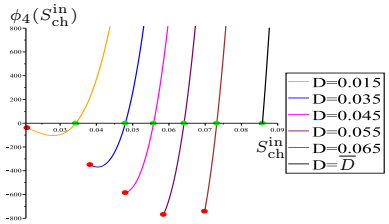

Figure 5.9: The curves of the function $\phi_4(S_{ch}^{in})$ for $S_{ch}^{in} > \sigma(D)$ (in red) and for several fixed values of D, showing the solution in green of $\phi_4(D, S_{ch}^{in}) = 0$.

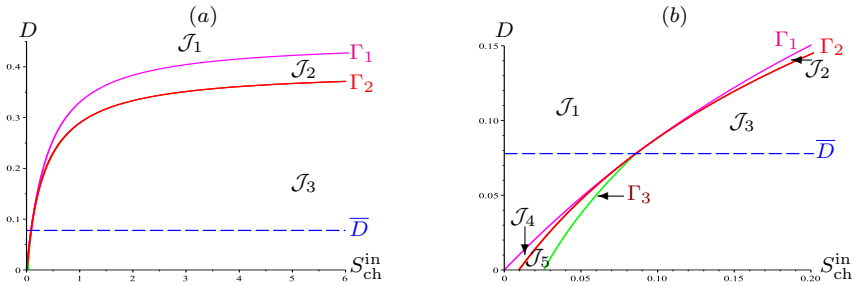

Figure 5.10: The curves Γ_1, Γ_2 and Γ_3, and the line $D = \overline{D}$ in the case without maintenance.

Table 5.5 summarizes the various regions in the operating diagrams in the case without maintenance for the different conditions according to S_{ch}^{in} and D.

Table 5.5: Existence and stability of steady states of (2.1) according to the five regions $\mathcal{J}_i$ of the operating diagrams of Figure 5.1(a) in the case without maintenance.

Condition 1	Condition 2	Region	E_{000}	E_{110}^1	E_{110}^2	E_{111}
$D > 0$	$(1-\omega)S_{ch}^{in}Y < \phi_1(D)$	$\mathcal{J}_1$	S			
$D \geq \overline{D}$	$\phi_1(D) < (1-\omega)S_{ch}^{in}Y < \phi_2(D)$	$\mathcal{J}_2$	S	U	S	
	$\phi_2(D) < (1-\omega)S_{ch}^{in}Y$	$\mathcal{J}_3$	S	U	U	S
$D < \overline{D}$	$\phi_2(D) < (1-\omega)S_{ch}^{in}Y$ and $\phi_4 > 0$	$\mathcal{J}_3$	S	U	U	S
	$\phi_1(D) < (1-\omega)S_{ch}^{in}Y < \phi_2(D)$	$\mathcal{J}_4$	S	U	U	
	$\phi_2(D) < (1-\omega)S_{ch}^{in}Y$ and $\phi_4 < 0$	$\mathcal{J}_5$	S	U	U	U

□

Hydrogen is in the input

We assume that $S_{ch}^{in} > 0$, $S_{ph}^{in} = 0$ and $S_{H_2}^{in} > 0$ and we illustrate the operating diagrams in $\left(S_{ch}^{in}, D\right)$-plane in both cases with and without maintenance. In this case, system (2.1) has further three steady states E_{001}, E_{100} and E_{101}, see Proposition 2.2.

We consider the inflowing concentrations $S_{ph}^{in} = 0$ and $S_{H_2}^{in} = 2.67 \times 10^{-5}$. These values are those of Figure 3(a) in [64]. Figure 5.11(a) represents the operating diagram in the plane $\left(S_{ch}^{in}, D\right)$, in the case without maintenance. The three magnifications shown in Figure 5.11(b-c-d) put in evidence the regions $\mathcal{J}_8$, $\mathcal{J}_{10}$ and $\mathcal{J}_i$, $i = 12, \ldots, 21$. Figure 5.12(a) represents the operating diagram in $\left(S_{ch}^{in}, D\right)$-plane, in the case with maintenance. The magnifications presented in Figure 5.12(b-c-d) show the regions $\mathcal{J}_1$ and $\mathcal{J}_i$, $i = 6, \ldots, 13$ are similar to those in Figure 5.11. The addition of hydrogen input substrate leads to the occurrence of sixteen new regions besides the region $\mathcal{J}_1$ which is identical to that of the operating diagram in Figure 5.1. Figures 5.11 and 5.12 are constructed using the same method as Figure 5.1, which consists in plotting the curves separating the regions.

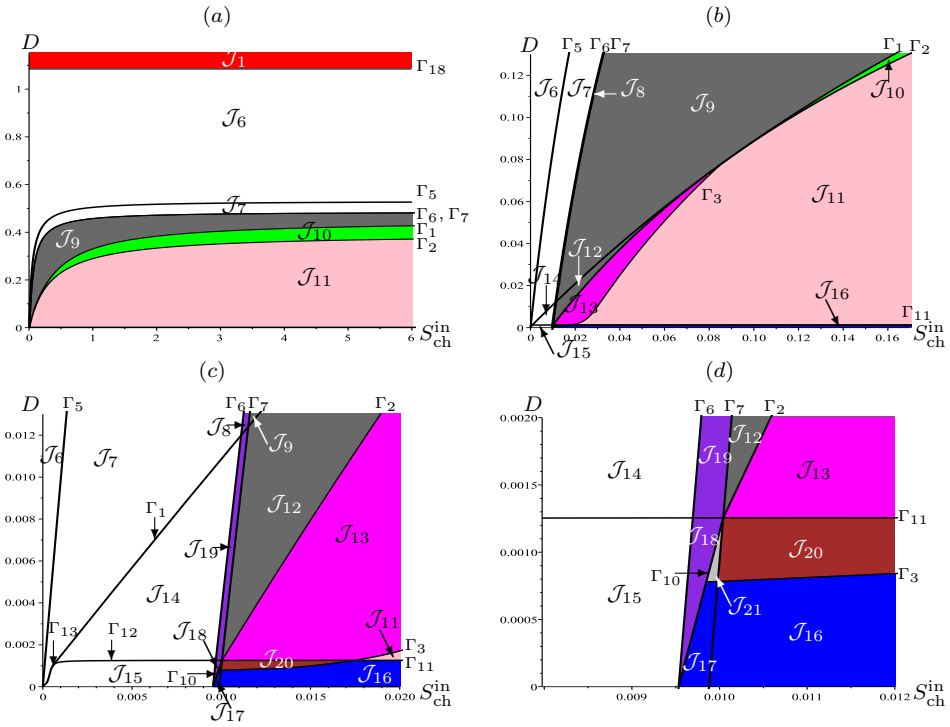

Figure 5.11: (a) Operating diagram in the plane $\left(S_{ch}^{in}, D\right)$, when $S_{ph}^{in} = 0$, $S_{H_2}^{in} = 2.67 \times 10^{-5}$ and $k_{dec,i} = 0$. (b) Magnification for $D \in [0, 0.13]$ showing the regions $\mathcal{J}_i$, $i = 12, \ldots, 16$. (c) Magnification for $D \in [0, 0.013]$ showing the regions $\mathcal{J}_8$ and $\mathcal{J}_i$, $i = 17, \ldots, 20$. (d) Magnification for $D \in [0, 0.002]$ showing the region $\mathcal{J}_{21}$.

The existence and the stability of the steady states of (2.1) in the seventeen regions $\mathcal{J}_1$ and $\mathcal{J}_i$, $i = 6, \ldots, 21$, of the operating diagrams in Figures 5.11 and 5.12, are determined in Table 5.6.

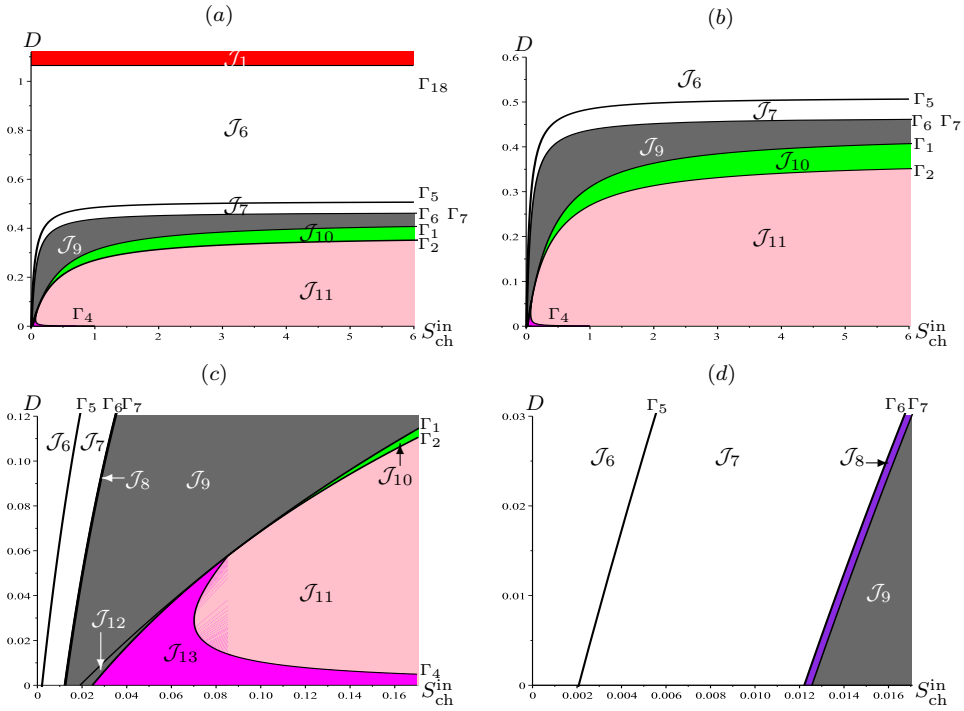

Figure 5.12: (a) Operating diagram in the plane $\left(S^{in}_{ch}, D\right)$, when $S^{in}_{ph} = 0$ and $S^{in}_{H_2} = 2.67 \times 10^{-5}$ with maintenance. (b) Magnification for $D \in [0, 0.6]$. (c) Magnification for $D \in [0, 0.12]$ showing the regions $\mathcal{J}_{12}$ and $\mathcal{J}_{13}$. (d) Magnification for $D \in [0, 0.03]$ showing the region $\mathcal{J}_8$.

The Hopf bifurcation occurs at the boundary between regions $\mathcal{J}_{11}$ and $\mathcal{J}_{13}$, see Figures 5.11 and 5.12, and in $\mathcal{J}_{13}$ close to the boundary with $\mathcal{J}_{11}$ a periodic orbit in E_{111} emerges, as illustrated in Figure 3.9 and Figure 4.17 in the previous chapters. We see also that the regions $\mathcal{J}_i$, $i = 14, \ldots, 21$ are empty in the case with maintenance. Thus, the maintenance has an effect on the disappearance of the regions. Moreover, in the case without maintenance and for small values of the dilution rate D, there cannot be any destabilization of E_{111}. However, the coexistence of the three species around a limit cycle can occur, in the case with maintenance. On the other hand, our study of the operating diagrams in both cases with and without maintenance show the emergence of new regions which are not reported in Figure 3(a), namely the stability region of E_{101} (SS5), the stability region of E_{100} (SS3) with the instability region of E_{111} (SS6), and the region $\mathcal{J}_{21}$ when all the steady states exist and are unstable, except E^1_{110} (SS4) which does not exist. For the positive initial conditions in a neighborhood of E_{111} all these steady states converge to the stable limit cycle. These regions are very thin and in a biological point of view, such regions would likely not be attained.

Construction of Figure 5.11. We illustrate the method used to plot the operating diagram presented in Figure 5.11 in the case without maintenance. We assume that $S^{in}_{ph} = 0$ and $S^{in}_{H_2} = 2.67 \times 10^{-5}$. E_{010} and E_{011} do not exist when $S^{in}_{ph} = 0$. Using Table 3.8, we see that:

Table 5.6: Existence and stability of steady states in the regions of the operating diagrams of Figures 5.11 and 5.12.

Region	E_{000} SS1	E_{001} SS2	E_{100} SS3	E^1_{110} $SS4^1$	E^2_{110} $SS4^2$	E_{101} SS5	E_{111} SS6	Color
$\mathcal{J}_1 = (1)$	S							Red
$\mathcal{J}_6 = (2, 1)$	U	S						White
$\mathcal{J}_7 = (2, 13)$	U	S	U					White
$\mathcal{J}_8 = (5, 123)$	U	U	U			S		Blueviolet
$\mathcal{J}_9 = (3, 12)$	U	U	S					Dimgray
$\mathcal{J}_{10} = (34^2, 124^1)$	U	U	S	U	S			Green
$\mathcal{J}_{11} = (36, 124^1 4^2)$	U	U	S	U	U		S	Pink
$\mathcal{J}_{12} = (3, 124^1 4^2)$	U	U	S	U	U			Dimgray
$\mathcal{J}_{13} = (3, 124^1 4^2 6)$	U	U	S	U	U		U	Magenta
$\mathcal{J}_{14} = (2, 134^1 4^2)$	U	S	U	U	U			White
$\mathcal{J}_{15} = (2, 134^2)$	U	S	U		U			White
$\mathcal{J}_{16} = (6, 1234^2)$	U	U	U		U		S	Blue
$\mathcal{J}_{17} = (6, 1234^2 5)$	U	U	U		U	U	S	Blue
$\mathcal{J}_{18} = (5, 1234^2)$	U	U	U		U	S		Blueviolet
$\mathcal{J}_{19} = (5, 1234^1 4^2)$	U	U	U	U	U	S		Blueviolet
$\mathcal{J}_{20} = (., 1234^2 6)$	U	U	U		U		U	Brown
$\mathcal{J}_{21} = (., 1234^2 56)$	U	U	U		U	U	U	Silver

E_{000} always exists. From Table 3.8, the first stability condition of E_{000} holds in the region bounded by the line Γ_{18} and located above this line. The second stability condition of E_{000} holds in the region bounded by the curve Γ_5 and located at the left of this curve. Then, E_{000} is stable in the region located above the line Γ_{18}, see Figure 5.13.

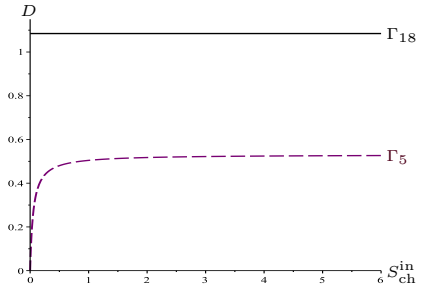

Figure 5.13: The line Γ_{18} and the curve Γ_5.

From Table 3.8, E_{001} exists in the region bounded by the line Γ_{18} and located below this line, and it is stable in the region bounded by the curve Γ_6 and located at the left of this curve, see Figure 5.14.

E_{100} exists in the region bounded by the curve Γ_5 and located below this curve (see Figure 5.13). From Table 3.8, the first (resp. second) stability condition of E_{100} holds for

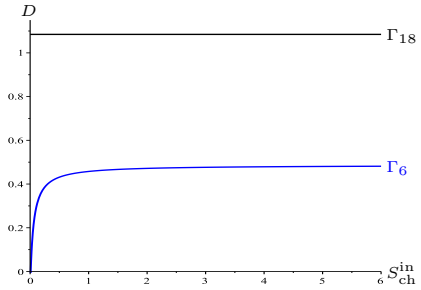

Figure 5.14: The line Γ_{18} and the curve Γ_6.

all $\left(S_{ch}^{in}, D\right)$ in the region bounded by the curve Γ_{11} (resp. Γ_7) and located above (resp. below) this curve. Then, E_{100} is stable in the region located between the two curves Γ_7 and Γ_{11}, see Figure 5.15.

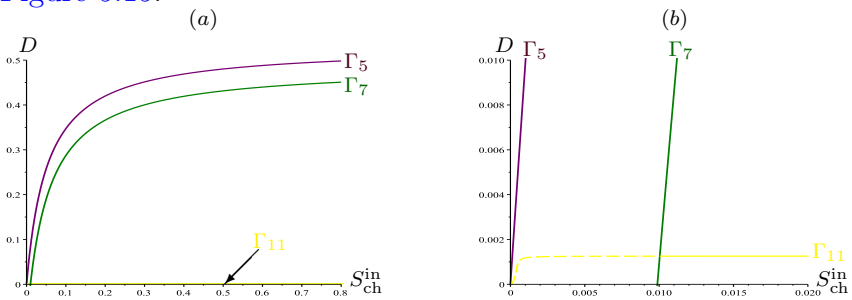

Figure 5.15: The curves Γ_5, Γ_7 and Γ_{11}.

From Table 3.8, the first existence condition of E_{110}^1 and E_{110}^2 holds in the region bounded by the curve Γ_1 and located at the right of this curve, see Figure 5.16. The second existence condition of E_{110}^1 (resp. E_{110}^2) holds for all $\left(S_{ch}^{in}, D\right)$ in the region bounded by the curve Γ_{12} (resp. Γ_{13}) and located at the left (resp. right) of this curve, see Figure 5.16. Then, E_{110}^1 exists in the region located between the curves Γ_1 and Γ_{12}, while E_{110}^1 exists in the region located at the right of the curves Γ_1 and Γ_{13}, see Figure 5.16. From Remark 3.1,

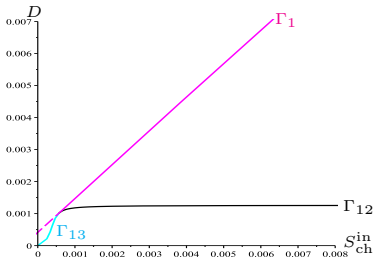

Figure 5.16: The curves Γ_1, Γ_{12} and Γ_{13}.

when it exists, E_{110}^1 is unstable and the second stability condition of E_{110}^2 in Table 3.8 is always satisfied. The third stability condition of E_{110}^2 holds for all $D > \overline{D}$ (see Figure 5.3). The first stability condition of E_{110}^2 holds for all $\left(S_{ch}^{in}, D\right)$ in the region bounded by the curve Γ_2 and located at the left of this curve. Then, E_{110}^2 is stable in the region located between the two curves Γ_1 and Γ_2 and above the line $D = \overline{D}$ (see Figure 5.17).

From Table 3.8, the first (resp. second) existence condition of E_{101} holds for all $\left(S_{ch}^{in}, D\right)$ in the region bounded by the curve Γ_6 (resp. Γ_7) and located at the right (resp. left) of

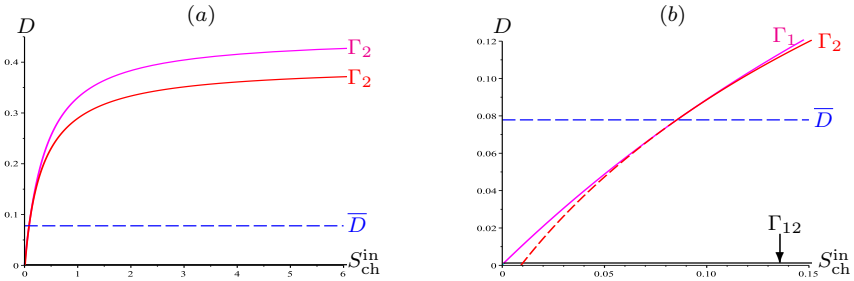

Figure 5.17: The curves Γ_1, Γ_2 and Γ_{12}, and the line $D = \overline{D}$.

this curve. Then E_{101} exists in the region located between the two curves Γ_6 and Γ_7, and it is stable in the region bounded by the curve Γ_{10} and located at the right of this curve (see Figure 5.18).

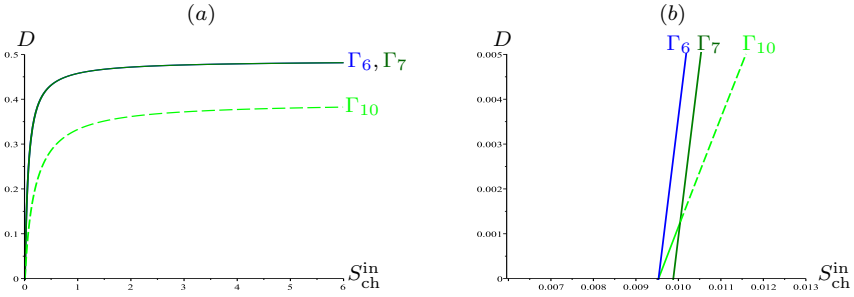

Figure 5.18: The curves Γ_6, Γ_7 and Γ_{10}.

From Table 3.8, the first and the second existence conditions of E_{111} hold for all $\left(S^{in}_{ch}, D\right)$ in the region bounded by the curves Γ_2 and Γ_{10} and located at the right of these curves, see Figure 5.20. From Table 3.8 and Figure 5.3(a), E_{111} is stable for all $D \geq \overline{D}$. Inversely, when $D < \overline{D}$, using similar arguments, we determine the sign of the function $\phi_4(D, S^{in}_{ch})$. To this end, we show in Figure 5.19 the signs of the function $S^{in}_{ch} \mapsto \phi_4(D, S^{in}_{ch})$ for several values of $D \in [0, \overline{D}[$, illustrate the uniqueness of the solution $S^{in,c}_{ch}(D)$ of equation $\phi_4(D, S^{in}_{ch}) = 0$. Then, we have $\phi_4(D, S^{in}_{ch}) < 0$ in the region bounded by the curve Γ_3 and located at the left of this curve (see Figure 5.20). Inversely, $\phi_4(D, S^{in}_{ch}) > 0$ in the region bounded by the curve Γ_3 and located at the right of this curve (see Figure 5.20).

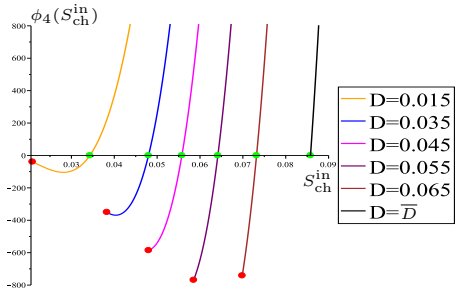

Figure 5.19: The curves of the function ϕ_4, for $S^{in}_{ch} > \sigma(D)$ (in red) and for several fixed values of D, showing the solution in green of $\phi_4(D, S^{in}_{ch}) = 0$.

Table 5.7 defines the various regions in the operating diagrams in the case without maintenance according to S^{in}_{ch} and D.

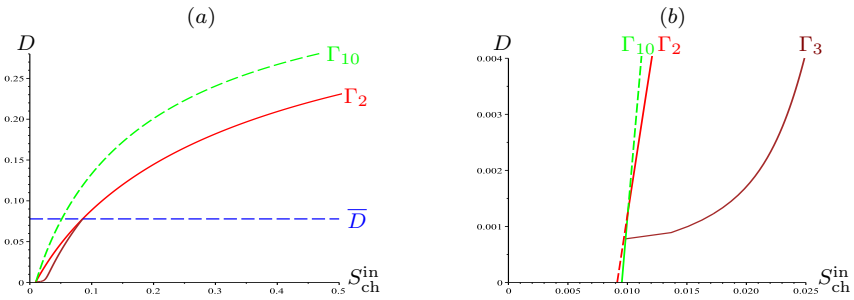

Figure 5.20: The curves Γ_2, Γ_3 and Γ_{10}, and the line $D = \overline{D}$.

Table 5.7: Definitions of the regions corresponding to the operating diagrams of Figure 5.11 when $S_{ph}^{in} = 0$ in the case without maintenance.

Region	Definition
$\mathcal{J}_1$	$\mu_2\left(S_{ch}^{in}\right) < D$ and for all $S_{ch}^{in} \geq 0$
$\mathcal{J}_6$	$\mu_2\left(S_{ch}^{in}\right) < D$ and $S_{ch}^{in}Y < M_0\left(D, S_{H_2}^{in}\right)$
$\mathcal{J}_7$	$M_0\left(D, S_{H_2}^{in}\right) < S_{ch}^{in}Y < \varphi_0(D)$, $S_{ch}^{in}(1-\omega)Y < \phi_1(D) - S_{H_2}^{in}$, $S_{ch}^{in}Y < M_0\left(D, s_2^{*2}\right) + M_1\left(D, s_2^{*2}\right)$
$\mathcal{J}_8$	$\varphi_0(D) < S_{ch}^{in}Y < \left(S_{H_2}^{in} + \omega\varphi_0(D) - M_2(D)\right)/\omega$ and $S_{ch}^{in}Y(1-\omega) < \phi_1(D) - S_{H_2}^{in}$
$\mathcal{J}_9$	$\left(S_{H_2}^{in} + \omega\varphi_0(D) - M_2(D)\right)/\omega < S_{ch}^{in}Y < \left(\phi_1(D) - S_{H_2}^{in}\right)/(1-\omega)$
$\mathcal{J}_{10}$	$\overline{D} < D$ and $\phi_1(D) - S_{H_2}^{in} \leq S_{ch}^{in}Y(1-\omega) < \phi_2(D) - S_{H_2}^{in}$
$\mathcal{J}_{11}$	$\phi_2(D) - S_{H_2}^{in} < S_{ch}^{in}Y(1-\omega)$, $\mu_1\left(S_{ch}^{in}Y - s_0, S_{H_2}^{in} - \omega\left(S_{ch}^{in}Y - s_0\right)\right) < D$ and $\phi_4\left(D, S_{ch}^{in}, S_{H_2}^{in}\right) > 0$,
$\mathcal{J}_{12}$	$D < \overline{D}$, $\phi_1(D) - S_{H_2}^{in} \leq S_{ch}^{in}Y(1-\omega) < \phi_2(D) - S_{H_2}^{in}$ and $S_{H_2}^{in} + \omega\varphi_0(D) - M_2(D) < S_{ch}^{in}\omega Y$
$\mathcal{J}_{13}$	$D < \overline{D}$, $\phi_2(D) - S_{H_2}^{in} < S_{ch}^{in}Y(1-\omega)$, $\mu_1\left(S_{ch}^{in}Y - s_0, S_{H_2}^{in} - \omega\left(S_{ch}^{in}Y - s_0\right)\right) < D$, and $\phi_4\left(D, S_{ch}^{in}, S_{H_2}^{in}\right) < 0$
$\mathcal{J}_{14}$	$\left(\phi_1(D) - S_{H_2}^{in}\right)/(1-\omega) \leq S_{ch}^{in}Y < \varphi_0(D)$ and $M_0\left(D, s_2^{*2}\right) + M_1\left(D, s_2^{*2}\right) < S_{ch}^{in}Y$
$\mathcal{J}_{15}$	$M_0\left(D, s_2^{*2}\right) + M_1\left(D, s_2^{*2}\right) < S_{ch}^{in}Y < M_0\left(D, s_2^{*1}\right) + M_1\left(D, s_2^{*1}\right)$, $S_{ch}^{in}Y < \varphi_0(D)$
$\mathcal{J}_{16}$	$\left(S_{H_2}^{in} + \omega\varphi_0(D) - M_2(D)\right)/\omega < S_{ch}^{in}Y < M_0\left(D, s_2^{*1}\right) + M_1\left(D, s_2^{*1}\right)$ and $\phi_4\left(D, S_{ch}^{in}, S_{H_2}^{in}\right) > 0$
$\mathcal{J}_{17}$	$\varphi_0(D) + \varphi_1(D) < S_{ch}^{in}Y < \left(S_{H_2}^{in} + \omega\varphi_0(D) - M_2(D)\right)/\omega$ and $\phi_4\left(D, S_{ch}^{in}, S_{H_2}^{in}\right) > 0$
$\mathcal{J}_{18}$	$\varphi_0(D) < S_{ch}^{in}Y < \varphi_0(D) + \varphi_1(D)$ and $S_{ch}^{in}Y < M_0\left(D, s_2^{*1}\right) + M_1\left(D, s_2^{*1}\right)$
$\mathcal{J}_{19}$	$\varphi_0(D) < S_{ch}^{in}Y < \left(S_{H_2}^{in} + \omega\varphi_0(D) - M_2(D)\right)/\omega$, $\phi_1(D) - S_{H_2}^{in} < S_{ch}^{in}Y(1-\omega)$ and $M_0\left(D, s_2^{*1}\right) + M_1\left(D, s_2^{*1}\right) < S_{ch}^{in}Y$
$\mathcal{J}_{20}$	$\left(S_{H_2}^{in} + \omega\varphi_0(D) - M_2(D)\right)/\omega < S_{ch}^{in}Y < M_0\left(D, s_2^{*1}\right) + M_1\left(D, s_2^{*1}\right)$, $\phi_4\left(D, S_{ch}^{in}, S_{H_2}^{in}\right) < 0$
$\mathcal{J}_{21}$	$\varphi_0(D) + \varphi_1(D) < S_{ch}^{in}Y < \left(S_{H_2}^{in} + \omega\varphi_0(D) - M_2(D)\right)/\omega$ and $\phi_4\left(D, S_{ch}^{in}, S_{H_2}^{in}\right) < 0$

□

Phenol is in the input

Assume that $S_{ch}^{in} > 0$, $S_{ph}^{in} > 0$ and $S_{H_2}^{in} = 0$, we construct the operating diagrams in (S_{ch}^{in}, D)-plane in both cases with and without maintenance terms. In this case, system (2.1) has further two steady states E_{010} and E_{011}. However, the steady states E_{001}, E_{100} and E_{101} do not exist since $S_{H_2}^{in} = 0$, see Proposition 2.2.

We consider the input concentrations $S_{ph}^{in} = 10^{-2}$ and $S_{H_2}^{in} = 0$. These values are those of Figure 5(a) in [64]. Figure 5.21(a) represents the operating diagram in the plane (S_{ch}^{in}, D), in the case without maintenance. The magnifications shown in Figure 5.21(b-c) put in evidence the regions $\mathcal{J}_i$, $i = 22, \ldots, 30$. Figure 5.22(a) represents the operating diagram in the case with maintenance. The magnification presented in Figure 5.22(b) shows that the regions $\mathcal{J}_i$ $j = 1, \ldots, 5$ and $\mathcal{J}_i$, $i = 22, \ldots, 30$ are similar to those in Figure 5.21. The addition of phenol input substrate leads to the emergence of twelve new regions $\mathcal{J}_i$, $i = 22, \ldots, 32$, besides the regions $\mathcal{J}_j$, $j = 1, \ldots, 5$ which are identical to those of the operating diagram in Figure 5.1. Figures 5.21 and 5.22 are constructed using the same method as Figure 5.11, which consists in plotting the curves separating the regions.

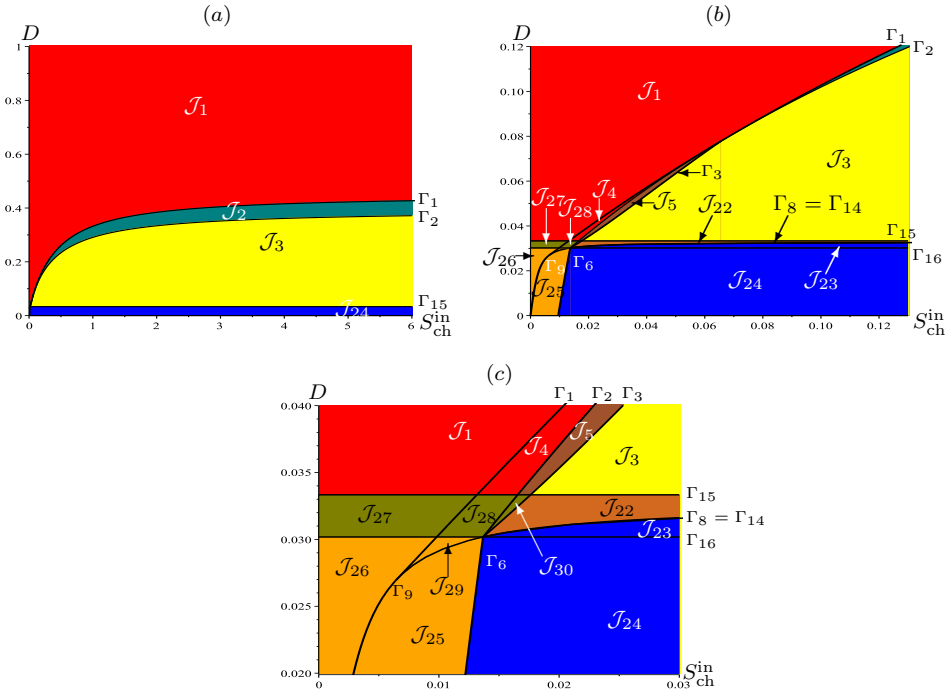

Figure 5.21: Operating diagram in the plane (S_{ch}^{in}, D), when $S_{ph}^{in} = 10^{-2}$, $S_{H_2}^{in} = 0$ and $k_{dec,i} = 0$. (b) Magnification for $D \in [0, 0.078]$ showing the regions $\mathcal{J}_i$, for $i = 22, \ldots, 28$. (c) Magnification for $D \in [0.02, 0.04]$ showing the regions $\mathcal{J}_{29}$ and $\mathcal{J}_{30}$.

The existence and the stability of the steady states of (2.1) in the sixteen regions $\mathcal{J}_i$, $i = 1, \ldots, 5$ and $\mathcal{J}_j$, $j = 22, \ldots, 32$ of the operating diagrams of Figures 5.21 and 5.22 are summarized in Table 5.8.

The positive steady state E_{111} loss its stability via a Hopf bifurcation by crossing the boundary from the region $\mathcal{J}_3$ to $\mathcal{J}_5$, see Table 5.8 and Figures 5.21 and 5.22, and in $\mathcal{J}_5$

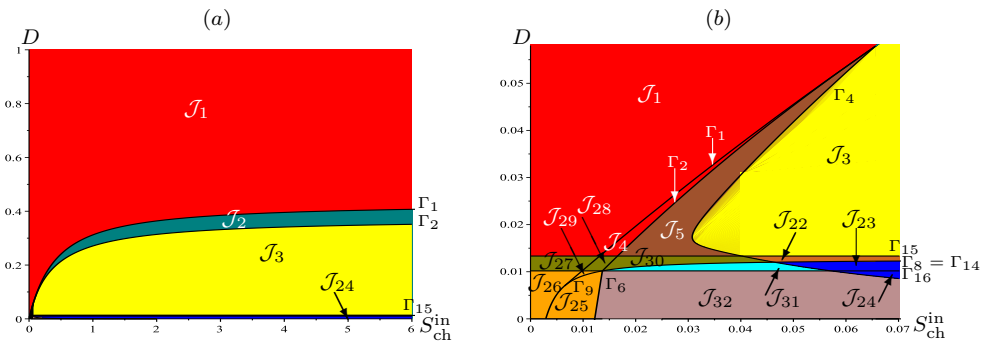

Figure 5.22: Operating diagram in the plane $\left(S_{ch}^{in}, D\right)$, when $S_{ph}^{in} = 10^{-2}$, $S_{H_2}^{in} = 0$ and $k_{dec,i} > 0$. (b) Magnification for $D \in [0, 0.058]$ showing the regions $\mathcal{J}_i$, for $i = 22, \ldots, 32$.

Table 5.8: Existence and stability of steady states in the regions of the operating diagrams of Figures 5.21 and 5.22.

Region	E_{000} SS1	E^1_{110} SS4^1	E^2_{110} SS4^2	E_{111} SS6	E_{010} SS7	E_{011} SS8	Color
$\mathcal{J}_1 = (1)$	S						Red
$\mathcal{J}_2 = (14^2, 4^1)$	S	U	S				Teal
$\mathcal{J}_3 = (16, 4^1 4^2)$	S	U	U	S			Yellow
$\mathcal{J}_4 = (1, 4^1 4^2)$	S	U	U				Red
$\mathcal{J}_5 = (1, 4^1 4^2 6)$	S	U	U	U			Sienna
$\mathcal{J}_{22} = (67, 14^1 4^2)$	U	U	U	S	S		Chocolate
$\mathcal{J}_{23} = (6, 14^2 7)$	U		U	S	U		Blue
$\mathcal{J}_{24} = (6, 14^2 78)$	U		U	S	U	U	Blue
$\mathcal{J}_{25} = (8, 14^2 7)$	U		U		U	S	Orange
$\mathcal{J}_{26} = (8, 17)$	U				U	S	Orange
$\mathcal{J}_{27} = (7, 1)$	U				S		Olive
$\mathcal{J}_{28} = (7, 14^1 4^2)$	U	U	U		S		Olive
$\mathcal{J}_{29} = (8, 14^1 4^2 7)$	U	U	U		U	S	Orange
$\mathcal{J}_{30} = (7, 14^1 4^2 6)$	U	U	U	U	S		Olive
$\mathcal{J}_{31} = (., 14^2 67)$	U		U	U	U		Cyan
$\mathcal{J}_{32} = (., 14^2 678)$	U		U	U	U	U	RosyBrown

close to the boundary with $\mathcal{J}_3$ a limit cycle in E_{111} occurs. We see also that there are new regions $\mathcal{J}_{31}$ and $\mathcal{J}_{32}$ that appear under the influence of the maintenance terms. Notice that, in the case with maintenance and for D fixed, the value of S_{ch}^{in} which E_{111} loss its stability is larger than in the case without maintenance. Moreover, in the case without maintenance and for small values of D, there cannot be any destabilisation of E_{111}, while the coexistence around a limit cycle can appears in the case with maintenance. On the other hand, our theoretical study of the operating diagrams in both cases with and without maintenance show that there are new behaviors, namely the existence of bistability region

$\mathcal{J}_{22}$ of E_{111} and E_{010} (SS7), which occurs in a small area between $\mathcal{J}_3$ and $\mathcal{J}_{23}$, the instability regions $\mathcal{J}_5, \mathcal{J}_{30}, \mathcal{J}_{31}$ of E_{111}, and the region $\mathcal{J}_{32}$ when all the steady states exist and are unstable, except E^1_{110} (SS4^1) which does not exist. For the positive initial conditions in a neighborhood of E_{111} all these steady states converge to the stable limit cycle. These regions are not reported in the case including maintenance in Figure 5(a) of [64].

Phenol and hydrogen are in the input

To better understand the effect of both control parameters the phenol and the hydrogen input concentrations on system (2.1), we assume that $S^{in}_{ch} > 0$, $S^{in}_{ph} > 0$ and $S^{in}_{H_2} > 0$ and we perform the operating diagram in both cases with and without maintenance terms.

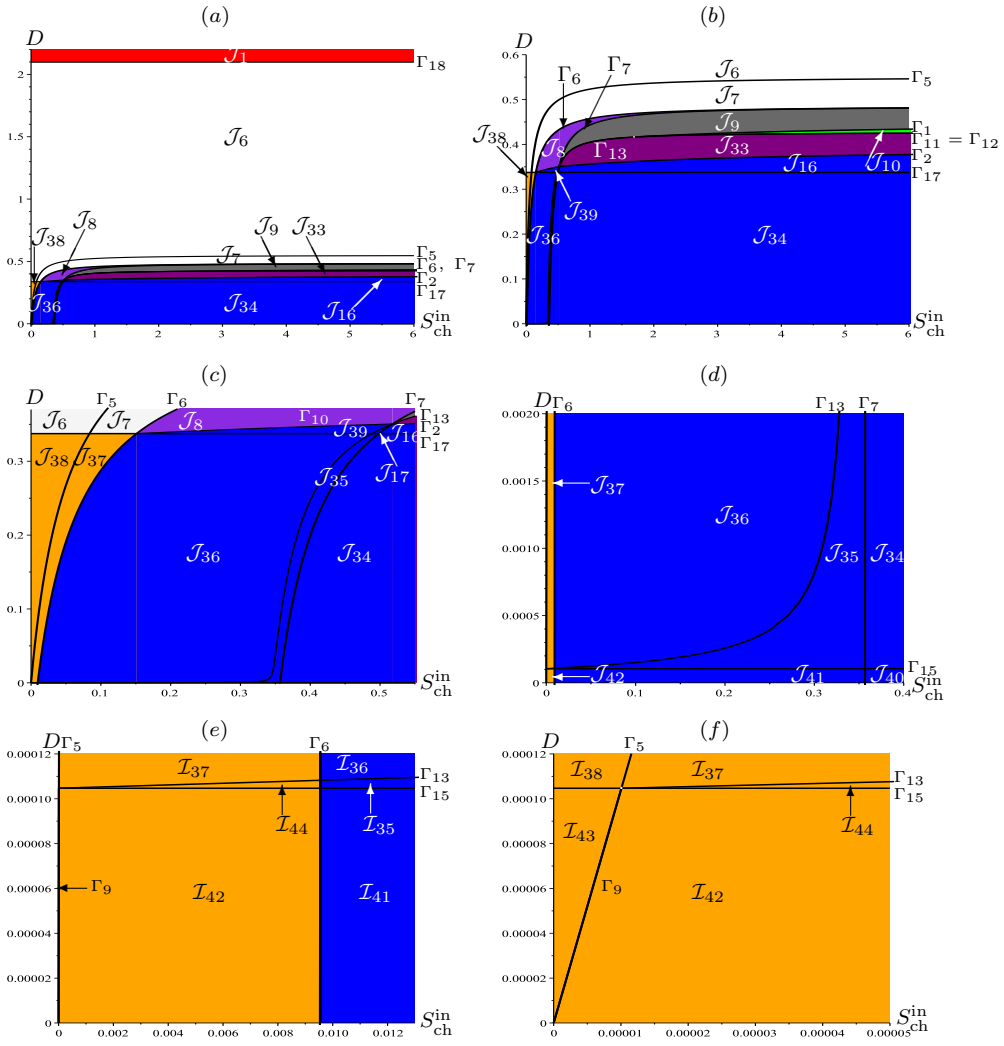

Figure 5.23: Operating diagram in the plane $\left(S^{in}_{ch}, D\right)$, when $S^{in}_{ph} = 1$, $S^{in}_{H_2} = 2.67 \times 10^{-2}$ and $k_{dec,i} = 0$. (b) Magnification for $D \in [0, 0.6]$ showing the regions $\mathcal{J}_{10}$ and $\mathcal{J}_{39}$. (c) Magnification for $D \in [0, 0.37]$ showing the regions $\mathcal{J}_{17}$, $\mathcal{J}_{35}$ and $\mathcal{J}_{37}$. (d) Magnification for $D \in [0, 0.002]$ showing the regions $\mathcal{J}_{40}$, $\mathcal{J}_{41}$ and $\mathcal{J}_{42}$. (e) Magnification for $D \in [0, 0.00012]$ showing the region $\mathcal{J}_{44}$. (f) Magnification for $S^{in}_{ch} \in [0, 0.00005]$ showing the region $\mathcal{J}_{43}$.

We consider the input concentrations $S_{ph}^{in} = 1$ and $S_{H_2}^{in} = 2.67 \times 10^{-2}$, corresponding to Figure 5(d) in [64]. Figure 5.23(a) represents the operating diagram in (S_{ch}^{in}, D)-plane, in the case without maintenance. The magnifications show in Figure 5.23(b-c-d-e-f) put in evidence the regions $\mathcal{J}_{16}$, $\mathcal{J}_{17}$, $\mathcal{J}_i$, $i = 33, \ldots, 44$. Figure 5.24(a) represents the operating diagram in the case with maintenance. The magnifications presented in Figure 5.24(b-c) show that the regions $\mathcal{J}_1$ and $\mathcal{J}_i$, $i = 6, \ldots, 13$ are defined as those in Figure 5.23. We see also that the maintenance has an effect on the disappearance of regions $\mathcal{J}_i$, $i = 39, \ldots, 44$. Moreover, the two input substrates hydrogen and phenol are added to the system contribute to the emergence of twelve new regions $\mathcal{J}_i$, $i = 33, \ldots, 44$ beside the regions $\mathcal{J}_1$, $\mathcal{J}_{16}$, $\mathcal{J}_{17}$, $\mathcal{J}_i$, $i = 6, \ldots, 10$ which are identical to that of the operating diagram in Figure 5.23. Since the concentrations of S_{ph}^{in} and $S_{H_2}^{in}$ are large enough comparing with the case of Figure 5.22 where $S_{ph}^{in} = 10^{-2}$ and $S_{H_2}^{in} = 0$, all asymptotic behaviors were detected in Figure 5(d) of [64]. Figures 5.23 and 5.24 are constructed using the same method as Figure 5.11, which consists in plotting the curves separating the regions.

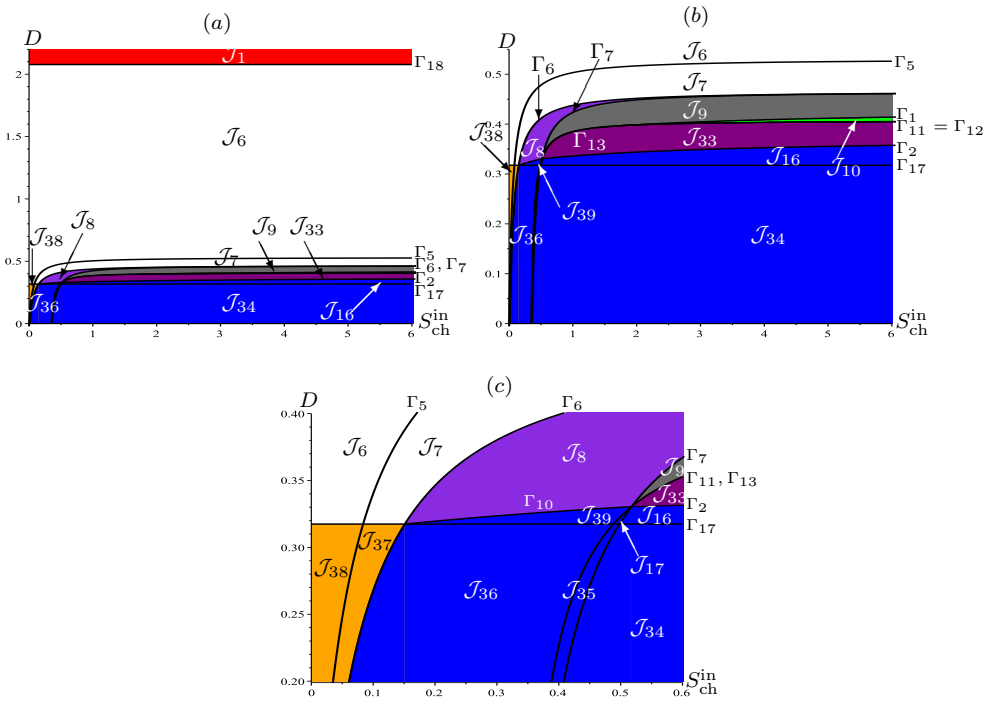

Figure 5.24: Operating diagram in the plane (S_{ch}^{in}, D), when $S_{ph}^{in} = 1$, $S_{H_2}^{in} = 2.67 \times 10^{-2}$ and $k_{dec,i} > 0$. (b) Magnification for $D \in [0, 0.55]$ showing the regions $\mathcal{J}_{10}$ and $\mathcal{J}_{39}$. (c) Magnification for $D \in [0.2, 0.4]$ showing the regions $\mathcal{J}_{17}$, $\mathcal{J}_{35}$ and $\mathcal{J}_{37}$.

The existence and the stability of the steady states of (2.1) in the twenty regions $\mathcal{J}_1$, $\mathcal{J}_{16}$, $\mathcal{J}_{17}$, $\mathcal{J}_i$ $i = 6, \ldots, 10$ and $\mathcal{J}_i$, $i = 33, \ldots, 42$, of the operating diagrams of Figures 5.23 and 5.24 are summarized in Table 5.9.

Table 5.9: Existence and local stability of steady states in the regions of the operating diagrams of Figures 5.23 and 5.24.

Region	E_{000} SS1	E_{001} SS2	E_{100} SS3	E^1_{110} SS4^1	E^2_{110} SS4^2	E_{101} SS5	E_{111} SS6	E_{010} SS7	E_{011} SS8	Color
$\mathcal{J}_1 = (1)$	S									Red
$\mathcal{J}_6 = (2,1)$	U	S								White
$\mathcal{J}_7 = (2,13)$	U	S	U							White
$\mathcal{J}_8 = (5,123)$	U	U	U			S				BlueViolete
$\mathcal{J}_9 = (3,12)$	U	U	S							DimGray
$\mathcal{J}_{10} = (34^2, 124^1)$	U	U	S	U	S					Green
$\mathcal{J}_{16} = (6, 1234^2)$	U	U	U		U		S			Blue
$\mathcal{J}_{17} = (6, 1234^2 5)$	U	U	U		U	U	S			Blue
$\mathcal{J}_{33} = (4^2, 123)$	U	U	U		S					Purple
$\mathcal{J}_{34} = (6, 1234^2 8)$	U	U	U		U		S		U	Blue
$\mathcal{J}_{35} = (6, 1234^2 58)$	U	U	U		U	U	S		U	Blue
$\mathcal{J}_{36} = (6, 12358)$	U	U	U			U	S		U	Blue
$\mathcal{J}_{37} = (8, 123)$	U	U	U						S	Orange
$\mathcal{J}_{38} = (8, 12)$	U	U							S	Orange
$\mathcal{J}_{39} = (6, 1235)$	U	U	U			U	S			Blue
$\mathcal{J}_{40} = (6, 1234^2 78)$	U	U	U		U		S	U	U	Blue
$\mathcal{J}_{41} = (6, 1234^2 578)$	U	U	U		U	U	S	U	U	Blue
$\mathcal{J}_{42} = (8, 1234^2 7)$	U	U	U		U			U	S	Orange
$\mathcal{J}_{43} = (8, 124^2 7)$	U	U						U	S	Orange
$\mathcal{J}_{44} = (8, 1234^2)$	U	U	U		U				S	Orange

5.2.2 Operating diagrams with respect to $\left(S^{in}_{H_2}, S^{in}_{ph}\right)$, S^{in}_{ch} and D fixed

Now, let D and S^{in}_{ch} be fixed, then, the intersections of the surfaces Γ_i for $i = 3, 4, 8, 9, 11, 12, 13, 15$ with the $\left(S^{in}_{H_2}, S^{in}_{ph}\right)$-plane are curves as functions of S^{in}_{ch} and D. However, the intersections of the surfaces Γ_j, $j = 1, 2, 5, 7, 10, 14, 16, 17, 18$ with this plane are straight lines.

We consider the input concentrations $S^{in}_{ch} = 0.5$ and $D = 0.25$. These values are those of Figure 6(a) in [64]. The operating diagram in the plane $\left(S^{in}_{H_2}, S^{in}_{ph}\right)$ is shwon in Figures 5.25 and 5.26 for the values of the chlorophenol input concentration and the dilution rate in both cases without and with considering maintenance, respectively. The magnification shown in Figure 5.25(b) put in evidence the regions $\mathcal{J}_2$, $\mathcal{J}_3$, $\mathcal{J}_{40}$, $\mathcal{J}_i$, $i = 22, \ldots, 24$ and $\mathcal{J}_j$, $j = 45, \ldots, 49$. The magnification presented in Figure 5.26(b) shows the regions $\mathcal{J}_1$, $\mathcal{J}_2$, $\mathcal{J}_3$, $\mathcal{J}_{40}$, $\mathcal{J}_i$, $i = 22, \ldots, 24$ and $\mathcal{J}_j$, $j = 45, \ldots, 51$. We see from the operating diagram

provided in Figure 5.26 that there are new regions $\mathcal{J}_1$, $\mathcal{J}_9$, $\mathcal{J}_{33}$, $\mathcal{J}_{50}$ and $\mathcal{J}_{51}$ that appear under the influence of the maintenance terms. Figures 5.25 and 5.26 are constructed using the same method as Figure 5.11, which consists in plotting the curves separating the regions.

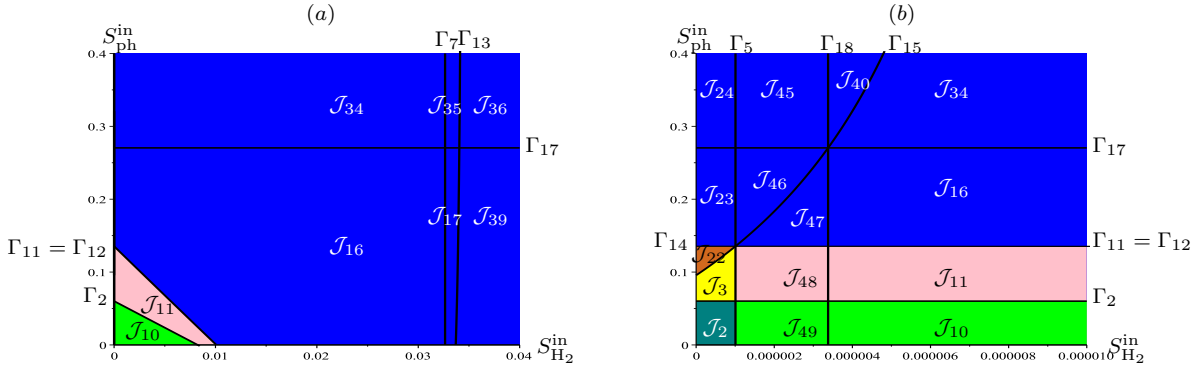

Figure 5.25: (a) Operating diagram in the plane $\left(S^{in}_{H_2}, S^{in}_{ph}\right)$, when $D = 0.25$, $S^{in}_{ch} = 0.5$ and $k_{dec,i} = 0$. (b) Magnification of (a) for $S^{in}_{H_2} \in [0, 10^{-5}]$ showing the regions $\mathcal{J}_2$, $\mathcal{J}_3$, $\mathcal{J}_{40}$, $\mathcal{J}_i$, $i = 22, \ldots, 24$ and $\mathcal{J}_j$, $j = 45, \ldots, 49$.

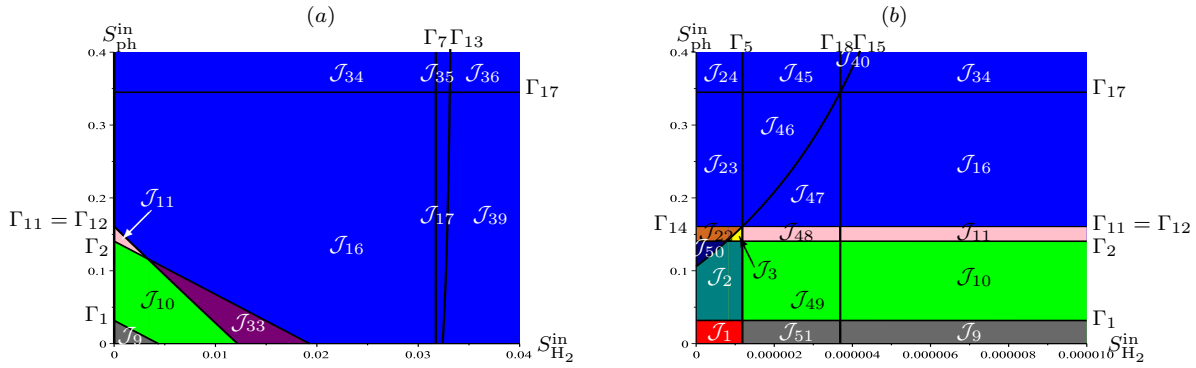

Figure 5.26: (a) Operating diagram in the plane $\left(S^{in}_{H_2}, S^{in}_{ph}\right)$, when $D = 0.25$, $S^{in}_{ch} = 0.5$ and $k_{dec,i} > 0$. (b) Magnification of (a) for $S^{in}_{H_2} \in [0, 10^{-5}]$ showing the regions $\mathcal{J}_1$, $\mathcal{J}_2$, $\mathcal{J}_3$, $\mathcal{J}_{40}$, $\mathcal{J}_i$, $i = 22, \ldots, 24$ and $\mathcal{J}_j$, $j = 45, \ldots, 51$.

The existence and the stability of the steady states of (2.1) in the twenty-four regions $\mathcal{J}_i$ of the operating diagrams of Figures 5.25 and 5.26 are summarized in Table 5.10.

We can deduce from Table 5.10 and the operating diagram shown in Figures 5.25 and 5.26 plotting for varying concentrations of hydrogen and phenol addition, that there are new regions that occur under the influence of the maintenance terms. Notice that the stability regions of the steady states E_{000}, E_{100} and E^2_{110}, and the bistability region of E^2_{110} and E_{010} do not exist in the case without maintenance. Moreover, the bistability region $\mathcal{J}_{50}$ of E^2_{110} and E_{010} (SS7) occurs between $\mathcal{J}_3$ and $\mathcal{J}_{23}$ which is very thin and is not reported in the case including maintenance in Figure 6(a) of [64].

Table 5.10: Existence and local stability of steady states in the regions of the operating diagrams of Figures 5.25 and 5.26.

Region	E_{000} SS1	E_{001} SS2	E_{100} SS3	E^1_{110} $SS4^1$	E^2_{110} $SS4^2$	E_{101} SS5	E_{111} SS6	E_{010} SS7	E_{011} SS8	Color
$\mathcal{J}_1 = (1)$	S									Red
$\mathcal{J}_2 = (14^2, 4^1)$	S			U	S					Teal
$\mathcal{J}_3 = (16, 4^1 4^2)$	S			U	U		S			Yellow
$\mathcal{J}_9 = (3, 12)$	U	U	S							DimGray
$\mathcal{J}_{10} = (34^2, 124^1)$	U	U	S	U	S					Green
$\mathcal{J}_{11} = (36, 124^1 4^2)$	U	U	S	U	U		S			Pink
$\mathcal{J}_{16} = (6, 1234^2)$	U	U	U		U		S			Blue
$\mathcal{J}_{17} = (6, 1234^2 5)$	U	U	U		U	U	S			Blue
$\mathcal{J}_{22} = (67, 14^1 4^2)$	U			U	U		S	S		Chocolate
$\mathcal{J}_{23} = (6, 14^2 7)$	U				U		S	U		Blue
$\mathcal{J}_{24} = (6, 14^2 78)$	U				U		S	U	U	Blue
$\mathcal{J}_{33} = (4^2, 123)$	U	U	U		S					Purple
$\mathcal{J}_{34} = (6, 1234^2 8)$	U	U	U		U		S		U	Blue
$\mathcal{J}_{35} = (6, 1234^2 58)$	U	U	U		U	U	S		U	Blue
$\mathcal{J}_{36} = (6, 12358)$	U	U	U			U	S		U	Blue
$\mathcal{J}_{39} = (6, 1235)$	U	U	U			U	S			Blue
$\mathcal{J}_{40} = (6, 1234^2 78)$	U	U	U		U		S	U	U	Blue
$\mathcal{J}_{45} = (6, 134^2 78)$	U		U		U		S	U	U	Blue
$\mathcal{J}_{46} = (6, 134^2 7)$	U		U		U		S	U		Blue
$\mathcal{J}_{47} = (6, 134^2)$	U		U		U		S			Blue
$\mathcal{J}_{48} = (36, 14^1 4^2)$	U		S	U	U		S			Pink
$\mathcal{J}_{49} = (34^2, 14^1)$	U		S	U	S					Green
$\mathcal{J}_{50} = (4^2 7, 14^1)$	U			U	S			S		Navy
$\mathcal{J}_{51} = (3, 1)$	U		S							DimGray

5.3 Bifurcations

In this section, we determines the nature of bifurcations of system (2.1) that might happen by crossing the various regions of the operating parameters space-$\left(D, S^{\text{in}}_{\text{ch}}, S^{\text{in}}_{\text{ph}}, S^{\text{in}}_{\text{H}_2}\right)$ through the surfaces of Γ_i where the steady states coalesce and can change their stability.

Proposition 5.1. *The bifurcations of the steady states of* (2.1) *arising on the boundaries of regions* $\mathcal{J}_i$ *for* $i = 1, \ldots, 51$*, according to the operating parameters* $S^{\text{in}}_{\text{ch}}$, $S^{\text{in}}_{\text{ph}}$, $S^{\text{in}}_{\text{H}_2}$ *and* D*, are listed in Table 5.11.*

Table 5.11: The bifurcations according to subsets of surfaces Γ_i. A saddle-node bifurcation is indicated by SNB, a transcritical bifurcation by TB and a Hopf bifurcation by HB.

Γ_i	Conditions	Transition	Bifurcation
Γ_1	$(1-\omega)S_{\text{ch}}^{\text{in}}Y \geq \phi_1(D) - S_{\text{ph}}^{\text{in}}Y_4 - S_{\text{H}_2}^{\text{in}}$	$\mathcal{J}_1$ to $\mathcal{J}_2$ $\mathcal{J}_1$ to $\mathcal{J}_4$ $\mathcal{J}_7$ to $\mathcal{J}_{14}$ $\mathcal{J}_8$ to $\mathcal{J}_{19}$ $\mathcal{J}_9$ to $\mathcal{J}_{10}$ $\mathcal{J}_9$ to $\mathcal{J}_{12}$ $\mathcal{J}_{26}$ to $\mathcal{J}_{29}$ $\mathcal{J}_{27}$ to $\mathcal{J}_{28}$ $\mathcal{J}_{51}$ to $\mathcal{J}_{49}$	SNB: $\text{E}_{110}^1 = \text{E}_{110}^2$
Γ_2	$(1-\omega)S_{\text{ch}}^{\text{in}}Y > \phi_2(D) - S_{\text{ph}}^{\text{in}}Y_4 - S_{\text{H}_2}^{\text{in}}$	$\mathcal{J}_2$ to $\mathcal{J}_3$ $\mathcal{J}_4$ to $\mathcal{J}_5$ $\mathcal{J}_{10}$ to $\mathcal{J}_{11}$ $\mathcal{J}_{12}$ to $\mathcal{J}_{13}$ $\mathcal{J}_{33}$ to $\mathcal{J}_{16}$ $\mathcal{J}_{28}$ to $\mathcal{J}_{30}$ $\mathcal{J}_{49}$ to $\mathcal{J}_{48}$ $\mathcal{J}_{50}$ to $\mathcal{J}_{22}$	TB: E_{110}^2=E_{111}
Γ_3	$\phi_4(D, S_{\text{ch}}^{\text{in}}, S_{\text{ph}}^{\text{in}}, S_{\text{H}_2}^{\text{in}}) < 0$	$\mathcal{J}_3$ to $\mathcal{J}_5$ $\mathcal{J}_{11}$ to $\mathcal{J}_{13}$ $\mathcal{J}_{16}$ to $\mathcal{J}_{20}$ $\mathcal{J}_{17}$ to $\mathcal{J}_{21}$ $\mathcal{J}_{22}$ to $\mathcal{J}_{30}$	HB of E_{111}
Γ_4	$r_5(D, S_{\text{ch}}^{\text{in}}, S_{\text{ph}}^{\text{in}}, S_{\text{H}_2}^{\text{in}}) < 0$	$\mathcal{J}_3$ to $\mathcal{J}_5$ $\mathcal{J}_{11}$ to $\mathcal{J}_{13}$ $\mathcal{J}_{22}$ to $\mathcal{J}_{30}$ $\mathcal{J}_{23}$ to $\mathcal{J}_{31}$ $\mathcal{J}_{24}$ to $\mathcal{J}_{32}$	HB of E_{111}
Γ_5	$S_{\text{ch}}^{\text{in}}Y > M_0(D + a_0, S_{\text{H}_2}^{\text{in}})$	$\mathcal{J}_1$ to $\mathcal{J}_{51}$ $\mathcal{J}_2$ to $\mathcal{J}_{49}$ $\mathcal{J}_3$ to $\mathcal{J}_{48}$ $\mathcal{J}_6$ to $\mathcal{J}_7$ $\mathcal{J}_{23}$ to $\mathcal{J}_{46}$ $\mathcal{J}_{24}$ to $\mathcal{J}_{45}$ $\mathcal{J}_{37}$ to $\mathcal{J}_{38}$ $\mathcal{J}_{43}$ to $\mathcal{J}_{42}$	TB: E_{000}=E_{100}
Γ_6	$S_{\text{ch}}^{\text{in}}Y > \varphi_0(D)$	$\mathcal{J}_7$ to $\mathcal{J}_8$ $\mathcal{J}_{14}$ to $\mathcal{J}_{19}$ $\mathcal{J}_{15}$ to $\mathcal{J}_{18}$ $\mathcal{J}_{25}$ to $\mathcal{J}_{24}$ $\mathcal{J}_{25}$ to $\mathcal{J}_{32}$ $\mathcal{J}_{37}$ to $\mathcal{J}_{36}$ $\mathcal{J}_{42}$ to $\mathcal{J}_{41}$	TB: E_{001}=E_{101} TB: E_{001}=E_{101} TB: E_{001}=E_{101} TB: E_{111}=E_{011} TB: E_{111}=E_{011} TB: E_{111}=E_{011} TB: E_{101}=E_{111}

		$\mathcal{J}_{44}$ to $\mathcal{J}_{35}$	TB: E_{101}=E_{111}
Γ_7	$S_{ch}^{in} Y\omega > S_{H_2}^{in} - M_2(D+a_2) + \omega\varphi_0(D)$	$\mathcal{J}_8$ to $\mathcal{J}_9$ $\mathcal{J}_{17}$ to $\mathcal{J}_{16}$ $\mathcal{J}_{19}$ to $\mathcal{J}_{12}$ $\mathcal{J}_{21}$ to $\mathcal{J}_{20}$ $\mathcal{J}_{35}$ to $\mathcal{J}_{34}$ $\mathcal{J}_{41}$ to $\mathcal{J}_{40}$	TB: E_{100}=E_{101}
$\Gamma_8 = \Gamma_{14}$	$S_{ch}^{in} Y > M_0(D+a_0, s_2^{*1})$ or $M_1(D+a_1, M_3(S_{ch}^{in} Y, D+a_0)$ $+M_3(S_{ch}^{in} Y, D+a_0) > S_{ph}^{in} Y_4 + S_{H_2}^{in}$	$\mathcal{J}_{22}$ to $\mathcal{J}_{23}$ $\mathcal{J}_{30}$ to $\mathcal{J}_{31}$	TB: E_{110}^1=E_{010}
Γ_{10}	$S_{ch}^{in} Y > \varphi_0(D) + \varphi_1(D) - S_{ph}^{in} Y_4$	$\mathcal{J}_8$ to $\mathcal{J}_{39}$ $\mathcal{J}_{18}$ to $\mathcal{J}_{17}$ $\mathcal{J}_{18}$ to $\mathcal{J}_{21}$	TB: E_{101}=E_{111}
$\Gamma_{11} = \Gamma_{12}$	$\mu_1(S_{ph}^{in} Y_4 + S_{ch}^{in} Y - s_0, S_{H_2}^{in} - \omega(S_{ch}^{in} Y - s_0)) > D + a_1$ or $S_{ch}^{in} Y > M_0(D+a_0, s_2^{*1}) + M_1(D+a_1, s_2^{*1}) - S_{ph}^{in} Y_4$	$\mathcal{J}_{10}$ to $\mathcal{J}_{33}$ $\mathcal{J}_{11}$ to $\mathcal{J}_{16}$ $\mathcal{J}_{13}$ to $\mathcal{J}_{20}$ $\mathcal{J}_{22}$ to $\mathcal{J}_{23}$ $\mathcal{J}_{48}$ to $\mathcal{J}_{47}$	TB: E_{100}=E_{110}^1
Γ_{13}	$S_{ch}^{in} Y > M_0(D+a_0, s_2^{*2}) + M_1(D+a_1, s_2^{*2}) - S_{ph}^{in} Y_4$	$\mathcal{J}_9$ to $\mathcal{J}_{33}$	TB: E_{100}=E_{110}^2
Γ_{15}	$\mu_1(S_{ph}^{in} Y_4, S_{H_2}^{in}) > D + a_1$	$\mathcal{J}_1$ to $\mathcal{J}_{27}$ $\mathcal{J}_2$ to $\mathcal{J}_{50}$ $\mathcal{J}_3$ to $\mathcal{J}_{22}$ $\mathcal{J}_4$ to $\mathcal{J}_{28}$ $\mathcal{J}_5$ to $\mathcal{J}_{30}$ $\mathcal{J}_{34}$ to $\mathcal{J}_{40}$ $\mathcal{J}_{35}$ to $\mathcal{J}_{41}$ $\mathcal{J}_{38}$ to $\mathcal{J}_{43}$ $\mathcal{J}_{44}$ to $\mathcal{J}_{42}$ $\mathcal{J}_{47}$ to $\mathcal{J}_{46}$	TB: E_{000}=E_{010}
Γ_{16}	$\varphi_1(D) + M_2(D+a_2) < S_{ph}^{in} Y_4 + S_{H_2}^{in}$	$\mathcal{J}_{23}$ to $\mathcal{J}_{24}$ $\mathcal{J}_{27}$ to $\mathcal{J}_{26}$ $\mathcal{J}_{28}$ to $\mathcal{J}_{29}$ $\mathcal{J}_{31}$ to $\mathcal{J}_{32}$	TB: E_{010}=E_{011}
Γ_{17}	$S_{ph}^{in} Y_4 > \varphi_1(D)$	$\mathcal{J}_6$ to $\mathcal{J}_{38}$ $\mathcal{J}_7$ to $\mathcal{J}_{37}$ $\mathcal{J}_{16}$ to $\mathcal{J}_{34}$ $\mathcal{J}_{17}$ to $\mathcal{J}_{35}$ $\mathcal{J}_{23}$ to $\mathcal{J}_{24}$ $\mathcal{J}_{39}$ to $\mathcal{J}_{36}$ $\mathcal{J}_{46}$ to $\mathcal{J}_{45}$	TB: E_{010}=E_{011}
Γ_{18}	$\mu_2(S_{H_2}^{in}) > D + a_2$	$\mathcal{J}_6$ to $\mathcal{J}_1$ $\mathcal{J}_9$ to $\mathcal{J}_{51}$ $\mathcal{J}_{10}$ to $\mathcal{J}_{49}$ $\mathcal{J}_{11}$ to $\mathcal{J}_{48}$ $\mathcal{J}_{16}$ to $\mathcal{J}_{47}$ $\mathcal{J}_{40}$ to $\mathcal{J}_{45}$	TB: E_{010}=E_{011}

Proof. From Table 5.2, the surface Γ_1 is defined by $S_{ch}^{in} Y(1-\omega) = \phi_1(D) - S_{ph}^{in} Y_4 - S_{H_2}^{in}$.

Using Tables 2.1 and 5.1, we can see that E^1_{110} and E^2_{110} coalesce and are non hyperbolic steady states on the surface Γ_1. Using Table 5.1, if $S^{in}_{ch}Y(1-\omega) \geq \phi_1(D) - S^{in}_{ph}Y_4 - S^{in}_{H_2}$, we have a transition from $\mathcal{J}_1$ to $\mathcal{J}_2$ where E^1_{110} and E^2_{110} emerge unstable and stable, respectively, in the positive octant $\mathbb{R}^4_+$, which correspond of the saddle node bifurcation.

From Table 5.2, the surface Γ_2 is defined by $S^{in}_{ch}Y(1-\omega) = \phi_2(D) - S^{in}_{ph}Y_4 - S^{in}_{H_2}$. Using Tables 2.1 and 5.1, we can see that E^2_{110} and E_{111} coalesce and are non hyperbolic steady states on the surface Γ_2. Using Table 5.1, if $S^{in}_{ch}Y(1-\omega) > \phi_2(D) - S^{in}_{ph}Y_4 - S^{in}_{H_2}$, we have a transition from $\mathcal{J}_2$ to $\mathcal{J}_3$ where E^2_{110} becomes unstable and E_{111} appears stable, which correspond of the transcritical bifurcation.

From Table 5.2, the surface Γ_3 is defined by $\phi_4(D, S^{in}_{ch}, S^{in}_{ph}, S^{in}_{H_2}) = 0$. Using Table 5.1, if $\phi_4(D, S^{in}_{ch}, S^{in}_{ph}, S^{in}_{H_2}) > 0$, we have a transition from $\mathcal{J}_3$ to $\mathcal{J}_5$ where the positive steady state E_{111} loss its stability via Hopf bifurcation on the surface Γ_3.

All other cases are left to the reader since they can be treated similarly.

□

Remark 5.2. We have studied the types of bifurcations of the various transitions by surfaces but not by the intersections of curves and lines which are generically points and represent special cases which are not possible from the biological point of view. However, their studies of bifurcations can be studied in the same way.

5.4 Conclusion

In this chapter, we gave an analytical study of the operating diagram of model (2.1). Our study incorporated the effect of the maintenance as well as the effect of the three input substrate concentrations on the process behavior. We compare with the results in [64], obtained by numerical methods. Our main aim was to present the mathematical analysis of the operating diagrams of the model. Using the characterization of existence and stability conditions of the steady states, we have presented the operating diagram of system (2.1) in order to analytically determine the dynamical behavior of the model according to the control parameters S^{in}_{ch}, $S^{in}_{ph}, S^{in}_{H_2}$ and D. In the operating diagrams shown in Figure 5.1 obtained for $S^{in}_{ph} = S^{in}_{H_2} = 0$ in the cases with and without maintenance, we have found the same regions in both cases, with variations only in their shape and extend, and we have confirmed the numerical results of [51] in the case with maintenance. Moreover, we have discovered interesting regions, which are unreported by the numerical study of the operating diagram in Figure 2 in [64]. In the operating diagrams shown in Figures 5.11 and 5.12 obtained for $S^{in}_{ph} = 0$, in Figures 5.21 and 5.22 obtained for $S^{in}_{H_2} = 0$ and in Figures 5.25 and 5.26 obtained for $D = 0.25$ and $S^{in}_{ch} = 0.5$, we have proven that there are regions appear and disappear under the influence of the maintenance terms, and the emergence of new important regions, which previously undetectable by the numerical analysis in [64]. For comparison, we have detected a stability region of the steady state E_{101} (SS5), the existence of the bistability regions between the steady states E_{111} (SS6) and E_{010} (SS7),

and between E^2_{110} (SS4) and E_{010} (SS7), where are not reported in Figure 3(a), Figure 5(a) and Figure 6(a), respectively, of [64]. More interestingly, we have also discovered instability regions of the positive steady state E_{111} (SS6) in the operating diagrams shown in Figures 5.11 to 5.22, which are unreported in [64] in the case when maintenance is included in the system.

Our results give a better understanding of the operating diagrams performed by the numerical method in [64] and allow us to answer the delicate question where the maintenance does not destabilize the steady states but modify the boundary between the region of stability and the region of instability, and has an effect on the appearance and the disappearance of some regions.

The results of this chapter are the subject of a submitted publication in [42].

General conclusion

In this thesis, we have investigated the dynamics of three interacting microbial species describing the anaerobic mineralization of chlorophenol, in a three-step food-web, introduced by Wade et al. [64]. More precisely, we have focused on the mathematical analysis of the model, extending the previous works. We have generalized the approach presented in [51] by including multiple substrate inflow into the model and characterizing the stability of steady state in the case including maintenance. We have extended [64] by allowing a larger class of growth functions and [18, 57] by including maintenance. Our main aim was to give a complete analysis of the model by a combination of theoretical results and numerical techniques to obtain information on the qualitative behaviors of this six-dimensional system and to fully clarify the findings of the previous numerical analysis. We have highlighted several complex dynamics of the process. In chapter 2, by considering a large class of growth kinetics, the phenol and hydrogen input concentrations together with maintenance terms, which were neglected in the previous analytical analysis, we have proven that our system can have up to eight steady states: the washout steady state which always exists, a positive steady state where all degrader microbial populations coexist, and six other steady states corresponding to the extinction of one or two degrader populations. When they exist, all steady states are unique, except the steady state where chlorophenol and phenol degraders are maintained and the hydrogen degrader is eliminated (E_{110}). We have developed the existence conditions of all steady states with respect to the operating parameters. The results on the existence of some steady states were obtained previously only numerically without knowing their exact number. In chapter 3, when decay terms are ignored, we could reduce the original six-dimensional system to an equivalent three-dimensional one. This made it possible to obtain explicitly the expressions of conditions of the local stability of all identified steady states according to the four operating parameters D, s_0^{in}, s_1^{in} and s_2^{in} which correspond to the dilution rate, the chlorophenol, phenol and hydrogen input substrate concentrations, respectively. We have analyzed the bifurcation diagrams by varying the chlorophenol input concentration when the hydrogen input is added to the model and the phenol input is excluded. We have proven that, except for the positive steady state, all the steady states can only appear or disappear through transcritical or saddle-node bifurcations. Then, we could show that the system exhibits a bi-stability and the coexistence steady state can destabilize undergoing a supercritical

Hopf bifurcation with the occurrence of a stable periodic solution. The destabilization of the positive steady state was not detected by the previous numerical analysis of the operating diagram in [64]. In order to gain more insight into the behavior of the system, from the bifurcation diagrams with S_{ch}^{in} as the bifurcating parameter (see Figures 3.5 to 3.7), we have proven that, if the concentration of the chlorophenol input S_{ch}^{in} is low, both the chlorophenol and phenol degraders are eliminated from the reactor and only the hydrogen degrader is maintained (E_{001} is the only stable steady state). Rising a little more the concentration of S_{ch}^{in}, only the chlorophenol and hydrogen degraders are maintained (E_{101} is the only stable steady state). Adding more S_{ch}^{in}, only the chlorophenol degrader is maintained (E_{100} is the only stable steady state). For higher concentration of S_{ch}^{in}, the system exhibits a bistability behavior where either only the chlorophenol degrader is maintained (E_{100} is stable) or the coexistence of three microbial species may occur around periodic oscillations (E_{111} is unstable and a stable limit cycle exists). In chapter 4, when the maintenance terms are present in the model, we have managed to characterize the stability of the steady states of the six-dimensional system. The stability analysis is much more delicate since the differential system cannot be reduced to a three-dimensional one as in the case without maintenance. We have used the Liénard-Chipart stability criterion to simplify the mathematical analysis by reducing considerably the number of the Routh-Hurwitz conditions to check. Then, we gave the necessary and sufficient conditions of the local stability of the steady states, with respect to the operating parameters of the process. On the other hand, we highlighted several possible asymptotic behaviors in this six-dimensional system, using two bifurcation diagrams with the dilution rate and then, with the chlorophenol input concentration as the bifurcating parameters (see Figure 4.8 and Figures 4.13 to 4.15). We have shown that one of the operating diagrams obtained numerically in [64] has omitted important transition phenomena between steady states. If the dilution rate is too low, only the chlorophenol degrader is maintained (E_{100} is the only stable steady state). Increasing slightly the dilution rate D, the system exhibits a bistability behavior where either only the chlorophenol degrader is maintained (E_{100} is stable) or the coexistence of three microbial species may occur around periodic oscillations (E_{111} is unstable and a stable limit cycle exists). Increasing a little more D, the system exhibits a bistability behavior where either only the chlorophenol degrader is maintained or the coexistence of three microbial species occurs at the positive steady state (E_{100} and E_{111} are both stable). Increasing further D, the system exhibits a bistability between only the chlorophenol degrader and both the chlorophenol and phenol degraders (E_{100} and E_{110}^2 are both stable). Rising a little more the value of D, only the chlorophenol degrader is maintained. Then, only the chlorophenol and hydrogen degraders are maintained (E_{101} is the only stable steady state). Adding a little more, both the chlorophenol and phenol degraders are eliminated from the reactor and only the hydrogen degrader is maintained (E_{001} is the only stable steady state). For higher dilution rate, there is washout of all three microbial populations (E_{000} is the only stable steady state). We proved that the positive steady state of coexistence of all species can be unstable and we give numerical evidence

for the supercritical Hopf bifurcation, in the case including chlorophenol and hydrogen input concentrations. The possibility of the Hopf bifurcation of the positive steady state was previously observed in [51] in the case without phenol and hydrogen input concentrations. In chapter 5, by using the operating diagrams we could show the behaviors of the system by varying the microbial operating parameters. To plot these operating diagrams, we must fix the values of the biological parameters and we must fix two of the four parameters while varying the others. These diagrams can be useful for interpreting experimental results. For $S_{ph}^{in} = S_{H_2}^{in} = 0$, the operating diagrams in the $\left(S_{ch}^{in}, D\right)$ plane of Figure 5.1 show the same number of regions in both cases with and without maintenance, with variations only in their shape and extension. In the case of maintenance, our analytical study of the operating diagrams confirms the numerical results of [51] where a stable limit cycle bifurcates from the positive steady state via a Hopf bifurcation. This behavior is unreported in the numerical operating diagram of Figure 2 in [64]. Considering the inflowing concentrations $S_{ph}^{in} = 0$ and $S_{H_2}^{in} = 2.67\times10^{-5}$ of Figure 3(a) in [64], Figure 5.11 shows the destabilization of the positive steady state in the case without maintenance. In the regions $\mathcal{J}_{20}$ and $\mathcal{J}_{21}$, all the steady states are unstable so that there is coexistence around a limit cycle for any positive initial conditions. Adding the maintenance terms to the system, the regions $\mathcal{J}_i$, $i = 14, \ldots, 21$ disappear. In addition, Figure 5.12 shows that the regions $\mathcal{J}_8$ (stability of E_{101} (SS5)) and $\mathcal{J}_{13}$ (stability of E_{100} (SS3) with instability of E_{111} (SS6)) have been omitted in [64]. Crossing $\mathcal{J}_{11}$ to $\mathcal{J}_{13}$, there is bistability of E_{100} and a limit cycle. In the regions $\mathcal{J}_8$ and $\mathcal{J}_{13}$, the outcome of the process is different than that found in the numerical operating diagram in [64]. Similarly, for the input concentrations $S_{ph}^{in} = 10^{-2}$ and $S_{H_2}^{in} = 0$ as in Figure 5(a) of [64], Figures 5.21 and 5.22 prove that the region $\mathcal{J}_{22}$ (bistability of E_{111} (SS6) and E_{010} (SS7)), and the regions $\mathcal{J}_5, \mathcal{J}_{30}, \mathcal{J}_{31}$ and $\mathcal{J}_{32}$ (instability of E_{111}) were not been detected. However, when the input concentrations $S_{ph}^{in} = 1$ and $S_{H_2}^{in} = 2.67\times10^{-2}$ are large enough as in Figure 5(d) of [64], our analytical operating diagrams in Figures 5.23 and 5.24 show that all asymptotic behaviors were detected. Finally, when $S_{ch}^{in} = 0.5$ and $D = 0.25$ are fixed as in Figure 6(a) of [64], our operating diagrams in $\left(S_{H_2}^{in}, S_{ph}^{in}\right)$ plane of Figures 5.25 and 5.26 prove that the regions $\mathcal{J}_i$, $i = 1, 3, 9, 11, 22, 48, 50, 51$ are unreported. In fact, there can be stability of only E_{000} (J_1) or E_{100} (J_9 and J_{51}), or bistability of E_{000} and E_{111} (J_3) or of E_{100} and E_{111} (J_{11} and J_{48}) or of E_{111} and E_{010} (J_{22}) or of E_{110} and E_{010} (J_{50}). The findings of our mathematical study permit a better understanding of the operating region of the coexistence of all species and its dependence on the biological parameters and show the omission of several important asymptotic behaviors in the numerical study of [64]. Especially validated models with realistic parametrization from experimental data, more attention should be paid to numerical resolution. However, the theoretical study of the operating diagram remains the only way to ensure the accuracy of the results. Moreover, our results allow us to answer the difficult question about the effect of maintenance on the destabilization of the steady states. We proved that it does not destabilize them but modifies the boundary between the region of stability and the region of instability and has an effect on the appearance

and the disappearance of some regions.

Several questions remain open and will be subject of future work, such as the study of the global behavior of the system. Indeed, using the Thieme's theory, we can deduce the global properties of the 6-dimensional system from the 3-dimensional reduced one, in the case without maintenance. A sensitivity study with relation to the biological parameters can be carryed out, in view to get an idea on the robustness and the genericity of the phenomena. We aim too to perform a theoretical and numerical study of the operating diagrams for different parameter values of the maintenance, in order to examine their effects on the stability regions and the attraction basins in the case of bistability.

Bibliography

[1] N. Abdellatif, R. Fekih-Salem, and T. Sari. Competition for a single resource and coexistence of several species in the chemostat. *Math. Biosci. Eng*, 13(4):631–652, 2016. 12, 102

[2] F. Assaneo, R. M. Coutinho, Y. Lin, C. Mantilla, and F. Lutscher. Dynamics and coexistence in a system with intraguild mutualism. *Ecological Complexity*, 14:64–74, 2013. 13

[3] B. Bar and T. Sari. The operating diagram for a model of competition in a chemostat with an external lethal inhibitor. *Discrete & Continuous Dyn. Syst. - B*, 25:2093–2120, 2020. 102

[4] B. Benyahia, T. Sari, B. Cherki, and J. Harmand. Bifurcation and stability analysis of a two step model for monitoring anaerobic digestion processes. *J. Proc. Control*, 22(6):1008–1019, 2012. 10, 11, 12

[5] O. Bernard, Z. Hadj-Sadok, D. Dochain, A. Genovesi, and J-P. Steyer. Dynamical model development and parameter identification for an anaerobic wastewater treatment process. *Biotechnol. Bioeng*, 75:424–438, 2001. 11, 12

[6] O. Bernard, M. Polit, Z. Hadj-Sadok, M. Pengov, D. Dochain, M. Estaben, and P. Labat. Advanced monitoring and control of anaerobic wastewater treatment plants: software sensors and controllers for an anaerobic digester. *Wat. Sci. Technol*, 43(7): 175–182, 2001. 10

[7] A. Bornhöft, R. Hanke-Rauschenbach, and K. Sundmacher. Steady-state analysis of the Anaerobic Digestion Model No. 1 (ADM1). *J. Nonlinear Dyn*, 73:535–549, 2013. 1, 15, 16

[8] F. Borsali and K. Yadi. Contribution to the study of the effect of the inter-specificity on a two nutrients competition model. *Int. J. Biomath*, 8(1):243–253, 2015. 10

[9] F. Borsali and K. Yadi. Persistent competition models on two complementary nutrients with density-dependent consumption rates. *Annali di Matematica Pura ed Applicata*, 8(1):1–25, 2019. 10

[10] J. Bryers. Structured modeling of anaerobic digestion of biomass particulates. *Biotechnol. Bioeng*, 27:638–649, 1985. 1, 16

[11] A. Burchard. Substrate degradation by a mutualistic association of two species in the chemostat. *J. Math. Biol*, 32:465–489, 1994. 10

[12] W. A. Coppel. *Stability and Asymptotic Behavior of Differential Equations*. D.C. Heath, Boston, 1965. 66

[13] Y. Daoud, N. Abdellatif, T. Sari, and J. Harmand. Steady state analysis of a syntrophic model: The effect of a new input substrate concentration. *Math. Model. Nat. Phenom*, 13:1–22, 2018. 10, 14

[14] M. Dellal, M. Lakrib, and T. Sari. The operating diagram of a model of two competitors in a chemostat with an external inhibitor. *Math. Biosci*, 302:27–45, 2018. 102

[15] B. Dubey and J. Hussain. Modelling the interaction of two biological species in a polluted environment. *J. Math. Anal. Appl*, 246(1):58–79, 2000. 10

[16] M. El-Hajji, J. Harmand, H. Chaker, and C. Lobry. Association between competition and obligate mutualism in a chemostat. *J. Biol. Dynam*, 3:635–647, 2009. 13

[17] M. El Hajji, F. Mazenc, and J. Harmand. A mathematical study of a syntrophic relationship of a model of anaerobic digestion process. *Math. Biosci. Eng*, 7:641–656, 2010. 14, 15

[18] M. El Hajji, N. Chorfi, and M. Jleli. Mathematical modelling and analysis for a three-tiered microbial food web in a chemostat. *Electron. J. Differ. Equ*, 255:1–13, 2017. 10, 20, 129

[19] R. Fekih-Salem. Modèles mathématiques pour la compétition et la coexistence des espèces microbiennes dans un chémostat. *University of Montpellier 2 and University of Tunis el Manar (ph.d. thesis)*, 2013. 12

[20] R. Fekih-Salem, T. Sari, and N. Abdellatif. Sur un modèle de compétition et de coexistence dans le chémostat. *ARIMA*, 14:15–30, 2011. 12

[21] R. Fekih-Salem, N. Abdellatif, and A. Yahmadi. Effect of inhibition on a syntrophic relationship model in the anaerobic digestion process. *in Proceedings of the 8th conference on Trends in Applied Mathematics in Tunisia, Algeria, Morocco*, pages 391–396, 2017. 14

[22] R. Fekih-Salem, C. Lobry, and T. Sari. A density-dependent model of competition for one resource in the chemostat. *Math. Biosci*, 286:104–122, 2017. 12, 102

[23] R. Fekih-Salem, Y. Daoud, N. Abdellatif, and T. Sari. A mathematical model of anaerobic digestion with syntrophic relationship, substrate inhibition and distinct removal rates. SIAM J. Appl. Dyn. Syst. SIADS, 2020, hal-02085693v2. 11, 102

[24] F.R. Gantmacher. *Application of the theory of matrices*. Interscience Publishers, INC. New York, 2004. 66, 67, 68

[25] J. Harmand, C. Lobry, A. Rapaport, and T. Sari. The chemostat: Mathematical theory of microorganism cultures. *Willy*, 1, 2017. 1, 6, 8, 9

[26] M. Henze, C. P. L. Jr. Grady, W. Gujer, G. v. R. Marais, and T. Matsuo. Activated Sludge Model No. 1. Technical Report 1, AWPRC Scientific and Technical Reports, London, UK, 1987. 16

[27] M. Henze, W. Gujer, T. Mino, T. Matsuo, M. C. Wentzel, G. v. R. Marais, and M. C. van Loosdrecht. Activated Sludge Model No. 2D, ASM2D. *Wat. Sci. Technol*, 39(1):165–182, 1999. 16

[28] S. B. Hsu, S. P. Hubbell, and P. Waltman. A mathematical theory for singlenutrient competition in continuous cultures of micro-organisms. *SIAM J. Appl. Math*, 32: 366–383, 1976. 9

[29] IWA Task Group for Mathematical Modelling of Anaerobic Digestion Processes. *Anaerobic Digestion Model No. 1 (ADM1)*. IWA Publishing, London, UK, 2002. 1, 15, 16

[30] J. P. Grover. *Resource Competition*. Chapman and Hall, 1997. 12

[31] R. Kreikenbohm and E. Bohl. A mathematical model of syntrophic cocultures in the chemostat. *FEMS Microbiol. Ecol*, 38:131–140, 1986. 14

[32] R. Kreikenbohm and E. Bohl. Bistability in the chemostat. *Ecol. Model*, 43:287–301, 1988. 14

[33] J. A. Leon and D. B. Tumpson. Competition between two species for two complementary or substitutable resources. *J. Theor. Biol*, 50:185–201, 1975. 10

[34] B. Li and H. L. Smith. Competition for essential resources: a brief review, in: Dynamical systems and its applications in biology. *Fields Institute Communications*, 36: 213–227, 2003. 10

[35] MAPLE. *version 17.0.0.0*. Waterloo Maple Inc., Waterloo, Ontario, 2018. 59, 97, 107, 109

[36] F. Mazenc and M. Malisoff. On stability and stabilization for models of chemostats with multiple limiting substrates. *J. Biol. Dyn*, 2(6):612–627, 2012. 10

[37] J. Monod. La technique de culture continue. théorie et applications. *Ann. Inst. Pasteur*, 41(79):390–410, 1950. 6

[38] A. Narang. The steady states of microbial growth on mixtures of substitutable substrates in a chemostat. *J. Theor. Biol*, 190:241–261, 1998. 10

[39] B.J. Ni, G.P. Sheng, and H.Q. Yu. Model-based characterization of endogenous maintenance, cell death and predation processes of activated sludge in sequencing batch reactors. *Chem. Eng. Sci*, 66:747–754, 2011. 14

[40] S. Nouaoura, R. Fekih-Salem, N. Abdellatif, and T. Sari. Mathematical analysis of a three-tiered food-web in the chemostat. *Discrete & Continuous Dyn. Syst. - B*, 26 (10):5601–5625, 2021. doi: 10.3934/dcdsb.2020369. 10, 20, 37, 62

[41] S. Nouaoura, N. Abdellatif, R. Fekih-Salem, and T. Sari. Mathematical analysis of a three-tiered model of anaerobic digestion. SIAM J. Appl. Math. SIAP, 1, 2021, https://hal.archives-ouvertes.fr/hal-02540350v2. 10, 20, 88, 100

[42] S. Nouaoura, R. Fekih-Salem, N. Abdellatif, and T. Sari. Operating diagrams for a three-tiered microbial food-web model. Preprint submitted to J. Math. Biol, 2021, https://hal.archives-ouvertes.fr/hal-03243013. 127

[43] A. Novick and L. Szilard. Description of the chemostat. *Science*, 112(3):715–716, 1950. 6

[44] S. L. Pimm. *Food Webs*. University of Chicago Press, Chicago, 2002. 18

[45] G. Powell. Stable coexistence of syntrophic associations in continuous culture. *J. Chem. Technol. Biotechnol. 35B*, pages 46–50, 1985. 10

[46] A. Rapaport and M. Veruete. A new proof of the competitive exclusion principle in the chemostat. *Discrete & Continuous Dyn. Syst. - B*, 24:3755–3764, 2019. 12

[47] P. J. Reilly. Stability of commensalistic systems. *Biotechnol. Bioeng*, 16(10):1373–1392, 1974. 11, 12

[48] G. Robledo, F. Grognard, and J. L. Gouzé. Global stability for a model of competition in the chemostat with microbial inputs, nonlinear analysis. *Real World Applications*, 13(2):582–598, 2012. 9

[49] T. Sari and B. Benyahia. The operating diagram for a two-step anaerobic digestion model. *J. Nonlinear Dyn*, 2020. 102

[50] T. Sari and J. Harmand. A model of a syntrophic relationship between two microbial species in a chemostat including maintenance. *Math. Biosci*, 275:1–9, 2016. 10, 14, 15, 21, 22

[51] T. Sari and M. J. Wade. Generalised approach to modelling a three-tiered microbial food-web. *Math. Biosci*, 291:21–37, 2017. 2, 10, 19, 20, 21, 24, 28, 35, 37, 62, 102, 106, 126, 129, 131

[52] T. Sari, M. El Hajji, and J. Harmand. The mathematical analysis of a syntrophic relationship between two microbial species in a chemostat. *Math. Biosci. Eng*, 9: 627–645, 2012. 14

[53] M. Sbarciog, M. Loccufier, and E. Noldus. Determination of appropriate operating strategies for anaerobic digestion systems. *Biochem. Eng. J*, 51(3):180–188, 2010. 10, 11, 12, 102

[54] SCILAB. *version 6.0.1(64-bit)*. Scilab Enterprises SAS, 2018. 59, 97

[55] I. Simeonov and S. Diop. Stability analysis of some nonlinear anaerobic digestion models. *Int. J. Bioautomation*, 14(1):37–48, 2010. 11

[56] H. L. Smith and P. Waltman. The theory of the chemostat, dynamics of microbial competition. *Cambridge University Press, Cambridge*, 1995. 6, 9, 12, 102

[57] S. Sobieszek, M. J. Wade, and G. S. K. Wolkowicz. Rich dynamics of a three-tiered anaerobic food-web in a chemostat with multiple substrate inflow. *Math. Biosci. Eng*, 17(1):7045–7073, 2020. 2, 10, 20, 56, 62, 97, 129

[58] G. Stephanopoulous. The dynamics of commensalism. *Biotechnol. Bioeng*, 23:2243–2255, 1981. 10, 11, 12

[59] D. Tilman. *Resource Competition and Community Structure*. Princeton University Press, Princeton, NJ, 1982. 10

[60] K. V. Venkatesh, P. Doshi, and R. Rengaswamy. An optimal strategy to model microbial growth in a multiple substrate environment. *Biotechnol. Bioengrg*, 56:635–644, 1997. 10

[61] S. Vet, K. SO de Buyl, Faust, J. Danckaert, D. Gonze, and L. Gelens. Bistability in a system of two species interacting through mutualism as well as competition: Chemostat vs. lotka-volterra equations. *PLoS ONE*, 13(6):e0197462, 2018. 13

[62] E. I. P. Volcke, M. Sbarciog, E. J. L. Noldus, B. De Baets, and M. Loccufier. Steady state multiplicity of two-step biological conversion systems with general kinetics. *Math. Biosci*, 228:160–170, 2010. 14

[63] M. J. Wade, J. Harmand, B. Benyahia, T. Bouchez, S. Chaillou, B. Cloez, J-J. Godon, B. Moussa Boudjemaa, A. Rapaport, T. Sari, R. Arditi, and C. Lobry. Perspectives in mathematical modelling for microbial ecology. *Ecol. Model*, 321:64–74, 2016. 6

[64] M. J. Wade, R. W. Pattinson, N. G. Parker, and J. Dolfing. Emergent behaviour in a chlorophenol-mineralising three-tiered microbial 'food web'. *J. Theoret. Biol*, 389: 171–186, 2016. x, 2, 10, 15, 16, 18, 19, 20, 24, 37, 49, 57, 62, 65, 78, 79, 80, 81, 82, 88, 89, 93, 94, 95, 99, 100, 102, 104, 105, 106, 111, 117, 119, 120, 121, 122, 126, 127, 129, 130, 131

[65] M.J. Wade. Not just numbers: Mathematical modelling and its contribution to anaerobic digestion processes. *Processes*, 8:888, 2020. 1, 16

[66] Y. Wang and H. Wu. A mutualism-competition model characterizing competitors with mutualism at low density. *Mathematical and Computer Modelling*, 53(9):1654–1663, 2011. 13

[67] M. Weedermann, G. Seo, and G. S. K. Wolkowicz. Mathematical model of anaerobic digestion in a chemostat: Effects of syntrophy and inhibition. *J. Biol. Dyn*, 7(1): 59–85, 2013. 1, 15, 16

[68] M. Weedermann, G. S. K. Wolkowicz, and J. Sasara. Optimal biogas production in a model for anaerobic digestion. *J. Nonlinear Dyn*, 81:1097–1112, 2015. 1, 14, 15, 16

[69] T. G. Wilkinson, H. H. Topiwala, and G. Harner. Interactions in a mixed bacterial population growing on methane in continuous culture. *Biotechnol. Bioeng*, 16:41–59, 1974. 14

[70] J. Wu, H. Nie, and G. S. K. Wolkowicz. A mathematical model of competition for two essential resources in the unstirred chemostat. *SIAM J. Appl. Math*, 65(1):209–229, 2004. 10

[71] A. Xu, J. Dolfing, T. P. Curtis, G. Montague, and E. Martin. Maintenance affects the stability of a two-tiered microbial 'food chain'? *J. Theoret. Biol*, 276(1):35, 2011. 14, 15, 16, 18, 102

[72] Z. Zhang. Mutualism or cooperation among competitors promotes coexistence and competitive ability. *Ecological Modelling*, 164(2-3):271–282, 2003. 13

Publications and communications related to the thesis

Publications:

i. **S. Nouaoura**, R. Fekih-Salem, N. Abdellatif, T. Sari, "*Mathematical analysis of a three-tiered food-web in the chemostat*", Discrete & Continuous Dynamical System Journal - B. 2021, 26 (10) : 5601–5625, doi/10.3934/dcdsb.2020369.

ii. **S. Nouaoura**, N. Abdellatif, R. Fekih-Salem, T. Sari, "*Mathematical analysis of a three-tiered model of anaerobic digestion*", SIAM - Journal on Applied Mathematics (SIAP), (Accepted in April, 2021). Available at https://hal.archives-ouvertes.fr/hal-02540350v2.

Submitted publication:

- **S. Nouaoura**, R. Fekih-Salem, N. Abdellatif, T. Sari, "*Operating diagrams for a three-tiered microbial food-web model*". Preprint submitted to Journal of Mathematical Biology, (2021). Available at https://hal.archives-ouvertes.fr/hal-03243013.

Communication:

- **S. Nouaoura**, N. Abdellatif, R. Fekih-Salem, T. Sari, "*Mathematical analysis of a three-tiered microbial food-web model with new input susbtrates*". Conference: Proceedings of the 9th conference on Trends in Applied Mathematics in Tunisia, Algeria, Morocco TAMTAM'19. At Tlemcen-Algeria, 23-27 February 2019, pages. 241–242. Available at https://hal.archives-ouvertes.fr

Seminars and Schools:

1. **S. Nouaoura**, N. Abdellatif, R. Fekih-Salem, T. Sari, "*Mathematical analysis of a three-tiered microbial food-web model*". TREASURE Seminar 2018. At Hammamet-Tunisia, 10-14 December 2018.

2. **S. Nouaoura**, N. Abdellatif, R. Fekih-Salem, T. Sari, "*Mathematical study of microbial food-web model: effects of input substrates and decay terms*". International School on Dynamical Systems and Applications (ISDSA 2019), "Third meeting of TWMA". At Monastir-Tunisia, 05-10 September 2019.

3. **S. Nouaoura**, N. Abdellatif, R. Fekih-Salem, T. Sari, "*Mathematical study of microbial food-web model: effects of input substrates and decay terms*". TREASURE Seminar 2019. At Hammamet-Tunisia, 02-06 December 2019.

4. **S. Nouaoura**, N. Abdellatif, R. Fekih-Salem, T. Sari, "*The effect of a new input substrates concentration on the microbial food-web model*".Maghrebian Meeting of Young Researchers in Pure and Applied Mathematics, "MYRPAM". At Hammamet-Tunisia, 09-12 December 2019.